Evolutionary Drivers of Mobile Colistin Resistance



Lois Ogunlana
Balliol College
University of Oxford

A thesis submitted for the degree of
Doctor of Philosophy

Thesis Abstract

Antibiotics are our strongest defence against disease causing bacteria. This makes the threat of widespread antibiotic resistance all the more concerning. Last-resort antibiotics such as colistin are especially important as they are effective against multiple-drug resistant pathogens. The recent emergence and spread of the mobile colistin resistance gene *mcr-1* threatens the efficacy of colistin. Although the gene incurs a large fitness cost, mechanisms such as compensatory adaptation could reduce costs associated with MCR-1 carriage and enable its maintenance and spread in the absence of colistin selection.

To test if compensatory adaptation was playing a role in *mcr-1* evolution, I first studied the impact of non-synonymous coding sequence variants and found that although some provided fitness benefits, most variants were deleterious (Chapter 2). Next, I focused on variants found in *mcr-1* regulatory sequences and found that regulatory variants generally caused increased fitness in the presence and absence of colistin selection (Chapter 3). Additionally, I discovered that *E. coli* carrying regulatory variants had reduced transcript levels and MCR-1 protein activity. From these results, I concluded that regulatory variants reduce the costs of MCR-1 by reducing protein levels via reduced transcription and/or translation. Interestingly, regulatory variants also increased colistin resistance suggesting that they are not traditional examples of compensation but rather regulatory fine-tuning to obtain optimal balances between MCR-1 activity and fitness costs. Lastly, I studied the impact of MCR-1 on cell morphology and behaviour, particularly in regards to bacterial conjugation (Chapter 4). I found that MCR-1 activity lead to increased conjugation rates and plasmid stability of transferable *mcr-1*-positive plasmids.

Overall, these results have important implications on the control of MCR-1 mediated colistin resistance. Although intragenic compensation is not prevalent, *mcr-1* regulatory variations are observed in multiple plasmid backgrounds and are increasing in prevalence among *mcr-1*-positive sequence isolates. Additionally, MCR-1 can facilitate its own transfer in the absence of selection though its effects on conjugation and plasmid stability. These factors could make *mcr-1* genes difficult to eliminate even in the absence of colistin selection.

Acknowledgements

Firstly, I want to thank my supervisors Prof. Craig Maclean and Dr. Stephan Uphoff. I feel very blessed to have two patient and enthusiastic mentors guiding me thorough my DPhil work. I have learned so much from them over the years and I have thoroughly enjoyed working on these projects. I have become a better researcher through this DPhil and I believe that having excellent supervisors is a big part of that.

I also thank the past and present members of the Maclean and Uphoff labs for being such a delight to work with, teaching me so much about science and just generally being a fun bunch to be around. I would like to especially thank Pramod Jagir, Andre Papkou, Valentine Lagage and Natalia Kapel for their lab mentorship. I want to thank the members of the Zoology department for making work life easier and more fun even through the pandemic. I also thank the Oxford Interdisciplinary Science DTP and Balliol College for the academic support and opportunities they provided throughout my studies.

I am blessed to have made so many wonderful friends in Balliol, The Department of Zoology and through the DTP who provided me with immense support and much needed entertainment. I want to thank Divjot Kuar and Sofia Miñano for all the much-needed coffee breaks. I also thank my partners in crime and welfare Dario Stein and Leonor Aidos for their never-ending puns, deep discussions and frequent brunch outings. I specially thank my dearest flatmates and life-long friends Chelsea Taylor, Chloe Casey and Stefania Vietti-Michelina who have made my life in Oxford so bright and full of life.

Lastly, I thank my amazing family who have been with me every step of the way. I am immensely blessed to have been born to such a loving and supportive household. I thank my big brother Samuel for all the late-night calls of support and his unwavering faith in me. I also like thank my little brother Daniel for being the cutest person to have ever lived and for never failing to brighten my day. And finally, I thank my loving parents Stephen and Elisabeth who have been there for me for as long as I can remember. Their love, support and faith has built me into the person I am today and I am grateful to call myself their daughter. I thank God for the blessings of family, friendship and mentorship I have in my life as this thesis would not be possible without them.

Contributions

I declare that this thesis is substantively my own work.

Contributions by others include:

- Chapter 3: I MG1655 with chromosomally integrated *mcr-1* was constructed by Divjot Kuar. Tables containing *mcr-1*-positive sequence isolate information were obtained from Liam Shaw

- Chapter 4: Liquid culture transfers in flow-cytometry based conjugation passage experiments were performed with support from Celia Souque.

Table of Contents

THESIS ABSTRACT **2**

ACKNOWLEDGEMENTS **3**

CONTRIBUTIONS **4**

TABLE OF CONTENTS **5**

ABBREVIATIONS **7**

1 INTRODUCTION **8**

1.1 The Growing Threat of Antibiotic Resistance 8
1.1.1 The Causes of Antibiotic Resistance *9*
1.1.2 The Consequences of Antibiotic Resistance *10*
1.2 Fitness, Compensation and Mobile Genetic Elements 11
1.2.1 The Evolutionary Conflicts of Mobile Genetic Elements *12*
1.2.2 MGE Maintenance by Compensatory Adaptation and Co-Selection *15*
1.2.3 Reducing Antibiotic Use: Will It Stop Resistance? *17*
1.3 Our Current Understanding of Mobile Colistin Resistance 18
1.3.1 Colistin: History and Mechanism of Action *18*
1.3.2 Colistin Resistance and MCR-1 Epidemiology *20*
1.3.3 The Fitness Costs of MCR-1 ..... *21*
1.4 Thesis Outline and Structure 22

2 INVESTIGATING THE FITNESS EFFECTS OF STRUCTURAL VARIATIONS IN MCR-1 ..... **25**

2.1 Abstract 25
2.2 Introduction 25
2.3 Materials and methods 27
2.4 Results 31
2.4.1 MCR-1 Variant Construction *31*
2.4.2 Individual Resistant and Fitness Assessments of mcr-1 Variants *32*
2.4.3 Fitness Competitions of MCR Variants *39*
2.4.4 Structural Variant Sequence Analysis *42*
2.5 Discussion 43
2.6 Supplementary Information 47

3 THE FITNESS EFFECTS OF MCR-1 REGULATORY SEQUENCE VARIATIONS **51**

3.1 Abstract 51
3.2 Introduction 51
3.3 Methods 53
3.4 Results 57
3.4.1 Regulatory Variations and their Predicted Effects *57*
3.4.2 Plasmid and Variant Construction *58*
3.4.3 Endpoint Optical Density Assessments of Regulatory Variants *58*
3.4.4 Growth Rate Estimations of Regulatory Variants *60*
3.4.5 Growth Rate and MIC of Chromosomally Integrated MCR-1 ..... *61*
3.4.6 Measuring Variant mcr-1 Expression via RT-qPCR *63*
3.4.7 Relative Surface Charge of Regulatory Variants *64*
3.4.8 Fitness Competitions of Regulatory Variants *66*
3.4.9 Proportion and Frequency Assessments of Regulatory Variants *68*
3.5 Discussion 70
3.6 Supplementary Information 74

4 THE IMPACTS OF MCR-1 ON CONJUGATION AND PLASMID MAINTENANCE **77**

4.1 Abstract 77
4.2 Introduction 77
4.3 Methods 79
4.4 Results 84
4.4.1 Effects of mcr-1 Overexpression on TOP10 E. coli Growth and Behaviour 84
4.4.2 Aggregation Analysis of MG1655 and β3914 85
4.4.3 Donor E. coli Construction and Analysis 89
4.4.4 Assessments of Donor Plasmid Stability 90
4.4.5 Conjugation Rate Measurements 92
4.4.6 Fluorometric Assessments of Plasmid Stability 93
4.4.7 Fluorometric Assays of Passaged Conjugation Cultures 95
4.5 Discussion 98
4.6 Supplementary Information 102
5 FINAL DISCUSSION AND SUMMARY 104
APPENDICES 109
REFERENCES 129

Abbreviations

AA……	Amino Acid
AMP……	Antimicrobial Peptide
Ara……	Arabinose
BP……	Base Pair
DRC……	Dose-Response Curve
HGT……	Horizontal Gene Transfer
IC50……	Half maximal inhibitory concentration
LB……	Luria/Lysogeny Broth
LPS……	Lipopolysaccharide
MCR……	Mobile Colistin Resistance
MDR……	Multi-Drug Resistance
MGE……	Mobile Genetic Element
MIC……	Minimum Inhibitory Concentration
MH/MH2……	Mueller Hinton Broth
MSA……	Multi-Sequence Alignment
OD……	Optical Density
PV……	Promoter Variant
SDV……	Shine-Dalgarno Variant
SNP……	Single Nucleotide Polymorphism

1 Introduction

As our arsenal of effective antibiotics continue to dwindle due to the imminent threat of antibiotic resistance, last-resort antibiotics such as Colistin have become increasingly important. This is why the discovery of *mcr-1*, a plasmid encoded colistin resistance gene, is of great significance. Although mobile genetic elements (MGEs), such as plasmids and transposons carrying *mcr-1*, play a large role in the acquisition and spread of antibiotic resistance genes, the maintenance of these elements and expression of genes they carry often comes with a large cost. In this introductory chapter, I present important evolutionary concepts that underpin the spread and maintenance of MGEs and are relevant to this thesis. I will then introduce *mcr-1* and the threat it imposes on colistin usage before outlining the thesis aims and structure.

1.1 The Growing Threat of Antibiotic Resistance

Before the 20th century, microbial infectious were largely unmanageable with pneumonia, tuberculosis, and enteritis being among the leading causes of death (ONS, 2017; Adedeji, 2016). It wasn't until the discovery and subsequent development of multiple antibiotics in the mid-to-late 20th century, often called the start of the "Antibiotic Era", that these deadly infections became treatable (Aminov, 2010; Ventola, 2015; Adedeji, 2016; Zaman *et al.*, 2017). Antibiotics effectively inhibit microbial growth and/or replication (**bacteriostatic**) or kill bacteria (**bactericidal**) due to their toxic effects on bacterial specific targets (Levy and Bonnie, 2004; Zaman *et al.*, 2017). Penicillin, the 1st antibiotic introduced to the market, successfully treated Word War II soldiers plagued with wound infections. Today, multiple surgical procedures, such as organ transplants, joint replacements and childbirth would be impossible without antibiotics (Ventola, 2015). It is clear that antibiotics have revolutionised medicine as their use has saved countless lives, improved the standard of living and increased global life expectancies (Davies and Davies, 2010; Blair *et al.*, 2015; Meek, Vyas and Piddock,

2015). However, the modern rise of **antibiotic resistance** is largely endangering the efficacy of these “wonder drugs”.

1.1.1 The Causes of Antibiotic Resistance

Bacteria are resistant to antibiotics once able to survive and grow in therapeutic concentrations of these drugs (Aminov, 2010; Ventola, 2015; Zaman *et al.*, 2017). Microbes can obtain antibiotic resistance via two main mechanisms. Firstly, **spontaneous mutations** conferring resistance can arise in bacterial genomes, usually in genes encoding antibiotic targets (Baym *et al.*, 2016). This is especially the case during antibiotic treatment as antibiotics often increase mutation rates since their effects often result in mutagenic DNA damage and error-prone replication (Long *et al.*, 2016). Secondly, exchange of genetic material between cells, referred to as **Horizontal Gene Transfer** (**HGT**), enables bacteria to acquire antibiotic resistance genes present on **mobile genetic elements** (**MGEs**) such as plasmids and transposons (Davies and Davies, 2010; Blair *et al.*, 2015; Meek, Vyas and Piddock, 2015). Resistance genes have varied molecular mechanisms, e.g. drug efflux, enzymatic inactivation, which ultimately reduce antibiotic efficacy (Blair *et al.*, 2015; Zaman *et al.*, 2017). Bacteria harbouring genetic resistance determinants are able to outcompete their susceptible counterparts in the presence of antibiotics (Levy and Bonnie, 2004; Aminov, 2010; Meek, Vyas and Piddock, 2015; Zaman *et al.*, 2017). This **selection pressure** facilitates the maintenance and spread of these genes when antibiotics are present (*Figure 1.1*).

The misuse and overuse of antibiotics has greatly accelerated the incidence and spread of resistance genes in bacterial populations (Levy and Bonnie, 2004; Aminov, 2010; Ventola, 2015; Zaman *et al.*, 2017). Between 2000 and 2015, global antibiotic consumption increased by 65% with 2030 projections predicting a 200% increase if no major policy changes are introduced (Klein *et al.*, 2018). Many countries have high antibiotic prescription rates and in others, antibiotics can be purchased from retail pharmacies without prescription (Ventola, 2015; World Health Organization, 2018). This accessibility promotes antibiotic overuse which is directly correlated with increased prevalence of resistant strains (Kallel *et al.*, 2008; Yang *et al.*, 2018). Furthermore, antibiotic misuse via inappropriate prescribing and agricultural overuse adds to the problem. In many countries, antibiotics are added to animal feed as

growth promoters and around 80% of antibiotics sold in the U.S. are solely used for animals (Ventola, 2015). This is problematic as some of these agricultural antibiotics are used in human treatment and/or possess similar modes of action to drugs used in the clinic (Saiful, Shiraj-Um-Mahmuda and Hazzaz-Bin-Kabir, 2016). Resistance determinants that arise in livestock associated bacterial populations can become clinically relevant by HGT into human pathogens or directly via zoonotic infections leading to reductions in antibiotic efficacy (ESFA, 2018; Ortega-Paredes *et al.*, 2020). Currently, resistance genes with diverse modes of action have been identified against all major classes of antibiotics. Additionally, as no new classes of antibiotic have entered the market since the 1980s, our arsenal of effective antibiotics is highly limited (Aminov, 2010; Blair *et al.*, 2015; Ventola, 2015; Zaman *et al.*, 2017).

1.1.2 The Consequences of Antibiotic Resistance

Antibiotic resistance has a devastating impact on healthcare with over 33,000 European patients dying from resistant bacterial infections every year (Cassini *et al.*, 2019). Increased use of multiple antibiotics has driven the emergence of multi-drug resistant (MDR) strains such as Methicillin-Resistant Staphylococcus Aureus (MRSA) which are extremely difficult to treat (Levy and Bonnie, 2004; Ventola, 2015). Additionally, antibiotic resistance has large economic impacts due to increased healthcare costs and productivity losses with the estimated cost of antibiotic resistance in the EU surpassing 1.5 billion euros each year (Prestinaci, Pezzotti and Pantosti, 2015; Dadgostar, 2019). If major interventions to limit antibiotic use and stop resistance spread are not implemented, we risk returning to the “Pre-Antibiotic Era”.

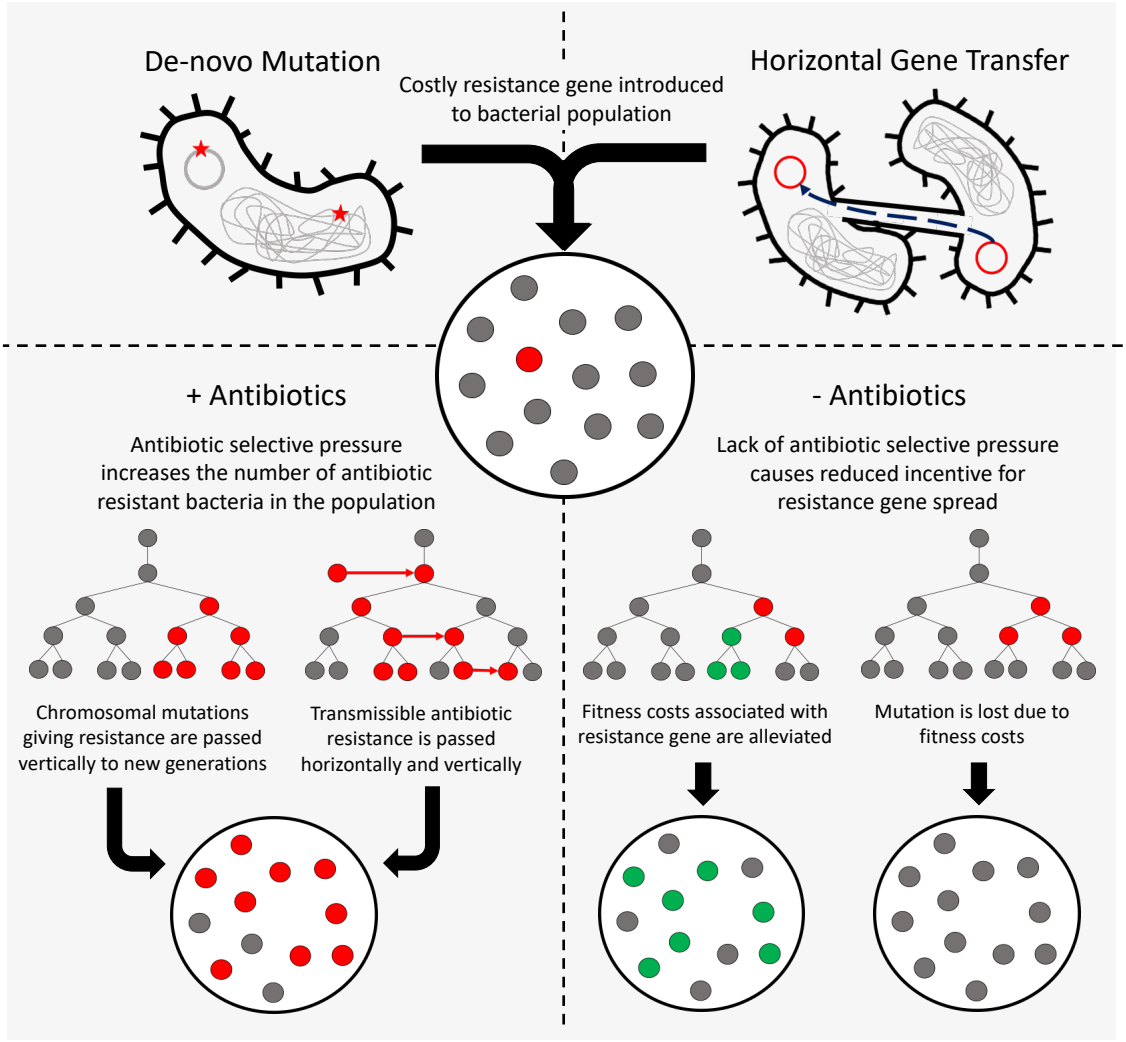


Figure 1.1: Antibiotic Resistance Emergence and Maintenance

Genes conferring antibiotic resistance can arise de-novo via spontaneous mutations or can be given to susceptible bacteria via horizontal gene transfer. In the presence of antibiotics, selective pressure drives the maintenance and spread of these resistance genes. Chromosomal mutations are clonally passed on to daughter cells while transmissible resistance genes can also be passed on horizontally to non-offspring neighbours. In the absence of antibiotics, the fitness costs imposed by resistance genes could cause them to be lost from the population. Alternatively, if these costs are alleviated or resistance is cost free, resistance genes can be maintained. (Figure made by thesis author)

1.2 Fitness, Compensation and Mobile Genetic Elements

The spread of antibiotic resistance genes becomes a clinically relevant problem once the frequency of resistant populations reduces effectiveness of an antibiotic therapy (Andersson and Hughes, 2010). It is unsurprising that resistance genes would persist in the presence of antibiotics. However, resistance gene persistence is not guaranteed in antibiotic-free

conditions. A key discovery from experimental studies on resistance genes it that they often reduce bacterial survival and reproduction in the absence of selection (Andersson and Levin, 1999; Andersson and Hughes, 2010a; Melnyk, Wong and Kassen, 2015). These **fitness costs** are highly variable and involve many factors (Vogwill and Maclean, 2015). Antibiotics often target vital bacterial pathways (e.g. cell wall synthesis, gene expression, DNA replication) and resistance mutations altering key proteins could perturb important pathways or reduce pathogen virulence (Andersson and Levin, 1999; Sommer, Dantas and Church, 2009; Melnyk, Wong and Kassen, 2015). Genetic background is also important as resistance genes do not exist in isolation. Chromosomal resistance mutations tend to carry larger costs than MGEs. Potentially because MGEs may already contain fitness adaptations obtained from previous hosts (Vogwill and Maclean, 2015). Additionally, plasmid type and/or strain can have pronounced effects on resistant gene fitness costs due to epistatic interactions with surrounding genes or certain plasmid properties (e.g. stability, conjugation rate and copy number) (Vogwill, Kojadinovic and Maclean, 2016; Dimitriu *et al.*, 2019). Fitness costs have important evolutionary implications as they provide selection against resistance and play key roles in resistance evolution dynamics (Andersson and Levin, 1999; Andersson and Hughes, 2010). These dynamics become more interesting when considering resistance obtained from MGEs as their maintenance is costly and their evolutionary interests are separate from their bacterial hosts (Andersson and Levin, 1999; Sommer, Dantas and Church, 2009).

1.2.1 The Evolutionary Conflicts of Mobile Genetic Elements

Pathogenic bacteria typically exist in populated communities that host multiple strains and species (Sommer, Dantas and Church, 2009). MGEs such as plasmids, transposons and integrons are commonly found in these environments and can be transferred between neighbours via three main HGT mechanisms: **conjugation**, **transformation** and **transduction** (*Figure 1.2*). These mechanisms can occur between bacterial species and facilitate adaptation, particularly in diverse microbial communities that carry various MGEs. Bacteria are able to acquire “ready-made” genes that can provide beneficial phenotypes, such as antibiotic resistance, without relying on rare *de novo* mutations that may disrupt conserved essential genes (Harrison and Brockhurst, 2012; Brockhurst *et al.*, 2019). MGEs can also be nested within each other, producing larger elements that encode multiple beneficial traits such as

pathogenicity islands and multi-resistance plasmids (Brockhurst *et al.*, 2019). For example, integrons, genetic elements which allow bacteria to incorporate and express new genes, can be found within transposons allowing the entire mechanism to change positions within a genome or between genetic backgrounds (Benler *et al.*, 2021). These cassettes can also be nested within conjugative plasmids which enables dissemination of these highly adaptive genetic structures to a range of bacterial strains and species (Martinez *et al.*, 2007).

In addition to potentially beneficial accessory genes, MGEs carry genes essential for their replication and transfer. For example, conjugative plasmids encode genes necessary for the formation of transfer pili and transposons encode transposases that facilitate their movement within the genome (Harrison and Brockhurst, 2012; Brockhurst *et al.*, 2019). These "backbone" genes are energetically costly to hosts as their maintenance and expression is resource intensive and occupies cellular machinery (Bentley *et al.*, 1990; Bergstrom, Lipsitch and Levin, 2000; Harrison and Brockhurst, 2012). Other MGE features can cause additional problems for hosts. Conjugative pili are often vulnerable to pili specific phage and high copy number plasmids can be toxic (Harrison *et al.*, 2012; Bottery, Wood and Brockhurst, 2017). Unless the overall benefits provided by accessory MGE genes outweigh the costs of their carriage, these elements are likely to be lost via **purifying selection** (Bergstrom, Lipsitch and Levin, 2000; Harrison and Brockhurst, 2012; Brockhurst *et al.*, 2019). However, it is possible for costly MGEs to be maintained as selfish parasites in the absence of selection e.g. by recurrent transfer (Stewart and Levin, 1977).

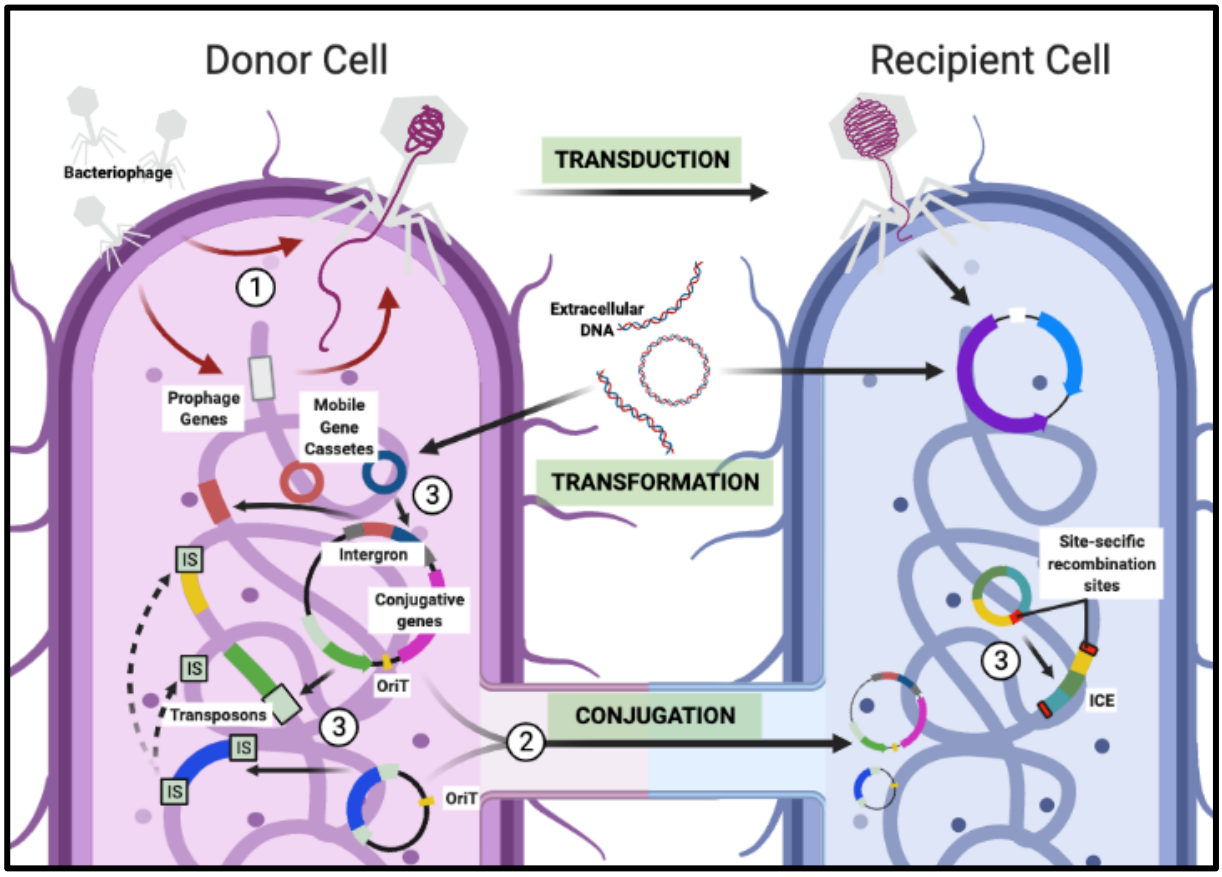


Figure 1.2: Mechanisms for Gene Acquisition and Transfer

Genetic material can be rearranged within cells and passed between cells using a variety of mechanisms. The three mechanisms by which bacteria can obtain and pass genetic material horizontally are T**ransduction** (introduction of foreign DNA by viral vectors) **Transformation** (uptake of genetic material from the environment) and **Conjugation** (transfer of genetic material between bacteria via direct contact). The schematic above illustrates these three mechanisms in addition to various gene transfer mechanisms. (**1**) Phage originating either from the environment or prophage genes) can package the host genome and therefore transfer genes to recipient cells they subsequently infect. (**2**) Conjugation genes are expressed allowing bacteria to form sex pili that attach to surrounding cells draw them closer. This facilitates cell-to-cell contact which form cytoplasmic connection between cells. Plasmids containing an origin of transfer (OriT) are able to move through these connections and therefore spread to other cells. (**3**) Genes can be rearranged using different modes of intracellular motility. Composite and unit transposons can jump from the plasmid to the genome or vice versa. Movement of insertion sequences (IS) can facilitate the mobility of previously non-mobile genetic elements. Mobile gene cassettes can be captured within integrons and transposons allowing their integration into plasmids or the bacterial genome. Site-specific recombination sequences can allow incorporation of foreign DNA into plasmids or the genome. (Figure made by thesis author via BioRender)

Due to fitness costs, the eventual genomic integration of beneficial MGE genes and elimination of the non-beneficial backbone is in the host's interests (Bergstrom, Lipsitch and Levin, 2000; Harrison and Brockhurst, 2012; Brockhurst *et al.*, 2019). This is in direct conflict

with the evolutionary interests of MGEs as they are semi-autonomous entities seeking to maximise their transmission both horizontally and vertically. Carrying genes that improve host fitness enhances the vertical transmission of MGEs. However, as these genes can eventually be integrated into bacterial chromosomes, it is unlikely that MGEs will persist in hosts even under constant selection (Bergstrom, Lipsitch and Levin, 2000; Brockhurst *et al.*, 2019). Consequently, MGEs mainly encode selfish genes that facilitate their spread in multiple genetic backgrounds with phage, plasmid and transposon maintenance genes being highly overrepresented in pangenomes (Bentley *et al.*, 1990). Resolution of intragenomic conflicts between host chromosomes and MGEs is essential for MGE maintenance. This is possible through subsequent evolutionary adaptations that minimise the costs that MGEs impose (Harrison and Brockhurst, 2012; Brockhurst *et al.*, 2019).

1.2.2 MGE Maintenance by Compensatory Adaptation and Co-Selection

Costs imposed by resistance mutations, genes and MGEs, increases the possibility of these resistance determinants becoming lost in antibiotic-free environments through purifying selection (Harrison and Brockhurst, 2012; Vogwill and Maclean, 2015). However, studies on fitness costs have revealed that even in these conditions, resistance can be maintained in three ways. The first and rarest is through **cost-free resistance** where there are no measurable differences in the fitness's of susceptible and resistant strains. Secondly, **linkage** to genes providing large fitness benefits could outweigh the costs of resistance. The final and most relevant mechanism to this thesis is **compensatory adaptation** which is the partial to full removal of fitness costs from resistance by additional mutations (Andersson and Hughes, 2010; Melnyk, Wong and Kassen, 2015; Vogwill and Maclean, 2015). It is important to note that **recurrent horizontal transfer** can theoretically maintain costly resistance genes, but it is unclear if horizontal transfer rates are high enough (Stewart and Levin, 1977; Lopatkin *et al.*, 2017).

Evidence of compensatory evolution has been detected by *in-vitro* experimental evolution studies (Andersson and Hughes, 2010). These studies involve the serial passage of resistant bacteria in the absence of antibiotics. Changes in fitness can be detected by assessing changes in colony size or measuring exponential growth rates (Baltrus, 2013). Competitive fitness can

also be assessed by co-incubation of evolved and ancestral lines *in-vitro* and/or *in-vivo* followed by assays that measure changes in their ratios. Whole genome sequencing or sequencing of targeted genes can reveal which genotypic alterations may be responsible for the resulting fitness differences (Andersson and Hughes, 2010). Compensation can occur through various mechanisms: intragenic or extragenic single nucleotide polymorphisms (SNPs) can increase fitness while maintaining or even increasing resistance; gene amplification can provide larger targets for fitness altering mutations; and reduced or induced gene expression could mean costs are lowered or only manifest in the presence of antibiotics (Andersson and Hughes, 2010; Bottery, Wood and Brockhurst, 2017). If resistance genes are present on MGEs, subsequent mutations on the MGE backbone and/or host chromosomes can lead to stable maintenance of these elements (Brockhurst *et al.*, 2019).

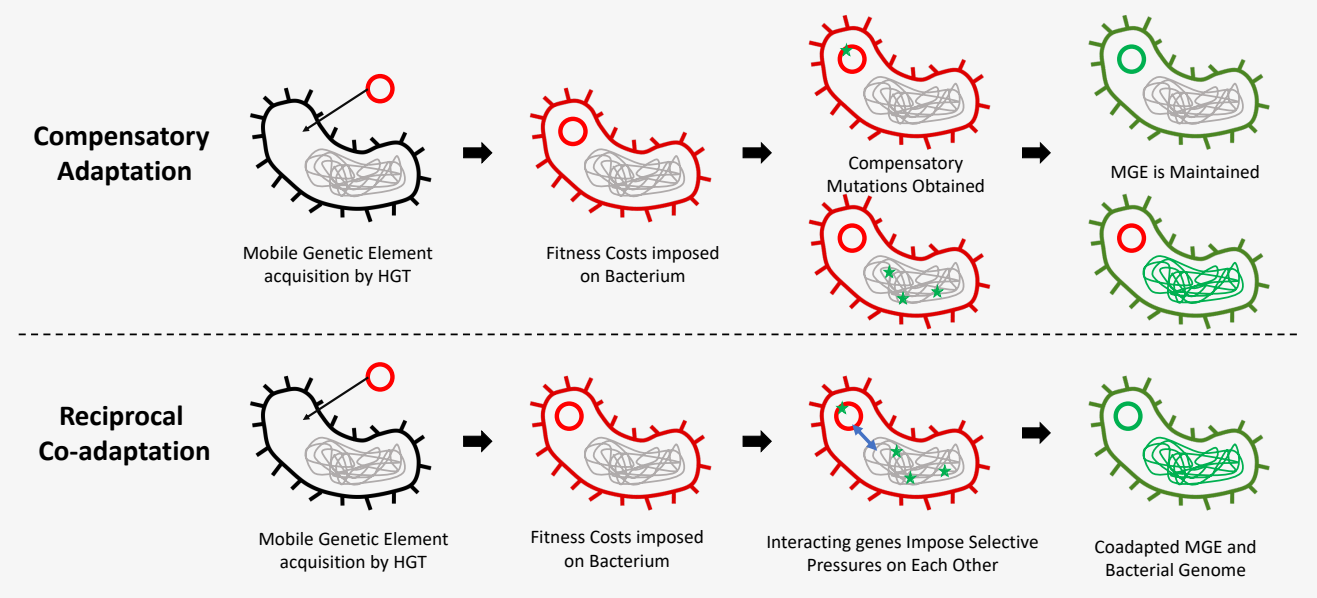


Figure 1.3: Fitness Compensation and Co-adaptation of MGEs

The schematic above illustrates compensatory adaptation and reciprocal adaptation. Mobile genetic elements obtained are initially costly and therefore result in fitness losses (demonstrated by red colourings). Mutations (demonstrated by stars) either on the host chromosome or the MGE can lead to alleviation of these fitness costs (demonstrated by green colouring) resulting in the maintenance of these elements. Additionally, interacting genes within these elements can impose selective pressures resulting in mutations within the element and/or the bacterial genome that are costly on their own but beneficial in combination. Due to this, the MGE and bacterial genome become co-dependent and removal of the MGE could result in fitness losses. This is the basis of reciprocal coadaptation. (Figure made by thesis author)

Compensation can also lead to the resolution of intragenomic conflicts between newly obtained MGEs and their hosts (*Figure 1.3*). Evidence from experimental evolutions have shown that in combination with positive selection for beneficial plasmid genes, compensatory adaptation is able to stabilise non-transmissible plasmids by reducing the costs of their carriage (Millan *et al.*, 2014; San Millan and MacLean, 2017). Additionally, multiple studies have also demonstrated cost reductions of transmissible/non-transmissible plasmids due to plasmid or chromosome mutations (Bouma and Lenski, 1988; Dahlberg and Chao, 2003; Sota *et al.*, 2010). Initial compensatory mutations can also pave the way for subsequent, more extensive co-evolution (*Figure 1.3*). **Reciprocal co-adaptation** between MGEs and host chromosomes can lead to domestication and co-dependence of MGEs (Harrison and Brockhurst, 2012; Bottery, Wood and Brockhurst, 2017; Brockhurst *et al.*, 2019). These adaptations can also help explain the "plasmid paradox" since, aside for parasitic, highly conjugative plasmids, it is unclear why plasmids are stably maintained in bacterial populations despite the costs they inflict (Millan *et al.*, 2014; San Millan and MacLean, 2017). Putting all of this together, it becomes clear that in addition to providing beneficial genes and spreading antibiotic resistance, HGT is a powerful adaptive force with the ability to dramatically transform evolutionary landscapes through compensation and reciprocal-coadaptation (Baltrus, 2013; Brockhurst *et al.*, 2019).

1.2.3 Reducing Antibiotic Use: Will It Stop Resistance?

Antibiotic treatment creates environments favouring the spread of resistant mutants since susceptible bacteria are eliminated and remaining resistant strains have reduced resource competition (Gullberg *et al.*, 2011). Due to their fitness costs, resistant bacteria have increased generation times and reduced growth rates in antibiotic-free environments giving susceptible isolates a competitive advantage (Wale *et al.*, 2017). This suggests that reducing antibiotic use would remove the selection pressures that antibiotics impose on bacteria and cause resistant variants to be outcompeted by their fitter, susceptible counterparts (Basra *et al.*, 2018; Bell and MacLean, 2018). Moreover, costly MGEs that carry resistance genes would no longer be positively selected for in these conditions. Many have suggested that the limitation of antibiotic use could lead to the reduction or even reversal of resistance in bacterial populations, an idea supported by both experimental studies and theoretical models

(MacLean *et al.*, 2010; Wale *et al.*, 2017; Bell and MacLean, 2018). However, if compensatory evolution has already occurred in resistant strains, removal of antibiotics would not alter the prevalence of resistance genes.

Compensation allows resistance to spread and stabilise in the absence of antibiotics since resistant mutants are no longer selected against (MacLean and Vogwill, 2015). Additionally, resistance reversion is unlikely once compensatory mutations arise as the fitness benefits of reversion are no longer relevant (Andersson and Hughes, 2010). Multiple studies have shown stable maintenance of resistance determinants for long time periods in the absence of selection (Besier *et al.*, 2005; Gifford and MacLean, 2013; MacLean and Vogwill, 2015; Qi *et al.*, 2016). If compensation is as common as these studies suggest, the spread of compensated resistance alleles by HGT and/or clonal expansion could lead to redundancy of clinically relevant antibiotics (MacLean and Vogwill, 2015; Melnyk, Wong and Kassen, 2015). There is evidence of compensatory adaptation occurring in natural populations, an example being adaptation to rifampicin resistance costs by *M. tuberculosis* (Comas *et al.*, 2012). However, compensatory adaptation is not readily detected in clinical settings and studies highlighting its occurrence provide no insights to its prevalence. On the contrary, most clinical studies have found that resistance declines in pathogen populations once antibiotic use is restricted or stopped completely (Costelloe *et al.*, 2010; MacLean and Vogwill, 2015). Such strong couplings of antibiotic consumption and resistance are unlikely if compensatory adaptation is common in nature. It is important to assess the prevalence of compensation in real-world settings to determine whether limiting antibiotic use will be effective in preventing the spread of antibiotic resistance.

1.3 Our Current Understanding of Mobile Colistin Resistance

1.3.1 Colistin: History and Mechanism of Action

The work carried out in this thesis involves the **antimicrobial peptide** (**AMP**) Colistin (also known as polymixin E) and the **mobile colistin resistance** (**MCR**) gene *mcr-1*. Colistin is bactericidal and contains hydrophobic and cationic regions vital for its antibacterial activity (*Figure 1.4*). Gram-negative bacteria possess a thin peptidoglycan cell wall sandwiched

between two cell membranes (Silhavy, Kahne and Walker, 2010). Unlike their inner membranes which are phospholipid bilayers, the gram-negative outer membrane only contains phospholipids within the inner leaflet. Outer leaflets contains glycolipids such as lipopolysaccharide (LPS) which are typically composed of O-antigen, core oligosaccharide and Lipid A (Silhavy, Kahne and Walker, 2010). The cationic tail of colistin facilitates initial binding of the AMP to negatively charged phosphate ions on the Lipid A portion of gram-negative bacteria outer membranes (Falagas, Kasiakou and Saravolatz, 2005; Bialvaei and Samadi Kafil, 2015). This action leads to the displacement of magnesium and calcium ions needed for membrane stabilisation (*Figure 1.4*). Colistin is thought to form pores on outer and inner membranes via subsequent interactions of its hydrophobic rings with membrane lipids (Falagas, Kasiakou and Saravolatz, 2005).

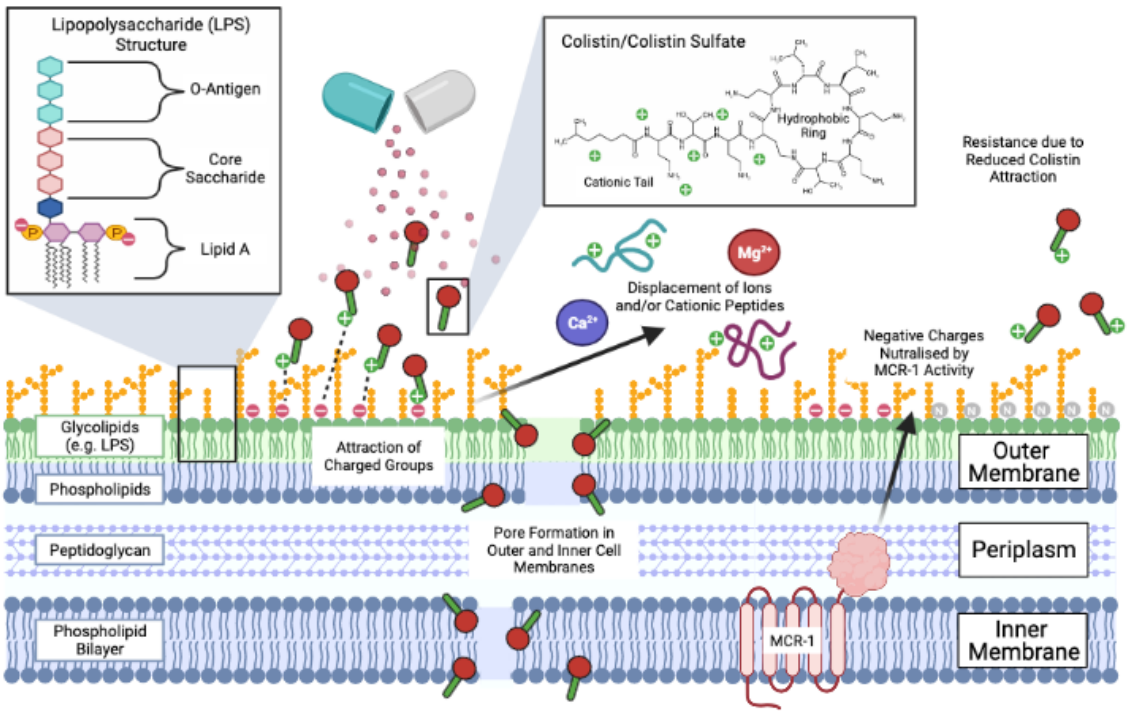


Figure 4: Colistin Mechanism of Action

The schematic above illustrates the structure and components of the gram-negative cell membrane and demonstrate colistin effects of the membrane structure. Due to its amphipathic nature, colistin is able to adhere to outer membranes via interactions with negative charges on LPS glycolipids. It is also able to interact with the hydrophobic lipid bilayer. This causes colistin to act as a detergent causing membrane solubilisation causing the formation of pores. Displacement of cationic ions and peptides on the outer membrane leads to permeability changes and further membrane destabilisation. (Figure made by thesis author via Biorender)

Colistin became available for clinical use in the 1960s but was largely replaced by aminoglycosides due to its neuro and nephrotoxicity (Falagas, Kasiakou and Saravolatz, 2005; Biswas *et al.*, 2012). However, increased prevalence of antibiotic resistance led to its resurgence as a "last-resort" against MDR gram-negative pathogens, particularly carbapenemase-producing and NDM-1 metallo-β-lactamase multidrug-resistant Enterobacteriaceae (Falagas, Kasiakou and Saravolatz, 2005; Biswas *et al.*, 2012; Gharaibeh and Shatnawi, 2019). Colistin's main use remains within the agricultural sector for treatment of livestock, disease prevention and, most controversially, as a growth promoter. Before 2016, production of agricultural colistin in China was estimated to about 12,000 tonnes yearly and colistin was heavily used in broiler and pig farms across European and southeast Asian countries (B McPhee and Lewenza, 2016). Despite the introduction of bans, agricultural misuse of colistin is widespread and has contributed to the increased prevalence of colistin resistance (Wang, Tian, *et al.*, 2017; Davies and Walsh, 2018; Gharaibeh and Shatnawi, 2019).

1.3.2 Colistin Resistance and MCR-1 Epidemiology

As its amphiphilic properties have destabilising and solubilising effects on gram-negative membranes, resistance mechanisms against colistin largely involve membrane modifications (Bialvaei and Samadi Kafil, 2015). Before the discovery of *mcr-1*, prominent mechanisms of colistin resistance included complex two-component regulatory systems, such as PhoPQ and PmrAB, which were chromosomally located and incur large fitness costs (Gunn, 2008; Cannatelli *et al.*, 2013). Because of these features, colistin resistance was considered rare as the costs of these genes made them difficult to maintain. Additionally, HGT was not involved in their dissemination. However, the emergence and spread of *mcr-1* has changed the situation.

In 2016, a routine surveillance study identified surges in colistin resistance among commensal bacteria from Chinese livestock. Upon closer investigation, Liu et.al associated the presence of the pHNSH45 plasmid with colistin resistance and identified *mcr-1* as the sole cause of resistance within this plasmid (Liu *et al.*, 2016). The encoded MCR-1 protein is a phosphoethanolamine (pEtN) transferase thought to confer colistin resistance by attaching pEtN to phosphate groups on Lipid A (Sun *et al.*, 2018). This diminishes the negative charges

on LPS therefore, reducing the ability of colistin to bind to its target (*Figure 1.4*). The study also found that porcine associated *E. coli* strains carrying pHNSH45 were able to rapidly transfer the plasmid to susceptible *E. coli* stains, showing potential of this gene to spread. Additionally, providing susceptible *E. coli*, *K. pneumoniae* and *P. aeruginosa* with *mcr-1*-positive plasmids increased their colistin **minimum inhibitory concentrations** (**MICs**) demonstrating its functionality in known human pathogens (Liu *et al.*, 2016).

Subsequent epidemiological and clinical studies have isolated colistin resistant bacteria from multiple environmental, animal and human sources. Additionally, *mcr-1* positive isolates have been identified in nearly 70 countries and include at least ten species of Enterobacteriaceae (Wang, Tian, *et al.*, 2017; Sun *et al.*, 2018). The rapid emergence of *mcr-1* is of growing concern as colistin is an important last-resort antimicrobial therapy. Should *mcr-1* become widespread, it would greatly reduce the efficacy of colistin treatment. Due to the selection pressures imposed, it is unsurprising that *mcr-1* prevalence is tightly correlated with colistin use. This is demonstrated well by surveillance data that show higher prevalence of *mcr-1* positive isolates in livestock, where colistin is mainly used (Maciuca *et al.*, 2019; Shen *et al.*, 2020). Additionally, a national effort to minimise colistin use in China lead to large decreases in *mcr-1* prevalence within the country further solidifying the links between antibiotic usage and resistance gene spread (Shen *et al.*, 2020; Wang *et al.*, 2020). However, to understand the evolutionary dynamics involved in the maintenance and spread of *mcr-1*, we must consider the costs that it imposes on bacteria and how these costs may change depending on its genomic context.

1.3.3 The Fitness Costs of MCR-1

Like most resistance genes, there are fitness costs associated with the expression of *mcr-1*. The initial study by Liu et.al reported plasmid stability of pHNSHP45 in trans-conjugants but murine infection assays showed a 1-log reduction in *mcr-1*-positive *E. coli* compared to susceptible bacteria in the absence of colistin (Liu *et al.*, 2016). These results hinted at *mcr-1* expression affecting cell viability. Supporting this, a thorough analysis into the fitness effects of *mcr-1* demonstrated the fitness trade-offs associated with high *mcr-1* expression by analysing growth rates, conducting competition assays and directly assessing cell morphology

and viability (Yang *et al.*, 2017). The study showed that plasmid-mediated *mcr-1* overexpression impaired cell growth, affected fitness, altered cell morphology and ultimately caused cell death. Based on transmission electron microscopy micrographs showing outer membrane damage and fluorescence assays showing increased entry of cell permeability markers, they hypothesised that MCR-1 increases membrane permeability resulting in reduced bacterial fitness (Yang *et al.*, 2017).

Successive studies support the observation that *mcr-1* carries a large fitness cost. Tietgen *et al.* showed that *E. coli* and *K. pneumoniae* transformed with *mcr-1* positive TOPO expression vectors had reduced growth rates and increased doubling times compared to control strains (Tietgen *et al.*, 2018). Their competitive growth experiments associate presence of *mcr-1* positive pKP2442 with reduced growth rates in *K. pneumoniae*. Nang *et.al* showed that plasmids containing *mcr-1* were less stable than their *mcr-1* negative counterparts in *K. pneumoniae* strains (Nang *et al.*, 2018). Due to these costs, bans on colistin use could lead to the loss of *mcr-1* mediated resistance which has been effectively demonstrated through the 2017 ban on colistin use in China (Shen *et al.*, 2020; Wang *et al.*, 2020). However, these costs could also provide a selective pressure for compensatory adaptation. Interestingly, allelic variations of *mcr-1* genes as well as homologs such as *mcr-3* have been identified globally. MCR-like genes have also been found in various genetic backgrounds and plasmid replicon types (Sun *et al.*, 2018). The effect of these varying genetic contexts on the fitness and resistance levels of bacteria carrying *mcr-1* is largely unexplored although some have speculated that these variants could be a result of ongoing evolution of *mcr-1* to an unknown selection pressure (Yang *et al.*, 2017; Sun *et al.*, 2018). Analysing genetic variations in *mcr-1* will help determine how this gene is evolving and if compensatory adaptation is playing a role in *mcr-1* evolution.

1.4 Thesis Outline and Structure

Much work has been done on the epidemiology of MCR and its prevalence is regularly monitored in multiple environments (Wang, Tian, *et al.*, 2017; Wang *et al.*, 2020). However, studies rarely focus on the evolutionary trajectory of MCR and the effect of its expression on bacterial fitness. If compensation is involved in MCR evolution, resistance could be

maintained in the absence of colistin. This would be problematic as further dissemination of this gene would ultimately lead to the inefficacy of colistin in the clinic and consequently limit our arsenal of effective defences against MDR gram-negative pathogens. Therefore, it is important to explore the genetic contexts and variations of *mcr-1* and determine the underlying factors that could be sources of compensatory adaptation. In the following work, I will be using quantitative growth and competition assays, molecular biology, and microscopy techniques to investigate the genetic variances found within and surrounding the *mcr-1* gene and the different genetic contexts that *mcr-1* is found in. I will then assess the impact of these variances on the fitness and resistance profiles of bacteria carrying them.

Chapter 2: Analysing the Structural Polymorphisms of MCR-1

I will be focusing on the variations found within the *mcr-1* coding sequence. The DNA sequences of multiple *mcr-1* positive isolates are available and show SNP variations that result in altered protein sequences (non-synonymous). I hypothesise that these naturally occurring *mcr-1* SNP variants could be examples of intragenic compensatory mutations. The main aim of this chapter was to analyse the non-synonymous sequence variations seen within *mcr-1* genes and determine their effects on colistin resistance and cell fitness in the presence and absence of selection.

Chapter 3: **Analysing the Variation in MCR-1 Expression**

Recent work that studied the *mcr-1* gene in various plasmid backgrounds identified a region of high variability that was located slightly upstream of *mcr-1*. Upon closer investigation, I found that this region overlapped with the *mcr-1* promoter and other regulatory regions. In this chapter, I test the hypothesis that these regulatory mutations reduce the levels of *mcr-1* gene expression therefore reducing the fitness costs associated with MCR-1. I reconstruct the regulatory variants and analyse the fitness and resistance changes they impose on host *E. coli* strains in comparison to the native regulatory sequence.

Chapter 4: The Impacts of MCR-1 Expression on Bacterial Conjugation

Conjugation is a pivotal part of *mcr-1* maintenance and distribution as these genes are largely found on conjugative plasmids. During experiments, I found that mcr-1 expressing bacteria showed increased interactions and “stickiness”. In this chapter, I will examine how expression

of *mcr-1* impacts bacterial conjugation and how this change could impact the maintenance and spread of transferable *mcr-1*-positive plasmids in the absence of selection pressures. I will assess the conjugation rates of *mcr-1* positive and negative bacteria and preform evolutionary experiments to determine the stability of *mcr-1* plasmids in the presence/absence of conjugation.

2 Investigating the Fitness Effects of Structural Variations in MCR-1

2.1 Abstract

Following the discovery of mobile colistin resistance, various *mcr-1* variant alleles have been identified, some of which demonstrate parallelism. The evolutionary cause of these variants and their phenotypic effects are largely unknown. I hypothesise that these variant SNPs are occurrences of compensatory adaptation to alleviate the fitness costs of *mcr-1* activity. In this chapter, I use a combination of individual fitness assessments and direct competition assays to study the effect of these variants on *E. coli* fitness and colistin resistance. Aside from a few weakly compensatory exceptions, we found that the majority of tested structural variants were deleterious. From this, I conclude that intragenic compensation is not widespread in *mcr-1* evolution.

2.2 Introduction

MCR-like genes have been identified in various geographical locations, animal/human hosts, *Enterobacteriaceae* species and genetic contexts (Sun *et al.*, 2018). As mentioned in the introductory chapter, *mcr-1* is plasmid localised and can therefore disseminate rapidly via HGT. However, *mcr-1* expression is associated with reduced growth rate, reduced competitive ability, and attenuated virulence (Yang *et al.*, 2017). These costs suggest that reducing colistin use would lower *mcr-1* prevalence (Basra *et al.*, 2018; Bell and MacLean, 2018).

Allelic variations of *mcr-1* containing single nucleotide polymorphisms (SNPs) have since been found. These SNPs are either synonymous or nonsynonymous, the former causing degenerate codon changes while the latter alters AA sequences of resultant MCR-1 proteins (Carretto *et al.*, 2018; Sun *et al.*, 2018). These mutations were identified in *Enterobacteriaceae* isolates

obtained from different geographical areas and hosts. As no in-depth studies have been done on these allelic variations, the evolutionary drivers behind these SNPs and their resultant effects are largely unknown. Annotated SNPs are overwhelmingly non-synonymous with some occurring at the same site or genetic region. This parallelism is suggestive of evolution to similar selection pressures and could mean that the SNPs are advantageous (Stern, 2013; Harrison *et al.*, 2015; Bailey, Guo and Bataillon, 2018). Additionally, non-synonymous SNPs may be signals of adaptive evolution if their frequency exceeds those of synonymous variations (i.e. $d_N/d_S>1$) (Bobay and Ochman, 2017). However, these SNPs could also be neutral or weakly deleterious as most non-synonymous mutations are non-advantageous due to their detrimental effects on gene function and fitness (Eyre-Walker and Keightley, 2007). Additionally, *mcr-1* was discovered relatively recently with phylogenetic analysis estimating its mobilisation into Enterobacteria genomes occurring in the mid 2000s (Wang *et al.*, 2018). As such, *mcr-1* may still be adapting to their Enterobacteriaceae hosts or undergoing purifying selection (Sheppard, Guttman and Fitzgerald, 2018).

It is known that compensatory mutations can alleviate fitness costs associated with resistance genes, therefore causing gene maintenance in the absence of antibiotic selection (Andersson and Hughes, 2010; San Millan and MacLean, 2017). What is unknown however is the likelihood of compensatory adaption over reversion to susceptible phenotypes (Levin, Perrot and Walker, 2000). A 2005 investigation found that compensatory mutations were more likely to be intergenic (92% of the time in prokaryotes) (Poon, Davis and Chao, 2005). A subsequent study found that compensatory mutations are non-randomly distributed in a gene and tended to appear in certain sites meaning it might be possible to predict when compensation was occurring by analysing resistance gene sequences (Davis, Poon and Whitlock, 2009). Using a combination of genetic and phenotypic assays, we could determine if identified SNPs are signals of compensatory adaptation.

The goal of this chapter is to test for compensatory evolution in *mcr-1*. Based on the parallel nature of some allelic variants and the high frequency of non-synonymous SNPs in named *mcr-1* alleles, I hypothesised that the structural variations are adaptive responses to the selective pressure imposed by *mcr-1* expression. I assessed these variants in comparison to the consensus *mcr-1* gene sequence and empty vector/inactivated *mcr-1* controls by cloning

them into identical genetic backgrounds, ensuring that any differences seen were solely due to variant SNPs. I then determined the fitness and resistance effects between variant isolates using a combination of individual fitness assessments and competition assays. Based on our results, it was found that although some resistance and fitness benefits were observed, variant SNPs were generally not compensatory.

2.3 Materials and methods

Bacterial Strains, Plasmids and Growth Conditions

Cloning experiments in this chapter involved the pBAD/HisA cloning vector (ThermoFisher Scientific). The vector was modified using PCR amplification and Gibson assembly to; remove the multiple cloning site, remove the hexa-HIS tag, introduce EcoRI and XhoI restriction sites and introduce Gibson overhangs. Primers used are listened in *appendix table 1*.

E. coli TOP10 was used for most experiments in this chapter. TOP10 *E. coli* containing consensus *mcr-1* cloned into pBAD/HisA was kindly supplied by Walsh lab (Oxford, Dunn School of Pathology) (Yang *et al.*, 2017). This vector was used to construct structural *mcr-1* gene variants (*appendix table 2*). TOP10 *E. coli* used were chemically (One Shot™ TOP10 *E. coli*, ThermoFisher Scientific) or electrically (TOP10 Electrocomp™, ThermoFisher Scientific) competent. Later experiments in this chapter used the common *E. coli* lab strain AB1155.

Bacteria were grown on Luria Broth (LB) broth (Sigma-aldrich), LB Millar agar (Sigma-aldrich) plates or Cation-adjusted Mueller Hinton Broth 2 (MH2, Sigma-aldrich). Media was un-supplemented or supplemented with the appropriate antibiotics, sugars and growth factors depending on assays preformed. Bacteria were grown at 37°C in shaking liquid culture (250 rpm) or in standing (LB Millar agar) incubation.

Variant Plasmid Construction

Eight allelic variants available prior to June 2018 were constructed. Plasmids containing consensus *mcr-1* or an *mcr-1* variant were constructed using Gibson assembly (GA) and site-directed mutagenesis. Variant SNPs were introduced into the consensus *mcr-1* sequence and the resulting inserts were assembled into identical pBAD vector backbones. SNP and amino

acid variations and localisations of each *mcr-1* variant created are listed in *table 2.1*. A random DNA sequence generator was used to design 15bp sequence tags for each plasmid (The Maduro Lab). Generated sequences were designed to have a GC content of around 50% and selected based on the following criteria:

- Does not contain a string of >4 identical bases
- Melting temperature (Tm) of 60-63°C
- No stable hairpins and dimers (Determined using OligoAnalyzer, (IDT))

Unique tags sequences for each variant are listed in *appendix table 1*. PCR amplification with Gibson primers (*appendix table 1*) were used to generate insert fragments with appropriate GA overhangs, sequence tags and SNPs. The desired cloning vector was generated using the primer pair pBADF and pBADR to amplify pBAD/HisA (*appendix table 1*). GA was carried out using the NEBuilder® HiFi DNA Assembly Master Mix (New England Biolabs). A schematic summarizing construction of the variant plasmids is given in *figure 2.1*. The inactivated *mcr-1* control (T285A) was created using the mutagenesis protocol described above and primers that targeted and replaced the *mcr-1* active site threonine codon (*appendix table 1 and 2*).

Transformation and Sequencing Verification

Plasmids constructed using GA were transformed into competent TOP10 *E. coli* (ThermoFisher Scientific). Bacteria were selected for colonies containing correctly assembled plasmids. The QIAprep Spin Miniprep Kit (QAIGEN) was used to isolate plasmids which were subsequently PCR and sequence verified. Colonies containing correct *mcr-1* consensus and variant plasmids were used for subsequent experiments.

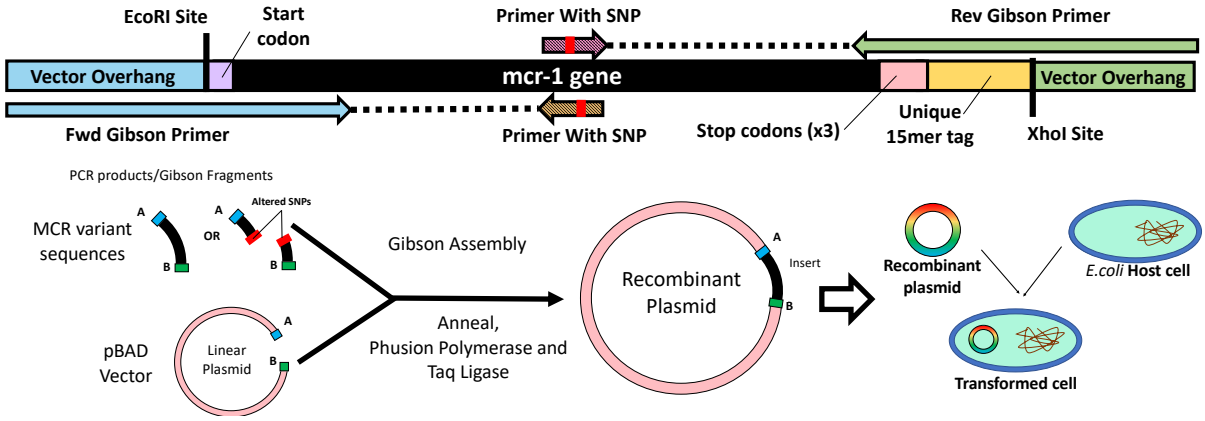


Figure 2.1 Variant Plasmid Construction: Gibson primers were designed to introduce vector-matching overhangs to regions flanking *mcr-1*. Tags to for variant identification were also introduced. pBAD was linearized by PCR for GA. Variant sequences were generated using *mcr-1* as a template and mutagenic primers to introduce variant SNPs. *mcr-1* variant fragments and linearized pBAD were assembled to create variant plasmids which were subsequently transformed to TOP10 *E. coli* hosts.

Minimum inhibitory Concentration (MIC) Determination

Colistin MICs of TOP10 *E. coli* control and variant stains were determined using broth microdilution and OD measurements. Bacteria were grown overnight (16 hours) in LB-ampicillin (50µg/ml, sigma-aldrich). Cultures were transferred to MH2+0.02% arabinose and grown for 3 hours at 37°C to induce MCR-1 expression. Bacteria were diluted to $5x10^5$CFU/ml in MH2 media (0.02% Arabinose) containing colistin (Cayman Chemical) of varying concentrations (0-8ug/ml). Bacteria were grown overnight at 37°C and OD measurements (595nm) were taken following incubation. Cultures were resuspended to ensure that OD measurements were not affected by aggregations. Bacterial growth was set to 0 if OD were less than 0.125 absorbance units. Dose response curve (DRC) models were fitted using the "drc" package (v2.5-12). All models obtained non-significant scores using lack-of-fit tests.

Growth Rate Measurements

Overnight bacterial cultures were diluted 1-in-10 into LB media in the presence/absence of 0.02% arabinose and incubated for 3hr. Resulting cultures were diluted $5x10^5$ into MH2 media containing colistin (0-4ug/ml). Bacteria were incubated overnight (16 hours) with OD measurements (595nm) taken every 10 minutes. DRC models were fitted using the "drc" package (v2.5-12). All models obtained non-significant scores using lack-of-fit tests.

qPCR Competitions

Variant qPCR primers were designed to match the unique sequence tags of variant plasmids and the empty pBAD vector control. Individual standard curves for every primer pair were generated using known plasmid concentrations. Overnight bacterial cultures were diluted 1-in-10 into MH2+0.02% arabinose. Bacteria were OD normalized and diluted to pooled bacterial mixes. Mixes were used to inoculate MH2 media of varying colistin concentrations (0-4ug/ml) and competitions were carried out over a 20hr incubation. Competition and initial bacteria mixes were boiled (100^{o}C for 20 minutes) and diluted for qPCR (Applied Biosystems, StepOnePlus Real-Time PCR System). Three technical repeats were preformed per competition and average CTs were used to determine plasmid concentrations. Relative fitness was calculated for each competition condition using the following equation.

$$Relative\ Fitness = {log_2\left(\frac{Vf}{Vi}\right)} \Big/ {log_2\left(\frac{Cf}{Ci}\right)}$$

Where Vf = variant plasmid concentration following competition, Vi = variant plasmid concentration of initial pools, Cf = consensus *mcr-1* plasmid concentration following competition and Ci = consensus *mcr-1* plasmid concentration of initial pools. Reconstitution experiments were conducted using known concentrations of variant bacteria as proof of concept experiments.

AB1155 Experiments

Control, consensus and variant plasmids were miniprepped (Qaigen QIAprep Spin Miniprep Kit) and transformed into chemically competent AB1155 *E. coli*. MIC assays were repeated for in the same way as previously described (see Methods: MIC Determination).

Structural Variant Sequence Analysis and Tree Building

mcr-1 variant gene sequences were downloaded from the NCBI MCR-1 phosphoethanolamine--lipid A transferase gene family reference gene catalogue. *mcr-1* alleles available as of December 2021 were included (32 structural variants, *Table 2.S1*). Gene sequences were translated and aligned (Geneious Prime software). MUSCLE v3.8.425 was

used for multiple alignment of gene and protein sequences (8 iterations, profile dependent parameters optimised). Alignments were used to construct phylogenetic trees using the Geneious Tree Builder algorithm. Genetic distance trees were built using the Neighbour-Joining method. *mcr-1.10* (Moraxella sp. MSG13-C03, GenBank: MF176238.1) or *mcr-POR* (Moraxella porci strain CIP110214 GenBank: MF432696.1, (Kieffer, Nordmann and Poirel, 2017)) were used as outgroups.

2.4 Results

2.4.1 MCR-1 Variant Construction

To assess the effects of the identified non-synonymous allelic *mcr-1* variations, I first reconstructed the sequences in pBAD (*Figure 2.1*). In addition to the consensus sequence, eight variants were constructed which at the time, represented all reported non-synonymous variants in *mcr-1*. Subsequently identified structural variants were not constructed. Variant I.D.s, localisation and sequence changes of variants are listed in *table 2.1*. Annotation differences between databases meant certain variants IDs do not match NDARO/NCBI annotations (naming discrepancies listed in *table 2.1*). Structural variants created will be referred using given variant IDs (*table 2.1*). Consensus/variant sequences were cloned downstream of the AraBAD inducible promoter enabling induced *mcr-1* expression in TOP10 *E. coli* following the addition of arabinose (Yang *et al.*, 2017). This ensured that differences seen were solely due to non-synonymous SNPs. Additionally, an inactivated version of *mcr-1* was made by replacing the crucial active site amino acid threonine with alanine (T285A). This was done to eliminate the crucial phosphorylation step required for the phosphotransferase activity of MCR-1 (Stojanoski *et al.*, 2016). Constructed plasmids were subsequently used for resistance and fitness assessments.

Variant ID	SNP location	Base change	AA number and domain localisation	AA Change	NDARO ID
mcr-1.3	Base 48	T to G	16 (1st transmembrane domain)	F to L	*mcr-1.3*
mcr-1.4	Base 1318	G to A	440 (Last periplasmic domain/ catalytic domain)	D to N	*mcr-1.4*
mcr-1.5	Base 1354	C to T	452 (Last periplasmic domain/ catalytic domain)	H to Y	*mcr-1.5*
mcr-1.7	Base 643	G to A	215 (Last periplasmic domain/ catalytic domain)	A to T	*mcr-1.7*
mcr-1.8	Base 8	A to T	3 (1st cytoplasmic domain)	Q to R	*mcr-1.8*
mcr-1.9	Base 1,238	T to C	413 (Last periplasmic domain/ catalytic domain)	A to T	*mcr-1.9*
mcr-k1.2	Base 8	A to G	3 (1st cytoplasmic domain)	Q to L	*mcr-1.2*
mcr-k1.9	Base 111+112	AA to GG	38 (1st periplasmic domain)	I to V	*mcr-1.14*
	Base 591	G to A	197 (Last periplasmic domain/ catalytic domain)	M to I	

Table 2.1: *mcr-1* Variant SNP Locations are listed. All variants were found in *E. coli* with the exceptions being *mcr-k1.2* and *mcr-k1.9* (found in *K. pneumoniae*). Notation discrepancies in the NDARO database and this study are noted in the last column.

2.4.2 Individual Resistant and Fitness Assessments of *mcr-1* Variants

MIC assays and Dose-Response Curves

Resistance and fitness effects of the *mcr-1* variants were determined in colistin-free and colistin supplemented medium. Endpoint OD595 measurements following overnight incubation (16 hours) were used to quantify variant growth (*Figure 2.2*) with isolates containing empty pBAD vector or inactivated (T285A) *mcr-1* as controls. A clear fitness cost of *mcr-1* expression, demonstrated by a marked reduction in the optical density (OD) in colistin-free medium, was identified for the consensus *mcr-1* sequence and in most the structural variants tested. *mcr-k1.2* was a clear exception to this as its optical densities mirrored that of the empty vector and inactivated controls (*Figure 2.2a*). Additionally, *mcr-1.8* had a significantly higher OD in colistin-free medium compared to the consensus sequence.

Endpoint OD measurements also allowed crude estimations of variant resistance differences. MICs of *mcr-1* variants and controls were obtained by growing arabinose induced cells in colistin-supplemented media (0.125 - 4 mg/l). Resistance functionally of MCR-1 was successfully removed by the T285A mutation as isolates gave similar MICs to empty vector

controls (*Figure 2.2b*). More stringent dilution scales were used (1 – 4 mg/l, steps of 0.2) in attempt to tease apart minor resistance differences between the structural variants. Aside from *mcr-k1.2*, MICs results showed little difference between the majority of structural variants and consensus *mcr-1* (*Figure 2.2b*). Only variant *mcr-1.8* gave consistently higher MICs while *mcr-k1.2* showed significant reductions in average colistin MIC from 2.85mg/ml to 1mg/ml (*Figure 2.2b*). Full MIC assay dynamics are given in *Figure 2.2c*.

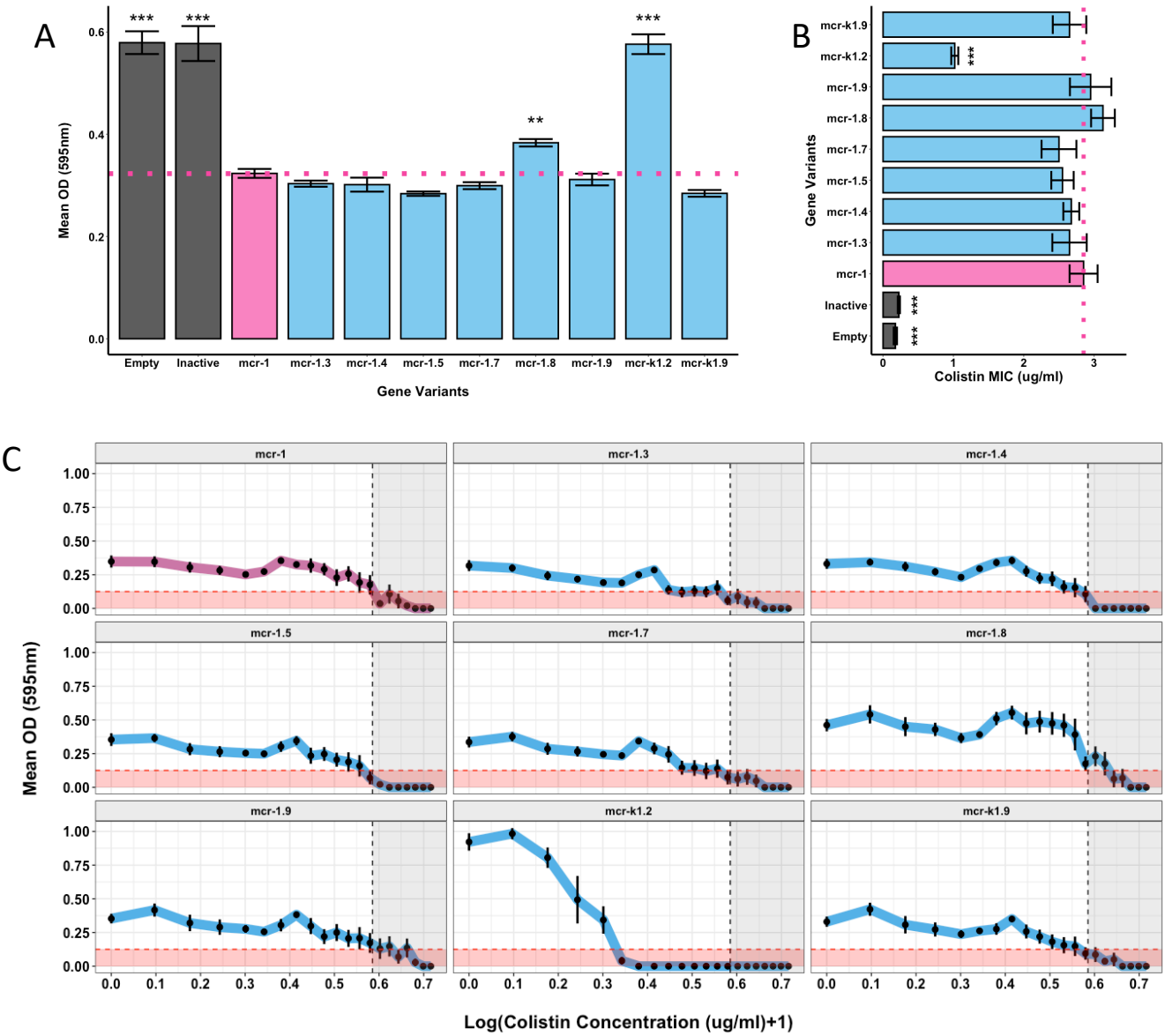


Figure 2.2: OD results from the MIC assays. (**A**) Mean OD in colistin-fee media for controls (empty vector and inactivated *mcr-1*, black), consensus *mcr-1* (pink) and structural *mcr-1* variants (blue). (Dotted pink line = consensus mean, n = 15, n=5 for inactive *mcr-1* control, error bars = standard error (SE), test = Dunnett's t-test adjusted for multiple comparisons using *mcr-1* consensus as the control group, p-values: ***<0.001). (**B**) MICs of variant(blue)/consensus(pink) *mcr-1* MICs and controls (black). (Dotted pink line = consensus

MIC, n=5-8, error bars = standard error (SE), test = Dunnett's t-test adjusted for multiple comparisons using *mcr-1* consensus as the control group, p-values: ***<0.001) (**C**) Mean ODs from MIC assays for variant (blue)/consensus (pink) *mcr-1* in stringent colistin ranges (0-4.2ug/ml, Log10 Scale). Red shading indicates OD ≤ 0.125, grey shading indicates colistin concentration ≥ consensus *mcr-1* average colistin MIC (n=8, error bar= SE).

Variant	Dose-Response Model Estimates and Comparisons						
	Predicted MIC (ug/ml)	**IC50 (e)** (ug/ml)	**p-value**	**Sig.**	**Uninhibited growth (d)** (OD595)	**p-value**	**Sig.**
mcr-1	**3.0**	**2.74**	NA	NA	**0.310**	NA	NA
mcr-1.3	2.8	**2.25**	0.00056	***	**0.258**	0.04127	*
mcr-1.4	2.8	**2.46**	0.17464		**0.306**	1.00000	
mcr-1.5	2.6	**2.49**	0.41971		**0.294**	1.00000	
mcr-1.7	2.4	**2.25**	0.00122	**	**0.305**	1.00000	
mcr-1.8	3.2	**2.91**	0.46058		**0.471**	< 0.00001	***
mcr-1.9	3	**2.81**	0.64402		**0.323**	1.00000	
mcr-k1.2	1.2	**0.79**	< 0.00001	***	**0.935**	< 0.00001	***
mcr-k1.9	2.6	**2.44**	0.10973		**0.306**	1.00000	

Table 2.2: Predicted MICs, e and d coefficients for *mcr-1* variants. Variant values lower than consensus *mcr-1* values are highlighted in red and higher values are in blue. P-value and significance show results of pairwise comparisons of each variant to consensus *mcr-1* (p-values adjusted using the Bonferroni correction for multiple comparisons).

To further probe into the fitness and resistance differences between the variant sequences, dose-response curves (DRCs) were fitted to consensus/variant bacteria ODs obtained using more stringent colistin concentrations Pairwise plots allowed one-to-one comparisons of variant and consensus DRC models (*Figure 2.3*). DRC models generated coefficients that quantify the fitness and resistances of variants with standard error values which allows comparison of variant strains with consensus *mcr-1* (*Table 2.2*). IC50s (i.e. half-maximal inhibitory colistin concentration, e-coefficient) were lower than the consensus for most tested variants with *mcr-1.3* and *mcr-k1.2* obtaining significance. Those with higher IC50s (*mcr-1.8* and *mcr-1.9*) did not differ significantly from the consensus control, indicating that most variants had similar colistin resistance levels to the consensus. The estimated OD at uninhibited growth (d-coefficient) was significantly increased for *mcr-1.8* and *mcr-k1.2* variants. All other variants showed decreases which was significant only for *mcr-1.3*.

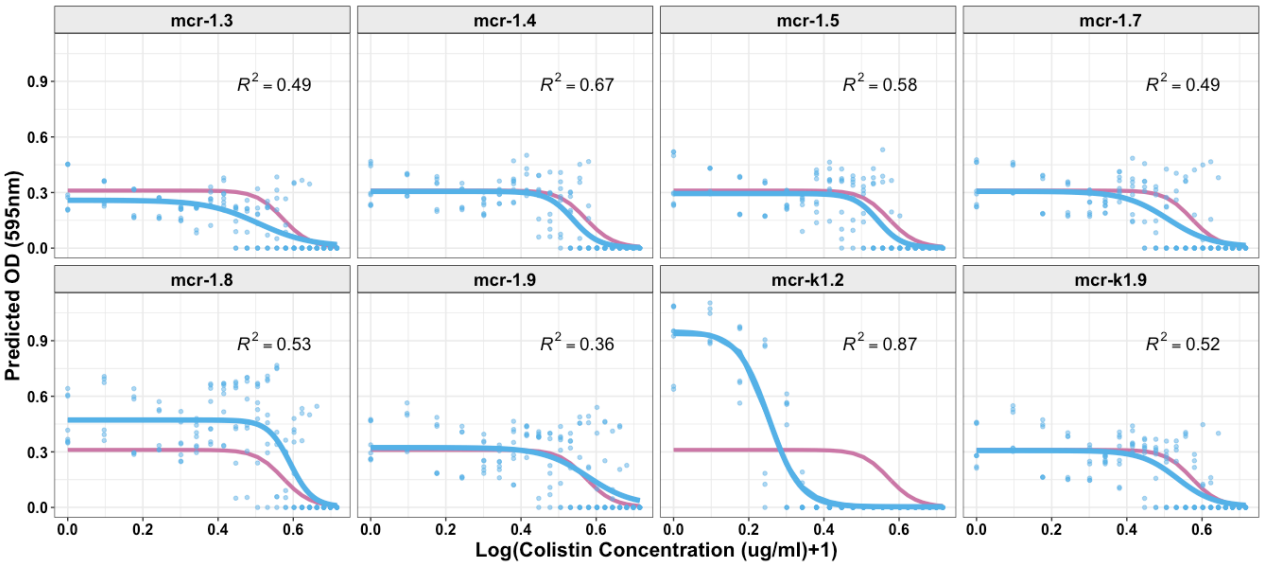


Figure 2.3: Pairwise dose-response curves comparing consensus (pink) to variant (blue) *mcr-1* in stringent colistin ranges (0-4ug/ml, Log10 Scale). Lines show DRM predictions, points show actual values. R-squared values for variant models are annotated. Consensus R-squared = 0.53.

MIC assays were repeated for variants and controls using AB1155 *E. coli*, a wild-type strain which has not been engineered for cloning/protein expression. DRCs were also fitted to the data to compare variant and consensus fitness (*Figure 2.S1*). Results largely reiterate those found using TOP10 *E. coli* with *mcr-k1.2* giving higher fitness but lowered resistance while most other variants showed similar/lower finesses and resistances. Interestingly, *mcr-1.8* showed a marginal but significant increase in resistance (*Figure 2.S1*).

Growth Curve Assays and DRC Assessments

Endpoint OD measurements suggests that most variants are not compensatory, but this fitness assessment is very coarse. For example, it is possible that *mcr-1* variants compensate for the cost of MCR-1 expression by increasing growth rate. To test this possibility, bacteria were grown in a range of colistin concentrations (0-4 mg/l) with OD measurements taken every 10 minutes over the course of 16 hours to generate growth curves (*Figure 2.4a*). Experiments were repeated with and without 0.02% arabinose to assess the effect of variant *mcr-1* gene expression. Maximum gradients obtained from growth curves (over 10 measurements) was used to estimate exponential growth rates (mOD/min) in all growth conditions (*Figure 2.S2*). Control measurements demonstrated the cost of *mcr-1* expression

on growth rate as consensus *mcr-1* showed significantly lower rates when compared to inactivated and empty vector plasmids (*Figure 2.4b*).

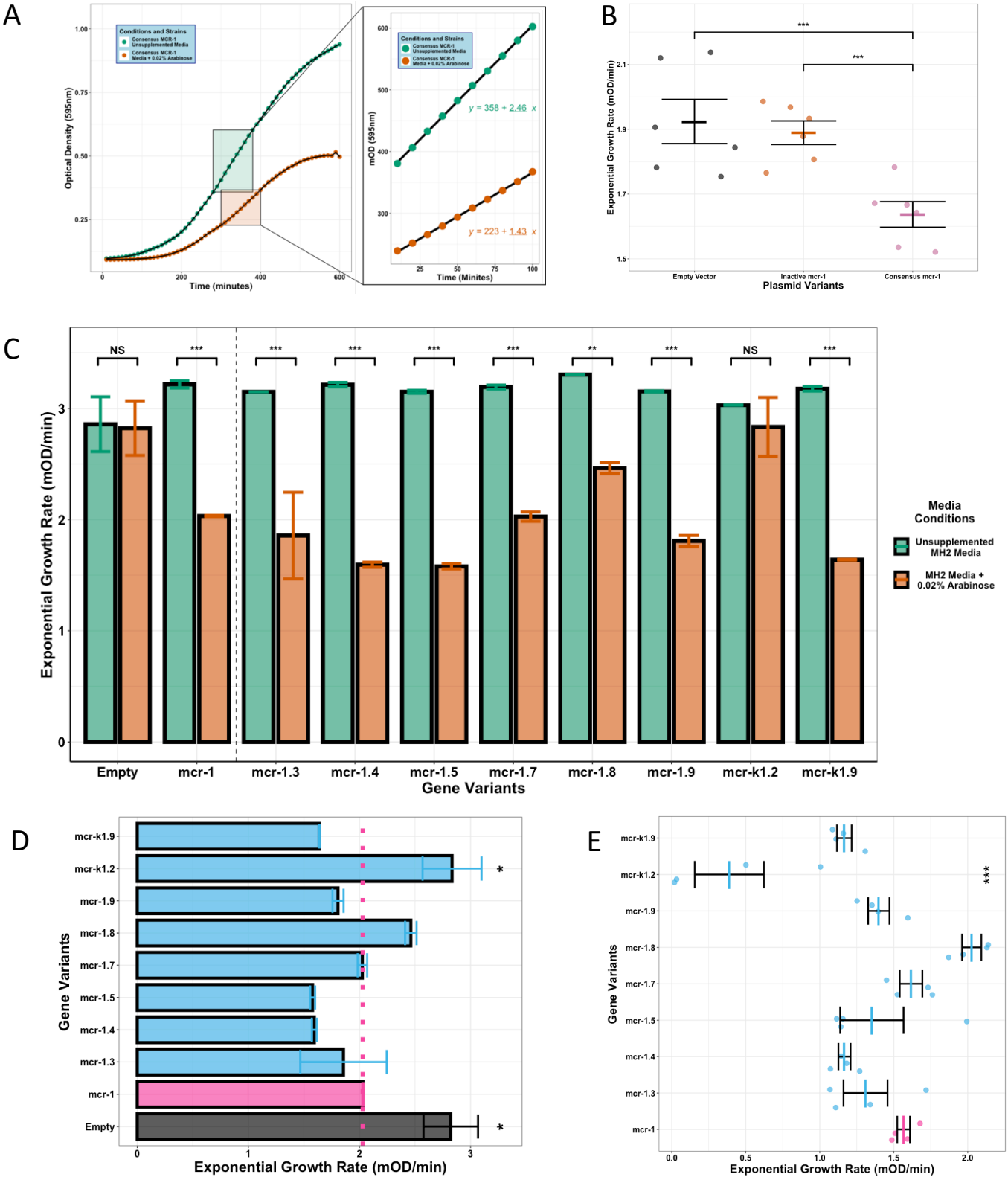


Figure 2.4: Growth rate assays for structural variants. (**A**) Example growth curves and exponential growth rate calculation. Bacteria are grown ON with OD measurements taken every 10 minutes. Points giving the

maximum gradient (10 points) are selected. Regression lines are fitted through points (note the mOD conversion) and gradients (underlined) give the exponential growth rates. Calculations are repeated for every condition allowing comparisons between strains/conditions. (**B**) Growth rates (mOD/min) for empty (black), inactive (orange) and consensus (pink) *mcr-1* plasmids in colistin-free media with 0.02% arabinose (Tukey's range test, adjusted for multiple comparisons, **<0.01, n = 6, error-bar=SE). (**C**) Exponential growth rate (mOD/min) in colistin-free medium shown for structural variants and controls in the absence (green) and presence (orange) of 0.02% arabinose. Pairwise comparisons of MH2 vs MH2+Ara growth rates for each variant/control is shown in black (Tukey's range test, adjusted for multiple comparisons, p-values: ***<0.001, **<0.01, ns=no significance, n-2, error-bar=SE). (**D**) Exponential growth rate (mOD/min) in colistin-free arabinose supplemented medium is shown for variants (blue) consensus *mcr-1* (pink) and empty vector control (black). Growth rate comparisons of variants with consensus *mcr-1* is shown in black (Tukey's range test, adjusted for multiple comparisons, p-values: *<0.05, n-2, error-bar=SE). (**E**) Exponential growth rate (abs/min) in 1mg/ml colistin is shown for consensus (pink) and variants (blue) *mcr-1*. Dotted black line shows average exponential growth rate of consensus *mcr-1*). (Dunnett's T- adjusted for multiple comparisons, ***<0.001, n=4, error-bar=SE)

Growth rates obtained in colistin-free medium indicate how variants/controls grow in the absence of selective pressures (*Figure 2.4c, 4d*). Pairwise comparisons between growth rates obtained from arabinose supplemented/un-supplemented media were used to determine if growth costs were seen upon expression of *mcr-1* variants (*Figure 2.4c*). Bar *mcr-k1.2,* all variants show significantly reduced growth rates in arabinose supplemented media showing that expression of all high-resistant variants was associated with fitness costs. Interestingly, the differences between arabinose supplemented/un-supplemented growth rates obtained for *mcr-1.8* were lower than that of the other affected *mcr-1* variants. To identify differences in variant growth, rates obtained in arabinose supplemented media were compared (*Figure 2.4d*). *mcr-k1.2* showed a significant increase in exponential growth rate when compared to the consensus which supports previous end-point OD measurements.

To asses variant growth in the presence of selective pressures, growth rates were obtained in arabinose (0.02%) and colistin (1mg/ml) supplemented media. Results show that most variants had reduced exponential growth rates at this concentration in comparison to the consensus *mcr-1* with *mcr-k1.2* giving a large significant reduction (p=<0.001). *mcr-1.8* and *mcr-1.7* showed higher mean growth rates at this concentration although significance was not obtained for either variant (*Figure 2.4e*).

Variant	Dose-Response Model Estimates and Comparisons					
	IC50 (e) (ug/ml)	**p-value**	**Sig.**	**Uninhibited growth rate (d)** (abs/min)	**p-value**	**Sig.**
mcr-1	**0.798**	NA	NA	**1.93**	NA	NA
Empty Vector	**0.099**	0.00042	***	**2.58**	< 0.00001	***
mcr-1.3	**0.775**	1.00000		**1.69**	0.00717	**
mcr-1.4	**0.804**	1.00000		**1.54**	< 0.00001	***
mcr-1.5	**0.945**	1.00000		**1.65**	0.02935	*
mcr-1.7	**0.899**	0.90155		**1.80**	0.09926	.
mcr-1.8	**0.952**	0.90155		**2.17**	0.00717	**
mcr-1.9	**0.809**	1.00000		**1.93**	0.96752	
mcr-1.2k	**0.521**	0.00410	**	**2.40**	0.00007	***
mcr-1.9k	**0.673**	1.00000		**1.74**	0.00186	**

Table 2.3: IC50 (e coefficient) and uninhibited exponential growth rate (d coefficient from DRC model) for all *mcr-1* variants growth data. Variant values lower than those obtained for consensus *mcr-1* are highlighted in red and higher values are shown in blue. Values were all compared to the consensus gene via Dunnett's t-test and adjusted for multiple comparisons. P values and significance levels are shown. Empty vector control parameters are also shown

DRC models were fitted in order to obtain model parameters for further in-depth comparisons (*Table 2.3, Figure 2.5*). Although IC50 values vary from MIC assays, the significantly reduced resistance of *mcr-k1.2* is maintained. Other variants show non-significant differences in IC50 values compared to the consensus suggesting that they maintain similar level of resistance. Similarly to MIC results, variants *mcr-1.8* and *mcr-k1.2*. showed a significantly increased d-coefficient (here predicting uninhibited exponential growth rate) when compared to consensus *mcr-1*. Uninhibited exponential growth rates of most other variants were significantly lower than that of *mcr-1* suggesting that they are deleterious.

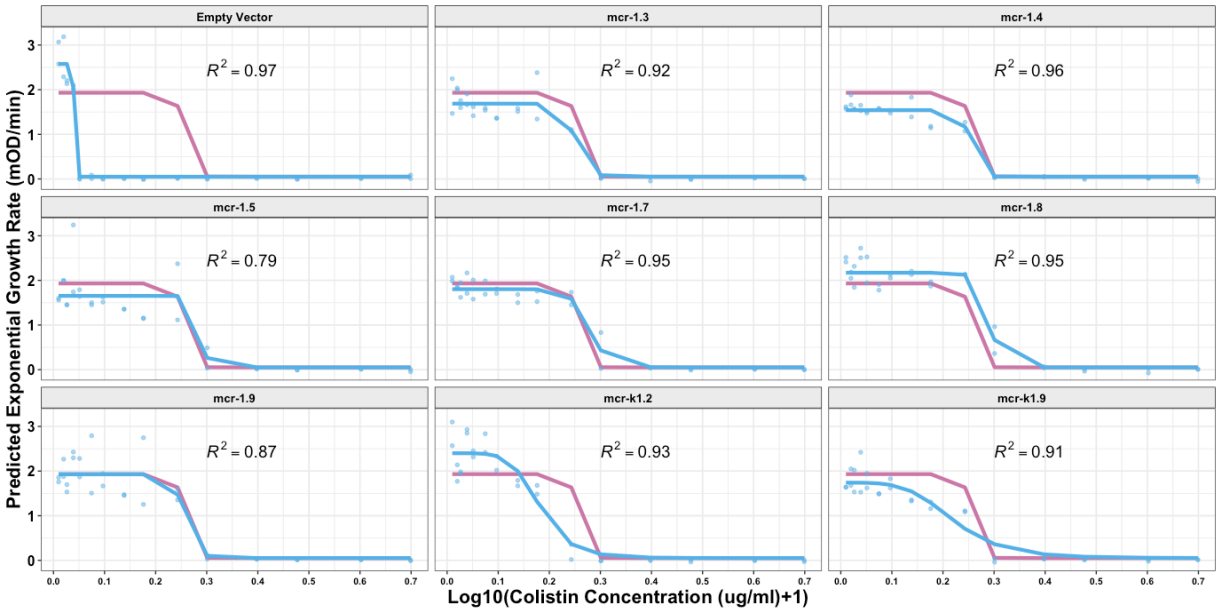


Figure 2.5: Pairwise dose-response curves comparing exponential growth rates consensus *mcr-1* (pink) to *mcr-1* variants (blue) in a range of colistin concentrations (0-4ug/ml, Log10 Scale). R-squared of fits are annotated. Consensus R-squared = 0.96 Curves fitted using the "drc" package in R.

2.4.3 Fitness Competitions of MCR Variants

Culture-based data suggests that most variants do not increase *mcr-1* fitness (*Figure 2.2*, *Figure 2.4*). However, these assays were all done individually and fitness results may differ when variants are in direct competition. To directly assess variant fitness and competitive ability, co-culture competition assays were performed. Consensus and variant bacteria were induced with arabinose (0.02%), pooled in equimolar proportions (OD normalised) and inoculated into colistin supplemented (0.25 - 4mg/l) and in colistin-free media. Unique 15mer tags on the consensus and variant *mcr-1* plasmids were used for plasmid specific qPCR. This allowed quantification of empty vector, consensus and variant plasmid concentrations in initial and competition mixes.

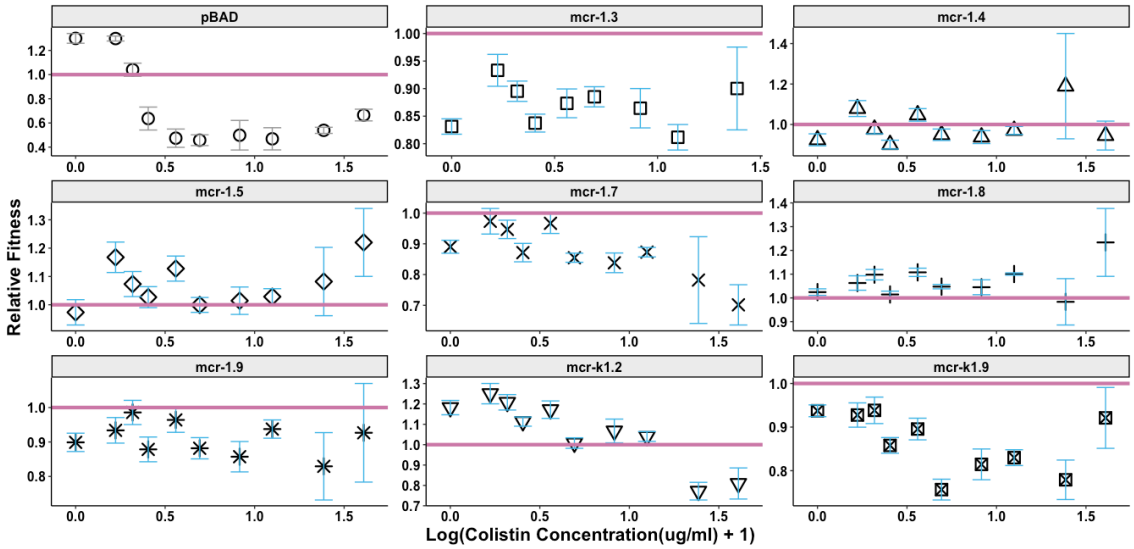


Figure 2.6: Results from qPCR competitions. Mean relative bacterial fitness of all variants is plotted in a range of colistin concentrations (0-4ug/ml, Log10 Scale) as compared to the consensus *mcr-1* (set to 1, pink line). Error bars=SE, n=4.

The relative fitness of each variant plasmid compared to the consensus *mcr-1* (set at 1) was determined by calculating the fold change for each plasmid at all tested colistin concentrations (*Figure 2.6*). CT values were converted to plasmid concentrations using variant primer specific standard curves (*Figure 2.S3*). To assess the effects of colistin concentrations on variant competitive ability, two-way ANOVA tests were run on relative fitness data. Results revealed that there were significant effects of variant ($p = < 2e\text{-}16$) and colistin concentration ($p = 0.00153$) on mean relative fitness. Additionally, significant interaction was identified between the variant and colistin concentration variables ($p = 2.176e\text{-}12$) meaning that the relationship between relative fitness and colistin concentration differs significantly depending on the *mcr-1* variant tested.

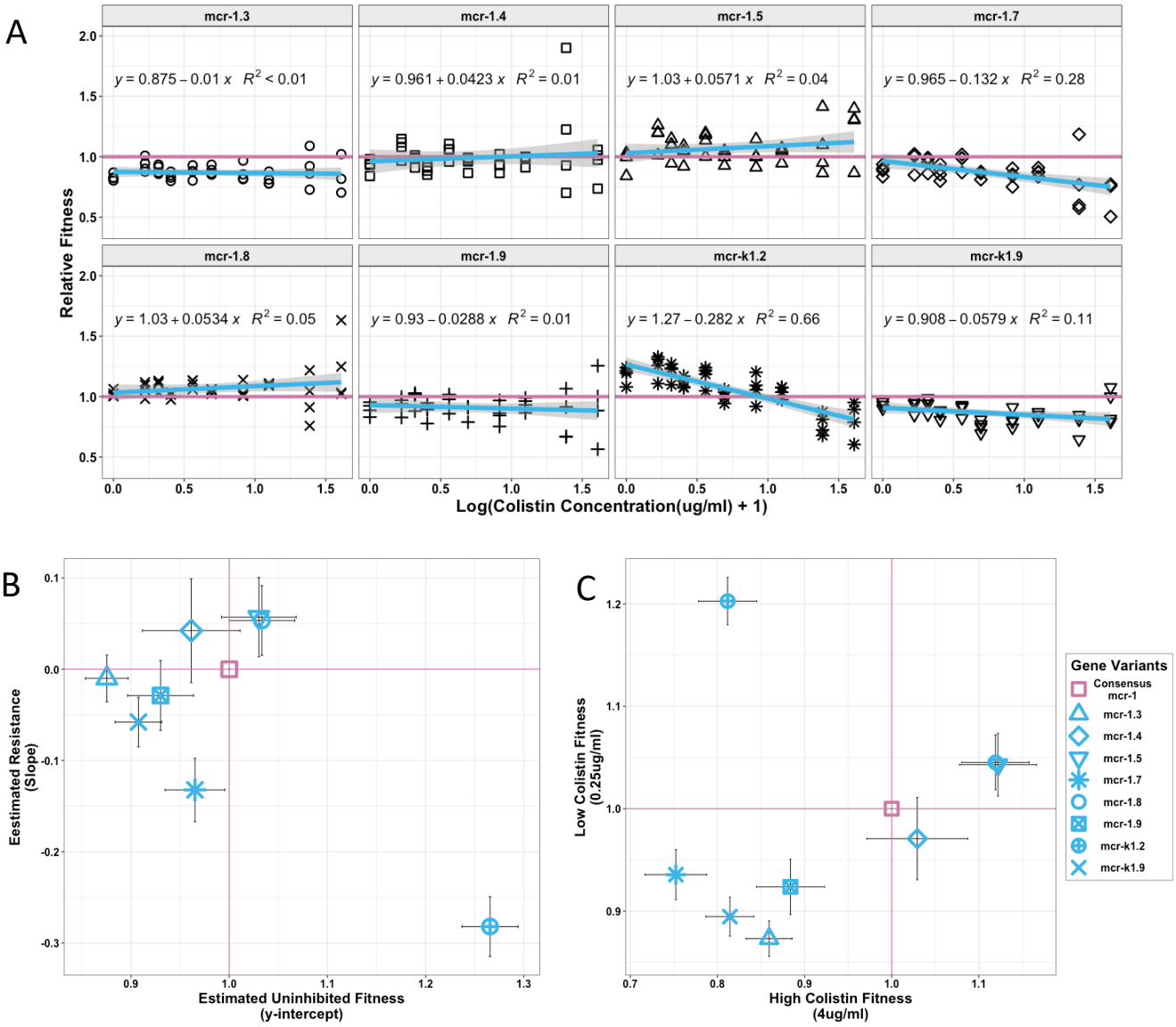


Figure 2.7: Linear models and estimations of relative competitive fitness. (**A**) Regression lines (blue) were fitted relative fitness data obtained for each variant plasmid in a range of colistin concentrations (0-4ug/ml, Log10 Scale). Points represent individual fitness competitions. Consensus *mcr-1* fitness was set to 1 (pink line). Equations of regression lines and r-squared values for models are shown. (n=4 biological replicates, line shading = SE) (**B**) Estimated uninhibited fitness (obtained from liner model y-intercepts) and estimated effect of colistin concentration (slope) are shown for each variant (blue). Consensus values (pink) were set to 1 and 0 respectively. (Error bars = SE) (**C**) Estimated fitness from the lowest (0.2ug/ml) and highest (4ug/ml) colistin concentration tested are shown for each variant (blue). Consensus values (pink) were set to 1. (Error bars = SE)

To pinpoint where significant changes in fitness were occurring and allow comparisons to consensus *mcr-1*, linear regressions were fitted to competition data (*Figure 2.7a*). Gradients gauge variant fitness in response to increasing colistin concentration while y-intercepts give

estimations of variant fitness in colistin-free media. Model coefficients were graphed to identify fitness patterns (*Figure 2.7b*). *mcr-k1.2* showed a significantly higher fitness (y-intercept = 1.27) at low concentrations of colistin which substantially drops as colistin concentration increases (negative gradient) due to its reduced resistance. *mcr-1.8* maintains small (y-intercept = 1.03) but consistent increase in fitness in comparison to the consensus which slightly increases in mid to high concentrations of colistin (positive gradient). Interestingly, *mcr-1.5* also shows a slight fitness increase at lower colistin concentrations (y-intercept = 1.03) which was not seen in cruder OD based assays. Remaining variants maintained similar (*mcr-1.4*) or lower fitness levels (*mcr-1.3*, *mcr-1.7*, *mcr-1.9* and *mcr-k1.9*) compared to consensus *mcr-1* across all tested colistin concentrations. In general, most variants had deleterious fitness and resistance effects when compared to consensus *mcr-1* (*Figure 2.7*).

2.4.4 Structural Variant Sequence Analysis

To obtain an updated picture of functional *mcr-1* variation, sequence analysis of all *mcr-1* variants annotated in the National Database of Antibiotic Resistant Organisms as of December 2021 were performed (NDARO). 32 non-synonymous *mcr-1* structural variant sequences were included, a majority of which were isolated from Escherichia coli (22/32) with some variants isolated from Salmonella, Klebsiella and Moraxella sp. Multiple sequence alignments (MSAs) were performed for *mcr-1* gene and protein sequences. A majority of variants differed from the consensus by a singular SNP (22/32, *Table 2.S1*) with only *mcr-1.10* (*Moraxella* sp.), *mcr-1.23* (*Salmonella* sp.) and *mcr-1.24* (*Escherichia coli*) showing >5 genetic differences. Interestingly, no SNPs were located in codons with known involvement in the MCR-1 active site or the catalytic domain cystine residues (Ma *et al.*, 2016; Stojanoski *et al.*, 2016). Additionally, SNPs and AA variances were overrepresented at the initial regions of the gene/protein (*Figure 2.8*). Unlike other areas where SNP/AA variations were due to a singular variant, N-terminal variation was seen in for 12/32 structural variants (*Figure 2.S4*) with some SNPs leading to the elimination of the initial start codon (*mcr-1.15* and *mcr-1.26*)

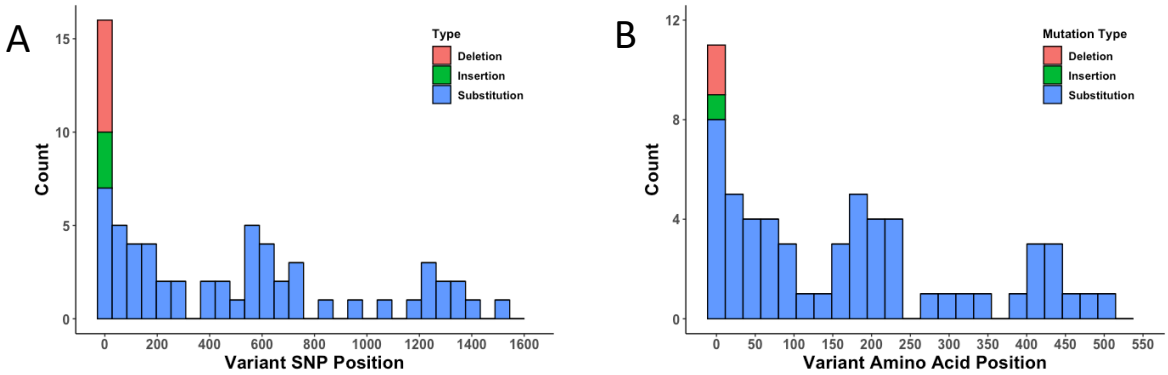


Figure 2.8: Histograms showing locations of all structural variant (**A**) bases and (**B**) amino acids across *mcr-1* gene and protein sequence respectively. Keys indicate the type of mutation (deletion, insertion or substitution). Variants were binned into 30 or 25 bins corresponding to 54bp or 21AA segments for histograms A and B respectively.

To understand the evolutionary organisation of the structural variants, neighbour joining trees were constructed from gene and protein MSAs. Alignments including an *mcr-1* like gene isolated from *M. porci* (*mcr-POR*) were also made as Moraxella is the proposed source of *E. coli mcr-1*. Structural variant *mcr-1.10* (Moraxella sp.) was used to root the original alignments due to its divergent genetic sequence (*Figure 2.S5*). Branch lengths of resultant trees were very short which reflected the low percentage variation between variant *mcr-1* genes. Some variants grouped together due to the presence of SNPs in the same position or in some cases, identical SNPs. Meta-data including isolation source, collection dates and country of origin was available for some of the variant sequence but there were no groupings based on these variables.

2.5 Discussion

Multiple epidemiological studies into colistin resistance have identified established genetic variations of the consensus *mcr-1* gene (Sun *et al.*, 2018). Based on fitness costs associated with *mcr-1* expression and the parallelism of some SNPs, I hypothesised that these that structural variants reflect ongoing compensatory adaptation. Evidence of compensation has been identified in the genetic homologue *mcr-3* which showed improved growth when compared to *mcr-1* while maintaining the same level of colistin resistance (Yang *et al.*, 2020). Moreover, a structural variant of *mcr-3* dubbed *mcr-3.5* demonstrated elevated fitness levels and differed by three substitutions which is suggestive of a recent mutation. In this chapter,

I analysed eight non-synonymous variants in-depth to identify fitness and resistance differences to the consensus *mcr-1* gene using individual variant analyses and direct competition with the consensus. Although these studies allowed us to pinpoint the effect of each individual variant analysed, I did not identify general trends arising as a result of non-synonymous allelic variants. Some of the variants appear to be compensatory and one variant showed a strong trade-off effect between resistance and fitness. However, these represent the exception rather than the rule. The majority of variants studied showed deleterious effects when compared to the consensus *mcr-1* gene (*Figure 2.6*).

Based on the low r-squared values, it is clear that linear regression models fitted do not explain a majority of the variance in fitness data. However, using these models to leverage fitness data obtained from all tested colistin concentrations increases confidence in our estimates of uninhibited fitness (y-intercept) and overall response to increasing colistin concentration (slope). Y-Intercept values for *mcr-1.3*, *mcr-1.9*, *mcr-k1.2* and *mcr-k1.9* were significantly different from 1 (*Figure 2.7b*). Meaning that with exception of *mcr-k1.2*, variants showed no significant difference or were significantly less fit than consensus *mcr-1* in the absence of selective pressures. Minor fitness increases were seen for *mcr-1.5* and *mcr-1.8* in colistin-free media and in low colistin concentrations with significance obtained in the later condition (*Figure 2.7c*). Although this result is consistent with *mcr-1.8* individual data, *mcr-1.5* growth rate results suggest that the variant is deleterious in colistin-free media (*Table 2.3*). This differential response in individual vs competitive conditions is surprising and may point to *mcr-1.5* somehow benefiting in the presence of other variants. Potential mechanisms explaining this phenomenon or benefits *mcr-1.5* containing *E. coli* may be receiving are unclear.

Linear regression slopes obtained for *mcr-1.7*, *mcr-k1.2* and *mcr-k1.9* were significantly different from 0, all three of which gave negative values (*Figure 2.7b*). This suggests that variant responses to increasing colistin concentration either largely mimic consensus patterns or show slight to strong reductions in resistance. Of the variants that gave positive relative fitness slopes in models, *mcr-1.5* and *mcr-1.8* significantly outperform the consensus gene at the highest colistin concentration (*Figure 2.7c*) and therefore, may demonstrate a marginally

increased colistin resistance. However, it is unknown if such small changes are competitively relevant in natural environments.

mcr-k1.2 regularly demonstrated increased fitness at low colistin concentrations, often comparable to the empty pBAD control. This, taken together with its reduced resistance, suggests a trade-off where resistance is sacrificed for increased fitness. As the SNP was located at the gene N-terminal and did not coincide with known enzymatic/active-site codons, it is mechanistically unclear how the SNP leads to this change. Previous studies reported on adverse effects of *mcr-1* expression on *E. coli* growth rates and membrane integrity (Wang, Zhang, *et al.*, 2017; Yang *et al.*, 2017). It is possible that in environments with low to no colistin prevalence, selective pressures drive *mcr-1* positive bacteria to evolve reduced resistance in favour of increased bacterial viability. A 2018 study looking at the worldwide dissemination of *mcr-1* included a database of 457 *mcr-1* positive sequences (Wang *et al.*, 2018). When this database was searched for 100% identity to the *mcr-k1.2* variant, it was found in two sequences originating from the Netherlands and Italy. Although these countries (particularly Italy) have used colistin in agricultural settings, usage levels are significantly lower than in southeast Asian countries and prior usages in Brazil and China (Wertheim *et al.*, 2013; 'ECDC/EFSA/EMA first joint report on the integrated analysis of the consumption of antimicrobial agents and occurrence of antimicrobial resistance in bacteria from humans and food-producing animals', 2015). Low to no colistin prevalence could create environments where *mcr-k1.2* variants are more likely to thrive.

As *mcr-1* provides colistin resistance but comes at large costs, I expected fitness at low and high colistin concentrations to be negatively correlated but this is not the case for the majority of variants tested (*Figure 2.7c*). Competition outcomes largely suggest that most variants are deleterious and it is therefore unlikely that they would become dominant in the presence or absence of colistin. It is unclear why these variants are found in nature as they would likely be outcompeted by fitter alternatives in all tested colistin concentrations. There are multiple explanations for this phenomenon. Deleterious variants could have arisen recently and would be outcompeted with time by purifying selection (Bosshard *et al.*, 2019). This could be the case for *mcr-1.3* which despite being one of the first variants identified, has the fewest BLAST hits (Altschul *et al.*, 1990). Additionally, consensus *mcr-1* remains overwhelmingly

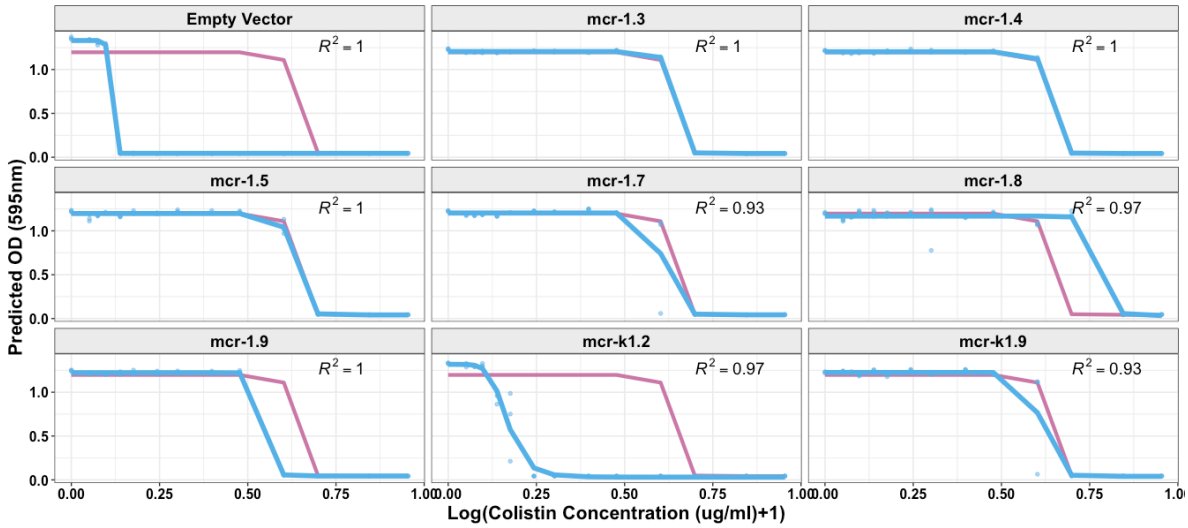
predominant in surveillance data (Mendes Oliveira, Paiva and Lima, 2019; Shen *et al.*, 2019, 2020). Interestingly, *mcr-k1.2* and *mcr-k1.9* variants were found in a recent study but in incredibly low proportions (n=5 and n=1 out of 688 respectively) (Shen *et al.*, 2020). Deleterious variants could also occupy a specific niche and therefore face no competition (Price and Arkin, 2015). Genetic background differed between variants and perhaps extragenetic factors or genetic linkage contribute to overall bacterial fitness and therefore facilitates their propagation (Vogwill and Maclean, 2015; Bell and MacLean, 2018).

In the extended variant sequence analysis, alignments showed that structural polymorphisms often occur in the initial part of MCR-1. Additionally, the more drastic changes in MCR-1 resistance and fitness was seen in variants that containing polymorphisms in N-terminal *mcr-1* regions (*mcr-1.8* and *mcr-k1.2*). I hypothesised that this region formed the signal peptide of MCR-1, an N-terminal region important for protein targeting and translocation (Freudl, 2018). This region is the first to be translated and interacts with transport proteins such as those involved in the twin-arginine protein translocation (Tat) and Sec pathways (Liu *et al.*, 2017). This enables delivery of resultant proteins to correct cellular locations. Despite its inner cell membrane localisation, involvement of MCR-1 in known protein transport has not been previously studied. Attempts to tag MCR-1 with HALO and YPET protein tags were made in order to test if structural variants led to changes in the resultant protein localisation. However, tagged proteins were unable to pass functional testing suggesting that aspects of tagged protein structure and function might be compromised (results not shown).

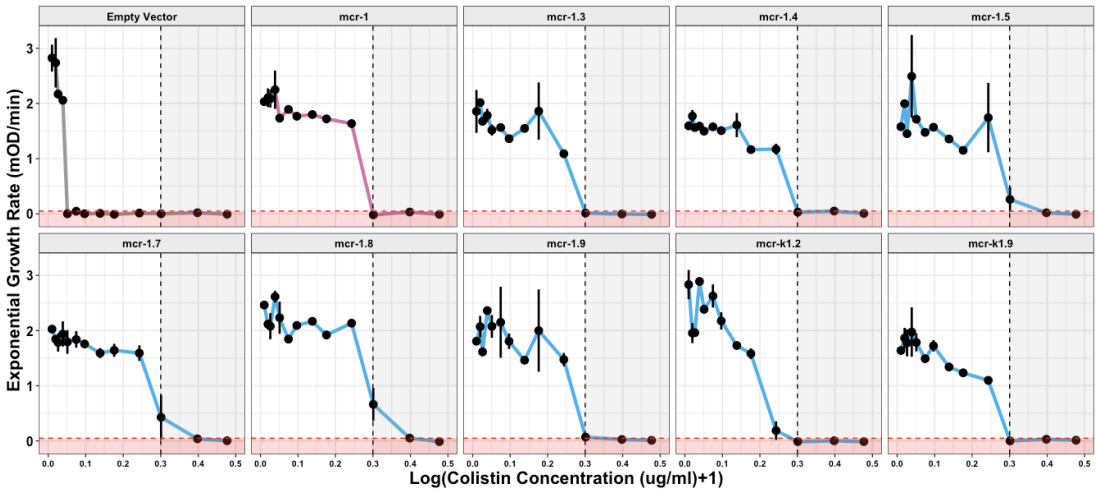
In conclusion, some variants compensate for the cost of colistin resistance, but the majority of structural variants are neutral or weakly deleterious (50% of variants tested). The *mcr-k1.2* variant regularly demonstrated increased fitness and decreased colistin resistance, suggesting that trade-offs between fitness and resistance may limit compensatory mutation by modification of the MCR-1 structure. There were some potential compensatory mutations with *mcr-1.8* being the strongest contender but results were not significant and support for *mcr-1.5* was not consistent across assays. Data suggests that *mcr-1.4* is largely similar to consensus *mcr-1* while *mcr-1.5* is potentially compensatory but do not give a high enough fitness increase to confirm this with certainty. The mutation seen in *mcr-1.8* mildly increases the resistance and fitness across all assays tested however, it represents the minority of

variants tested. Non-synonymous SNPs largely clusters at the N-terminal of MCR-1 which could point to the functional importance of this region but this was not examined further due to problems encountered in tagging and microscopy experiments.

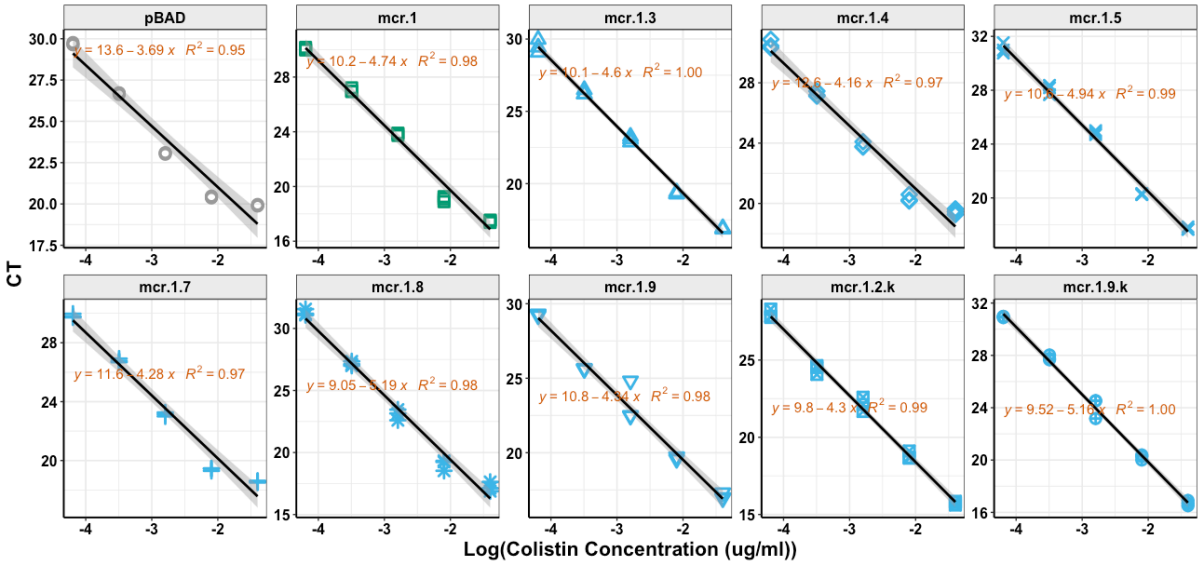
2.6 Supplementary Information



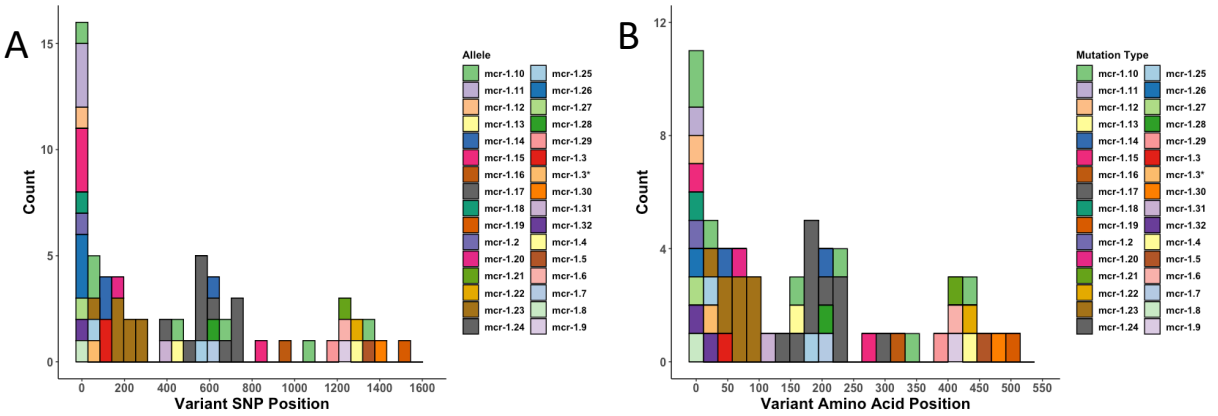
Supplementary Figure 2.S1: DRC model curves from AB1155 MIC data. Pairwise dose-response curves comparing consensus *mcr-1* (pink) to *mcr-1* variants (blue) in colistin (0-8ug/ml, Log10 Scale) were fitted using DRC package in R. Points show actual values. R-squared of fits are annotated. Consensus R-squared = 0.99



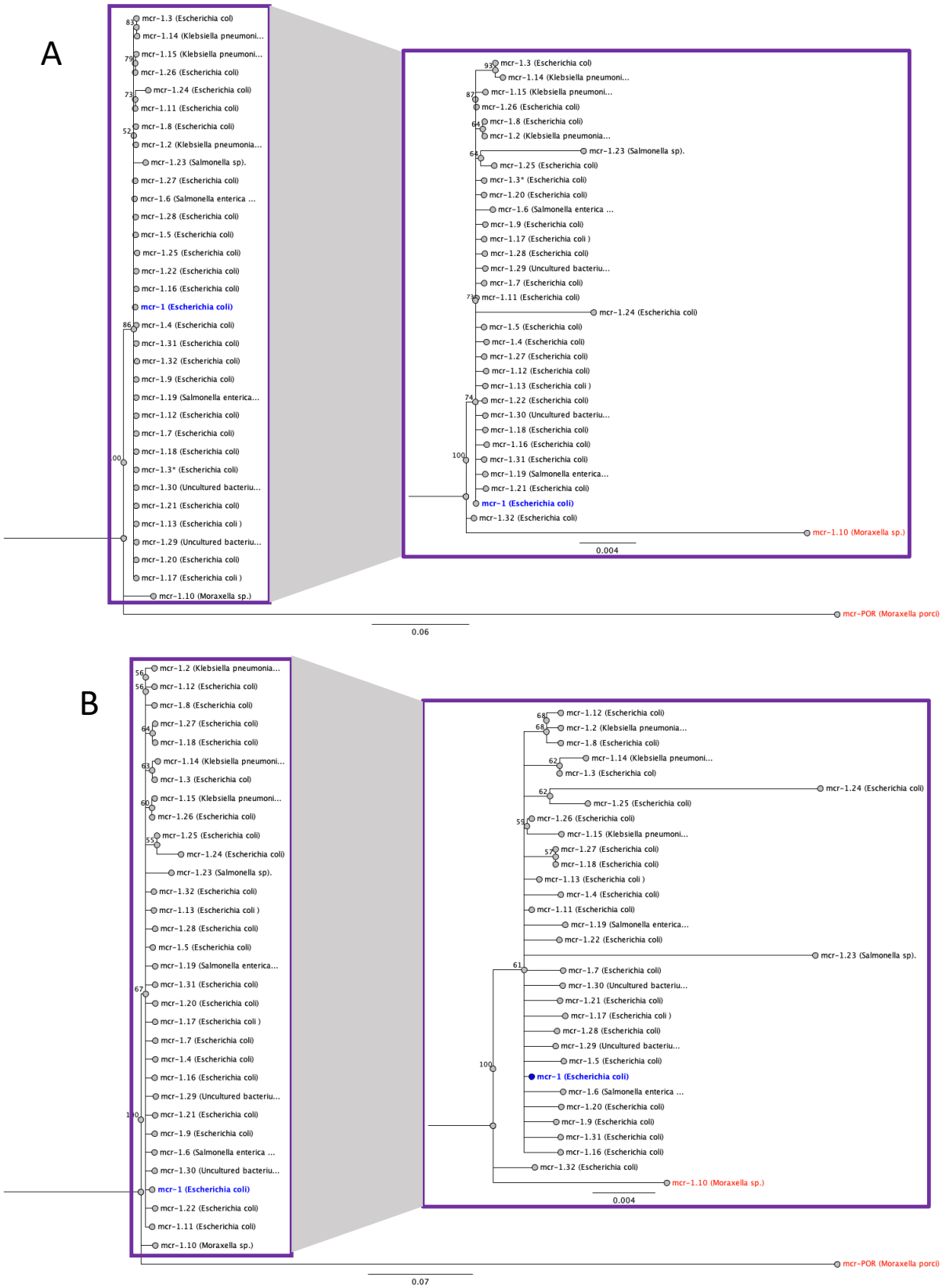
Supplementary Figure 2.S2: Mean exponential growth rate (mOD/min) results from growth rate assays for empty vector (black), variant (blue) and consensus (pink) *mcr-1* in colistin (0-4ug/ml, Log10 Scale). The horizontal red dotted line and shading indicates growth rates ≤ 0.05 and the vertical black dotted line and grey shading shows colistin concentrations ≥ the consensus *mcr-1* MIC (1ug/ml). n=2, error bar = SE.



Supplementary Figure 2.S3: Graph shows qPCR CT values obtained (y-axis) for each qPCR in known target plasmid concentrations (x-axis, Log10 Scale) n=6. Blank lines show linear regression models fitted to the data with confidence intervals in grey shading. Line equations and R-squared values for each regression line are shown in brown.



Supplementary Figure 2.S4: Histograms showing locations of all structural variant (**A**) bases and (**B**) amino acids across *mcr-1* gene and protein sequence respectively. Keys indicate variant name. Variants were binned into 30 or 25 bins corresponding to 54bp or 21AA segments for histograms A and B respectively.



Supplementary Figure 2.S5: Figure RD1: *mcr-1* structural variant gene (**A**) and protein (**B**) multiple alignment genetic distance trees. Alignments were made using MUSCLE v3.8.42 (eight iterations). Consensus *mcr-1* is highlighted in blue on all trees. Genetic distance trees were built using the Neighbour-

Joining method with *mcr-POR* (outer trees) or *mcr-1.10* (inner trees) and outgroups (highlighted in red). Scale bars show the percentage variation from the consensus

MCR-1 Allele	Total BP differences	SNP variation locations	Mutation Type	Total AA differences	AA variation locations	Genbank ID
mcr-1.1	-	-	-	-	-	KP347127.1
mcr-1.2	1	8	Substitution	1	3	LXQO01000025.1
mcr-1.3	2	111, 112	Substitution	1	38	KU934208.1
*mcr-1.3**	1	48	Substitution	1	16	KY400027.1
mcr-1.4	1	1318	Substitution	1	440	KY041856.1
mcr-1.5	1	1354	Substitution	1	452	KY283125.1
mcr-1.6	1	1263	Substitution	1	420	KY352406.1
mcr-1.7	1	643	Substitution	1	215	KY488488.1
mcr-1.8	1	8	Substitution	1	3	KY683842.1
mcr-1.9	1	1238	Substitution	1	413	KY964067.1
mcr-1.10	41	4, 31, 67, 463, 701, 1060, 1327	Substitution	7	2, 11, 23, 155, 234, 354, 443	MF176238.1
mcr-1.11	3	19, 20, 21	Insertion	1	8	KY853650.2
mcr-1.12	1	9	Substitution	1	3	LC337668.1
mcr-1.13	1	465	Substitution	1	155	MG384739.1
mcr-1.14	3	111, 112, 593	Substitution	2	38, 197	KX443408.2
mcr-1.15	4	1, 2, 3, 836	Deletion, Substitution	2	1, 279	MG763897.1
mcr-1.16	1	952	Substitution	1	318	MK568462.1
mcr-1.17	1	410	Substitution	1	137	MK568463.1
mcr-1.18	1	25	Substitution	1	9	PGLM01000025.1
mcr-1.19	1	1534	Substitution	1	512	MK490674.1
mcr-1.20	1	184	Substitution	1	62	LS398440.1
mcr-1.21	1	1234	Substitution	1	412	MK965883.1
mcr-1.22	1	1277	Substitution	1	426	MN017134.1
mcr-1.23	12	41, 154, 169, 181, 202, 214, 232, 260, 272	Substitution	9	14, 52, 57, 61, 68, 72, 78, 87, 91	MN873697.1
mcr-1.24	13	500, 534, 538, 566, 567, 568, 623, 655, 703, 715, 756	Substitution	10	167, 178, 180, 189, 190, 208, 219, 235, 239, 289	MN879257.1
mcr-1.25	2	41, 565	Substitution	2	14, 189	MN879259.1
mcr-1.26	3	1, 2, 3	Deletion	1	1	JAAGSA010000042.1
mcr-1.27	1	26	Substitution	1	9	JAAGSB010000042.1
mcr-1.28	1	641	Substitution	1	214	MT770924.1
mcr-1.29	1	1189	Substitution	1	397	MT731964.1
mcr-1.30	1	1421	Substitution	1	474	MT731965.1
mcr-1.31	1	371	Substitution	1	124	MW940640.1
mcr-1.32	2	4, 40	Substitution	2	2, 14	MF084991.1

Supplementary Table 2.S1: List of all MCR-1 alleles available from the National Database of Antibiotic Resistant Organisms as of December 2021. Number of base pair and AA differences and their locations are listed.

3 The Fitness Effects of MCR-1 Regulatory Sequence Variations

3.1 Abstract

Cis-acting elements such as promoters, enhancers and Shine-Dalgarno (SD) sequences have measurable effect on prokaryotic transcription and translation. Sequence changes within these regions can alter resultant protein levels causing changes in protein activity and bacterial behaviour. Previous studies have identified points of high sequence variability that coincide with potential *mcr-1* regulatory sequences. In this chapter, I test the hypothesis that these variants are compensatory mutations that reduce the cost of MCR-1 carriage. I discover that regulatory variations show reduced *mcr-1* expression and protein activity while also improving host fitness and resistance.

3.2 Introduction

Gene regulation allows gene expression to occur in appropriate conditions and quantities (Kumar and Bansal, 2018). Rates of mRNA production (transcription) and conversion of transcripts into functional proteins (translation) greatly impacts resulting protein levels. These processes are facilitated by cis-regulatory elements located in non-coding genomic regions (Kaberdin and Bläsi, 2006; Kumar and Bansal, 2018). Promoters, located directly upstream of transcription start sites (TSS), are crucial for transcription initiation. Prokaryotic promoters have two main components: the -10 element (TATAAT consensus sequence) and the -35 element (TTGACA consensus sequence). Sigma factors (usually sigma70/RpoD in Escherichia coli) form interactions with these elements to recruit RNA Polymerase (RNAP) leading to transcription initiation (Murakami and Darst, 2003; Shultzaberger *et al.*, 2007; Feklistov and Darst, 2011). Sequence alterations within these elements can cause measurable changes in transcription initiation levels (Bauer *et al.*, 1988). Shine-Dalgarno (SD) sequences are cis-regulatory elements found upstream of prokaryotic transcript start codons (Shine and

Dalgarno, 1975; Kaberdin and Bläsi, 2006). The region is purine rich (GGAGGA consensus sequence) allowing complementary interactions with anti-SD sequences on 16S ribosomal RNA (rRNA) components of prokaryotic ribosomes (Saito, Green and Buskirk, 2020). This interaction leads to initiator tRNA binding, recruitment of ribosome subunits and progression to translational elongation (Kaberdin and Bläsi, 2006).

In 2018, a landmark study used a dataset of over 450 *mcr-1*-positive sequence reads to characterise the genetic contexts of this *mcr-1* (Wang *et al.*, 2018). The study identified a 186bp region directly upstream of the *mcr-1* gene that had an unusually high level of sequence diversity. A significant proportion of these polymorphisms coincided with the mcr-1 promoter. Structural SNPs investigated in chapter 2 did not coincide with MCR-1 functional regions (e.g. active site/cystine residues). However, these upstream SNPs are directly associated with a functional sequence with known involvement in *mcr-1* levels. Although compensatory mutations usually alter protein function, evolutionary changes in bacterial regulatory networks have been shown to provide fitness benefits (Davis, Poon and Whitlock, 2009; Stoebel *et al.*, 2009; Patel and Matange, 2021). Mutations within *mcr-1* regulatory regions could be examples of gene expression fine-tuning to find the optimum balance between fitness costs and colistin resistance.

Observed regulatory *mcr-1* polymorphisms are of high incidence and cause changes in well-established consensus regulatory sequences. I hypothesise that these mutations will reduce *mcr-1* expression therefore dampening associated fitness costs. In this chapter, I study the fitness and resistance consequences of the regulatory variants identified in the Wang dataset. Important changes were made between the current and previous chapter. The well-established *E. coli* model strain MG1655 was used instead of highly modified TOP10 stains. Additionally, the arabinose inducible promoter of pBAD made it unsuitable to use for assessing regulatory variations. A switch was made to the pSEVA121 vector which does not contain built-in promoters for cargo gene expression allowing utilisation of natural *mcr-1* regulatory sequences (Silva-Rocha *et al.*, 2013). Additionally, its RK2 origin maintains a similar copy number to natural plasmids (about 4-7 copies per cell) (Kües and Stahl, 1989). Using in-silico tools, RT-qPCR and cell surface charge assays, I found that most regulatory mutants reduced gene expression and protein activity. Through individual and competitive fitness

assessments, I discovered that regulatory variants generally increased fitness in the presence and absence of colistin. Furthermore, investigations of recent sequence datasets found increases in regulatory variant prevalence. Taken together, results suggest that *mcr-1* regulatory variants provide marked fitness and resistance benefits to *E. coli* hosts.

3.3 Methods

Bacterial Strains, Plasmids and Growth Conditions

Cloning experiments involved the pSEVA121 cloning vector (SEVA) generously provided by the Standard European Vector Architecture (SEVA) database and material repository. *E. coli* MG1655 was used for experiments in this chapter. TOP10 (ThermoFisher Scientific) *E. coli* was used for cloning. MG1655 with chromosomally integrated *mcr-1* was constructed by Divjot Kuar. Briefly, lambda red recombineering was used to integrate consensus *mcr-1* gene and regulatory sequences into the MG1655 chromosome in replacement of the non-essential lacZ gene. Isolates were confirmed for correct assemblies using blue-white screening and sequence verification.

Bacteria were grown in Luria Broth (LB) broth (Sigma-aldrich), LB Millar agar (Sigma-aldrich) plates or Mueller Hinton Broth (MH, Sigma-aldrich). All bacteria were grown at 37°C in shaking (liquid culture, 250 rpm) or standing (LB Millar agar) incubation.

Wang Dataset Sequence Analysis and *In-Silico* Assessments

The 2018 Wang dataset of 457 *mcr-1*-positive isolates was used to characterise regulatory sequences and variants. Sequences were mapped to the consensus *mcr-1* gene using Geneious alignment software. A 308bp query of the alignment which included the 183bp upstream region and the 1st 125 base pairs of the *mcr-1* gene was used for silico promoter predictions using BPROM, BacPP and De Novo DNA (Salis Lab) software. Regulatory variants found within identified *mcr-1* -10 promoter box and Shine-Dalgarno sequences were given variant IDs. De Novo DNA (Salis Lab) and BacPP software were used to assign scores and/or predict transcription/translation rates for the identified variants.

Variant Plasmid Construction

Consensus *mcr-1* and the regions 150bp upstream and 40p downstream were amplified from the IncI2 plasmid PN16 and cloned into pSEVA121. Plasmids containing one of the eight regulatory variants (*Table 3.1*) and inactivated (T285A) *mcr-1* were generated using GA and site-directed mutagenesis. Variant SNPs were introduced into regulatory regions and inserts were assembled into identical pSEVA121 backbones. A random DNA sequence generator was used to design unique 32bp sequence tags for each variant plasmid (The Maduro Lab). Generated sequences were designed to have a GC content of 50% and selected based on the following criteria:

- Does not contain a string of >4 identical bases
- Melting temperature (Tm) of 60-63°C
- No stable hairpins and dimers (Determined using OligoAnalyzer (IDT))

Chosen sequences (*appendix table 1*) were aligned using Geneious Prime software (MUSCLE v3.8.425, 8 iterations, profile dependent parameters optimised). Gibson primers (*appendix table 1*) PCR amplification generated insert fragments with appropriate GA overhangs, sequence tags and SNPs. GA was carried out using the NEBuilder® HiFi DNA Assembly Master Mix (New England Biolabs). Sequence verified plasmids were transformed into TOP10 and MG1655 *E. coli* strains.

Minimum inhibitory concentration (MIC) Determination

Colistin MICs of MG1655 *E. coli* control or regulatory variant stains were determined using broth microdilution and OD measurements. Bacteria were grown overnight in LB+Amp (50µg/ml, sigma-aldrich). Bacteria were diluted to $5x10^5$ CFU/ml in colistin free or colistin supplemented MH media (Cayman Chemical, 0-8ug/ml). Bacteria were grown overnight at 37°C and OD measurements (595nm) were taken following incubation. Dose response curve (DRC) models were fitted using the "drm" package (v2.5-12). All models obtained non-significant scores using lack-of-fit tests.

Growth Rate Measurements

Overnight MG1655 and TOP10 *E. coli* cultures containing control or regulatory variant plasmids were diluted to $5x10^5$ CFU/ml in MH media. Bacteria were incubated overnight at 37°C with OD measurements (595nm) taken every 10 minutes.

Cell Surface Charge Assessments

Fluorescein isothiocyanate-labelled poly-L-lysine (FITC-PLL, Sigma) binding assays were used to determine MCR-1 activity. Positively charged FITC-PLL is able to bind gram-negative outer membrane in a charge dependant manner due to negative charges on lipid A (Rossetti *et al.*, 2004). MCR-1 activity reduces these negative charges allowing estimations of MCR-1 activity by measuring cell fluorescence. Bacterial cells containing control or regulatory variant plasmids were grown overnight in MH media. Cells were centrifuged and washed twice with 1X Phosphate-buffered saline (PBS) buffer. Washed cells were re-suspended in 1× PBS buffer to a final OD600 of 0.1. FITC-PLL solution was added to re-suspended cells (5 µg/ml). The bacteria and dye mixtures were incubated at room temperature for 12 min and centrifuged (6000xg for 5 minutes). Fluorescence measurements (excitation at 500 nm and emission at 530 nm) of supernatants were compared with PBS controls to determine the proportion of bacterial-bound dye.

qPCR Competitions

Primers designed to match unique sequence tags were used for variant plasmid specific amplification. Specificity and optimisation tests were performed using PCR and qPCR. Quality and efficiency tests were performed for all primers. Standard curves for each variant primer pair were generated using known plasmid concentrations. Overnight bacterial cultures were OD normalized and diluted 1-in-10 to pooled mixes. Mixes were used to inoculate MH media of four conditions (0, 0.375, 0.75 and 1.5ug/ml colistin) and competitions were carried out over a 20hr incubation at 37°C. Competition media and inoculation mixes were boiled (100^{o}C for 20 minutes) and qPCR (Applied Biosystems, StepOnePlus Real-Time PCR System) was performed using the ten variant primers. Three technical repeats were preformed per competition and average CTs were used to determine variant plasmid concentrations. Relative fitness was calculated for each condition using the following equation.

$$Relative\ Fitness = \frac{log_2\left(\frac{Vf}{Vi}\right)}{log_2\left(\frac{Cf}{Ci}\right)}$$

Where Vf = variant plasmid concentration following competition, Vi = variant plasmid concentration of initial pools, Cf = consensus *mcr-1* plasmid concentration following competition and Ci = consensus *mcr-1* plasmid concentration of initial pools.

RT-qPCR Gene Expression

mcr-1 expression levels were quantified in MG1655 *E. coli* containing control or regulatory variant plasmids. Total RNA was extracted from bacteria following incubation in MH+Amp (50ug/ml). Bacteria were sub-cultured, grown to an OD of 0.5 (600nm) and washed in PBS. Bacterial digestion was performed using RNAprotect Bacteria Reagen (Qiagen) as per manufacturer's instructions. Digested bacteria were subjected to RNA extraction using the RNeasy Mini Kit (Qiagen) and QiaCube liquid handling platform (Qiagen) as per manufacturer's instructions. Extracted RNA was DNAse treated using the TURBO DNA-free kit (ThermoFisher) and quantified using the Quantifluor® RNA system (Promega).

Extracted RNA was diluted to 5ug/ml and subjected to one step RT-qPCR on the StepOnePlus™ Real-Time PCR System (Applied Biosystems) using the Luna® Universal One-Step RT-qPCR Kit (New England Biolabs). *mcr-1* and *trfA* (reference) expression were quantified using appropriate primers (*appendix table 1*). *trfA* was selected as a reference due to its pSEVA121 localisation allowing normalisation of plasmid copy number across all control and regulatory variant plasmids tested. Relative *mcr-1* expression was calculated using the delta-delta (2–ΔΔCt) Ct method where expression levels of the variant promoter and Shine-Dalgarno sequences were compared to the consensus regulatory sequence.

Shen Dataset Variant Frequency Analysis

The 2020 *mcr-1* dataset was utilised to compare the variant frequency of *mcr-1*-positive bacterial isolates from China in 2016 (pre colistin ban), 2017 and 2018 (post colistin ban) (Shen *et al.*, 2020). Bioinformatic analysis and annotation of Shen dataset were done by Liam Shaw. Isolate information tables were obtained from Liam Shaw and analysed using R Studio.

3.4 Results

3.4.1 Regulatory Variations and their Predicted Effects

To determine if regions of high diversity found in the Wang dataset coincided with *mcr-1* regulatory regions, I first mapped out potential promoter and Shine–Dalgarno motifs then characterised SNPs located within mapped regions. *mcr-1*-positive isolate sequences (466 in total) were aligned and mapped to consensus *mcr-1*. BPROM *in-silico* promoter prediction software identified a potential promoter with -10 and -35 boxes located -50bp to -42bp and -74bp to 69bp respectively. This coincided well with the putative *mcr-1* promoter region mapped in a previous study (Poirel *et al.*, 2016). Of the 457 sequences, 473 contained -10 regions and 454 sequences contained -35 regions. Promoter variants (PVs) located within the -10 region where named and characterised (*Table 3.1*). As minimal single SNP variations was found within the putative -35 regions, these regions were not studied further.

As shine–Dalgarno (SD) motifs are short G-rich sequences located immediately upstream of start codons, a 20bp region 5' to the *mcr-1* start codon was analysed for sequence variation. A 6bp region was selected as a putative SD sequence due to guanines overrepresentation in this region. SNPs within this region were named and classified as SD sequence variants (SDVs). Occurrences of PVs and SDVs in the Wang dataset were recorded (*Table 3.1*). Overall, regulatory variants were frequent and demonstrated parallelism.

Variant ID	Regulation Type	Region	Sequence	Occurrences (Wang Dataset)
CP	-10 Promoter	(-47 to -42)	**TATAAT**	353
PV1	-10 Promoter	-45	TA**A**AAT	63
PV2	-10 Promoter	-45	TA**G**AAT	14
PV3	-10 Promoter	-44	TAT**G**AT	31
PV4	-10 Promoter	-43	TATA**G**T	2
CSD	Shine-Dalgarno	(-10 to -6)	**GAGTAG**	349
SDV1	Shine-Dalgarno	-8	GA**T**TAG	46
SDV2	Shine-Dalgarno	-10 and -8	**T**AA**T**AG	41
SDV3	Shine-Dalgarno	-8	GA**A**TAG	22
SDV4	Shine-Dalgarno	-9	G**C**GTAG	5

Table 3.1: Consensus and variant *mcr-1* regulatory sequences and their properties. CP and CSD indicate consensus -10 promoter and shine-Dalgarno sequences respectively. Variant regulatory IDs and sequence changes are highlighted in blue. SNP locations are respective to the *mcr-1* start codon.

Variants found outside 6 base-pair -10 promoter box and Shine-Dalgarno sequence are not included. PV= Promoter variant, SDV=Shine-Dalgarno variant.

In-silico promoter and SD assessment software was used to computationally asses regulatory variants effects. Query sequences of different lengths were submitted to BacPP and DeNovoDNA to give promoter scores, transcription and translation initiation rates (*Table 3.S1*). In most conditions, regulatory variants reduce scores and/or rates of initiating transcription or translation compared to consensus sequences.

3.4.2 Plasmid and Variant Construction

In order to assess the effects of the regulatory variants in more natural systems, *mcr-1* along with the regions 150bp upstream and 40bp downstream of the gene were amplified from the natural *mcr-1*-positive PN16 plasmid to obtain the gene's natural regulatory regions and surroundings. The 1823bp fragment was then cloned into the pSEVA121 plasmid which allowed *mcr-1* expression through native promoters and in copy numbers similar to natural *mcr-1*-positive plasmids (4-6 copies per cell). Regulatory variants and inactivated (T285A) *mcr-1* were subsequently created.

3.4.3 Endpoint Optical Density Assessments of Regulatory Variants

To assess the fitness and resistance consequences of regulatory SNPs, MIC assays using endpoint OD measurements were done for individual *mcr-1* regulatory variants and controls (Fig.1a). Mean optical densities show that in comparison to consensus *mcr-1*, regulatory variants show slightly increased MICs (excluding PV1 and SDV3). In colistin-free media, higher OD measurements are observed for most variants. However, changes in endpoint OD measurements are not ideal fitness indicators.

Variant	Dose-Response Model Estimates and Comparisons						
	Predicted MIC (ug/ml)	**IC50 (e)** (ug/ml)	**p-value**	**Sig.**	**Uninhibited growth (d)** (OD595)	**p-value**	**Sig.**
Consensus	**0.75**	**0.491**	NA	NA	**0.917**	NA	NA
PV1	0.75	**0.565**	< 0.00001	***	**0.852**	0.02909	*
PV2	1	**0.764**	0.19110		**0.943**	0.60246	
PV3	1	**0.719**	< 0.00001	***	**0.921**	1.00000	
PV4	1	**0.921**	< 0.00001	***	**0.964**	0.16919	
SDV1	1	**0.772**	< 0.00001	***	**0.925**	1.00000	
SDV2	1	**0.825**	< 0.00001	***	**0.905**	1.00000	
SDV3	0.75	**0.452**	< 0.00001	***	**0.875**	0.50919	
SDV4	1.5	**1.018**	0.03208	*	**0.990**	0.00059	***

Table 3.2: Predicted MICs, e and d coefficients consensus and regulatory variants. Variant values lower than the consensus regulatory value are highlighted in red and higher values are in blue. P-value and significance show results of pairwise comparisons of each variant to consensus *mcr-1* (p-values adjusted using the Bonferroni correction for multiple comparisons)

To directly compare resistance differences of regulatory variants to consensus sequences, DRC models were fitted onto OD results (*Table 3.2*). Pairwise plots clearly show the increased resistance that most variants (*Figure 3.1b*). Additionally, IC50s (e-coefficient) of most regulatory variants are significantly increased when compared to consensus regulatory sequences (*Table 3.2*, Dunnett's T-test with Bonferroni adjustment). Most variants also demonstrated higher uninhibited OD (d-coefficient) however, comparisons largely did not obtain significance.

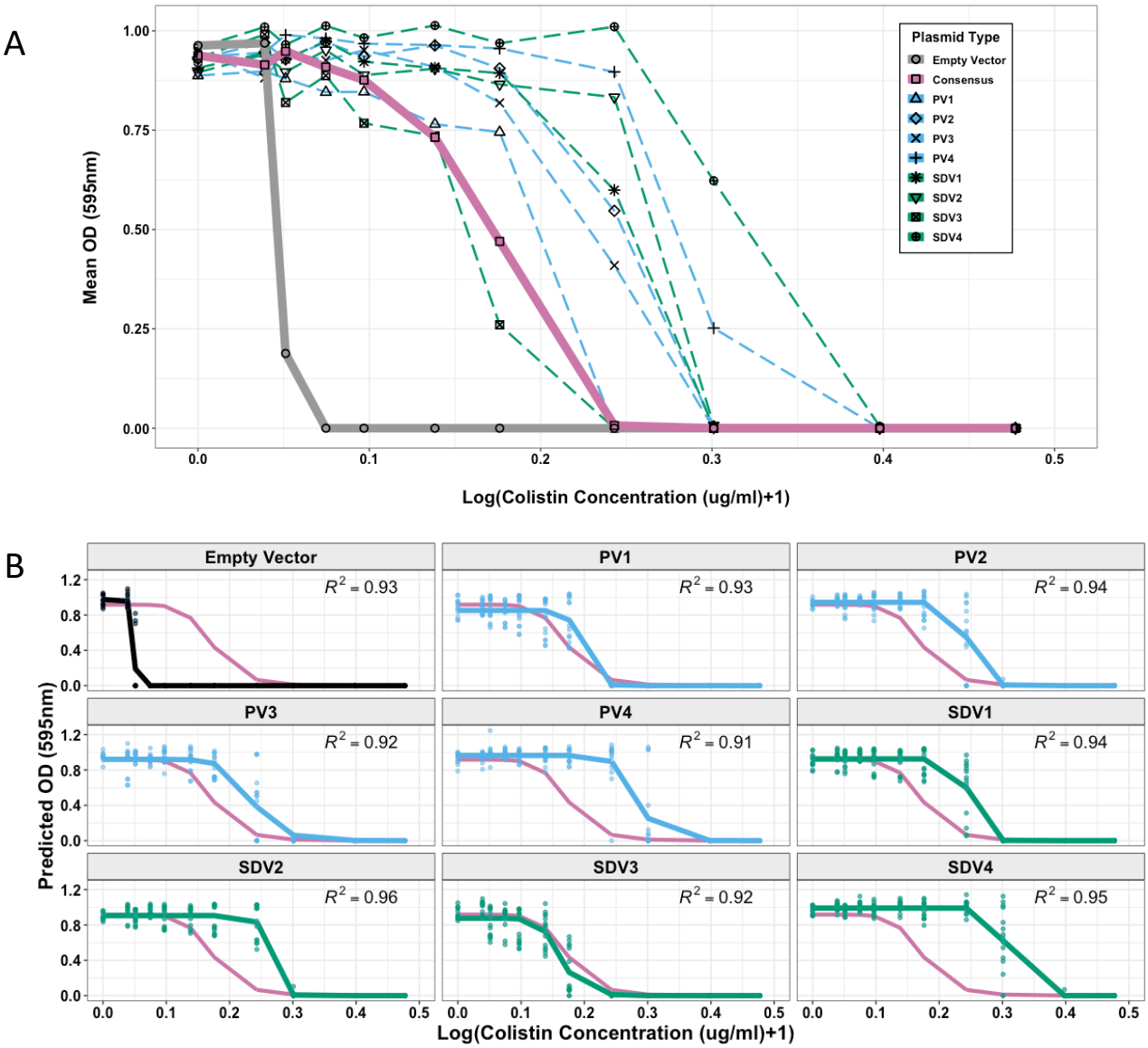


Figure 3.1: Results from the MIC assays (**A**) Mean OD in a range of colistin concentrations (0 – 2ug/ml, Log10 Scale). Points show mean values. Thicker lines indicate controls and dashed lines show regulatory variants (n=15). (**B**) Pairwise dose-response curves comparing consensus *mcr-1* regulatory sequence (pink) to promoter variants (blue), SD variants (green) and empty vector control (black) in a range of colistin concentrations (0-8ug/ml, Log10 Scale). Points show actual values. R-squared values for variant models are annotated. Consensus R-squared = 0.97.

3.4.4 Growth Rate Estimations of Regulatory Variants

Although MIC results showed that most variants demonstrated higher colistin resistance, endpoint OD measurements are course and did not provide much clarity regarding the fitness consequences of variants in colistin-free conditions. To assess regulatory variant fitness, exponential growth rates were measured for each variant plasmid and compared to

consensus sequences and controls (*Figure 3.2*). Results showed that besides PV1, regulatory variants gave significantly higher exponential growth rates than consensus sequences. This suggests that most variants provide fitness benefits as some were comparable to inactivated and empty vector controls. Additionally, results demonstrate that *mcr-1* fitness costs are still significant with native promoter expression and using lower copy number plasmids.

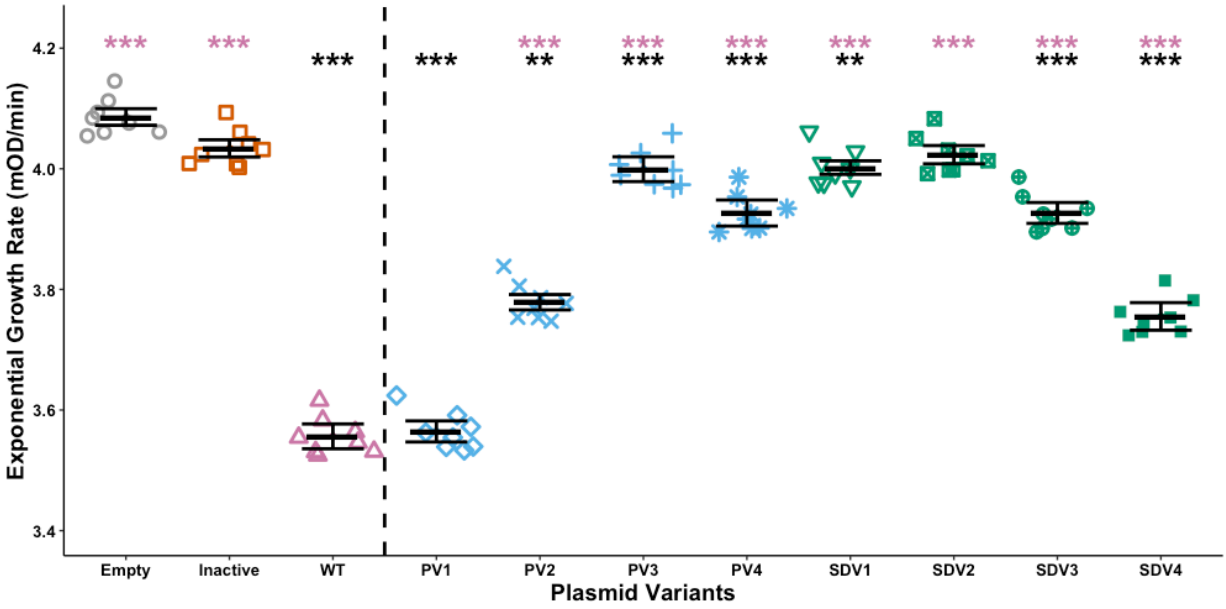


Figure 3.2: Exponential growth rates (abs/min) in colistin-free media is shown for the consensus regulatory sequence (WT, pink) and promoter (blue) and Shine-Dalgarno (green) variants. Empty (grey) inactivated *mcr-1* (orange) controls are included. Lines show mean exponential growth rates after blocking for daily variation. Points show adjusted daily averages. Significance of comparisons to empty (black) and WT (pink) controls are indicated above each variant (p-values: ****<0.001, **<0.01. Dunnett's t-test adjusted for multiple comparisons, n = 5 replicates per day, Error bars = SE)

3.4.5 Growth Rate and MIC of Chromosomally Integrated MCR-1

One method of reducing MCR-1 levels is to clone the gene and its promoter into *E. coli* chromosomes (single-copy) rather than plasmids (multi-copy). To determine whether resistance (*Figure 3.1*) and fitness (*Figure 3.2*) changes seen between regulatory variants and consensus sequences were caused by reduced MCR-1 levels, MG1655 strains containing chromosomally integrated *mcr-1* and its consensus regulatory elements were compared to plasmid controls. Growth rate assessments in colistin-free media show that MG1655 containing integrated *mcr-1* had higher exponential growth rates than their plasmid

counterparts (*Figure 3.3a*). Additionally, MIC results show that the integrated strain had slightly increased colistin MIC (*Figure 3.3b*). Results from DRC models significantly confirm resistance observations as the integrated strain had a significantly higher IC50 than pSEVA121-*mcr-1* carrying MG1655 (*Table 3.3*). These results show that integrated strains with the consensus regulatory demonstrate higher fitness in the presence and absence of colistin than plasmid carrying strains. Fitness and resistance trends seen for chromosomally integrated *mcr-1* largely mimicked those of most regulatory variants suggesting that decreased MCR-1 levels may explain the fitness and resistance benefits seen in the regulatory variants.

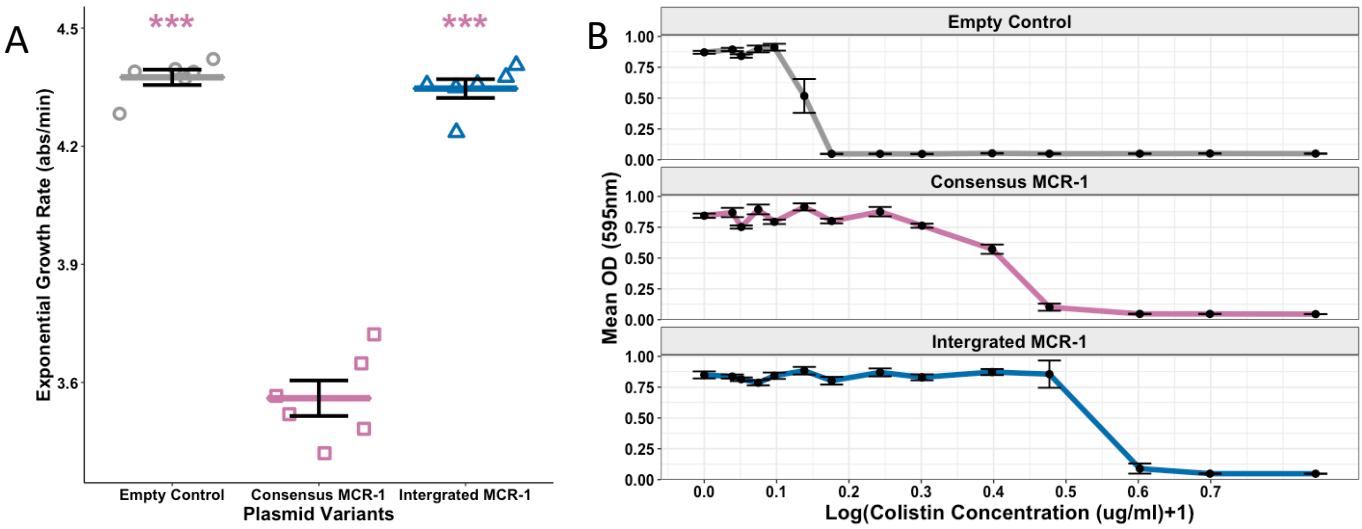


Figure 3.3: Growth rate and MIC assessments of chromosomally integrated *mcr-1*. (**A**) Exponential growth rates (abs/min) in colistin-free media is shown empty vector (grey) plasmid *mcr-1* (pink) and chromosomally integrated *mcr-1* (dark blue). (p-values: ***<0.001. Dunnett's t-test, n = 6, error bars=SE) (**B**) Mean OD in a range of colistin concentrations (0 – 6ug/ml, Log10 Scale) is indicated for empty vector (grey) plasmid *mcr-1* (pink) and chromosomally integrated *mcr-1* (dark blue). (n=8)

Variant	**Dose-Response Model Estimates and Comparisons**						
	Predicted MIC (ug/ml)	**IC50 (e)** (ug/ml)	**p-value**	**Sig.**	**Uninhibited growth (d)** (OD 595)	**p-value**	**Sig.**
Plasmid	2	**1.596**	NA	NA	**0.835**	NA	NA
Empty	0.5	**0.379**	<0.00001	***	**0.883**	0.02121	*
Chromosome	3	**2.748**	<0.00001	***	**0.839**	0.65582	

Table 3.3: Predicted MICs, e and d coefficients for stains containing the consensus *mcr-1* regulatory and gene sequence on either the pSEVA121 plasmid (Plasmid) or chromosomally integrated (Chromosome). Empty pSEVA121 was used as a control. Values lower/higher plasmid results are highlighted in red/blue respectively. Significance tests show results from Dunnett's T-test (compared to Plasmid values) adjusted using the Bonferroni correction for multiple comparisons.

3.4.6 Measuring Variant *mcr-1* Expression via RT-qPCR

Although thought to reduce *mcr-1* transcription/translation, previous assessments of regulatory variants are based on *in-silico* predictions. These tools are less accurate for determining outcomes of single SNP changes (e Silva and Echeverrigaray, 2012; Cassiano and Silva-Rocha, 2020). To experimentally determine if *mcr-1* promoter variations led to transcription changes, RT-qPCR was performed to measure relative *mcr-1* expression in comparison to the consensus promoter using the delta-delta Ct ($2^{-\Delta\Delta Ct}$) method (*Figure 3.4*). *mcr-1* SD variant expression levels of were measured as control. pSEVA121 located *trfA* was used as a reference gene to control for plasmid copy number. Results show excluding PV1, promoter variants showed lower relative expressions with significance obtained for PV2 (p=0.00536) and PV4 (p<1e-04). Although most SD variants had similar relative *mcr-1* expression values, SDV4 had a significantly reduced relative *mcr-1* expression level. Despite this, a one-way ANOVA comparing relative expression of consensus controls to pooled promoter and SD variants found significant differences between the promoter group (p-value=0.0244, Dunnett's test) but not the SD group. This means that promoter variants were generally found to reduce relative *mcr-1* expression which supports *in-silico* predictions.

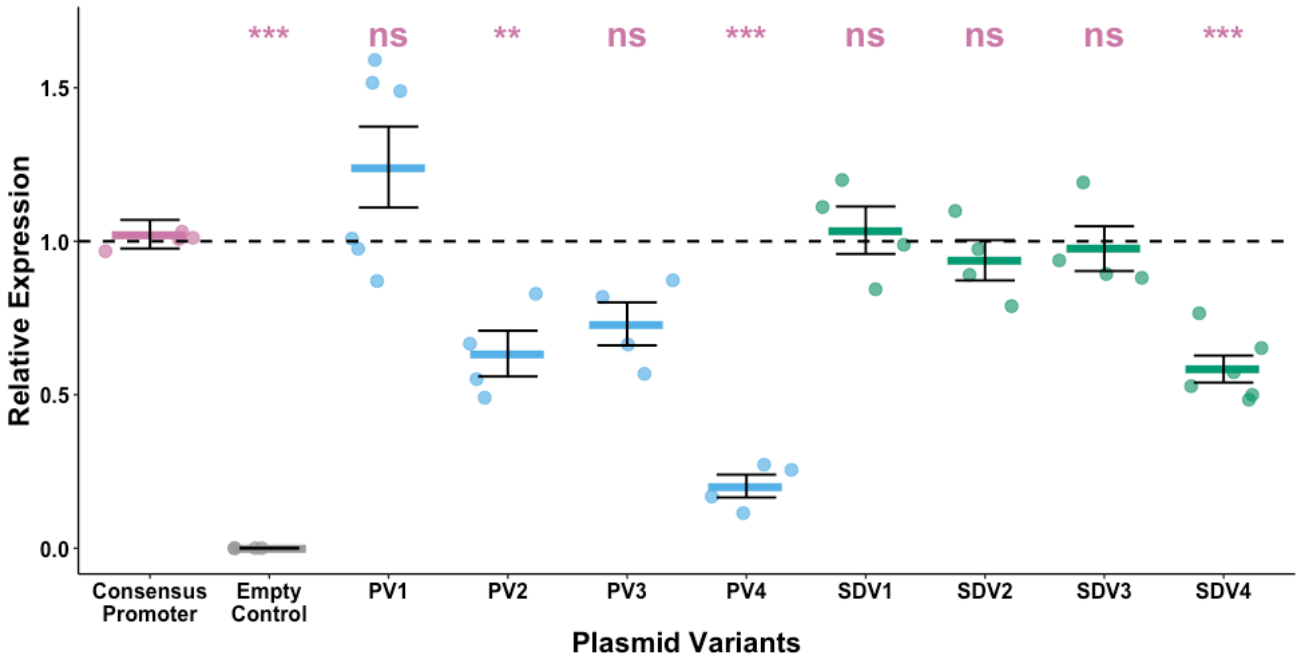


Figure 3.4: Relative *mcr-1* expression of regulatory variants (PV = blue, SDV= green) and empty control (grey) compared to the consensus regulatory sequence (pink). Solid variant lines show mean relative expression, points individual values. Significance in comparison to consensus are indicated above the respective plasmid variants (p-values: ****<0.001, **<0.01, ns=not significant. Dunnett's t-test adjusted for multiple comparisons, n = 4-6, error bars = SE, Dotted line at y=1).

3.4.7 Relative Surface Charge of Regulatory Variants

As expression data only provides information on mRNA levels, surface charge measurements were used to asses if regulatory variants led to reduced MCR-1 activity. *mcr-1* encodes a phosphoethanolamine (pEtN) transferase that adds phosphoethanolamine (pEtN) groups to negatively charged phosphates on gram-negative outer membranes. This reduces the negative surface charge on MCR-1 positive bacterial membranes. As regulatory variants likely reduce *mcr-1* transcription and translation (*Figure 3.4, Table 3.S1*), they would likely decrease MCR-1 levels and there have reduced surface charges. Altering the active site of MCR-1 almost completely eliminates the cost associated of carrying the gene, suggesting that it is the activity of the protein, and not the biosynthetic burden of expressing the protein, that generates a majority of fitness cost.

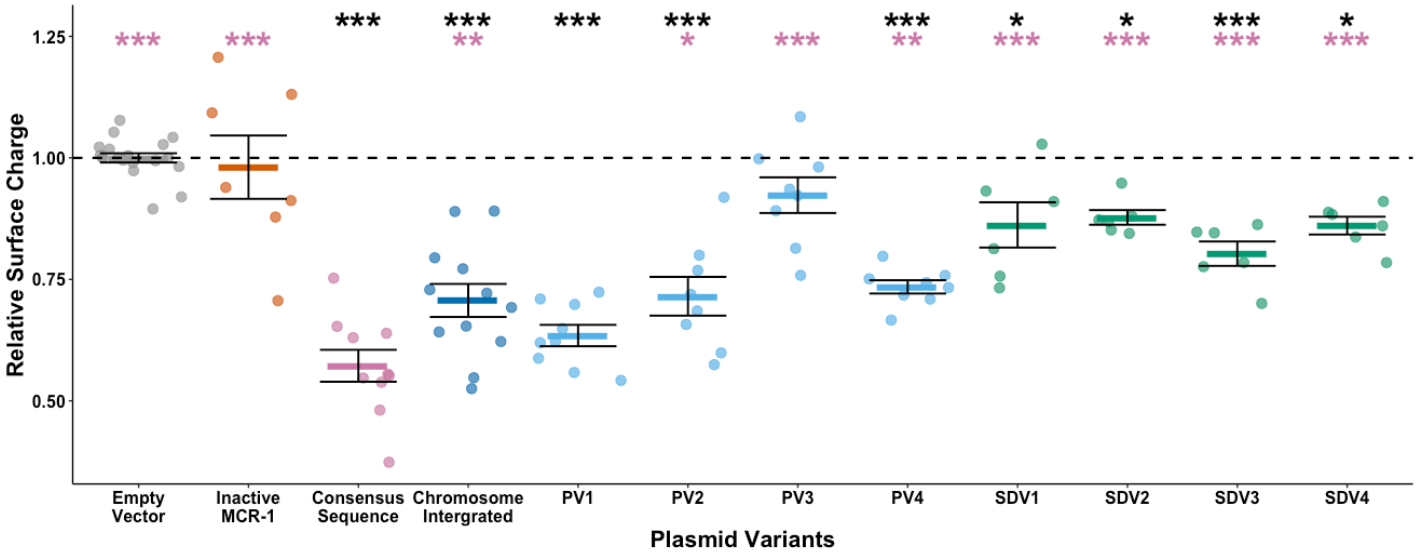


Figure 3.5: Relative surface charges of regulatory *mcr-1* variants (PV = light blue, SDV= green), integrated *mcr-1* (dark blue), inactivated *mcr-1* (orange) consensus sequence (pink) and empty control (grey). Surface charges were compared to the empty control which was set to 1 (dashed black line). Significance in comparison to the empty vector (grey) and consensus expression (pink) are indicated above the respective plasmid variants (p-values: ****<0.001, **<0.01, *<0.05, Dunnett's t-test adjusted for multiple comparisons, n=6-12, Error bar = SE)

To explore the relationship between protein activity and fitness more broadly, the cell surface charge of regulatory variants and controls was assessed by measuring the binding of the cationic FITC-PLL dye. Relative surface charge of each variant was calculated in comparison to empty vector controls (*Figure 3.5*). Surface charges of MG1655 containing the consensus regulatory sequence, inactivated MCR-1 or chromosomally integrated *mcr-1* were included as controls. Results show that excluding PV1, regulatory variants showed significantly increased relative surface charges than consensus regulatory sequences (*Figure 3.5*). This suggests that regulatory variants reduce MCR-1 activity in comparison to the consensus control, supporting the idea that these mutations decrease the *mcr-1* expression (*Figure 3.4*, *Table 3.S1*). Additionally, the PV3 variant did not show any significant differences in relative surface charge when compared to the empty control (*Figure 3.5*). Comparisons of pooled variant groups showed that promoter and SD variant groups generally had increased relative surface charges when compared to the consensus (p-value<0.001, One-way ANOVA, Tukey's test). SD variants had increased overall gains in relative surface charge when compared to the promoter variations (p-value = 0.008, One-way ANOVA, Tukey's test).

3.4.8 Fitness Competitions of Regulatory Variants

To directly assess variant fitness and competitive ability of the regulatory variants relative to the consensus, competition assays were performed. The relative fitness of each regulatory variant plasmid compared to the consensus (set at 1) was determined by calculating the fold change for each plasmid at all tested colistin concentrations (*Figure 3.6*). Most variants show clear increases in relative fitness in both the absence and presence of colistin suggesting that they increase fitness in all conditions. To confirm if this is the case, a two-way ANOVA was performed to assess the effects of variant plasmids (excluding inactive control) and colistin concentration on relative fitness. Main effects analysis showed that variant type alone had significant effects on relative fitness (p-value<0.001). Additionally, no significant interactions between variant plasmids and colistin concentration were identified (p-value= 0.396) therefore, further analysis disregarded concentration differences and focused purely on variant effects.

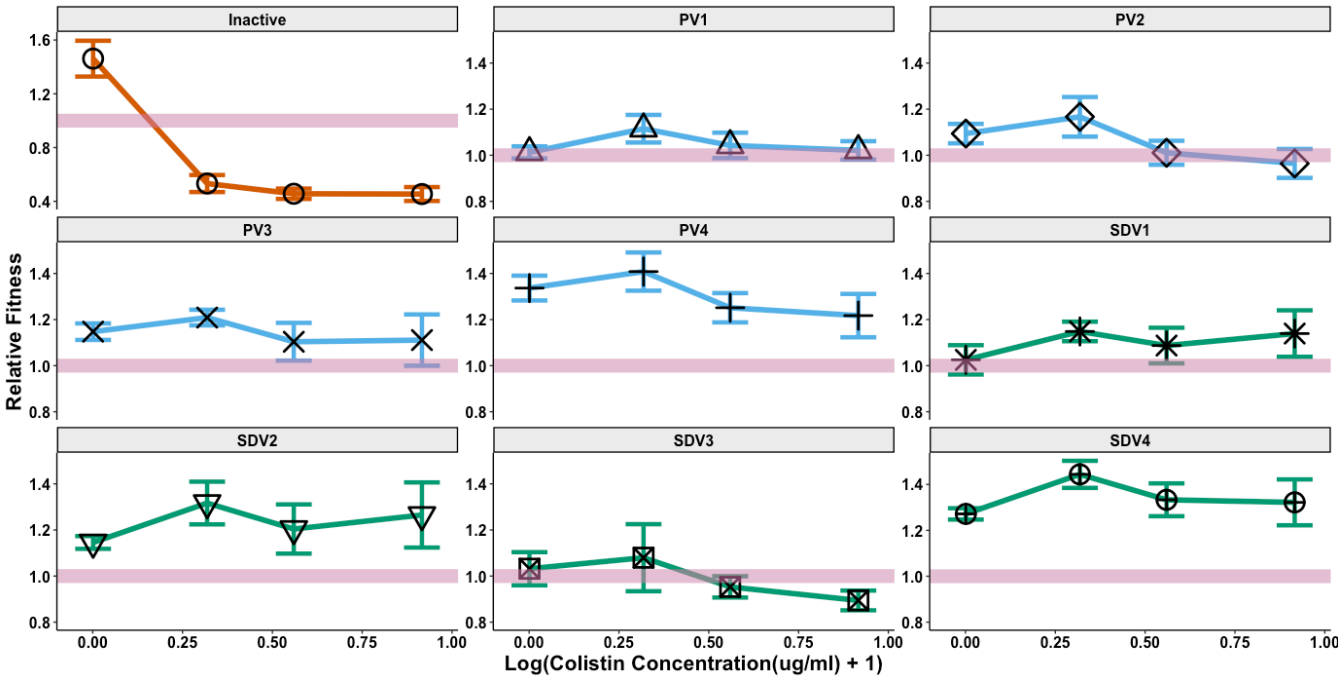


Figure 3.6: Relative fitness results from fitness competitions. Mean relative bacterial fitness of all regulatory variants and the inactivated control are plotted in comparison to the consensus regulatory sequence in a range of colistin concentrations (0-2ug/ml, Log10 Scale) (set to 1, pink line, Error bars=SE, n=4).

To determine which variants had significant increases in fitness, One Sample t-tests adjusted for multiple comparisons (Bonferroni) were run on relative fitness data. Results showed that PV3 p-value= 0.005), PV4 (p-value<0.001), SDV2 (p-value<0.001) and SDV4 (p-value<0.001) were significantly different from 1. Overall, results from pooled variants showed that both promoter and SD variants significantly increase relative fitness (p-value<0.001).

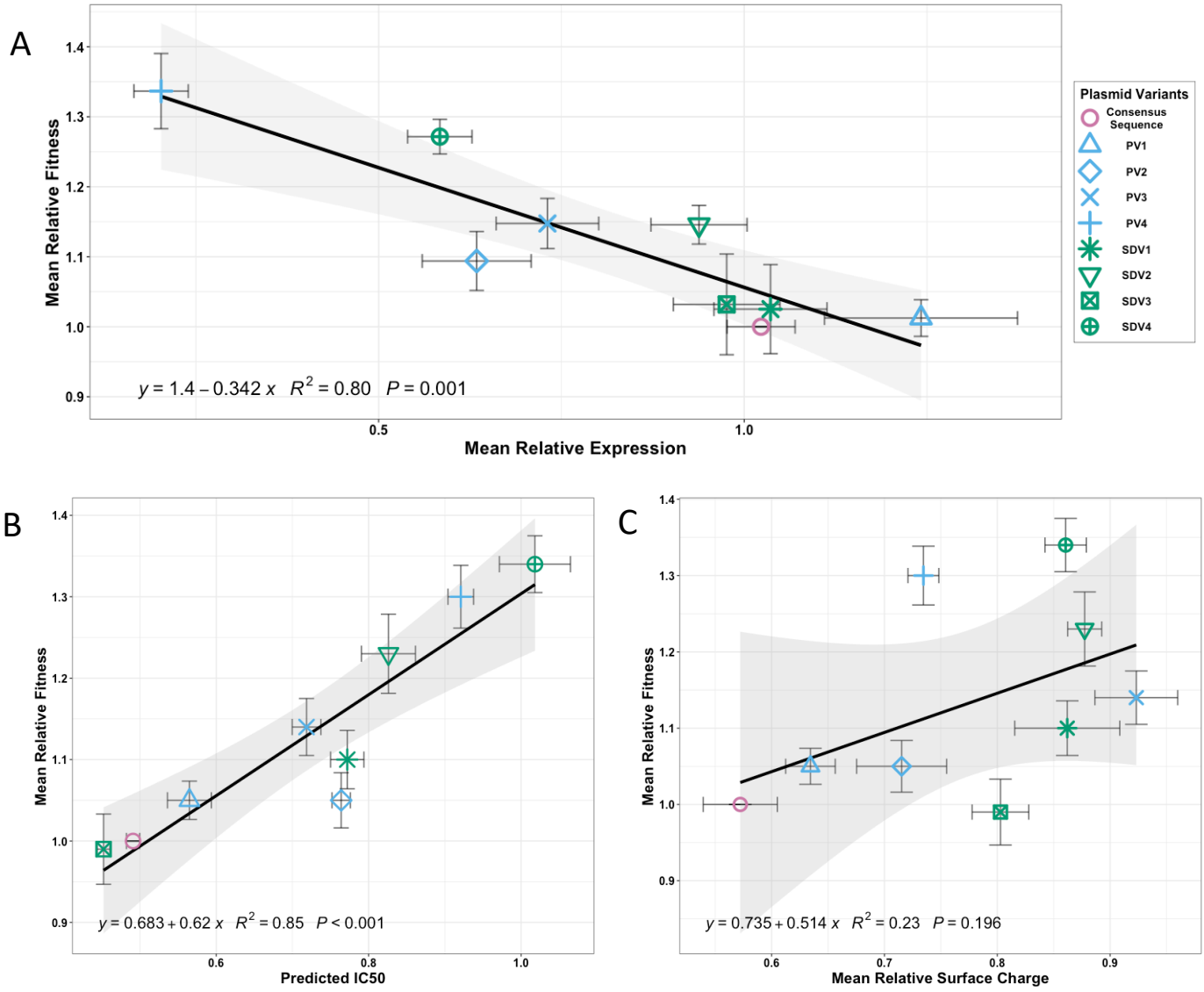


Figure 3.7: Scatterplots showing relationships between relative fitness (y-axis) and (**A**) Relative *mcr-1* expression, (**B**) predicted IC50 and (**C**) relative surface charge of regulatory variants and controls. Points assigned to particular variants/controls are shown in the legend (error bars = SE). Blank lines show linear regression models fitted to the data with confidence intervals in grey shading. Regression line equations, model r-squared and p-values indicated in black text. Variant legend from graph A is applicable to graphs B and C.

In order to identify relationships between fitness results and previous assessments on regulatory variant expression and activity, linear regression models were fitted to the relevant scatter plot data (*Figure 3.7*). A clear negative correlation was seen between relative expression and fitness (p-value = 0.001, *Figure 3.7a*) suggesting that reduced expression of *mcr-1* leads to increased fitness. Interestingly, a strong positive correlation was seen between variant IC50 and fitness (p-value= 0.0004) meaning expression and IC50 are also negatively correlated (*Figure 3.S2a*). Although, the model correlating fitness with surface charge showed a weak positive gradient, significance was not obtained (p-value = 0.1669, *Figure 3.7c*). Additional correlations showed that growth rate was correlated with surface charge but none of the other variables (*Figure 3.S2b*).

3.4.9 Proportion and Frequency Assessments of Regulatory Variants

MCR-1 surveillance has increased since its discovery, leading to a surplus sequencing data looking at *mcr-1* and its surrounding generic areas. We took advantage of the recent Shen dataset (2020) which monitored *mcr-1* prevalence before and after the introduction of the 2017 Chinese ban on colistin usage. Alignments of Shen and Wang dataset sequences were analysed to identify structural and regulatory mutations (*Figure 3.8*). Percentage proportions of variants within their relevant datasets show that over the years, proportions of regulatory variants have increased on a whole seem to have increased (*Figure 3.8a*).

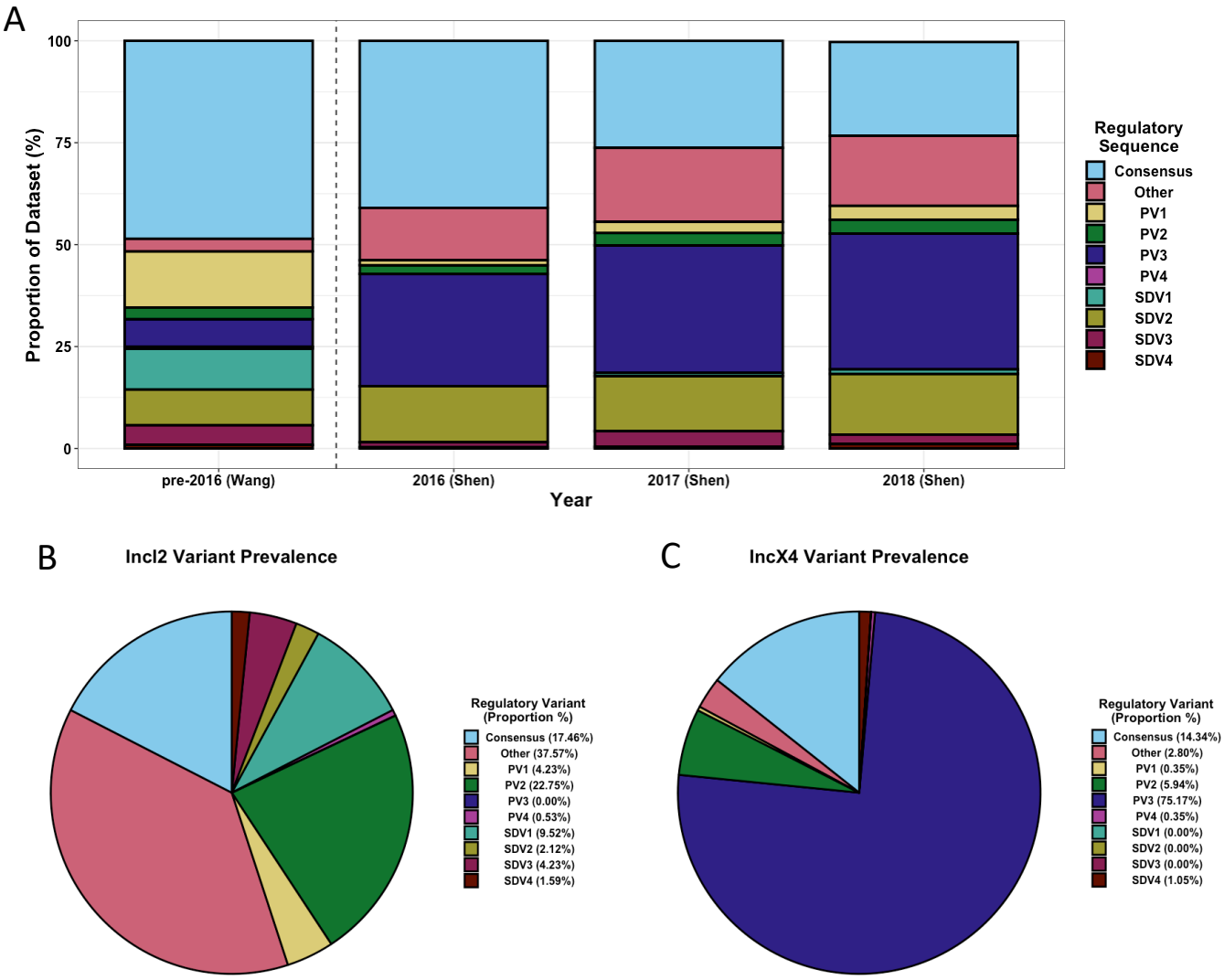


Figure 3.8: Analysis of regulatory variants in Shen (2020) and Wang (2018) datasets. (**A**) Percentage proportion of *mcr-1* positive sequences that contain certain regulatory sequences is indicated for each dataset. Shen dataset was separated by year while Wang dataset indicated sequences obtained before Shen dataset. Pie charts show proportion of regulatory variants within plasmids annotated as (**B**) IncI2 and (**C**) IncX4 in pooled Shen and Wang datasets.

IncX4 and IncI2 plasmids are common carriers of *mcr-1* genes. In order to see if regulatory variants were prominent within these plasmids, regulatory sequence proportion were calculated in both plasmid types (*Figure 3.8b, Figure 3.8c*). Results show that variant regulatory sequences are more prevalent than consensus sequences in both plasmid types. Interestingly, certain variants seem strongly linked with particular plasmids e.g. PV3 is exclusively present on IncX4 plasmids.

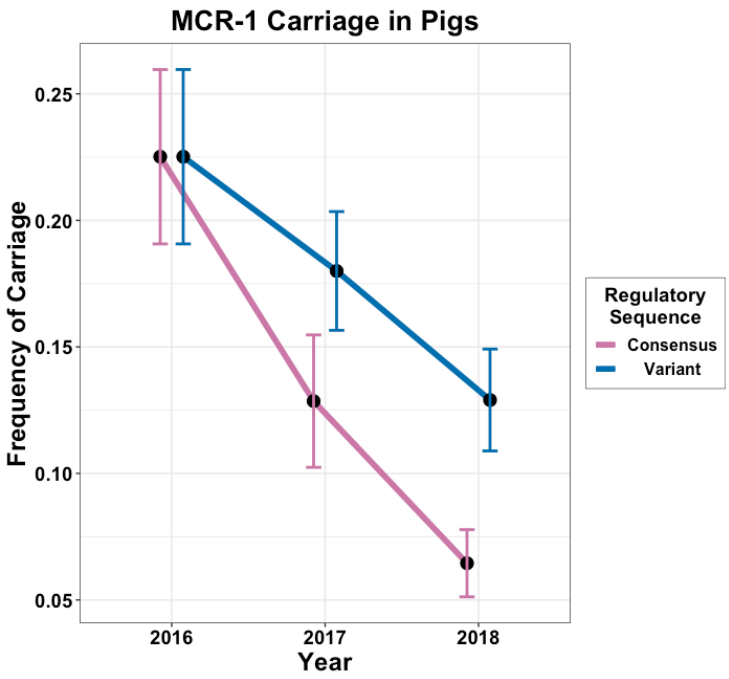


Figure 3.9: Frequency of carriage (i.e. Frequency of *mcr-1* prevalence * frequency of variant prevalence) was determined for consensus (pink) and variant (blue) sequences across the years for pig samples. Each sample was treated as an independent sampling unit.

Shen et al found that *mcr-1* prevalence significantly decreased in pig and human samples after the ban. To determine if this decrease differed for regulatory variants, the frequency of carriage was calculated for consensus and variant regulatory sequences in pig samples across the years spanning the ban (*Figure 3.9*). Results show that the frequency of MCR-1 carriage drops off more sharply for consensus regulatory sequences than variants. This suggests that loss of MCR-1 is largely driven by the decline of consensus regulatory sequences.

3.5 Discussion

It is well known that cis-acting non-coding DNA elements are important for regulating transcription and translation (Bulyk, 2005; Kumar and Bansal, 2018). Promoter sequences are crucial for RNA polymerase recruitment and transcription modulation while SD sequences pair with 16S rRNA to recruit ribosome components and initiate translation (Shine and Dalgarno, 1975; Shultzaberger *et al.*, 2007; e Silva and Echeverrigaray, 2012; Saito, Green and Buskirk, 2020). In this chapter, I show that mutations in both promoter and SD sequences increase overall fitness and colistin resistance of *mcr*-1-positive E. *coli*. Additionally, by analysing more recent datasets, I show that regulatory variants are increasing in prevalence

among *mcr-1*-positive sequences. Additional variants were identified in these datasets, however, those experimentally investigated in this study remain the most prevalent (*Table 3.S2*). -35 box variants were also seen but are uncommon partially due to this region being associated with large changes in its sequence depending on genetic background.

All observed variants were predicted to reduce the rate of transcription or translation (*Table 3.S1*), and these *in-silico* predictions are well supported by measurements of MCR-1 expression (*Figure 3.4*) and activity (*Figure 3.5*). PV1 was the only exception as gene expression and activity measurements were generally similar to or higher than the consensus. As a thymine to adenine change is less drastic than the introduction of a guanine, it is possible that PV1 makes too small of an impact to be distinguished from the consensus. Furthermore, PV1 shows consistent similarity to the consensus in the growth rate, MIC and competitive fitness measurements. Surprisingly, SDV4 also reduced *mcr-1* transcript levels despite not affecting the promoter sequence (*Figure 3.4*). However, SD sequences have previously been shown to effect downstream processing of mRNA and transcript stability (Wagner *et al.*, 1994; Bhattacharyya *et al.*, 2018; Wakabayashi, Warnasooriya and Ermolenko, 2020). It is possible that SDV4 has similar effects which could be misinterpreted as a reduction in gene expression. Nevertheless, reduced *mcr-1* transcription is well correlated with relative fitness suggesting that this metric is a good predictor of competitive regulatory variant fitness (*Figure 3.7a*).

As SD variants are involved in post-transcriptional processes, methods other than RT-qPCR were needed to determine if SD variants led to changes in MCR-1 levels. Surface charge assessment were used as a proxy of MCR-1 activity as the protein reduces anions on gram-negative bacterial membranes (Stojanoski *et al.*, 2016). All SD variants showed increased relative surface charges when compared to the consensus which indicates reduced MCR-1 activity (*Figure 3.5*). This increase in charge was also seen in promoter variants that showed reduced *mcr-1* transcript levels (*Figure 3.4*, *Figure 3.5*). Interestingly, variants show charges similar to or exceeding those obtained for chromosomally integrated *mcr-1* (copy number = 1) despite being present on pSEVA plasmids and therefore having a copy number of >1 in bacterial cells. These results suggest that regulatory variants reduce transcription/translation of *mcr-1* to a level below that of a singular *mcr-1* copy with consensus regulation. Although the general trend shows that increased surface charge is associated with increased

competitive fitness, linear models don't obtain significance (*Figure 3.7c*) which may be due to the error associated with surface charge measurements. Surface charge was positively correlated with growth rates (*Figure 3.S2b*) suggesting that it is a strong predicter of individual variant fitness.

The increased colistin resistance regulatory variants was unexpected. As these variants reduced MCR-1 expression and activity, it was hypothesised that they would also reduce colistin resistance. However, 6/8 of the regulatory variants showed increased in colistin resistance. Additionally, *mcr-1* expression was negatively correlated with colistin resistance in linear models (*Figure 3.S2a*). A potential explanation is that regulatory variants have a reached an optimum equilibrium between MCR-1 activity and fitness costs from its production. Increased resistance gene expression is not always positively correlated with increased antibiotic resistance (Palmer and Kishony, 2014). Once reaching a certain level of expression, further increases may not lead to resistance changes but still increase fitness costs. Therefore, limiting gene expression might keep resistance levels largely similar but increase overall fitness which could produce a higher MIC. As MCR-1 compromises the structural integrity of *E. coli* membranes, reduced production/activity of MCR-1 might reduce membrane permeability making variants less prone to colistin damage (Yang *et al.*, 2017). Another important note is that MCR-1 originated as a single copy chromosomal gene which was moved to multi-copy plasmids. As single copy costs are low and also show increased MICs (*Figure 3.3*), regulatory variants might be recovering ancestral levels of expression through cis-regulatory mutations that reduce expression level. Overall, results suggest that the *mcr-1* consensus regulatory sequence has yet to reach the optimal trade-off between resistance and fitness. This may explain why regulatory variants are more prominent in recent datasets (*Figure 3.8a*). Interestingly, regulatory variants are more prominent in sequences lacking both *mcr-1* flanking ISApl1 (*Figure 3.S3*), further associating them with more recent evolutionary adaptations.

Chromosomally integrated *mcr-1* containing consensus regulatory sequences regularly showed increased fitness and resistance than its plasmid located counterpart (*Figure 3.3*). However, chromosomal integration of *mcr-1* is not regularly seen in nature and presence of *mcr-1* is still highly plasmid associated (Shen *et al.*, 2020; Liu *et al.*, 2021). Since *mcr-1* is found

within composite transposons, it is surprising that integration of *mcr-1* is not more common due to the increased fitness and resistance benefits it provides (Wang *et al.*, 2018; He *et al.*, 2019). One possible reason is that regulatory variants on plasmids may be fitter and quicker to produce than chromosomal integrations of *mcr-1*. Furthermore, transposable elements required for integrations often contain additional promoters which may cause increased expression located upstream of *mcr-1.* Plasmids carrying *mcr-1* are often large and carry multiple uncharacterised genes which may provide unknown benefits to *E. coli* hosts.

Although the experimental system has been altered to mimic natural conditions of *mcr-1*, pSEVA does not contain multiple elements present on natural *mcr-1* plasmids. Natural plasmids contain factors that are not investigated in this study such as neighbouring genes (e.g. PAP2), natural origin of transfers and other elements that may have unknown effects on the *mcr-1* regulatory sequences and variants (Sun *et al.*, 2018). One way to test this would be to introduce regulatory variants into natural *mcr-1* plasmids and repeat assessments to determine if variants have similar effects. However, the current study provides a clear insight on regulatory variant effects in the absence of confounding factors.

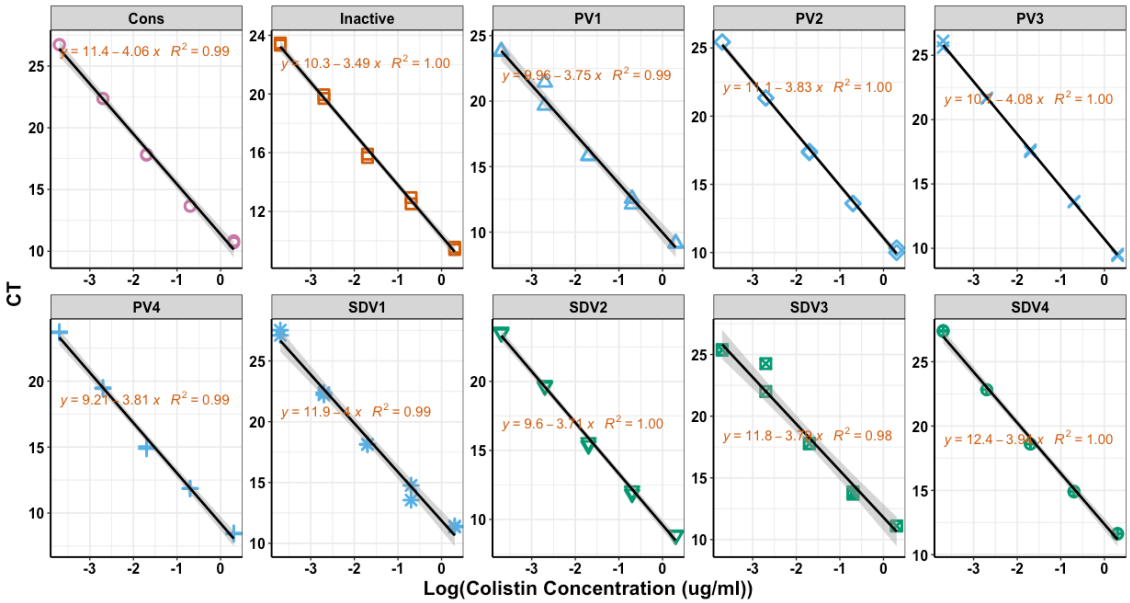
Unlike the structural variations investigated in data chapter 1, there is clear evidence that regulatory variants have increased fitness. Although the general levels of *mcr-1*-positive isolates is reducing due to government implemented colistin bans, regulatory variant prevalence is increasing in *mcr-1*-positive sequences (*Figure 3.8a*) and frequency of carriage calculations show that regulatory variants are declining at slower rates than consensus sequences in pig hosts (*Figure 3.9*). However, sequence results from recent datasets show that the most prevalent variants are not necessarily the fittest. Both PV4 and SDV4 gave high fitness and resistance scores but less fit variants such as SDV3 and PV1 are relatively common. This suggests that surveillance data does not simply reflect selection and fitness capacity of variants but likely also reflects other factors such as linkage and timing of variant incidence. Variants such as SDV1 and PV2 are more commonly seen in IncI2 plasmids while the hugely common PV3 variant is exclusively found in IncX4. This strong linkage could play an important role in determining the prevalence of regulatory variants.

The general takeaway from this chapter is that regulatory variations increase fitness and are increasing in prevalence. However, it is unclear whether these variants are examples of compensatory evolution. Previous examples of compensation are found within protein sequences and result in fitness increases by altering protein function. Additionally, compensatory mutations usually recover fitness costs without altering resistance but the identified regulatory mutations increase fitness and resistance. Evolution induced alterations in gene regulation have previously been shown to increase resistance and/or compensate for fitness costs caused by environmental/antibiotic stressors (Depardieu *et al.*, 2007; Stoebel *et al.*, 2009; Patel and Matange, 2021). However, no examples of compensatory adaptation via antibiotic gene expression alterations were found. Therefore, rather than compensation, regulatory variants could be examples of fine-tuning of *mcr-1* expression to obtain optimum cost to resistance ratios.

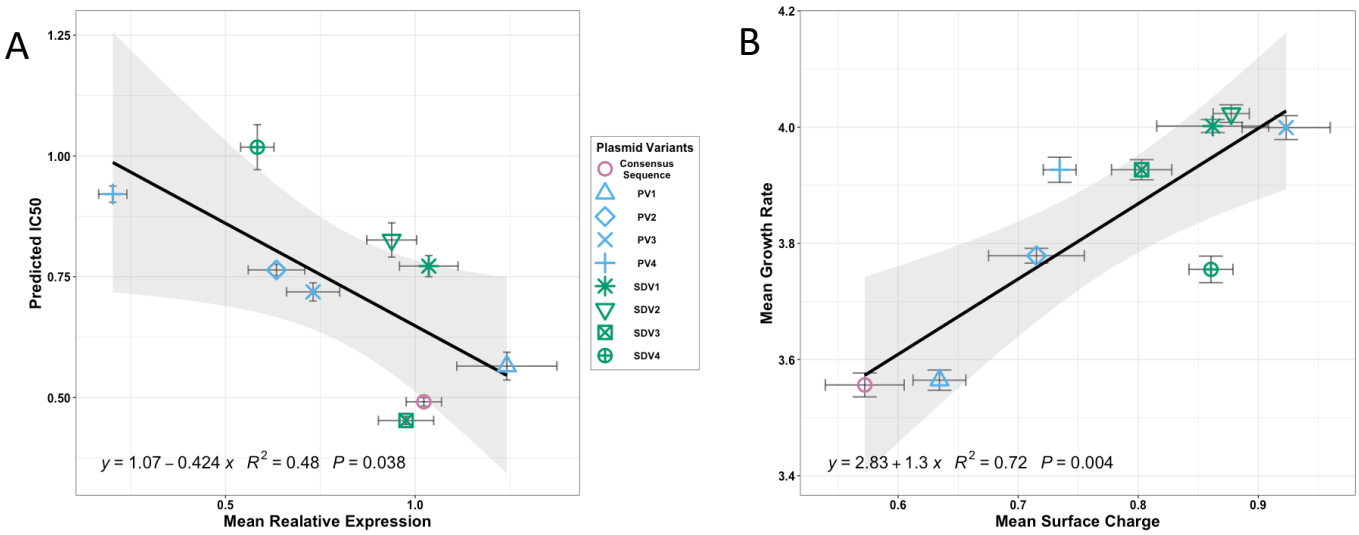
3.6 Supplementary Information

Regulatory Variant	***Promoter Assessments***				***Shine-Dalgarno Assessments***	
	BacPP Score (100)	BacPP Score (75)	BacPP Score (25)	DeNovoDNA Transcription Initiation Rate (au) (100)	DeNovoDNA Translation Initiation Rate (au) (35)	DeNovoDNA Translation Initiation Rate (au) (45 + full *mcr-1*)
Consensus	**72.375**	**86**	**40**	**7419.839125**	**832.0925053**	**708.14**
PV1	69.5625	81	45	5311.77532	-	-
PV2	67.5625	77	36	4313.308475	-	-
PV3	70.4375	77	31	4204.091093	-	-
PV4	69.0625	77	31	4788.265912	-	-
SDV1	-	-	-	-	526.1665373	526.17
SDV2	-	-	-	-	526.1665373	526.17
SDV3	-	-	-	-	526.1665373	526.17
SDV4	-	-	-	-	253.7995844	145.25

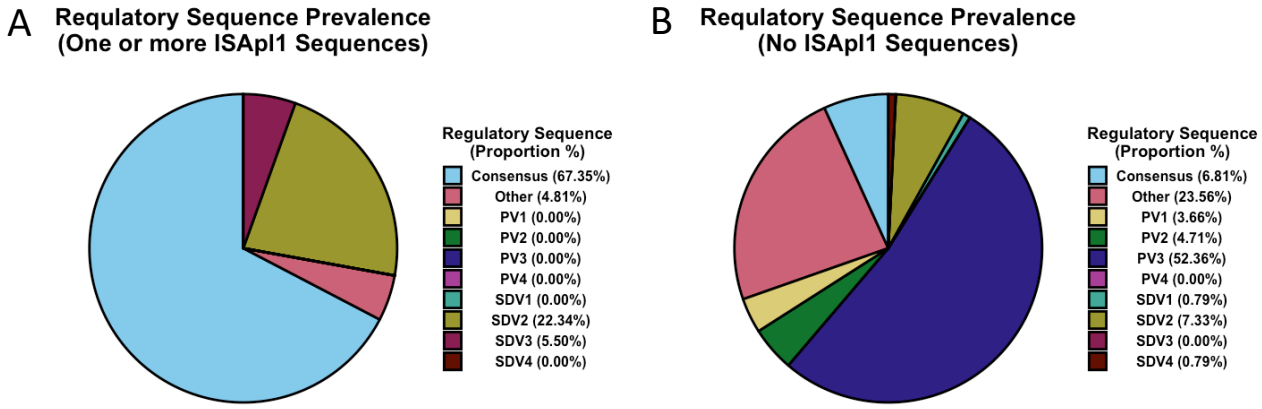
Supplementary Table S3.1: Scores obtained for promoter and Shine-Dalgarno using *In-Silico* analysis. Numbers in brackets indicate query length (in base pairs).



Supplementary Figure 3.S1: Graph shows qPCR CT values obtained (y-axis) for each qPCR in known target plasmid concentrations (x-axis, Log10 Scale) n=6. Blank lines show linear regression models fitted to the data with confidence intervals in grey shading. Line equations and R-squared values for each regression line are shown in brown.



Supplementary Figure 3.S2: Scatterplot showing correlations between (A) relative expression (x-axis) and predicted IC50 prediction (DRC model e-coefficient, y-axis) and (B) surface charge (x-axis) and growth rate (y-axis) of regulatory variants and controls. Points assigned to particular variants/controls are shown in the legend (error bars = SE). Blank lines show linear regression models fitted to the data with confidence intervals in grey shading. Regression line equations, model r-squared and p-values indicated in black text.



Supplementary Figure 3.S3: Pie charts show proportion of regulatory variants found on sequence reads (**A**) with or (**B**) lacking ISApl1 sequences in Shen dataset. Percentage proportion of regulatory sequences is indicated.

Variant Name	Location	Variant Prevalence in Dataset						Sequence
		All Datasets	Wang	Shen (Total)	Shen (2016)	Shen (2017)	Shen (2018)	
Consensus	NA	521	225	268	150	90	29	AAAATTGCAGTATAATTGCCGCAATTAT CCCACCGTTTATTTTTTGAGTAGTTTCTC
PV1	-10 promoter box	78	63	14	4	7	3	AAAATTGCAGTA**A**AATTGCCGCAATTAT CCCACCGTTTATTTTTTGAGTAGTTTCTC
PV2	-10 promoter box	32	14	18	7	8	3	AAAATTGCAGTA**G**AATTGCCGCAATTAT CCCACCGTTTATTTTTTGAGTAGTTTCTC
PV3	-10 promoter box	231	31	200	57	81	29	AAAATTGCAGTAT**G**ATTGCCGCAATTAT CCCACCGTTTATTTTTTGAGTAGTTTCTC
PV4	-10 promoter box	2	2	0	0	0	0	AAAATTGCAGTATA**G**TTGCCGCAATTAT CCCACCGTTTATTTTTTGAGTAGTTTCTC
SDV1*(including SNP1)	Shine-Dalgarno + Mid	80	46	34	15	16	3	both SDV1*(without SNP1) and SNP1 (CAATTATCCCACCGTTTATTTTTTGA**T**T AGTTTCTC)
SDV1*(without SNP1)	Shine-Dalgarno	22	19	3	0	2	1	AAAATTGCAGTATAATTGCCGCAATTAT CCCACCGTTTATTTTTTGA**T**TAGTTTCTC
SDV2	Shine-Dalgarno	142	41	93	45	35	13	AAAATTGCAGTATAATTGCCGCAATTAT CCCACCGTTTATTTTTT**A**A**A**TAGTTTCTC
SDV3	Shine-Dalgarno	38	22	16	4	10	2	AAAATTGCAGTATAATTGCCGCAATTAT CCCACCGTTTATTTTTTGA**A**TAGTTTCTC
SDV4	Shine-Dalgarno	8	5	3	1	1	1	AAAATTGCAGTATAATTGCCGCAATTAT CCCACCGTTTATTTTTTG**C**GTAGTTTCTC
SNP1	From Mid to SD	58	27	31	15	14	2	AAAATTGCAGTATAATTGCC**A**CAATTAT CCCACCGTTTATTTTTTGA**T**TAGTTTCTC
SNP2	Mid: Between -10 and SD	14	6	8	2	4	2	AAAATTGCAGTATAATTGCCGCAATTAT **A**CCACCGTTTATTTTTTGAGTAGTTTCTC
SNP3	Mid: Between -10 and SD	2	2	0	0	0	0	AAAATTGCAGTATAATTGCCG**T**AATTAT CCCACCGTTTATTTTTTGAGTAGTTTCTC
SNP4	Mid: Between -10 and SD	4	3	1	0	1	0	AAAATTGCAGTATAATTGCCGCAATTAT CCC**G**CCGTTTATTTTTTGAGTAGTTTCTC
SNP5	Mid: Between -10 and SD	6	0	0	0	0	0	AAAATTGCAGTATAATTGCCGCAATTAT CCCACCGTTT**G**TTTTTTGAGTAGTTTCTC
SNP6	Shine-Dalgarno	1	0	1	0	1	0	AAAATTGCAGTATAATTGCCGCAATTAT CCCACCGTTTATTTTTT**A**AGTAGTTTCTC
SNP7	Mid: Between -10 and SD	5	0	5	3	2	0	AAAATTGCAGTATAATTGCCGCAATTAT C**A**CACCGTTTATTTTTTGAGTAGTTTCTC
Consensus (including -35)	NA	459	208	224	135	69	21	TTGTACTGGATTTCTTAAAAAATTGCA GTATAATTGCCGCAATTATCCCACCGT TTATTTTTTGAGTAGTTTCTC
SNP8	-35 promoter box	13	6	6	0	4	2	TTGTACTG**A**ATTTCTTAAAAAATTGCA GTATAATTGCCGCAATTATCCCACCGT TTATTTTTTGAGTAGTTTCTC
SNP9	-35 promoter box	4	2	2	0	2	0	**C**TGTACTGGATTTCTTAAAAAATTGCA GTATAATTGCCGCAATTATCCCACCGT TTATTTTTGAGTAGTTTCTC

Supplementary Table 3.S1: Counts of consensus and variant sequences in Shen and Wang datasets. Variant sequences are listed with variants highlighted (blue) in bold underline.

4 The Impacts of MCR-1 on Conjugation and Plasmid Maintenance

4.1 Abstract

Membrane surface charge is an important factor in enabling microbial interactions with surfaces and other bacteria. Additionally, other structural and physiochemical changes in microbial membranes can facilitate biofilm formation. MCR-1 activity is known to alter microbial LPS composition and chapter 2 work has shown that MCR-1 reduces the net surface charge of gram-negative bacterial membranes. I hypothesize that the consequences of MCR-1 activity results in increased cell-to-cell interaction due to reduced electrostatic repulsion between individual cells. I also propose that these interactions result in increased conjugation stemming from the previously characterised positive association between cellular contact and conjugation rate. In this chapter, I use optical density measurements, plate counts and fluorometric assays to determine the stabilities and transfer rates of MCR-1-positive plasmid vectors. I found a clear conjugation dependant association between the presence of functional *mcr-1*, prolonged plasmid stability and increased conjugation rates. These results have implications on the stability of MCR-1-positive plasmids in the absence of antibiotic selection.

4.2 Introduction

Horizontal gene transfer (HGT) is a major contributor to the emergence and spread of antimicrobial resistance genes (AMR) (Norman, Hansen and Sørensen, 2009). Conjugation in particular is deeply involved in the spread of AMR plasmids, some of which are conjugative and have broad host ranges (Maiden, 1998; Barlow, 2009). This allows microbes to access "ready-made" antibiotic resistance (Rozwandowicz *et al.*, 2018). In addition to conjugative genes and transfer origins (oriT), there are multiple biotic and abiotic factors that influence plasmid transfer via conjugation. Mating experiments have demonstrated that factors such

as taxonomic relatedness, temperature, growth phase, pH etc. have significant impacts on the frequency of bacterial conjugation (Fernandez-Astorga *et al.*, 1992; Alderliesten *et al.*, 2020).

Cell density and motility are important factors affecting conjugation efficiently. Studies have consistently found that conjugation happens at higher rates when cells are spatially constrained and less motile (Alderliesten *et al.*, 2020). Licht et al found that when donors and recipients were fixed in biofilms as opposed to continuous mixing, significantly higher initial plasmid transfer rates were achieved (Licht *et al.*, 1999). Furthermore, certain microbiomes have high plasmid diversity and are often viewed as conjugation hotspots (Aarts and Margolles, 2015; Shterzer and Mizrahi, 2015). Biofilms and intestinal microbiomes are also associated with reduced cellular motility and increased cell-to-cell contact therefore resulting in increased opportunity for conjugation (Giacomucci *et al.*, 2019).

Antibiotics use has been shown to stimulate conjugation in scenarios where the conjugation machinery is not constitutively expressed (Lopatkin *et al.*, 2016). In the presence of antibiotics, plasmid transfer genes can be up-regulated resulting in increased conjugative transfer (Headd and Bradford, 2018; Liu *et al.*, 2019). Antibiotics can also act as promoters of HGT in cases where trans-conjugants have a selective advantage (Lopatkin *et al.*, 2016). However, in the absence of antibiotics, it is unlikely that trans-conjugants which may be receiving costly plasmids would outcompete their susceptible counterparts (Lopatkin *et al.*, 2016). Using a mathematical model, Stewart and Levin outlined multiple conditions where costly plasmids can be maintained in the absence of selection (Stewart and Levin, 1977). They argue that lab-obtained plasmid transfer rates are too low for conjugative plasmids be maintained as selfish parasites however, it is unclear if these measurements reflect conjugation rates in natural environments. Lopatkin et al showed that common conjugal plasmids containing resistance genes had high enough conjugation rates to be maintained in the absence of antibiotic selection (Lopatkin *et al.*, 2017). Although the study involved AMR plasmids covering the six major Inc types, it is unknown whether their conjugation rates are representative of most plasmids. Furthermore, it is unclear whether these AMR plasmids persisted based on transfer rates alone or whether other factors such as compensatory adaptation or unknown effects of resistant gene cargos were involved.

As *mcr-1* is predominantly associated with plasmids, conjugation has been a key part of its widespread dissemination. Therefore, factors that increase conjugation efficiency such as association with promiscuous Inc types would lead to further spread (Sun *et al.*, 2018). In chapter 1, it was observed that MCR-1 producing cells regularly formed aggregations in liquid media and were generally "stickier" than control *E. coli*. MCR-1 activity leads to reductions of negative charges in gram-negative outer membranes which may result in reduced electrostatic repulsion between cells. Additionally, MCR-mediated changes in membrane charge and composition may have physical effects on bacterial membranes such as altering membrane stiffness. These physical membrane properties have been previously linked with biofilm formation in multiple bacterial pathogens (Renner and Weibel, 2011). I hypothesised that *mcr-1* expression may increase cell-to-cell interactions which could facilitate conjugation. This chapter focus on testing this hypothesis by studying the impact of *mcr-1* expression of cellular aggregation, conjugation rates and plasmid stability and maintenance. I find that *mcr-1* expression has measurable effects on bacterial morphology and *mcr-1*-positive *E. coli* have higher conjugation rates than *mcr-1*-negative controls. Additionally, I discovered that production of functional MCR-1 increases the long-term stability of transferrable *mcr-1*-positive plasmids. Taken together, this suggests that MCR-1 activity leads to maintenance of and *mcr-1*-positive plasmids.

4.3 Methods

Bacterial Strains, Plasmids and Growth Conditions

Cloning experiments performed during this chapter made use of pSEVA121 and the pSEVA621 cloning vectors (SEVA) provided by the Standard European Vector Architecture (SEVA) database and material repository. *E. coli* MG1655, TOP10, J53 and β3914 were used throughout this chapter (Le Roux *et al.*, 2007; Yi *et al.*, 2012). All plasmids and bacterial strains and used and constructed in this chapter are listed in *appendix table 2* and *appendix table 3* respectively.

Bacteria were grown on Luria Broth (LB) broth (Sigma-aldrich), LB Millar agar (Sigma-aldrich) plates or Mueller Hinton Broth (MH, Sigma-aldrich) either un-supplemented or supplemented

with the appropriate antibiotics depending. Bacteria were grown at 37°C/30°C in shaking (liquid culture, 250 rpm) or in standing (LB Millar agar/liquid culture) incubation.

Plasmid Construction and Cloning

Plasmids were constructed for cloning and experimental purposes (*appendix table 2*). Necessary backbones, genes and features were PCR amplified from source plasmids. Amplified fragments were Gibson assembled to form the final products using the NEBuilder® HiFi DNA Assembly Master Mix (New England Biolabs). PCR primers are listed in *appendix table 1*. Plasmids were heat-transformed into competent stains. Non-transferrable pSEVA121 and pSEVA621 were created using PCR amplification and site-directed mutagenesis (Q5® Site-Directed Mutagenesis Kit, New England Biolabs) for OriT deletions.

Donor Strain Generation

Donor strains were created that contained one of the four following plasmids:

- Empty Vector: No cargo gene. Contains OriT (conjugative)
- Inactive Vector: Inactive *mcr-1* as cargo gene. Contains OriT (conjugative)
- WT MCR Vector: Consensus *mcr-1* as cargo gene. Contains OriT (conjugative)
- Orit- MCR Vector: Consensus *mcr-1* as cargo gene. No OriT (non-conjugative).

Plasmids were either of the pSEVA121 or pSEVA621 background. Created plasmids were transformed into *E. coli* β3914 and/or MG1655.

Microscopy

TOP10 and MG1655 *E. coli* containing pBAD and pSEVA121 plasmids respectively with empty, WT *mcr-1* or inactivated *mcr-1* cargos were incubated overnight. Cell cultures were diluted and were visualised using a Nikon Eclipse TI. Representative images were taken for each *E. coli* strain and isolate type.

Flow Cytometric Measurements of Cell Aggregation

Overnight cultures of *E. coli* MG1655 and β3914 donor stains were washed and diluted in 1x diluted Phosphate-buffered saline (PBS). Flow cytometry was conducted on donors using BD Accuri™ C6 (BD Biosciences) with a threshold of FSC-H: 10,000 and SCC-H: 8,000. 10,000 events were collected for each sample.

OD Measurements and Sedimentation Tests

Sedimentation tests were conducted with pBAD positive TOP10 *E. coli* and pSEVA121 positive MG1655 *E. coli*. pBAD carrying TOP10 containing *mcr-1* genes or empty controls were grown overnight in MH2 medium. MG1655 containing *mcr-1* positive pSEVA121, inactivated *mcr-1* or empty controls were incubated overnight in MH media. Both stain sets were grown for 48 hours at 37°C with OD measurements (600nm) taken every 10 minutes. OD measurements taken at early and late exponential stage were recorded. Bacteria were resuspended following incubation and a final OD measurement was taken. Sedimentation rates were calculated by measuring the maximum slope post sedimentation over 10 measurements.

MICs and Growth Rates

Colistin MIC and growth rate measurements were used to determine the resistance and fitness of donor and recipient strains. Bacteria were incubated overnight and OD adjusted before incubating them for 16 hours at a range of colistin concentrations (0 – 8ug/ml) at 37°C or 30°C. Growth rate measurements were done in the presence and absence of plasmid selecting antibiotics (ampicillin and gentamicin). Bacteria were grown in MH media for 24 or 36 hours at 37°C or 30°C. OD measurements were taken every 10 minutes and growth rates were calculated using the maximum gradients over 10 points.

Overnight Plasmid Stability Plating Experiments

β3914 and MG1655 stains containing pSEVA121 plasmids all four donor types (see: Donor Strain Generation) were grown LB-ampicillin (100 ug/ml). Strains were OD normalised and grown in LB for 16 hours (37°C). Cultures were serially diluted and plated on ampicillin supplemented (100 ug/ml) and un-supplemented LB agar. Colonies were counted for each donor stain and condition. Plasmid loss was confirmed for a subset of colonies using PCR.

Construction of Fluorescent Recipient Strains

Kanamycin resistant (KanR) red florescent (mKate2) MG1655 and chloramphenicol resistant (CmR) green florescent (msfGFP) β3914 recipient strains were made for use in plating and flow cytometry conjugation experiments respectively.

P1 transduction was used to make recipient MG1655 KanR, mKate2 strains. AB1157 *E. coli* containing mKate2 (AB1157 ΔflhD, Tn7::mKate2, gift from Uphoff lab, (Uphoff, 2018)) were incubated with P1 phage. Phase separation was used to obtain P1 lysate which was used for to transduce MG1655 cells. Transduced cell suspensions were plated on kanamycin selective plates to obtained colonies with the Tn7 cassette inserted in the glmS transcriptional terminator. Colonies were confirmed for the desired alleles by selective plating and microscopy.

Gibson assembly and lambda red recombineering was used to make β3914 CmR msfGFP recipient strains. CmR and msfGFP genes were cloned into pSEVA621. The Cmr-msfGFP cassette was amplified and transformed into MG1655 containing pKD46 to enable chromosomal integration of this cassette in replacement of the lacZ (β3914 ΔLacZ::CmR, msfGFP). Desired alleles were confirmed using plating, PCR, sequencing and microscopy.

Conjugation Rate Measurements

Two sets of conjugation rate assessments were performed. The first set used β3914 containing pSEVA121 plasmids with empty or WT *mcr-1* cargos as donors and J53 as a recipient. The secound set used β3914 containing pSEVA121 plasmids with empty, WT *mcr-1* or inactivated *mcr-1* cargos as donors and MG1655 (KanR, mKate2) as a recipient.

Donor and recipient strains were streaked incubated in the presence of selective antibiotics. Overnight cultures were diluted and grown to late exponential phase. Donor and Recipient cells were plated onto selective agar plates and incubated overnight at 37° to obtain T0 plate counts. Cells were then washed and resuspended in NaCl (0.9%). Donor and recipient cells were then mixed 1:1 ratio and incubated for 2 hours in LB. Mixed cultures were serially diluted and plated onto selective LB agar plates and incubated to obtain T1 plate counts for donor,

recipient and trans-conjugant cells. Donor conjugation rates were calculated using the Simonsen end-point method via the following equation:

$$Conjugation\ Rate\ (\gamma_{ep}) = \psi_{max}(N - N_0)^{-1} \ln\left\{1 + \frac{T * N}{D * R}\right\}$$

Where N = total cell count (CFU/ml) at T1, N_0 = total cell count (CFU/ml) at T0, T= trans-conjugant cell count (CFU/ml), D = donor cell count (CFU/ml) and R = recipient cell count (CFU/ml). ψ_{max} refers to the sum of TCs, donors and recipients for T0 and Tf in CFUs/ml and is calculated using the following equation:

$$\psi_{max} = \ln\left\{\frac{[total\ CFUs\ per\ ml\ at\ T1]}{[total\ CFUs\ per\ ml\ at\ T0]}\right\} \Big/ T1 - T0$$

Trans-conjugate to donor (TC:D) ratios for each conjugation were also calculated using plate counts of donors and TCs

RFP Passage and Stability Experiments

mScarlet (red florescent) was cloned into the cargo region of pSEVA621 ($Gent^R$). Plasmids of all four donor types (see: Donor Strain Generation) were generated using pSEVAE6S1-mScarlet as a backbone and subsequently transformed into β3914. RFP donors were OD normalised and grown in gentamicin supplemented (50 ug/ml) and un-supplemented MH media. 200ul of liquid culture was used for OD (595nm) and RFP measurements (Ex:595, Em:620). Cultures were also plated on gentamicin supplemented (50 ug/ml) and un-supplemented LB agar plates and incubated for plate counts. Donor cultures were passaged in the absence of gentamicin selection for 4 days. RFP measurements, OD measurements and plate counts (LB agar) were obtained for each subsequent passage.

Flow Cytometry Based Conjugation Experiments

Conjugation passage experiments were done using pSEVA621-mScarlet plasmids of all four donor types and β3914 ΔLacZ::CmR, msfGFP (recipient). Donors and recipients were mixed 1:1 and incubated for 24-hours at 30°C. Mixed cultures were passaged in fresh media for three

transfers. Flow cytometry and plating were used to measure donor (red, AmpR), recipient (green, CmR), TC (red and green, AmpR and CmR) and plasmid-negative donor proportions. Flow cytometry was performed for initial mixtures and all passages. Mixtures were diluted (x10,000) in PBS and recorded on a Cytoflex LX (Beckman) machine. Fluorescent marker compensation, event gating and data analysis was carried out using FlowJo™ v10 software (BD Biosciences). Samples were initially gated on FSC-A/SSC-A plots using a threshold of 8000 and 5000 respectively. Donor, recipient, TC and plasmid-negative donor populations were selected based on presence or absence of fluorescence in 488-527/40 (mScarlet) and 561-601/20 (msfGFP) channels (*Figure 4.S4*). Compensation was performed for each run using fresh pure cultures of donor, recipient, TC and plasmid-negative cells. A minimum of 3,000 events were recorded for each mixed culture sample. Selective plating was carried out for the final transfers of all passage experiments to obtain donor, recipient and TC CFU counts.

4.4 Results

4.4.1 Effects of *mcr-1* Overexpression on TOP10 *E. coli* Growth and Behaviour

While using pBAD expression vectors, it was regularly observed that MCR-positive TOP10 *E. coli* formed visible and surface adherent aggregations in liquid culture while control cultures remained planktonic. Additionally, this phenomenon was not observed in uninduced cells carrying pBAD-*mcr-1* plasmids suggesting that is was an MCR-1 specific effect. Phase-contrast microscopy images show that MCR-1+ cells form large aggregates in liquid suspension while control cells rarely interact (*Figure 4.1a*).

Although microscopy suggests that MCR-1 leads to enhanced cell aggregation, it is difficult to measure this phenotype quantitatively using image analysis alone. To tackle this problem, I analysed growth curves of control and MCR-1-positive TOP10 *E. coli* (*Figure 4.1b*). Induced cells carrying pBAD-*mcr-1* showed clearly altered growth kinetics when compared to uninduced and empty vector controls. The reduced exponential growth rate was expected and discussed in chapter 2. However, significant reductions in ODs of induced MCR-positive cells were observed (*Figure 4.1b*). To quantify this effect, the maximum gradient observed past the 9-hour timepoint (referend hereafter as sedimentation rate, (Trunk *et al.*, 2018)) was calculated for induced (0.02% Arabinose) and uninduced TOP10 *E. coli* carrying pBAD-*mcr-1*

or empty controls (*Figure 4.1c*). Significant decreases in sedimentation rates were seen for induced MCR-positive E. coli. Furthermore, this effect decreased upon induction with 0.002% arabinose suggesting that this effect is correlated with the level of *mcr-1* expression (results not shown).

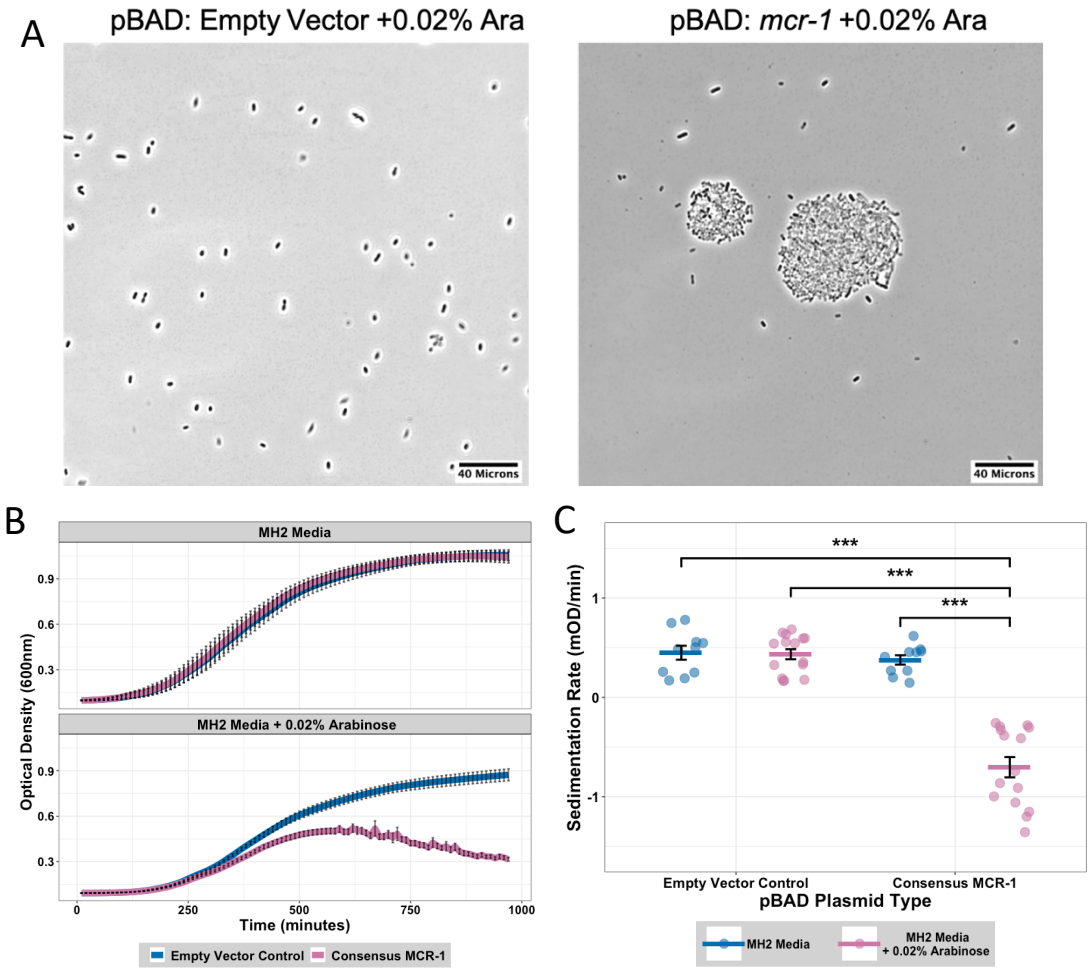


Figure 4.1: Effect of MCR-1 on TOP10. (**A**) Representative images of induced TOP10 carrying empty (left) or *mcr-1*-positive (right) pBAD plasmids. Scale bars are shown on the bottom left. (**B**) Growth curves (OD measurements over time) of control (blue) and *mcr-1*-positive (pink) TOP10 *E. coli* in the presence (n=15) and absence (n=8) of 0.02% arabinose. Error bars (black) show standard error (**C**) Sedimentation rates of control and *mcr-1* positive TOP10 *E. coli* in the presence (pink, n=15) and absence (blue, n=8) of 0.02% arabinose. (p-values: ***<0.001, Tukey's range test, black error bars show standard error, line at mean)

4.4.2 Aggregation Analysis of MG1655 and β3914

Although results using pBAD vectors suggest that *mcr-1* expression and activity leads to cell aggregation, *mcr-1* overexpression due to high pBAD copy-number and gene expression

complicates the validity of this connection. To counter this, microscopy experiments were repeated using MG1655 carrying *mcr-1*-positive and control pSEVA121 plasmids (*Figure 4.2*). Although the effect was less clear than pBAD results, cells with active MCR-1 formed distinct aggregates which were not seen in empty vector and inactive MCR-1 controls. This suggests that native expression of active *mcr-1* also results in cell aggregation.

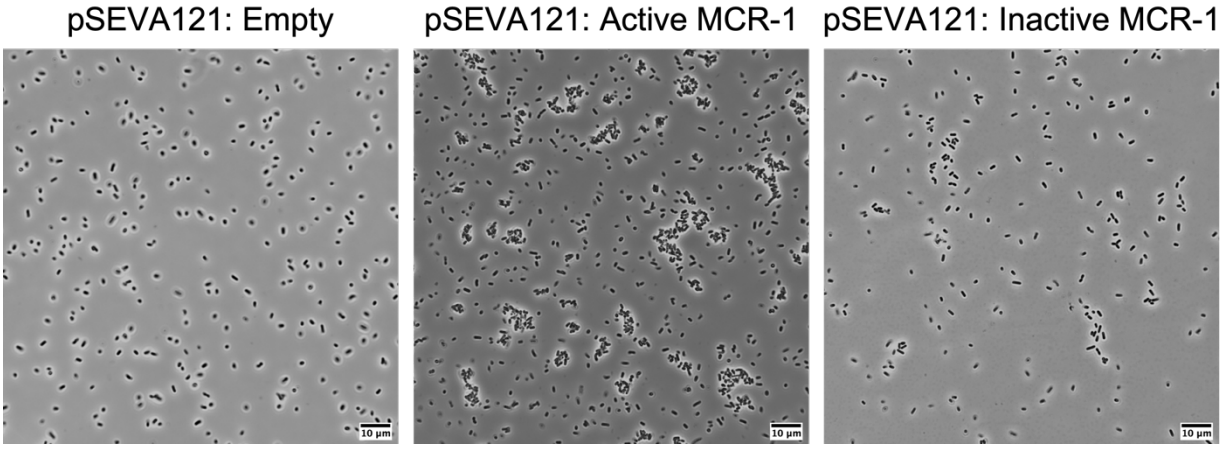


Figure 4.2: Effect of native *mcr-1* expression on MG1655. Representative images of MG1655 carrying empty pEVA121 (left), pEVA121 with active MCR-1 (middle) or pSEVA121 with inactivated MCR-1 (right). Scale bars are shown on the bottom left.

As aggregate formation decreases the OD of surrounding media, OD measurements were used quantify the MCR-1 induced this effect in MG1655 and β3914. The post stationary phase of MG1655 and β3914 cultures were analysed to obtained sedimentation rates (*Figure 4.3a*). Results show that MG1655 strains expressing *mcr-1* have an inconsistent yet stark reduction in their sedimentation rates when compared to cells carrying inactivated *mcr-1* or empty controls. However, this MCR-1 specific sedimentation effect is not seen in β3914 as all three plasmid types obtain similar rates. Despite this, MCR-1 positive β3914 *E. coli* have clear growth kinetic differences when compared to empty controls as their OD plateau at much lower values (*Figure 4.S1*). Therefore, it would seem that active MCR-1 severely impacts post-stationary phase growth kinetics of *E. coli*, either in the form of aggregate formation and sedimentation in MG1655 or via dramatically reduced final ODs in β3914.

To confirm that the low ODs of active MCR-1 producing MG1655 was due to increased cell sedimentation rather than other factors (e.g. cell death), OD measurements were taken after

resuspension of stationary phase cells (*Figure 4.3b*). Results show that MG1655 carrying active *mcr-1* had more dramatic changes between their peak and final ODs when compared to inactive *mcr-1* or empty vector controls. Additionally, all cell types had highly similar resuspended ODs suggesting that these reductions are not a result of cell death.

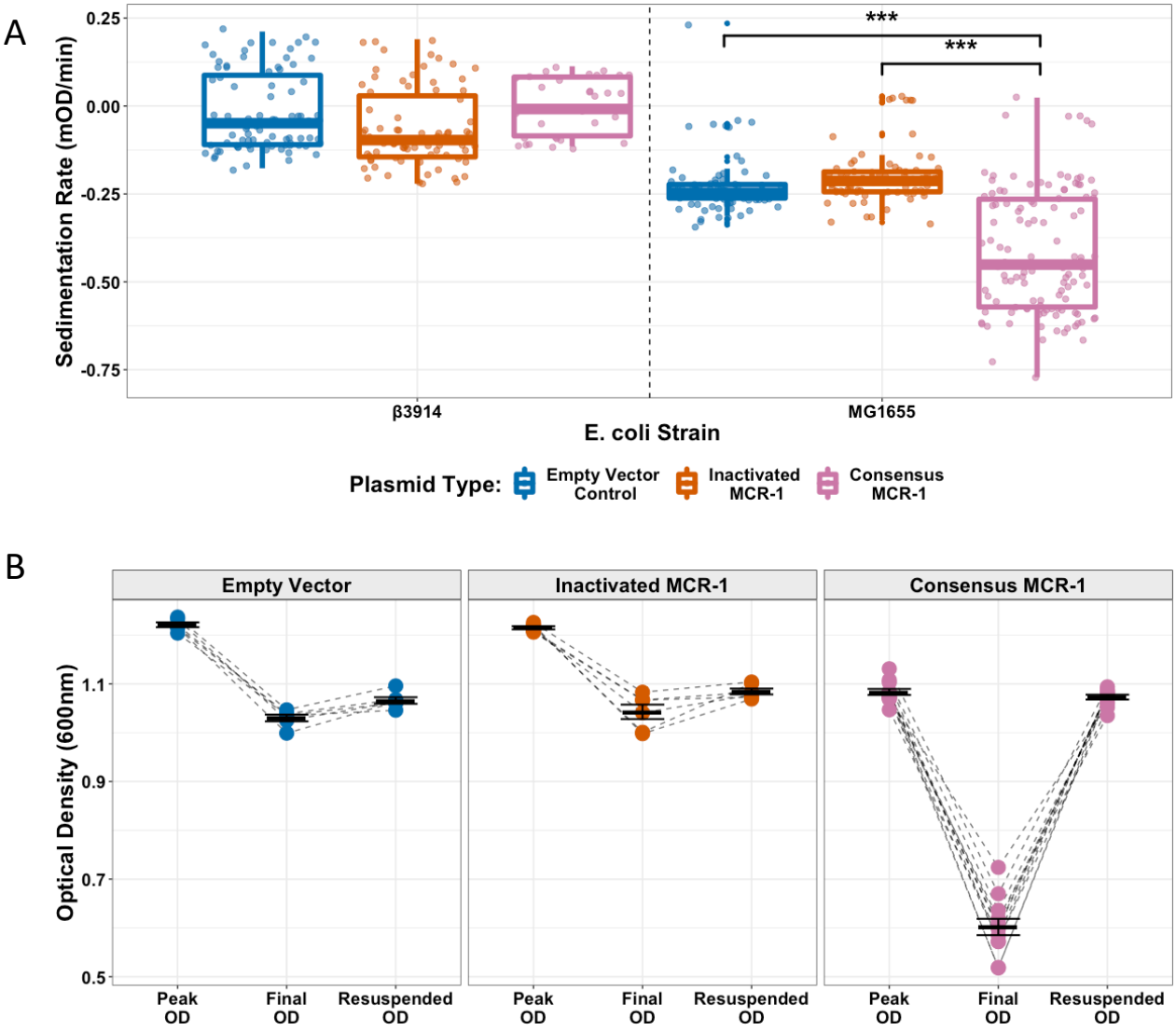


Figure 4.3: OD analysis of *mcr-1* positive MG1655 and β3914 strains. (**A**) Boxplots show sedimentation rates of empty (blue), inactive (orange) and *mcr-1* positive (pink) MG1655 and β3914 *E. coli* (n=30-100, p-values: ***<0.001, Tukey's range test, error bars =SE, line at mean). (**B**) OD measurements obtained for MG1655 carrying empty, inactivated and functional *mcr-1* at different growth stages. Measurements reflect the peak OD values, final OD values and resuspended OD values. Dotted lines connect individual repeats. (n=6, error bar=SE, line at mean)

Although OD results quantified aggregation in bulk culture, turbidity measurements are more unreliable at later phases of bacterial growth due to the presence of debris and dead cells.

Unlike OD, flow cytometric methods are able to distinguish live cells from dead cell debris (Pan *et al.*, 2014; Trunk *et al.*, 2018). Additionally, particle forward scatter (FSC) can be used to determine particle size meaning if MCR-1 increases cell aggregation, this size increase would be detectable by flow cytometry. Thusly, flowcytometric measurements were done for MCR-1-positive and control MG1655 and β3914 *E. coli*. Results show that cells containing enzymatically active MCR-1 had a significantly higher FSCs than inactivated and empty vector controls (*Figure 4.4*). These results support previous assessments and suggests that active MCR-1 either makes larger aggregations or causes aggregation to become more common. Interestingly, cells carrying inactivated MCR-1 show marginally increased FSC in some cases which may indicate that this aggregation effect could be influenced by the presence of a membrane integrated protein.

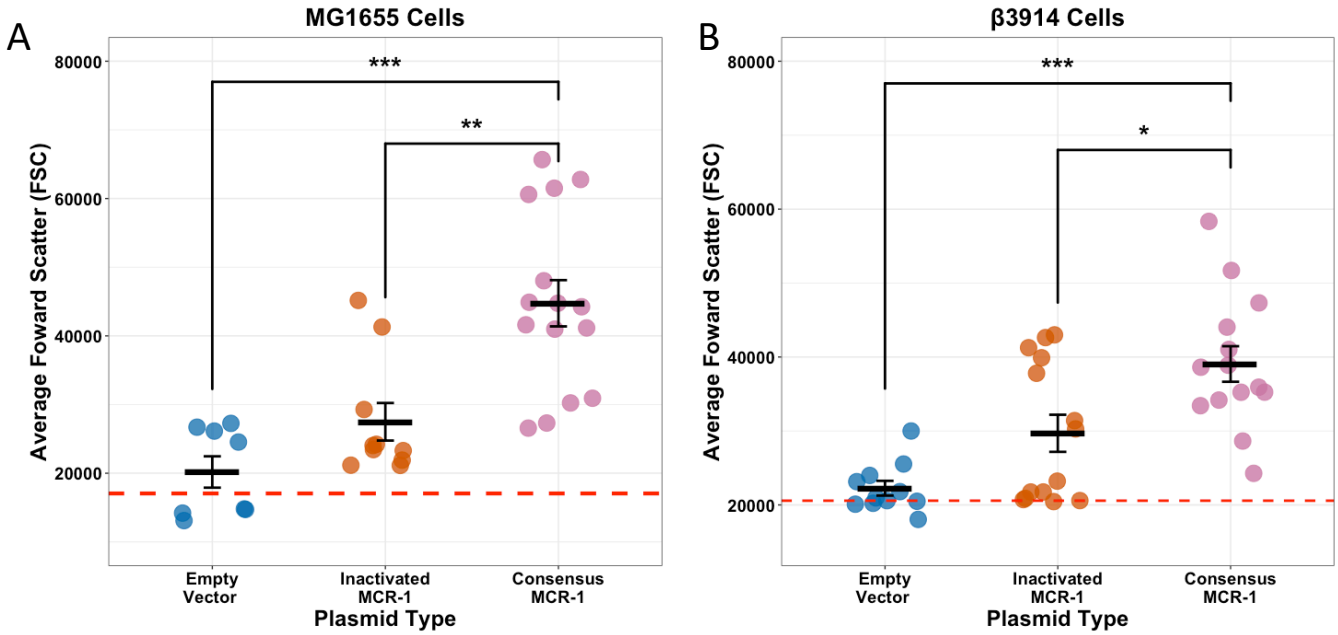


Figure 4.4: Individual (points) and mean (line) forward scatter (FSC) are indicated for (**A**) MG1655 and (**B**) β3914 *E. coli* carrying either empty vector (blue), inactivated (orange) or functional (pink) *mcr-1*. Dashed red line indicates the mean FSC of MG1655/β3914 *E. coli* without pSEVA plasmids. (n=8-15, p-values: ***<0.001, **<0.01, * <0.05, Tukey's range test, error bars show standard error, line at mean)

4.4.3 Donor *E. coli* Construction and Analysis

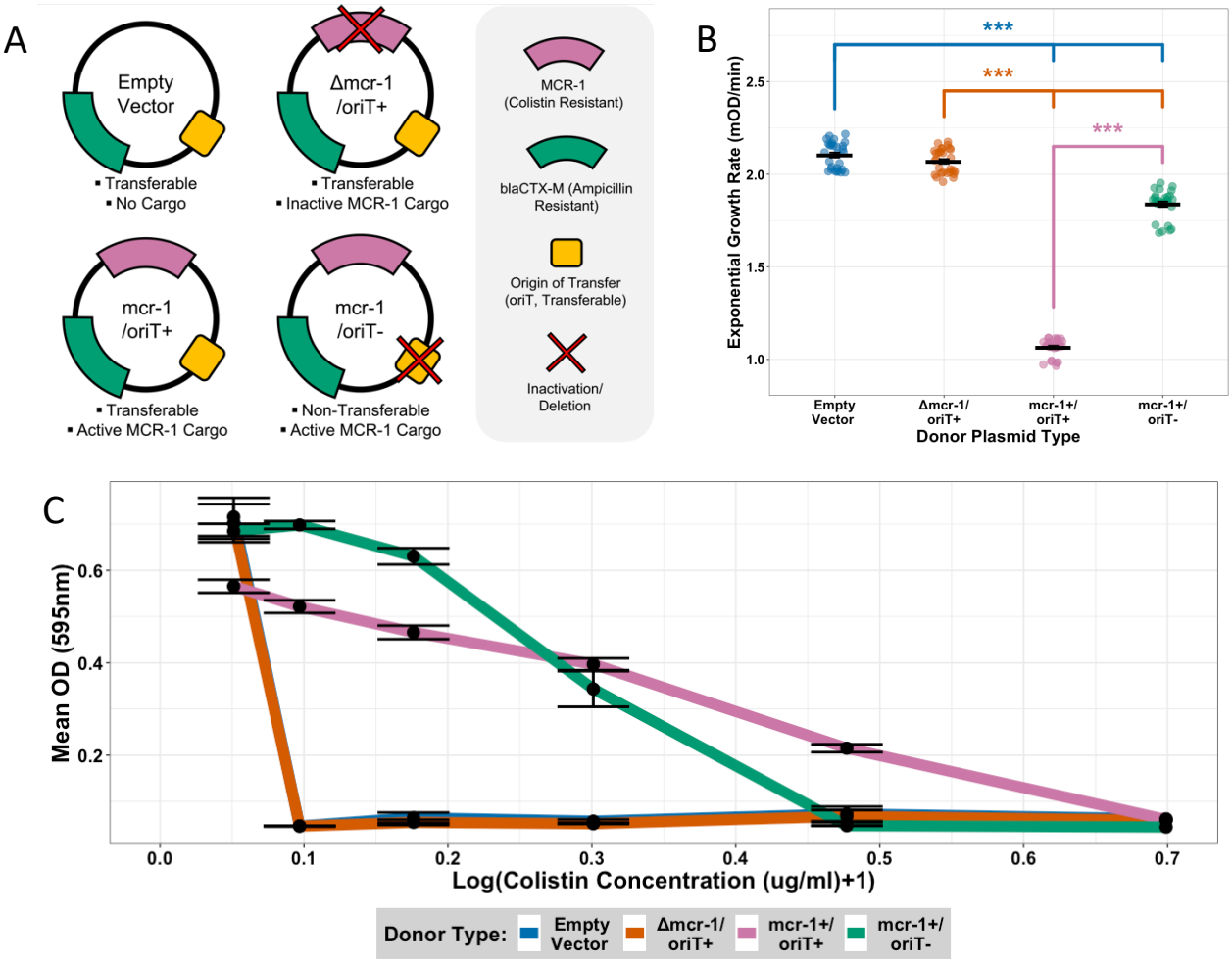


Figure 4.5: Creation and fitness/resistance of β3914 pSEVA121 donors. (**A**) Schematic representations of pSEVA121 donor plasmids created. The four donor plasmids are empty vector, Δ*mcr-1*/oriT+, *mcr-1*+/oriT+ and *mcr-1*+/oriT-. Plasmid features are also noted. (**B**) Growth rates of β3914 carrying empty (blue), Δ*mcr-1*/oriT+ (orange), *mcr-1*+/oriT+ (pink) and *mcr-1*+/oriT- (green) plasmids (n=28, p-values: ***<0.001, Tukey's range test, colour of significance brackets indicate left most donor being compared, error bars=SE, line at mean) (**C**) OD results in a range of colistin concentrations (0-8ug/ml, Log10 Scale) for β3914 carrying empty (blue), Δ*mcr-1*/oriT+ (orange), *mcr-1*+/oriT+ (pink) and *mcr-1*+/oriT- (green) plasmids (n=4, error bars=se, point at mean).

From previous experiments, it is clear that MCR-1 expression increases cell-to-cell interaction. I wanted to test the hypothesis that these interactions led to increased conjugation of MCR-1+ plasmids. To test this, MCR-1 positive and control donor stains were constructed. β3914 strains were selected as donors due to their chromosomal carriage of the RP4 conjugation machinery which allowed conjugative transfer of oriT-positive (mobilizable) pSEVA plasmids. Additionally, their autotrophic dependence on diaminopimelic acid (DAP) allowed counter-

selection in plating experiments. oriT sequences were deleted from pSEVA121-*mcr-1* plasmids to create non-mobilizable controls. This resulted in four donor plasmid types (*Figure 4.5a*): (**1**) transferable empty vector controls, (**2**) transferable plasmids expressing inactivated *mcr-1* (Δ*mcr-1/*oriT+), (**3**) transferable plasmids expressing functional *mcr-1* (*mcr-1+*/oriT+), and (**4**) non-transferable plasmids expressing functional *mcr-1* (*mcr-1*+/oriT-). Fitness and resistance assessments of β3914 donors carrying one of the 4 donor plasmid types unsurprisingly showed that *mcr-1* expression results in decreased growth rates (*Figure 4.5b*) and increased colistin resistance (*Figure 4.5c*). Interestingly, costs of MCR-1 in *mcr-1*+/oriT- donors are significantly lower than their oriT+ counterparts (*Figure 4.5b*). These donors also show slightly reduced colistin resistance levels (*Figure 4.5c*).

To determine if the higher fitness observed in *mcr-1*+/oriT- donors was due to the oriT deletion, deletions were performed on empty and inactive *mcr-1* vectors (*Figure 4.S3*). Results show that although the difference is larger for cells with active MCR-1, oriT deletions gave fitness increases for all three plasmid types (*Figure 4.S3*). Conjugation assays using oriT- donor plasmids confirmed that these plasmid types failed to produce trans-conjugants (data not shown) therefore confirming that deleting these sequences successfully eliminated transfer of donor plasmids.

4.4.4 Assessments of Donor Plasmid Stability

An optimal balance between plasmid transfer rate and the factors influencing plasmid loss (e.g. segregational loss/purifying selection) is important for the maintenance of costly plasmids in the absence of selection pressures (Hall *et al.*, 2017). If the aggregate phenotype of MCR-1-positive cells leads to increased conjugation, we would expect *mcr-1*+/oriT+ plasmids to have increased stability than Δ*mcr-1/*oriT+ or *mcr-1*+/oriT- plasmids in antibiotic-free media. To assess the impacts of MCR-1 on the stability of transferrable plasmids, β3914 of the 4 donor types were cultured in antibiotic-free media and subsequently plated on selective (+100ug/ml Ampicillin) and non-selective plates. Plate count results show that *mcr-1*+/oriT+ plasmids were maintained while ∆*mcr-1*/oriT+ and *mcr-1*/oriT- plasmids were largely unstable (*Figure 4.6a*). These results suggest that carriage of functional MCR-1 and oriT is necessary for short-term stability of costly plasmids.

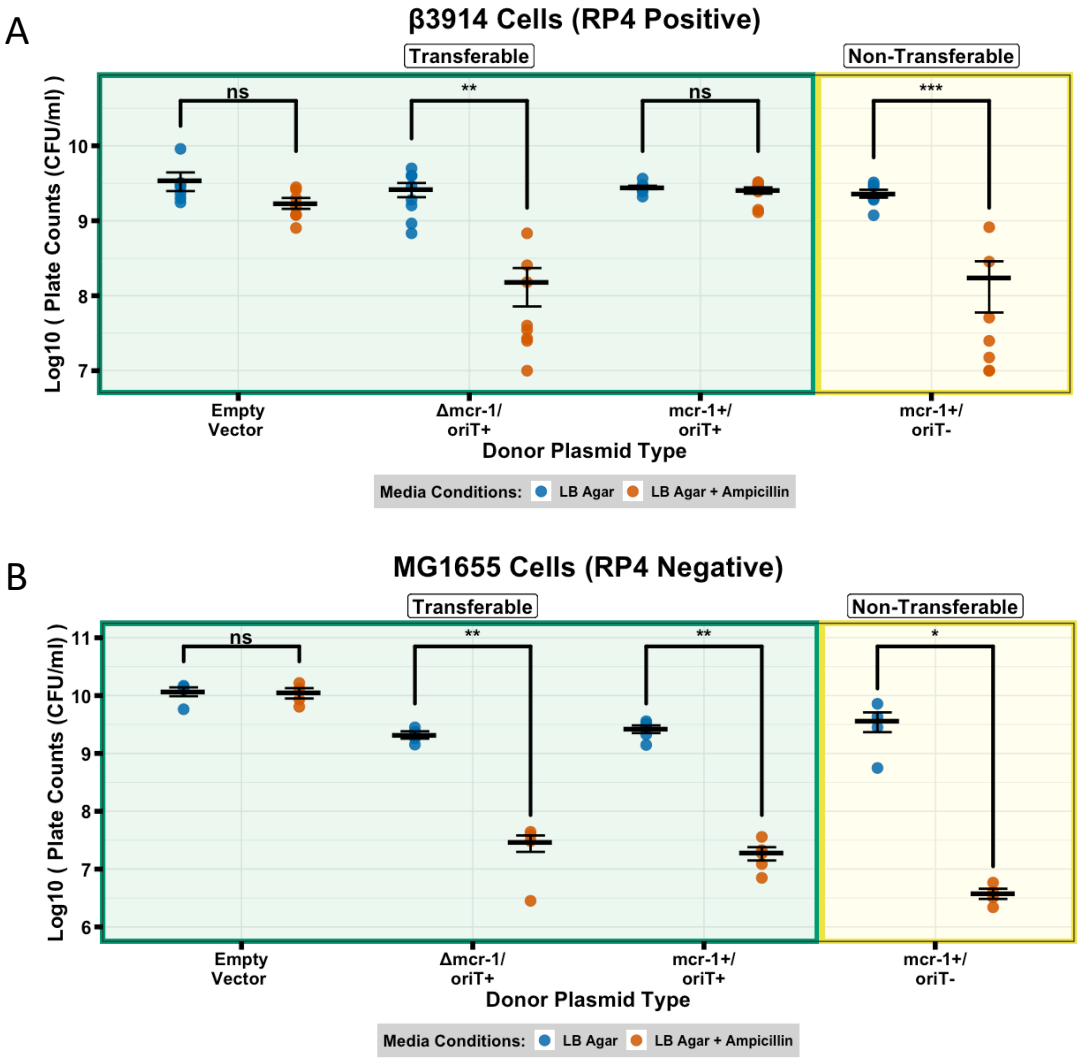


Figure 4.6: β3914 and MG1655 plasmid stability assessments. Plate counts for (**A**) β3914 (**B**) MG1655 donors carrying empty Δ*mcr-1*/oriT+, *mcr-1*+/oriT+ and *mcr-1*+/oriT- plasmids are shown in the absence (blue) and presence (orange) of ampicillin (100ug/ml) selection. Shaded regions show transferable (green) and non-transferable (yellow) plasmids. (n=7-9, p-values: ***<0.001, **<0.01, *<0.05, pairwise t-test with Bonferroni method adjustment, error bars = SE, line at mean).

To determine if this stability effect was due to conjugation, stability experiments were repeated with MG1655 cells which lack the RP4 conjugation machinery (*Figure 4.6b*). Results show that *mcr-1*+/oriT+ MG1655 had drastic decreases in plasmid maintenance when compared to their β3914 counterparts. This strongly suggests that the conjugation is the reason for the increased maintenance of *mcr-1*+/oriT+ plasmids.

4.4.5 Conjugation Rate Measurements

Although plate counts strongly suggest that conjugation is the mechanism driving the observed increases in *mcr-1*+/oriT+ plasmid stability, I wanted to determine the extent to which MCR-1 influenced plasmid conjugation. The Simonsen "End-point" method was used to estimate plasmid transfer rates with empty vector and *mcr-1*+/oriT+ β3914 (ΔdapA, Sm^R) as donors and J53 (NaN_3^R) as recipients (Simonsen *et al.*, 1990). Selective plate counts were used to calculate conjugation rates (CFU/hour) and Transcojugant:Donor (TC:D) ratios with results blocked for day-to-day variations (*Figure 4.7a*).

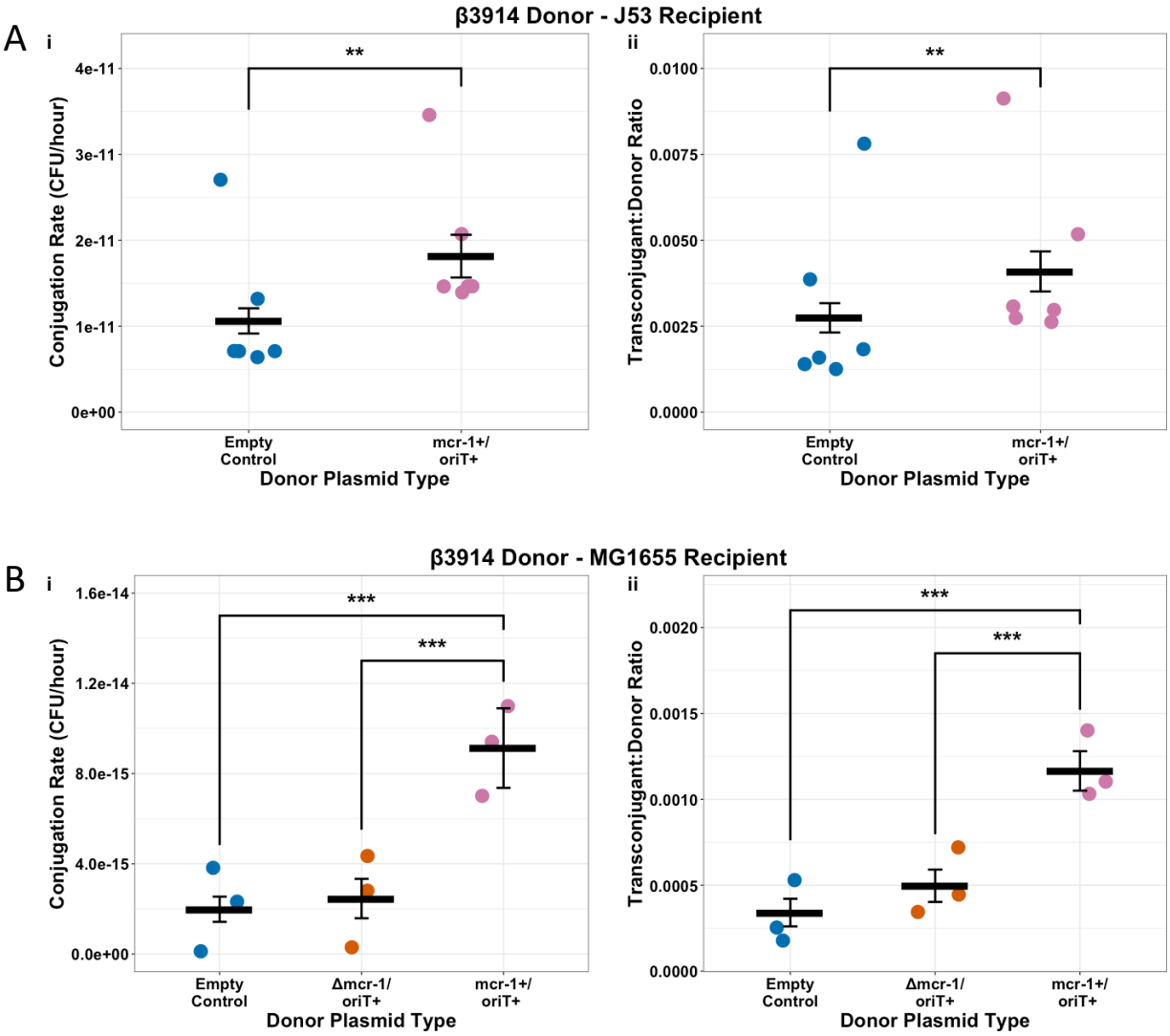


Figure 4.7: Conjugate rate (**i**) and TC:D (**ii**) estimations using J53(**A**) and MG1655 (**B**) recipients. (**A**) β3914 donors carrying empty (blue) and *mcr-1*+/oriT+ (pink) plasmids were inoculates with J53 recipients. 25 separate conjugative mixes per plasmid were plated for (i) conjugation rate and (ii)TC:D assessments. Results were blocked for day-to-day variation (n=5, p-values: ***<0.001, **<0.01, Type II ANOVA with Sidak correction for multiple comparisons, error bars = SE, line at mean) **(B)** β3914 donors carrying empty (blue),

Δ*mcr-1/*oriT+ (orange) and *mcr-1*+/oriT+ (pink) plasmids were inoculates with MG1655 recipients. 9 separate conjugative mixes per plasmid were plated for **(i**) conjugation rate and **(ii**) TC:D assessments. Results were blocked for day-to-day variation (n=3, p-values: ***<0.001, Type II ANOVA with Sidak correction for multiple comparisons, error bars = SE, line at mean)

Results show that *mcr-1*+/oriT+ plasmid achieved higher conjugation rates and TC:D ratios, suggesting that MCR-1 increases the rate of plasmid transfer. However, as empty vectors do not carry cargos, it was unclear whether this was due to the presence of a membrane protein or the specific action of MCR-1. To determine whether the observed transfer rate increase was due to MCR-1 activity, further conjugation rate assessments were done using empty vector, Δ*mcr-1/*oriT+ and *mcr-1*+/oriT+ β3914 donors and MG1655 (Kan^R, mKate2) recipients. Results were once again blocked for day-to-day variability in experiments (*Figure 4.7b*). Conjugation rates and TC:D ratios were consistently higher in cultures containing *mcr-1*+/oriT+ donor plasmids. These results strongly suggest that it is the activity of MCR-1 that is causing the higher rate of plasmid transfer. Additionally, these results are replicable for two different recipient strains (J53 and MG1655) showing that the effect of MCR-1 on conjugation is not restricted to a particular *E. coli* strain.

4.4.6 Fluorometric Assessments of Plasmid Stability

Previous assessments have definitively shown that the action of MCR-1 leads to increased conjugation and stability of transferable plasmids. However, it is unclear if these effects lead to the long-term stability of these plasmids in the absence of selection pressures. To determine this, I generated fluorescent donor plasmids which allowed us to rapidly track the transfer and/or loss of donor plasmids in the absence of selection. pSEVA621-mScarlet vectors (RP4 oriT, $Gent^R$) of the four donor plasmid types were constructed (*Figure 4.8a*) and their phenotypes confirmed with subsequent MIC and growth rate assessments (*Figure 4.S3*).

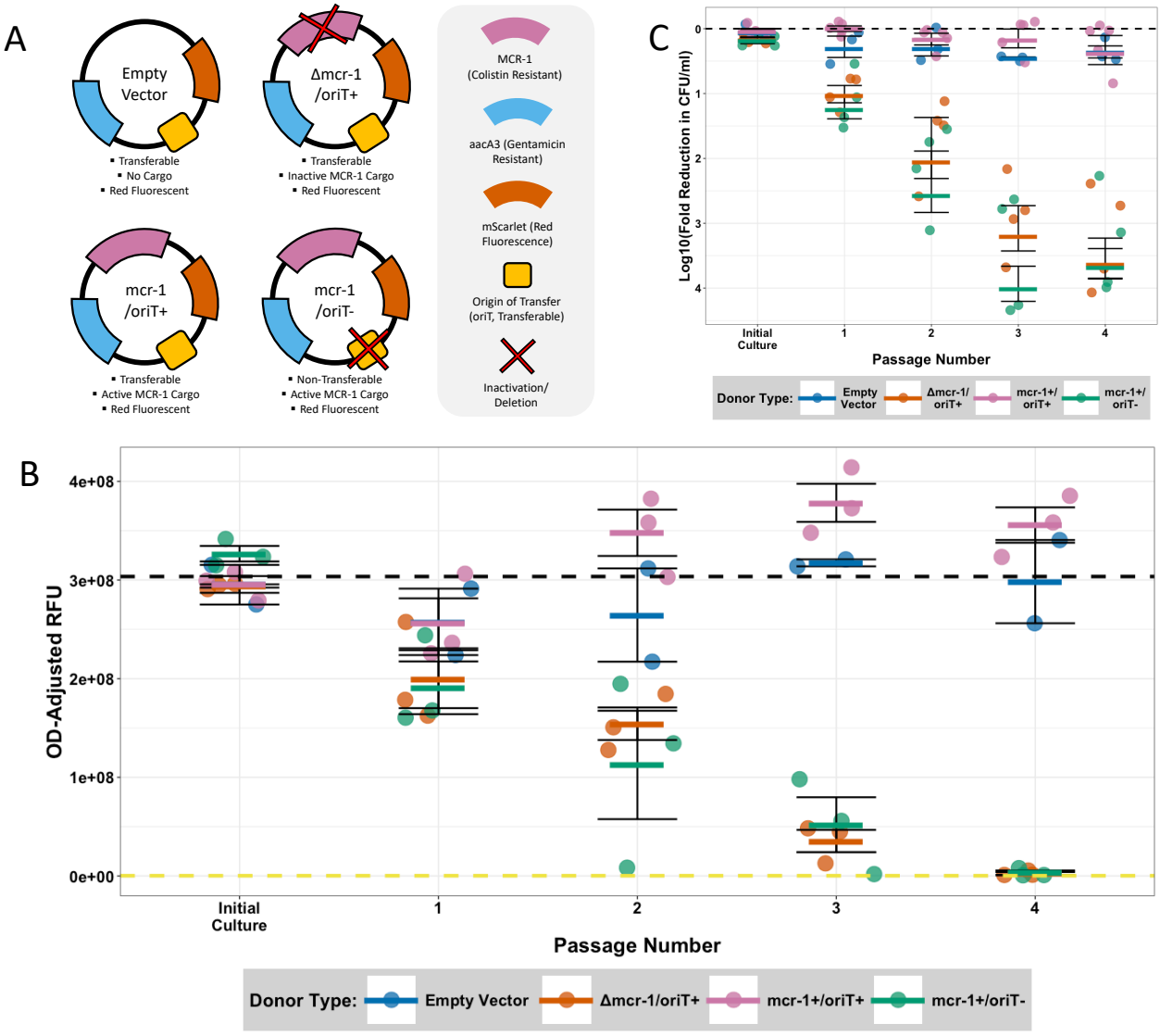


Figure 4.8: mScarlet+ β3914 Donor stability analysis. (**A**) Schematic representations of pSEVA627-mScarlet donor plasmids created. The four donor plasmids are empty vector, Δ*mcr-1*/oriT+, *mcr-1*+/oriT+ and *mcr-1*+/oriT-. Plasmid features are also noted. (**B**) OD adjusted RFU values for β3914 strains carrying mSacrlet+ empty (blue), Δ*mcr-1*/oriT+ (orange), *mcr-1*+/oriT+ (pink) and *mcr-1*+/oriT- (green) plasmids are shown for all passages and initial cultures (n=2/3, error bars = SE, line at mean, black dotted line at y= $3x10^8$ showing average initial OD-adjusted RFU, yellow line at y= $3x10^4$ showing background OD-adjusted RFU using mScarlet- bacteria). (**C**) Fold reduction between LB agar and LB agar + gentamicin plate counts for β3914 strains carrying mSacrlet+ empty (blue), Δ*mcr-1*/oriT+ (orange), *mcr-1*+/oriT+ (pink) and *mcr-1*+/oriT- (green) plasmids for all passages and initial cultures (n=3-5, error bars = SE, line at mean, black dotted line at y=0 i.e. no fold reduction)

To measure the long-term stability of donor plasmids, β3914 carrying fluorescent donor plasmids were grown in the presence of gentamicin selection and subsequently passaged four

times without selection. Fluorescence and OD measurements allowed quantification of mScarlet as a proxy of plasmid prevalence (*Figure 4.8b*). Results show that the OD adjusted RFU measurements for empty and *mcr-1*+/oriT+ plasmids remain as high as initial values for the duration of the serial passage experiments. In contrast, RFU values for donors carrying Δ*mcr-1*/oriT+ and *mcr-1*+/oriT- plasmids rapidly decline to background levels by passage 4. Initial and passaged donor liquid cultures were also plated on LB gentamicin agar which allowed estimations of fold reduction in observed colonies (*Figure 4.8c*). Results largely mirror RFU measurements as empty and *mcr-1*+/oriT+ plasmids are maintained while counts for gentamicin resistant Δ*mcr-1*/oriT+ and *mcr-1*+/oriT- donors drastically reduce after 4 transfers. Taken together, these results show that MCR-1 activity is required for the efficient transfer and maintenance of transferable *mcr-1* positive plasmids.

4.4.7 Fluorometric Assays of Passaged Conjugation Cultures

From previous experiments, it is clear that active MCR-1 increases the short and long-term plasmid stability of transferable plasmids (*Figure 4.6, Figure 4.8*). Additionally, strains carrying active MCR-1 demonstrate increased plasmid conjugation rates (*Figure 4.7*). Due to these results, I hypothesised that despite its cost, transferable and/or conjugative MCR-1-positive plasmids would have increased plasmid persistence in mixed populations. To test this, I measured the persistence of *mcr-1*+/oriT+ plasmids compared to non-transferable and no MCR-1 controls in conjugation-based passage experiments. Previously described β3914 pSEVA621-positive donors (*Figure 4.8a*) as well as newly constructed β3914 ΔLacZ::CmR, msfGFP recipients were used to conduct passage experiments with fluorometric outputs (*Figure 4.9*). In brief, donors and recipients mixed cultures were incubated in standing liquid LB culture and subsequently passaged three times without selection. Fluorometric measurements were made for initial mixes and passaged cultures allowing estimation of donors (mScarlet), recipients (msfGFP), trans-conjugants (mScarlet+ msfGFP) and plasmid-negative “uncoloured” donors in mixed populations (*Figure 4.10*, *Figure 4.S5*). Calculating event percentage within the specified gates quantified the proportion of each cell type in populations containing empty (*Figure 4.10a*), Δ*mcr-1*/oriT+ (Fig.10b), *mcr-1*+/oriT+ (*Figure 4.10c*) and *mcr-1*+/oriT- (*Figure 4.10d*) donor plasmids.

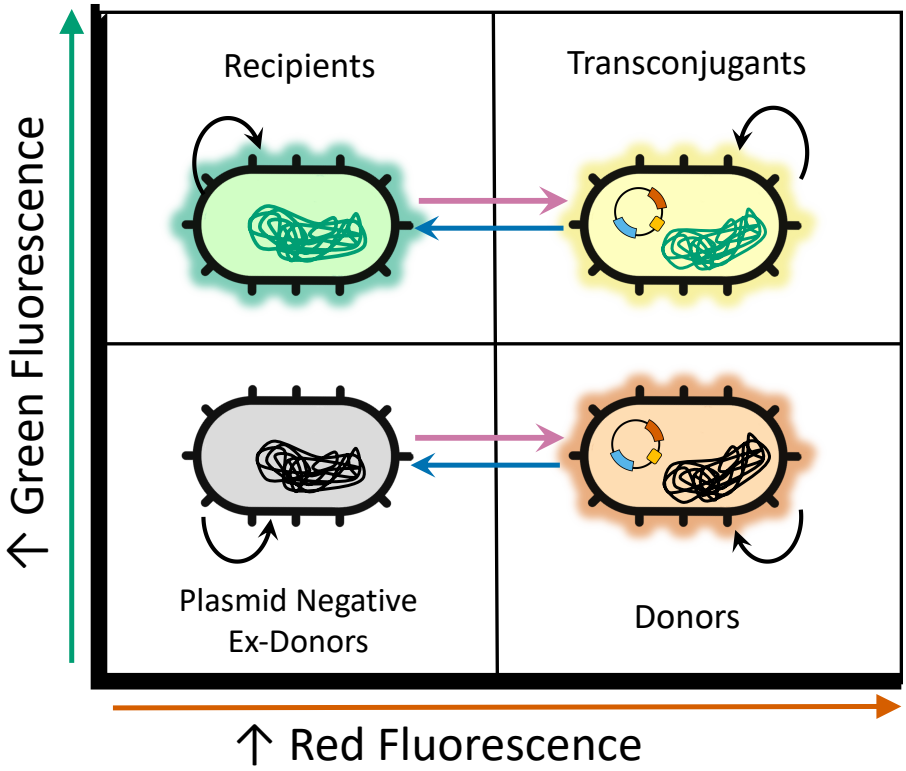


Figure 4.9: Schematic illustrates properties of cell populations involved in fluorometric conjugation assays. Coloured arrows in right panel represent conjugation (pink) plasmid loss (blue) and cell growth (black).

Results show that during the course of 3 transfers, donors carrying *mcr-1*+/oriT+ were largely maintained in the mixed culture populations (*Figure 4.10c*). This level of maintenance is still lower than that of empty vector controls (*Figure 4.10a*) but far exceeds the donor proportions of Δ*mcr-1*/oriT+ and *mcr-1*+/oriT- conjugation passage cultures (*Figure 4.10b, Figure 4.10c*). By day 3, mean donor percentages had declined to below 10% for all Δ*mcr-1*/oriT+ and *mcr-1*+/oriT- populations. Additionally, the plasmid-negative ex-donor cell fraction rapidly dominates these populations. The plasmid-negative ex-donor cell fraction also rises in empty and *mcr-1*+/oriT+ populations but this rise is much slower and confirms previous results showing increased stability of empty and *mcr-1*+/oriT+ plasmids. Although transconjugant levels remain low in all tested populations, *mcr-1*+/oriT+ and empty vector populations maintain their TC populations at around 1% of the total population across all passages. Conversely, Δ*mcr-1*/oriT+ and *mcr-1*+/oriT- TC populations rapidly decline to undetectable levels in subsequent transfers. Overall, the low TC levels combined with the abundance and prolonged maintenance of *mcr-1*+/oriT+ donors suggest that donor-donor transfer is the key driver of plasmid stability.

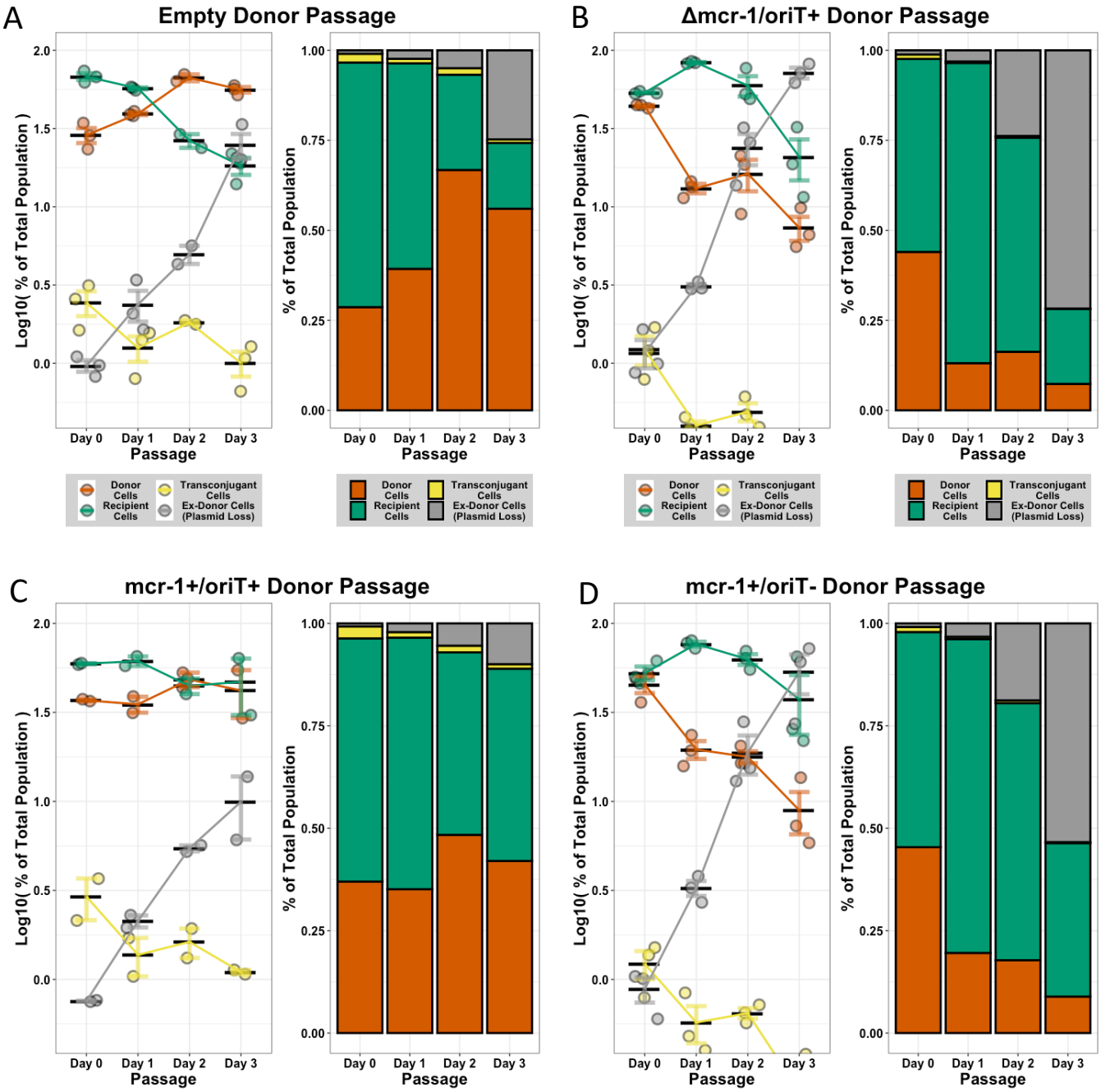


Figure 4.10: Individual and summary flow cytometry results from standing conjugation transfer experiments are shown for populations containing empty (A, n=3), Δ*mcr-1*/oriT+ (B, n=3), *mcr-1*+/oriT+ (C, n =2) and *mcr-1*+/oriT- (D, n=3) plasmids. Scatter plot points show percentage of total population for donor (orange), recipient (green), TC (yellow), and plasmid-negative ex-donor (grey) cells. (black line at mean, error bars = SE, points show values for individual populations, coloured lines connect the means). X axes show passages number. Y-axes for scatter plots show log10 percentage proportion of the total population and are constrained at a minimum of 0.5% and a maximum of 100%. Stacked bar plot y-axes show percentage of total population for donor (orange), recipient (green), TC (yellow), and plasmid-negative ex-donor (grey) cells as individual bars.

4.5 Discussion

MCR-1 activity reduces the negative surface charge of bacteria and previous studies have shown that MCR-1-positive bacteria demonstrate altered morphologies. I aimed to study the consequences of these features on cell interaction and plasmid maintenance. I hypothesised morphological and electrostatic differences in MCR-1-positive bacteria would result in increased cell-to-cell contact which would potentially alter their conjugative ability. Through in-depth analysis of MCR-1-positive and control *E. coli*, it is clear that the presence of a functionally active MCR-1 causes increased cell-to-cell contacts. Additionally, transferable *mcr-1*-positive plasmids demonstrated increased stability, conjugation rates and long-term plasmid maintenance.

The reduction of membrane surface charge by MCR-1 activity was demonstrated experimentally in Chapter 2. Initial observations with pBAD vectors showed that *mcr-1* expression was correlated with increased cell-to-cell interaction and sedimentation. *E. coli* carrying functional MCR-1 formed visible biofilm like aggregations in liquid culture and plate colonies were noticeably viscus in comparison to MCR-1 negative *E. coli*. In this chapter, the association of native *mcr-1* expression with increased aggregation was quantitively proven by OD-based sedimentation assays (*Figure 4.3*) and flow cytometric assessments of cell size (*Figure 4.4*). Additionally, I have shown that the presence of functional MCR-1 increases conjugation rates and plasmid stability of transferrable plasmids but exactly how it causes this is unclear. One possible explanation for the aggregative phenotype is that the reduction of electrostatic repulsion between MCR-1-positive cells leads to increased cell-to-cell contact which in turn increases in conjugation rates. Membrane charges have been previously shown to be important for cell adhesion and the initial stages of biofilm formation as these stages are largely influenced by van der Waals forces and electrostatic interactions between bacterial cell walls and surfaces (McClaine and Ford, 2002; Vigeant *et al.*, 2002). Due to the reductions of negative charges on MCR-1-positive bacterial membranes, it is possible that this effect could also extend to interactions with other bacteria and therefore be facilitating the observed increases in cellular adhesion. As adhesive behaviour induced by electrostatic interactions is lost in media of high ionic strength, studying MCR-1-positive cells in media of

different salt could determine if the aggregative behaviour is associated with MCR-1 mediated changes to the physiochemical properties of bacterial cell membranes.

The observed aggregate phenotype may also be caused by factors other than reduced surface charge. MCR-1 activity result in the addition of pEtN groups to gram-negative outer membranes which could have unknown effects on the structural composition and properties of bacteria. Previous studies show that altering LPS composition can change bacterial behaviour including enhancing biofilm formation (Nakao *et al.*, 2012; Chalabaev *et al.*, 2014). Additionally, other Lipid A modifications have been shown to promote biofilm formation and increase in vivo biofilm survival (Chalabaev *et al.*, 2014; Segev-Zarko *et al.*, 2018). Although Δ*mcr-1*/oriT+ donors did not show increased conjugation rates and plasmid stability, cells producing inactivated MCR-1 did exhibit some mild aggregative properties (*Figure 4.2, Figure 4.4*). It is possible that the production of a membrane protein alone might cause changes in bacterial behaviour but a mechanism for how this increases cell aggregation is unclear.

Previous studies show that plasmid transfer happens at higher rates when cells are in close proximity, likely due to increased opportunity as cells encounter each other more frequently. Although donor populations in *mcr-1*+/oriT+ maintained high levels in fluorometric passage experiments, TC populations remained at relatively low levels and marginally decreased at each subsequent passage (*Figure 4.10b*). This suggests that although MCR-1 activity led to increased conjugation, this increase largely comes plasmid transfer among donor populations. As MCR-1 is costly, it is likely that cells would lose *mcr-1*-positive plasmids. However, reinfection of these plasmids from neighbouring donors maintains their levels in bacterial populations. As maintenance is mainly seen amoung donors, this reinfection is likely due to mother-daughter transmission as these cells are inherently in closer proximity. While other assays show that *mcr-1*+/oriT+ plasmids are increasingly transferred to confirmed non-daughter cells (*Figure 4.7*), mixed fluorometric passages suggests that mother-daughter transmission is dominant in mixed populations. These results link well to the impact of conjugation in biofilm forming communities. Previous studies show that although biofilm formation increases initial conjugation rate, this effect largely declined over time as donor bacteria were constrained. In contrast, well-mixed populations demonstrate reduced but consistent plasmid transfer rates which eventually results in all recipients obtaining plasmids

(Licht *et al.*, 1999). These results have important implications on MCR-1 epidemiology as they suggest that although this conjugative boost stabilises MCR-1 within MCR-1-positive communities, it may have limited impacts in the ability of these plasmids to transfer between strains/species.

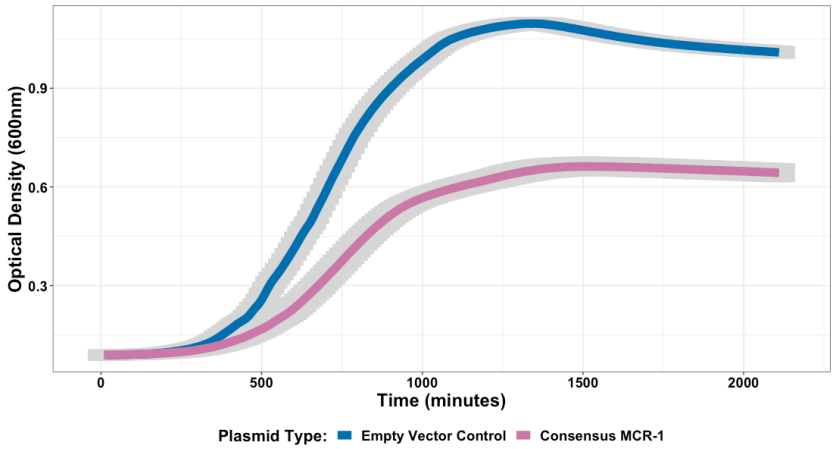
A surprising result from this study was that the deletion of oriT regions lead to fitness increases in bacterial fitness in all donor types tested (*Figure 4.5a, Figure 4.S2*). This could be due plasmid loss as oriT- plasmids are unable to be transferred via the integrated RP4 conjugation machinery. Additionally, pSEVA plasmids have lower copy numbers than traditional expression vectors and they don't contain active partitioning systems (Silva-Rocha *et al.*, 2013). This could mean that plasmid loss is being amplified in oriT- populations. Indeed, we see that *mcr-1*+/oriT- pSEVA plasmids have a higher degree of plasmid loss in the absence of antibiotic selection (*Figure 4.8, Figure 4.10d*). However, this boost in fitness is also seen in the presence of antibiotics (*Figure 4.S3b*). This result could reflect the cost of conjugation itself or could simply be due to a smaller oriT- plasmid exhibiting a lower cost of carriage. Interestingly, *mcr-1*+/oriT- plasmids also showed marginally reduced colistin resistance when compared to oriT+ counterparts. A possible reason for this is that plasmid loss due to poor partitioning and inability to transfer is still occurring in the presence of colistin selection leading to reduced resistance. Alternatively, the rapid growth of oriT- *E. coli* may result in increased colistin sensitivity. However, these conclusions contradict with chapter 3 results as reduced MCR-1 production was associated with increased resistance and exponential growth.

High variability was seen in a number of experiments carried out in this chapter. Sedimentation behaviour was not consistent in all MCR-1-positive MG1655 bacteria tested (*Figure 4.3a*) and for J53 and MG1655 recipients, conjugation transfer rates showed a high degree of day-to-day variability (*Figure 4.7*). This variability is likely due to other factors involving media composition and surrounding temperature that are hard to control for. Other studies have shown that factors such as glucose concentration, temperature and bacterial growth stage lead to large differences in conjugation rate and TC:D measurements (Lopatkin *et al.*, 2016; Hüttener *et al.*, 2022). Although results were significant without adjusting for day-to-day variations, the significance levels largely improved once taking this variation into account. Other variabilities seem to stem from strain differences. While, TOP10 and MG1655

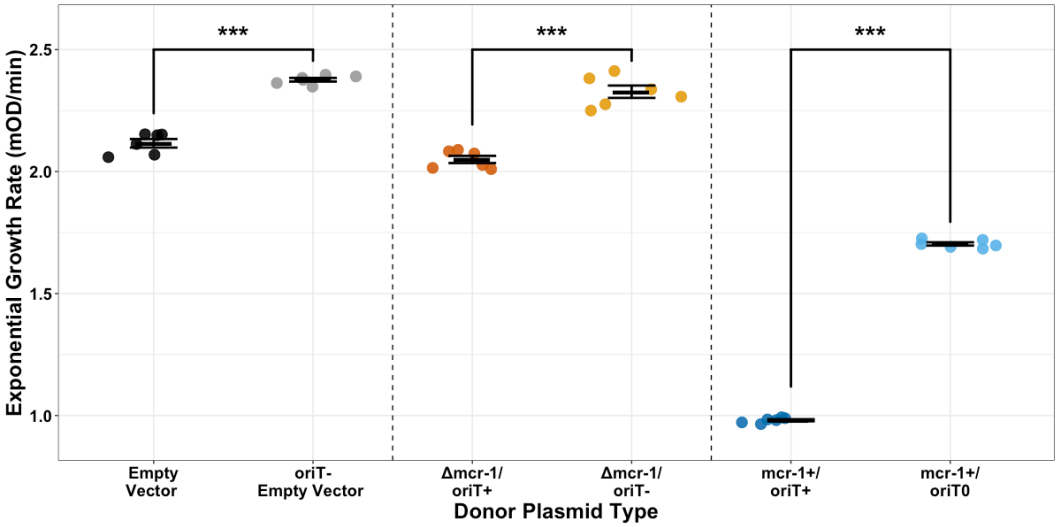
E. coli carrying functional MCR-1 showed increased sedimentation, this feature was not seen in β3914 *E. coli*. However, MCR-1-positive β3914 reached lower final ODs than MCR-1-negative counterparts (*Figure 4.S1*). These may simply be a result of fitness differences, but OD measurements are largely influenced by changes in cell morphology (Stevenson *et al.*, 2016). Additionally, flow cytometry results suggest aggregate formation in MCR-1-positive β3914 (*Figure 4.4b*). The variable behaviour seen in response MCR-1 activity may be due to underlying differences in outer-membrane LPS composition between *E. coli* strains (Darveau, 1998).

Although the results of this chapter show a clear link between the presence of *mcr-1*+/oriT+ and increased bacterial conjugation and plasmid stability, it is important to note that experiments were conducted using non-natural pSEVA vectors. It is also unclear whether the MCR-1 mediated boost in plasmid transfer is biologically relevant. In order to test the biological relevance of the data collected here, it is important that experiments are repeated using natural plasmids. Increased colony viscosity has been observed in *E. coli* J53 cells that carry natural MCR-1-positive plasmids. Further experiments that involve deleting *mcr-1* from natural plasmids and measuring the conjugation rates of *mcr-1*-positive and negative natural plasmids will ascertain if this MCR-1 mediated conjugation boost is a naturally occurring phenomenon. However, the take-away message from this chapter is that MCR-1 activity increases donor-to-donor plasmid transfer and this has important implications regarding epidemiology of MCR-1 and the spread of clinically relevant MCR-1-positive plasmids.

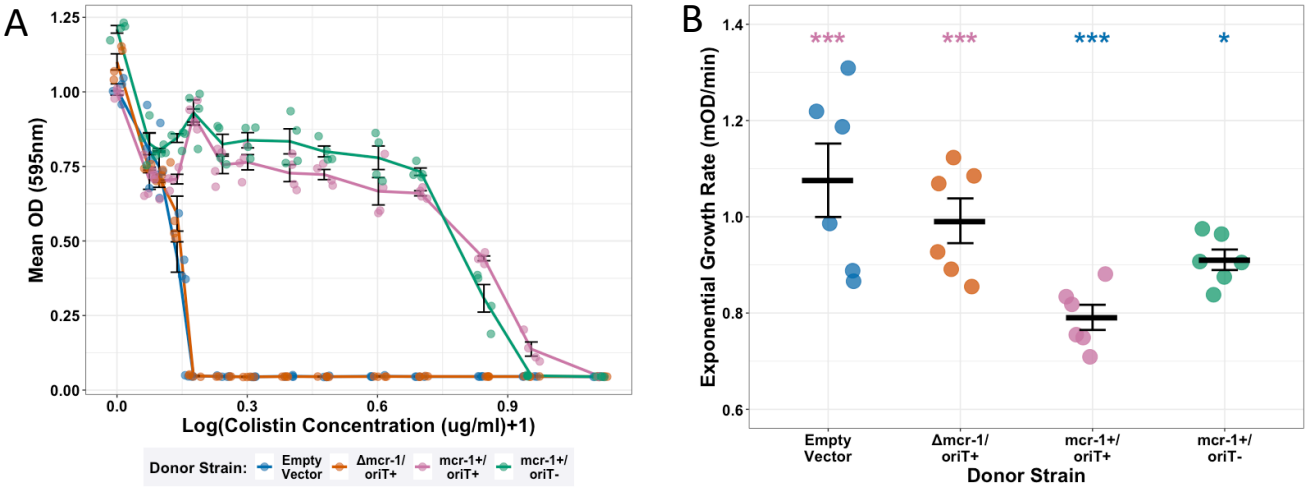
4.6 Supplementary Information



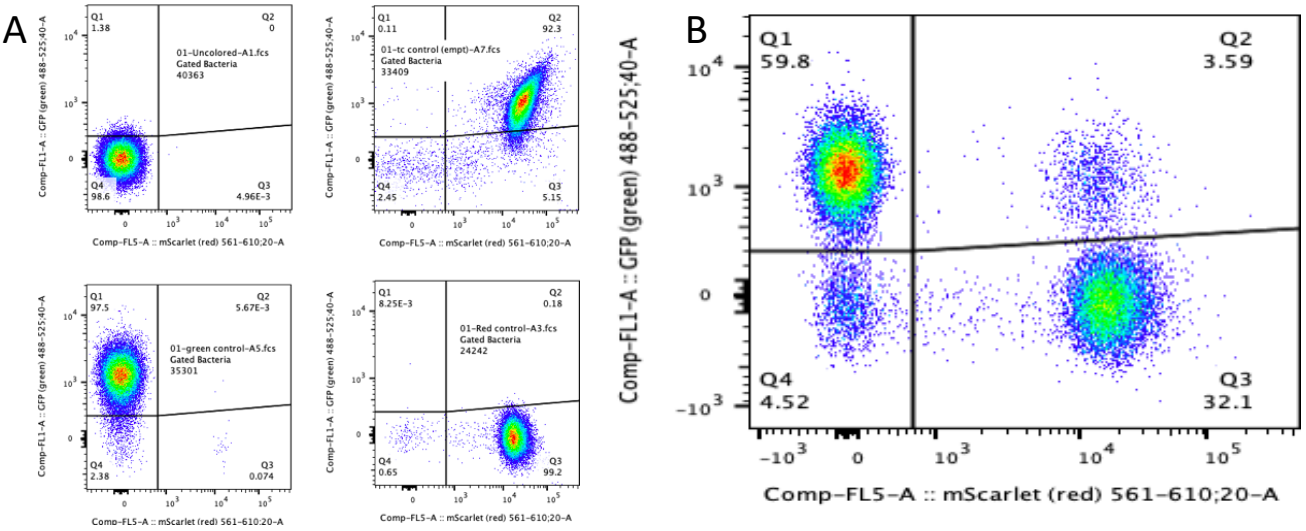
Supplementary Figure 4.S1: Growth curves for β3914 cells containing pSEVA121 empty vectors (blue) or pSEVA121-*mcr-1* (pink) are shown. Bacteria were grown in shaking liquid culture for 35-hours with OD measurements taken every 10 minutes. (n=6, grey shading = SE).



Supplementary Figure 4.S2: Effect of oriT deletions on β3914 donor growth rates. Exponential growth rate measurements obtained for β3914 carrying oriT+ or oriT- empty, inactivated *mcr-1* and functional *mcr-1* pSEVA121 plasmids (n=16, p-values: ***<0.001, Tukey's range test).



Supplementary Figure 4.S3: Resistance and fitness assessments of fluorescent β3914 donors. (**A**) Individual OD values (pints) and means (line) for β3914 strains carrying pSEVA627-mSacrlet+ empty (blue), Δ*mcr-1/*oriT+ (orange), *mcr-1*+/oriT+ (pink) and *mcr-1*+/oriT- (green) donor plasmids. Measuments were taken in a range of colistin concentrations (0-8ug/ml, Log10 Scale, n=4). (**B**) Exponential growth rates for empty (blue), Δ*mcr-1/*oriT+ (orange), *mcr-1*+/oriT+ (pink) and *mcr-1*+/oriT- (green) β3914 donor strains (n=6, p-values: ***<0.001, *<0.05, Dunnett test with comparisons to empty and consensus *mcr-1* plasmids in blue and pink respectively, error bars = SE, line at mean)



Supplementary Figure 4.S4: Scatter plots showing representative results of flow cytometry events. (**A**) Panels show control donor (Q3), recipient (Q1), TC (Q2) and plasmid-negative ex-donor cell (Q4) results after compensation. Gates were tested over two control populations each. (**B**) Representative scatter plot showing results for a mcr-1+/oriT+ population. Events were recorded until at least 3,000 events were obtained.

5 Final Discussion and Summary

The threat of widespread antibiotic resistance is of immense concern due to our heavy reliance on antibiotic treatment for human and animal healthcare. This is particularly the case regarding resistance to last-resort antibiotics (e.g. colistin) as this breaches our defence against disease causing microbes. Additionally, horizontal transmission of antimicrobial resistance (AMR) genes accelerates this problem. AMR generally infers fitness costs in the absence of antibiotic selection. However, many studies have shown that evolutionary adaptations such as compensatory mutations can remedy these costs leading to AMR gene maintenance. This effect has important implications on antibiotic management as limiting antibiotic use may not eradicate AMR genes if such adaptations are widespread. To minimise the spread of AMR, we must understand how these genes are evolving, determine if compensation is widespread and assess the impact of AMR on bacterial fitness and behaviour.

This thesis focused on mobile colistin resistance (MCR) and aimed to study the impacts of emerging variations in *mcr-1* coding and regulatory sequences to make inferences on how the gene was evolving and determine if these variants were compensatory. Furthermore, insights into MCR-induced bacterial behavioural changes allowed us to speculate on how MCR-1 facilitates its own maintenance in bacterial populations.

I first analysed the *mcr-1* coding sequence in chapter 2. Due to the parallelism witnessed and the high frequency of non-synonymous SNPs, I hypothesised that the structural variations found were adaptive and potentially compensatory. With some exceptions, I found that structural variants were largely deleterious in both the presence and absence of colistin (*Figure 5.1*). Only one variant (*mcr-1.8*) showed potential compensatory effects while another (*mcr-k1.2*) was a clear trade-off mutation where high fitness in colistin-free media was obtained as a consequence of reduced resistance. From this result, I concluded that within-gene compensatory adaptation was not common in *mcr-1* evolution which was further confirmed by the low prevalence of structural mutations in recent MCR-1 sequence datasets (*Figure 5.2*). Other studies have shown that costly resistance genes can be compensated for

by extragenic polymorphisms and AMR plasmids can be stabilised by reciprocal co-adaptation between MGEs and host chromosomes (Harrison *et al.*, 2015; Bottery, Wood and Brockhurst, 2017). Future work in this area should assess whether MCR-1 carriage can be compensated by non-intragenic mechanisms.

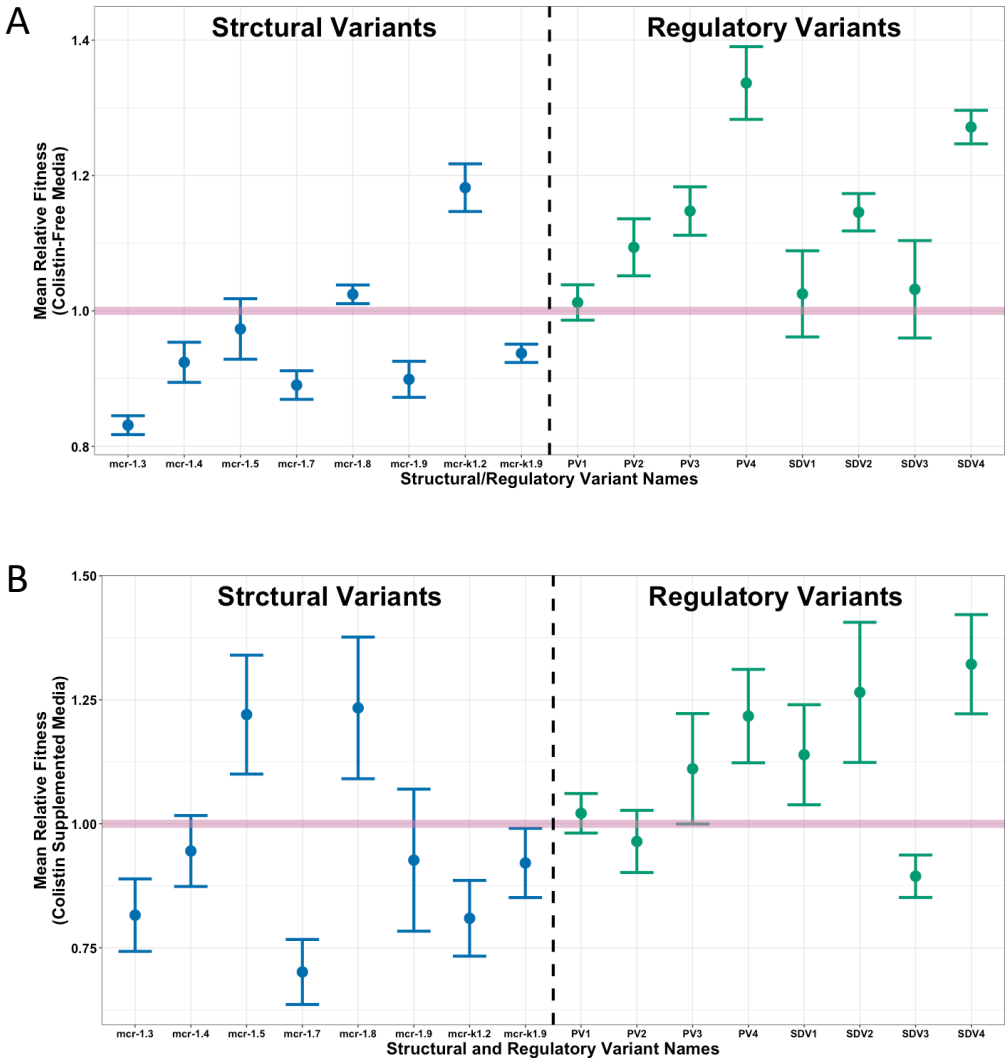


Figure 5.1: Summary figures showing the relative competitive fitness of all structural (blue) and regulatory (green) variations analysed in this study. The top panel (**A**) shows the fitness in colistin free media while the bottom panel (**B**) shows fitness in the highest tested levels of colistin.

When analysing the locations of currently available non-synonymous SNPs, I found that these mutations were highly clustered in MCR-1 N-terminal regions. Additionally, the two high-fitness variants *mcr-1.8* and *mcr-k1.2* exhibited parallel SNPs within the immediate N-terminal region of MCR-1. This suggests that this region may be of functional importance as SNPs lead to more drastic fitness changes. Studies on protein translocation have determined that N-

terminal regions of certain proteins encode signalling sequences that are vital in protein targeting (Hegde and Bernstein, 2006; Freudl, 2018). Future work expanding the analysis of N-terminal structural variations would be able to determine whether these regions are important for MCR-1 localisation.

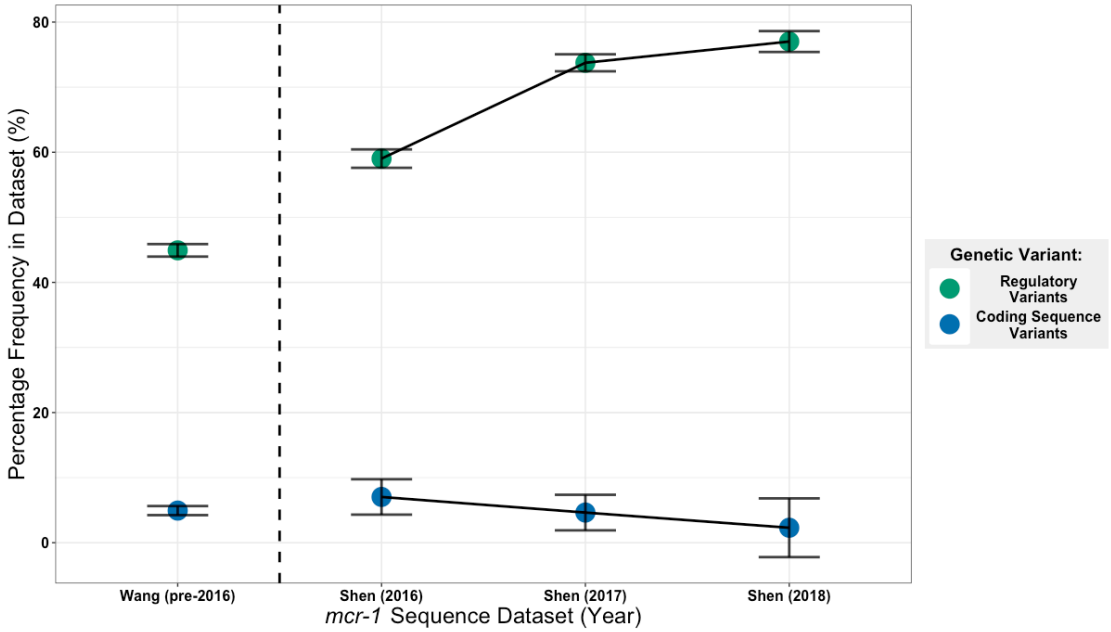


Figure 5.2: Percentage proportion of structural (blue) and regulatory (green) variation in *mcr-1* sequence datasets arranged according to year collected. Error bars = SE.

In chapter 3, I focused on variations found within MCR-1 regulatory sequences. When analysing the 2018 Wang *et al* dataset, I found that most variant SNPs were predicted to reduce MCR-1 transcription and/or translation. By reconstructing these variants, I discovered that these regulatory SNPs generally increased the competitive fitness of MCR-1-positive bacteria compared to consensus sequences (*Figure 5.1*). I also experimentally confirmed that the observed regulatory variants resulted in reduced MCR-1 gene expression and protein activity. From these results I concluded that reduced production of MCR-1 resulted in the high fitness observed for regulatory variants in the absence of colistin selection. Interestingly, I also found that these variants marginally increased colistin resistance suggesting that they are examples of regulatory fine-tuning in order to obtain optimal MCR-1 levels that maximise colistin resistance while minimising fitness costs. Further work that assesses the impacts of these variants in native MCR-1-positive plasmids would determine whether they have similar effects in their natural *mcr-1* gene contexts.

When assessing fitness results obtained from the two variation types, it is clear that regulatory mutations have a greater positive impact on the fitness of MCR-1 positive bacteria (*Figure 5.1*). Comparisons of genetic variant competitive fitness revealed that regulatory variants had higher relative fitness in both colistin-free (p-value= 2.597e-07, Mann-Whitney test) and colistin-supplemented media (p-value= 0.001341, Mann-Whitney test). However, it is important to note that structural and regulatory fitness assessments were preformed using differential cloning vectors. Recent sequence data shows that regulatory variants are more widespread and are increasing in prevalence among MCR-1-positive isolates. In contrast, structural variants exist in low proportions and seem to be reducing in prevalence further other the years (*Figure 5.2*). Fitness results from chapters 2 and 3 provide explanations to observed trends. Although a degree of linkage was observed between variants and certain plasmid Inc types, regulatory SNPs were widespread across all Inc types. These results have important implications of *mcr-1* epidemiology as increased prevalence of fitter regulatory variants could enable persistence of *mcr-1*-positive plasmids in the absence of selection.

Lastly, I investigated the effects of MCR-1 on bacterial behaviour and plasmid stability. I observed that MCR-1-positive *E. coli* regularly formed aggregates. As this behaviour is linked to biofilm formation and increased plasmid exchange, I hypothesised that this phenotype facilitates increased conjugative transfer of *mcr-1*-positive plasmids. I discovered that transferable plasmids carrying functional MCR-1 demonstrated long-term plasmid stability and increased transfer rates in the absence of antibiotic selection. Additionally, conjugative passages showed that plasmid prevalence was mainly due to donor maintenance rather than transconjugant emergence. From these results, I concluded that the observed stability was due to MCR-1 activity as increased cell-to-cell interactions led to increased rates of plasmid transfer within strains. Further work is needed to determine the mechanism leading to increase cellular interactions and to confirm if this effect is observed in natural plasmids. However, these results have important clinical implications as native *mcr-1* plasmids are highly conjugative. Since MCR-1 can facilitate its own spread in the absence of selection, these plasmids could be difficult to eradicate in clinical and agricultural settings.

In conclusion, I discovered key genetic and phenotypic factors involved in the evolution and transmission of MCR. Within-gene compensatory mutations are rare, however regulatory

mutations are widespread and confer fitness increases in all tested colistin concentrations. Additionally, production of active MCR-1 results in an aggravative phenotype which stabilises MCR-1-positive plasmids in the absence of selection by increasing plasmid transfer rates between mother and daughter cells.

Appendices

Appendix 1: Primers used in this thesis

CHAPTER 2 PRIMERS			
Primer Name	**Length (bp)**	**Sequence (5'-> 3')**	**Primer Use**
pBADF	26	GGTCTCGAGTTTAAACGGTCTCCAGC	pBAD vector amplification
pBADR	27	CATGCTGAATTCCTCCTGTTAGCCCAA	pBAD vector amplification
mcr fwd	24	ATGATGCAGCATACTTCTGTGTGG	mcr-1 gene amplification
mcr rev	23	TTACTATCAGCGGATGAATGCGG	mcr-1 gene amplification
mcr-1 consens fwd	60	CCATACCCGTTTTTTGGGCTAACAGGAGGAATTCAGCATGATGCAGCATACTTCTGTGTG	gibson primer
mcr-1 consens rev	57	GACCGTTTAAACTCGAGACCGCGGGGTGGGTCTGATTACTATCAGCGGATGAATGCG	gibson primer
mcr-k1.2 fwd	60	CCATACCCGTTTTTTGGGCTAACAGGAGGAATTCAGCATGATGCTGCATACTTCTGTGTG	gibson and mutgenisis
mcr-1.8 fwd	60	CCATACCCGTTTTTTGGGCTAACAGGAGGAATTCAGCATGATGCGGCATACTTCTGTGTG	gibson and mutgenisis
mcr-k1.9 rev	57	GACCGTTTAAACTCGAGACCCACATGATGCGTACGTTACTATCAGCGGATGAATGCG	gibson primer
mcr-1.2 rev	57	GACCGTTTAAACTCGAGACCGAACATGTGGCTGCGTTACTATCAGCGGATGAATGCG	gibson primer
mcr-1.4 rev	57	GACCGTTTAAACTCGAGACCTAACTCTGCCGGGCTTTACTATCAGCGGATGAATGCG	gibson primer
mcr-1.7 rev	57	GACCGTTTAAACTCGAGACCCCATCGGCGTCCTGTTTACTATCAGCGGATGAATGCG	gibson primer
mcr-1.8 rev	57	GACCGTTTAAACTCGAGACCCTCGACCTAATGTCCTTACTATCAGCGGATGAATGCG	gibson primer
mcr-1.5 rev	57	GACCGTTTAAACTCGAGACCCTCTCCGCTACCGAATTACTATCAGCGGATGAATGCG	gibson primer
mcr-1.3 rev	57	GACCGTTTAAACTCGAGACCAGTCAAGTACGCCGCTTACTATCAGCGGATGAATGCG	gibson primer
mcr-1.9 rev	57	GACCGTTTAAACTCGAGACCAGCTAACACGGGAACTTACTATCAGCGGATGAATGCG	gibson primer
mcr1.3 mut fwd	60	CAGTCCGTTGGTTCTTGTGGCGAGTGTTGCCGTTTTCTTGACCGCGACCGCCAATCTTAC	gibson and mutgenisis
mcr1.3 mut rev	60	GTAAGATTGGCGGTCGCGGTCAAGAAAACGGCAACACTCGCCACAAGAACCAACGGACTG	gibson and mutgenisis
mcr1.4 mut fwd	56	CAATGCTTATGACAATGCCTTGCTTGCCACCGATAATTTCATCGCTCAAAGTATCC	gibson and mutgenisis
mcr1.4 mut rev	56	GGATACTTTGAGCGATGAAATTATCGGTGGCAAGCAAGGCATTGTCATAAGCATTG	gibson and mutgenisis
mcr1.5 mut fwd	58	GATGATTTCATCGCTCAAAGTATCCAGTGGCTGCAGACGTACAGCAATGCCTATGATG	gibson and mutgenisis
mcr1.5 mut rev	58	CATCATAGGCATTGCTGTACGTCTGCAGCCACTGGATACTTTGAGCGATGAAATCATC	gibson and mutgenisis
mcr1.9 mut fwd	58	GCGATATGATGAAAAGTTTGCCAAATTCACGCCAGCGTGTGAAGGTAATGAGCTTGCC	gibson and mutgenisis
mcr1.9 mut rev	58	GGCAAGCTCATTACCTTCACACGCTGGCGTGAATTTGGCAAACTTTTCATCATATCGC	gibson and mutgenisis
mcr1.7 mut fwd	66	CGGTGGGTAAGCTTGCCAGTATTGAGTATAAAAAAGCCAGTACGCCAAAAGATACCATTTATCACG	gibson and mutgenisis
mcr1.7 mut rev	66	CGTGATAAATGGTATCTTTTGGCGTACTGGCTTTTTTATACTCAATACTGGCAAGCTTACCCACCG	gibson and mutgenisis
mcrk1.9 mut fwd	60	CGTAGCTATGTCAATCCGATCATACCAATCTACTCGGTGGGTAAGCTTGCCAGTATTGAG	gibson and mutgenisis
mcrk1.9 mut rev	60	CTCAATACTGGCAAGCTTACCCACCGAGTAGATTGGTATGATCGGATTGACATAGCTACG	gibson and mutgenisis
mcr_SDM_F	21	CGGCACATCGGCGGCGTATTC	mcr-1 inactivation
mcr_SDM_R	27	CACGATGTGACATTGCTAAAATTGGTC	mcr-1 inactivation
allTAGrev	15	CAGACCGCTTCTGCG	variant specific qpcr
qPCR_pBAD	17	GGGAATTCGAAGCTTGG	variant specific qpcr
qPCR_cons	14	TCAGACCCACCCCG	variant specific qpcr
qPCR_1.3	15	GCGGCGTACTTGACT	variant specific qpcr
qPCR_1.4	15	AGCCCGGCAGAGTTA	variant specific qpcr
qPCR_1.5	15	TTCGGTAGCGGAGAG	variant specific qpcr
qPCR_1.7	18	AAGGACATTAGGTCGAGG	variant specific qpcr
qPCR_1.8	14	ACGCCGATGGGGTC	variant specific qpcr
qPCR_1.9	17	GTTCCCGTGTTAGCTGG	variant specific qpcr
qPCR_k1.2	15	CGCAGCCACATGTTC	variant specific qpcr
qPCR_k1.9	17	CGTACGCATCATGTGGG	variant specific qpcr
mcr gibson fwd	49	GCTAACAGGAGGAATTAACCATGATGCAGCATACTTCTGTGTGGTACCG	fluorescent tag gibson
mcr gibson rev	44	CCAGCAGCGGAGCCAGCCGAGCGGATGAATGCGGTGCGGTCTTT	fluorescent tag gibson
ypet gibson fwd	30	CACCGCATTCATCCGCTCGGCTGGCTCCGC	fluorescent tag gibson
ypet gibson rev	71	GCAAAACACCCAAGTGACCTATCATTATTTGTACAATTCATTCATACCCTCGG	fluorescent tag gibson
halo gibson fwd	33	GCACCGCATTCATCCGCTCGGCTGGCTCCGCTG	fluorescent tag gibson
halo gibson rev	71	AAACTCAGTGCAAAACACCCAAGTGACCTATCATTAACCGGAAATCTCCAGAGTAGACAGC	fluorescent tag gibson
CHAPTER 3 PRIMERS			
Primer Name	**Length (bp)**	**Sequence (5'-> 3')**	**Primer Use**
p16 mcr fwd	38	GATAACAATTTCACACAGGAGGATTGCGCAATGATTGC	mcr-1 and regulatory amplification from pn16
p16 mcr rev	41	AGGGTTTTCCCAGTCACGACCATAATACGAATGGAGTGTGC	mcr-1 and regulatory amplification from pn16
pSEVA fwd	21	GTCGTGACTGGGAAAACCCTG	Amplification of pSEVA121 backbone
pSEVA Rev	24	TCCTGTGTGAAATTGTTATCCGCT	Amplification of pSEVA121 backbone

MisoSDMF	38	CGTGCGGCACATCGGCGGCGTATTCTGTGCCGTGTATG	mcr-1 inactivation
MisoSDMR	38	CATACACGGCACAGAATACGCCGCCGATGTGCCGCACG	mcr-1 inactivation
Gibson Fwd	39	GCTTTCTACGTGGCTGCCATTTTTGGGGTGAGGCCGTTC	Introduction of regulatory variant SNPs
MisoPV1F	51	GTACTGGATTTCTTAAAAAATTGCAGTAAAATTGCCGCAATTATCCCACCG	Introduction of regulatory variant SNPs
MisoPV1R	51	CGGTGGGATAATTGCGGCAATTTTACTGCAATTTTTTAAGAAATCCAGTAC	Introduction of regulatory variant SNPs
MisoPV2F	51	GTACTGGATTTCTTAAAAAATTGCAGTAGAATTGCCGCAATTATCCCACCG	Introduction of regulatory variant SNPs
MisoPV2R	51	CGGTGGGATAATTGCGGCAATTCTACTGCAATTTTTTAAGAAATCCAGTAC	Introduction of regulatory variant SNPs
MisoPV3F	51	GTACTGGATTTCTTAAAAAATTGCAGTATGATTGCCGCAATTATCCCACCG	Introduction of regulatory variant SNPs
MisoPV3R	51	GGTGGGATAATTGCGGCAATCATACTGCAATTTTTTAAGAAATCCAGTAC	Introduction of regulatory variant SNPs
MisoPV4F	51	GTACTGGATTTCTTAAAAAATTGCAGTATAGTTGCCGCAATTATCCCACCG	Introduction of regulatory variant SNPs
MisoPV4R	51	GGTGGGATAATTGCGGCAACTATACTGCAATTTTTTAAGAAATCCAGTAC	Introduction of regulatory variant SNPs
MisoSDV1F	50	GCCGCAATTATCCCACCGTTTATTTTTTGATTAGTTTCTCATGATGCAGC	Introduction of regulatory variant SNPs
MisoSDV1R	50	CTGCATCATGAGAAACTAATCAAAAAATAAACGGTGGGATAATTGCGGC	Introduction of regulatory variant SNPs
MisoSDV2F	50	GCCGCAATTATCCCACCGTTTATTTTTTTAATAGTTTCTCATGATGCAGC	Introduction of regulatory variant SNPs
MisoSDV2R	50	GCTGCATCATGAGAAACTATTAAAAAAATAAACGGTGGGATAATTGCGGC	Introduction of regulatory variant SNPs
MisoSDV3F	50	GCCGCAATTATCCCACCGTTTATTTTTTGAATAGTTTCTCATGATGCAGC	Introduction of regulatory variant SNPs
MisoSDV3R	50	GCTGCATCATGAGAAACTATTCAAAAAATAAACGGTGGGATAATTGCGGC	Introduction of regulatory variant SNPs
MisoSDV4F	50	GCCGCAATTATCCCACCGTTTATTTTTTGCGTAGTTTCTCATGATGCAGC	Introduction of regulatory variant SNPs
MisoSDV4R	50	CTGCATCATGAGAAACTACGCAAAAAATAAACGGTGGGATAATTGCGGC	Introduction of regulatory variant SNPs
wt_sdm_fwd	37	TAGAATGGTCGACGTCGTCGTGACTGGGAAAACCCTG	Inserting unique sequence tags by SDM
wt_sdm_rev	37	CACTTCGCGATTGAGTCATAATACGAATGGAGTGTGC	Inserting unique sequence tags by SDM
inact_sdm_fwd	37	GCCTGCGATATACCGTGTCGTGACTGGGAAAACCCTG	Inserting unique sequence tags by SDM
inact_sdm_rev	37	TTATCTTACCGGACTGCATAATACGAATGGAGTGTGC	Inserting unique sequence tags by SDM
pv1_sdm_fwd	37	CGCATGGACACTATTAGTCGTGACTGGGAAAACCCTG	Inserting unique sequence tags by SDM
pv1_sdm_rev	37	AGCGCTCCAGGTCAATCATAATACGAATGGAGTGTGC	Inserting unique sequence tags by SDM
pv2_sdm_fwd	37	GTCTAATCAGCGACAGGTCGTGACTGGGAAAACCCTG	Inserting unique sequence tags by SDM
pv2_sdm_rev	37	TGACTGCGTACTCTGACATAATACGAATGGAGTGTGC	Inserting unique sequence tags by SDM
pv3_sdm_fwd	37	AGGAATCATTCGGTCCGTCGTGACTGGGAAAACCCTG	Inserting unique sequence tags by SDM
pv3_sdm_rev	37	CATCTCGAATGCTGGTCATAATACGAATGGAGTGTGC	Inserting unique sequence tags by SDM
pv4_sdm_fwd	37	CTGGCAACGCAGTCAGGTCGTGACTGGGAAAACCCTG	Inserting unique sequence tags by SDM
pv4_sdm_rev	37	ATCGAGGTAAGGATAACATAATACGAATGGAGTGTGC	Inserting unique sequence tags by SDM
sdv1_sdm_fwd	37	CCTGAGCAGCCTGATCGTCGTGACTGGGAAAACCCTG	Inserting unique sequence tags by SDM
sdv1_sdm_rev	37	ATGCACTACTCCTAATCATAATACGAATGGAGTGTGC	Inserting unique sequence tags by SDM
sdv2_sdm_fwd	37	TGATCGACCGAGAGCTGTCGTGACTGGGAAAACCCTG	Inserting unique sequence tags by SDM
sdv2_sdm_rev	37	GCCGTAATTTAGAGTCCATAATACGAATGGAGTGTGC	Inserting unique sequence tags by SDM
sdv3_sdm_fwd	37	ATATGTGGTGCAGCCAGTCGTGACTGGGAAAACCCTG	Inserting unique sequence tags by SDM
sdv3_sdm_rev	37	TATCAGGCGACATGAGCATAATACGAATGGAGTGTGC	Inserting unique sequence tags by SDM
sdv4_sdm_fwd	37	TGAGAGTCGCAACTGTGTCGTGACTGGGAAAACCCTG	Inserting unique sequence tags by SDM
sdv4_sdm_rev	37	GAAGGTTGTTCCAACCCATAATACGAATGGAGTGTGC	Inserting unique sequence tags by SDM
tWT	32	ACTCAATCGCGAAGTGTAGAATGGTCGACGTC	primers for variant specific qPCR
tInactive	32	CAGTCCGGTAAGATAAGCCTGCGATATACCGT	primers for variant specific qPCR
tPV1	32	ATTGACCTGGAGCGCTCGCATGGACACTATTA	primers for variant specific qPCR
tPV2	32	TCAGAGTACGCAGTCAGTCTAATCAGCGACAG	primers for variant specific qPCR
tPV3	32	ACCAGCATTCGAGATGAGGAATCATTCGGTCC	primers for variant specific qPCR
tPV4	32	TTATCCTTACCTCGATCTGGCAACGCAGTCAG	primers for variant specific qPCR
tSDV1	32	ATTAGGAGTAGTGCATCCTGAGCAGCCTGATC	primers for variant specific qPCR
tSDV2	32	GACTCTAAATTACGGCTGATCGACCGAGAGCT	primers for variant specific qPCR
tSDV3	32	CTCATGTCGCCTGATAATATGTGGTGCAGCCA	primers for variant specific qPCR
tSDV4	32	GGTTGGAACAACCTTCTGAGAGTCGCAACTGT	primers for variant specific qPCR
new_qtag_rev	30	CAACCGAGCGTTCTGAACAAATCCAGATGG	primers for variant specific qPCR
qmcr_F	22	CCACAGCTTGCCAAGATCGATG	RT-qpcr expression primers
qmcr_R	22	ATACTCATCCGCGCCCAGATAG	RT-qpcr expression primers
TRFA F	22	GTGCGAGCTGAAATAGTCGAAC	RT-qpcr expression primers
TRFA R	22	GAGGAAATCGTCGTGCTGTTTG	RT-qpcr expression primers

CHAPTER 4 PRIMERS

Primer Name	Length (bp)	Sequence (5'-> 3')	Primer Use
OriT_fwd1	18	CCGGAACTGACCCCACAA	OriT Deletion by site directed mutagenisis
OriT_rev2	23	AAGGAGCCTTTAATTGTATCGGT	pSEVA121 OriT Deletion by site directed mutagenisis
orit_sdm_rev	23	GTCCAATTTACCGAACAACTCCG	pSEVA621 OriT Deletion by site directed mutagenisis
627scar_p2FWD	43	GAGTTTAAGGAGGTATATACATATGAGTAAAGGAGAAGCTGTG	Gibson of mScaelet into pSEVA621
627scar_rev	46	TCAACAGGAGTCCAAGACTAGTTTATTTGTATAGTTCATCCATGCC	Gibson of mScaelet into pSEVA622
fwd_prom2	62	ATTCATGGATGCAAAATAAGGAGTTTAAGGAGGTATATACATATGCGTAAAGGTGAAGAACT	Biofab Promoter SDM into pSEVE627M for msfGFP expression
rev_prom2	62	CTATTATAGGTACAAAAAGATGCGAAGTCAATACTCTATCGTTTCCTCCTAAGCTTGCATGC	Biofab Promoter SDM into pSEVE627M for msfGFP expression
CmR_PS_fwd	48	AGCGGATAACAATTTCACACAGGAGGCTAGCATCTCGAGGTGAAGACG	CmR Amplification for gibson into pSEVE627M
CmR_PS_nTerm_rev	47	TGCCTGCAGGTCGACTCTAGAGGATCCGATATCAAATTACGCCCCGC	CmR Amplification for gibson into pSEVE627M
Chloro2_merged_fwd	60	ACGCGAAATACGGGCAGACATGGCCTGCCCGGTTATTACTAGCATCTCGAGGTGAAGACG	CmR-msfGFP fragment amplification for recombineering

GFP_lacZ_rev	62	AATTGTGAGCGGATAACAATTTCACACAGGAAACAGCTTTATTTGTAGAGTTCATCCATGCC	CmR-msfGFP fragment amplification for recombineering

Appendix 2: Plasmids used/constructed in this thesis

CHAPTER 2 PLASMIDS		
Plasmid	**Relevant features**	**Source/Reference**
pBAD/His A	AmpR, ARA induced, MCS, Hexa-HIS tag	Thermo Fisher (Cat.#: V43001)
pBAD/His A:mcr-1	AmpR, ColistinR, ARA induced MCS, Hexa-HIS tag	Walsh Lab [Paper source]
pBAD*	modified pBAD (no MCS, Hexa-HIS tag), AmpR	this study
pBAD:mcr-1	Consus mcr-1 in pBAD* + unique tag	this study
pBAD:mcr-k1.2	mcr-k1.2 in pBAD* + unique tag	this study
pBAD:mcr-1.3	mcr-1.3 in pBAD* + unique tag	this study
pBAD:mcr-1.4	mcr-1.4 in pBAD* + unique tag	this study
pBAD:mcr-1.5	mcr-1.5 in pBAD* + unique tag	this study
pBAD:mcr-1.7	mcr-1.7 in pBAD* + unique tag	this study
pBAD:mcr-1.8	mcr-1.8 in pBAD* + unique tag	this study
pBAD:mcr-1.9	mcr-1.9 in pBAD* + unique tag	this study
pBAD:mcr-k1.9	mcr-k1.9 in pBAD* + unique tag	this study
pBAD:inactive mcr-1	(T285A) mcr-1 in pBAD	this study
pROD50	mYPET tag and linker	Uphoff Lab
pSU005	HALO tag and linker	Uphoff Lab
pBAD:mcr-1-mYPET	mcr-1 with c-terminal mYPET fusion	this study
pBAD:mcr-1-HALO	mcr-1 with c-terminal HALO fusion	this study
CHAPTER 3 PLASMIDS		
Plasmid	**Relevant features**	**Source/Reference**
pSEVA121	AmpR, OriT+	SEVA material repository
pn16	mcr-1+, IncI2 plasmid	Walsh Lab [Paper source]
pSEVA121:mcr-1	consensus mcr-1 sequence, consensus regulatory sequence	this study
pSEVA121:inactive mcr-1	(T285A) mcr-1 in pSEVA121	this study
pSEVA121:PV1	mcr-1.1 + promoter variant 1 + unique tag	this study
pSEVA121:PV2	mcr-1.1 + promoter variant 2 + unique tag	this study
pSEVA121:PV3	mcr-1.1 + promoter variant 3 + unique tag	this study
pSEVA121:PV4	mcr-1.1 + promoter variant 4 + unique tag	this study
pSEVA121:SDV1	mcr-1.1 + shine-delgarno variant 1 + unique tag	this study
pSEVA121:SDV2	mcr-1.1 + shine-delgarno variant 2 + unique tag	this study
pSEVA121:SDV3	mcr-1.1 + shine-delgarno variant 3 + unique tag	this study
pSEVA121:SDV4	mcr-1.1 + shine-delgarno variant 4 + unique tag	this study
CHAPTER 4 PLASMIDS		
Plasmid	**Relevant features**	**Source/Reference**
pSEVA121	AmpR, OriT+, ori:RK2	SEVA material repository
pSEVA121:mcr-1	AmpR, consensus mcr-1 gene and regulatory sequence, ori:RK2	this study
pSEVA121:inactive mcr-1	AmpR, T285A mcr-1 in pSEVA121, ori:RK2	this study
pSEVA121:oriT-	AmpR, OriT-, ori:RK2	this study
pSEVA121:mcr-1, oriT-	AmpR, consensus mcr-1 gene and regulatory sequence, OriT-, ori:RK2	this study
pSEVA121:inactive mcr-1, oriT-	AmpR, T285A mcr-1 in pSEVA121, OriT-, ori:RK2	this study
pSEVA621:mScarlet	CmR, red fluorescence, ori:RK2	this study
pSEVA621:mcr-1, mScarlet	CmR, consensus mcr-1 gene and regulatory sequence, red fluorescence, ori:RK2	this study
pSEVA621:inactive mcr-1, mScarlet	CmR, T285A mcr-1 in pSEVA121, red fluorescence, ori:RK2	this study
pSEVA621:mScarlet,oriT-	CmR, AmpR, OriT-, ori:RK2	this study
pGRG25-Pmax-mScarlet-I	Souece of mScarlet gene and Biofab promoter	Gift from Foster lab
pMS_131	Source of CmR gene	Lab Stocks
pSEVA627M	Source of msfGFP gene	SEVA material repository
pKD46	Temperature sensitive replication (repA101ts); encodes lambda Red genes (exo, bet, gam); native terminator (tL3) after exo gene; arabinose-inducible promoter for expression (ParaB); encodes araC for repression of ParaB promoter; Ampicillin resistant.	Gift from Uphoff lab

Appendix 3: Strains used in this thesis

Strain	Relevant Features	Source/Reference
E. coli TOP10	common lab *E. coli* cloning strain	ThermoFisher Scientific (Cat no: C404010)
E. coli AB1157	common lab *E. coli* strain	Uphoff Lab
E. coli MGI655	common lab *E. coli* strain	lab stocks
E. coli MGI655 (KanR, mCherry)	As above + Kanamycin Resistance, mKate2 gene (flourecent marker)	this work
E. coli J53	K-12 mutant, Sodium Azide (NaN_3) resistant	lab stocks (Matsumura, Peirano and Pitout, 2018)
E. coli ß3914	Genotype: F− RP4-2-Tc::Mu ΔdapA::(erm-pir), gyrA462 zei-298::Tn10 (KmR, EmR, TcR, SmR)	San-Milan Lab (Le Roux *et al.*, 2007)
E. coli ß3914 (CmR, msfGFP, ΔLacZ)	As above + CmR(pMS_131), BioFab promoter(pGRG25-Pmax-mScarlet-I), msfGFP gene (pSEVA627M)	this work
AB1157 ΔflhD, Tn7::mKate2, KanR	mKate2, KanR	Uphoff Lab (Uphoff, 2018)

Appendix 4: Wang and Shen Dataset Isolate Sequencing Tables

Constructed with aid from Liam Shaw

Wang Dataset						
#	Isolate ID	Promoter	Plasmid	Year	Host	SRA
1	11HE3	Consensus		2012	Human	-
2	12HE4	SDV2		2011	Human	-
3	12HE5	PV1	IncI2	2016	Chicken	-
4	12HE6	PV3	IncX4	2016	Human	-
5	12HE7	SDV1	IncI2	2016	Chicken	-
6	12HE8	Consensus		2016	Pig	-
7	12HE9	Consensus		2016	Pig	-
8	12HE10	PV3		2016	Pig	-
9	13HE2	PV3		2016	Chicken	-
10	13HE11	SDV1		2016	Chicken	-
11	13HE12	PV3	IncX4	2016	Chicken	-
12	13HE13	SDV1		2016	Chicken	-
13	13HE16	SDV1		2016	Human	-
14	13HE17	PV1		2016	Chicken	-
15	14HE18	SDV2		2016	Human	-
16	14HE19	SDV1		2016	Human	-
17	14HE20	SDV1	IncI2	2016	Human	-
18	14HE21	PV1	IncI2	2016	Chicken	-
19	14HE22	PV1		2016	Chicken	-
20	14HE23	PV1		2016	Chicken	-
21	B07_1_WFA61	SDV2		2016	Chicken	-
22	BJ34	SDV1		2016	Chicken	-
23	BJ36	Consensus		2016	Pig	-
24	BJ37	Consensus		2016	Pig	-
25	BJ72	Consensus		2016	Pig	-
26	BJ16008	SDV1		2016	Chicken	-
27	C07_1_1052	Consensus		2016	Pig	-
28	C1279	Consensus		2016	Human	-
29	C1461	SDV1		2016	Chicken	-
30	C1555	SDV1		2016	Chicken	-
31	C1616	SDV1		2016	Chicken	-
32	C1858	PV1		2016	Chicken	-
33	C1930	PV2		2016	Chicken	-
34	CC09	Consensus		2016	Pig	-
35	CC14	PV1		2016	Chicken	-
36	CC22	PV1		2016	Chicken	-
37	CC47	PV1		2016	Chicken	-

38	CP17	SDV2		2016	Chicken	-
39	CP81	PV1		2016	Chicken	-
40	CP85	PV1		2016	Chicken	-
41	CP015913.1	PV1		2016	Chicken	-
42	CP015977.1	PV2		2016	Chicken	-
43	CP016183.1	PV1		2016	Chicken	-
44	CP016184.1	SDV2	IncP1	2016	Chicken	-
45	CP016185.1	SDV2		2016	Chicken	-
46	CP016186.1	PV2		2016	Chicken	-
47	CP016187.1	PV1		2016	Chicken	-
48	CP016405.1	PV1		2016	Chicken	-
49	CP017246.1	PV1		2016	Chicken	-
50	CP018106.1	Consensus		2016	Pig	-
51	CP018112.1	PV1		2016	Human	-
52	CP018118.1	PV3	IncX4	2016	Human	-
53	CP018124.1	SDV1		2013	Human	-
54	CP018773.1	SDV1		2013	Chicken	-
55	CP019214.1	SDV1		2013	Chicken	-
56	CY24	PV1		2013	Chicken	-
57	D07_1_WFA16	SDV1		2013	Chicken	-
58	DRR065946	PV1		2013	Chicken	-
59	DRR065947	PV1	IncI2	2013	Chicken	-
60	DRR065948	PV1		2016	Human	-
61	ERR135710	Consensus	IncI2	2016	Environmental	-
62	ERR197184	Consensus		2016	Environmental	-
63	ERR702345	SDV2	IncP1	2016	Pig	-
64	ERR715581	Consensus		2016	Pig	-
65	ERR1035693	PV3		2016	Pig	-
66	ERR1046133	SDV2		2016	Chicken	-
67	ERR1149371	SDV2		2016	Chicken	-
68	ERR1163291	PV3	IncX4	2016	Pig	-
69	ERR1163331	SDV2		2016	Chicken	-
70	ERR1218581	PV3	IncX4	2016	Pig	-
71	ERR1218643	PV3	IncX4	2016	Chicken	-
72	ERR1218720	PV3	IncX4	2016	Human	-
73	ERR1229296	PV1	IncI2	2016	Human	-
74	ERR1360256	Consensus		2016	Human	-
75	ERR1366473	Consensus		2016	Human	-
76	ERR1399393	PV1	IncI2	2016	Pig	-
77	ERR1399394	PV3		2016	Pig	-
78	ERR1399395	PV1	IncI2	2016	Pig	-
79	ERR1399396	SDV1		2016	Chicken	-
80	ERR1399397	SDV1		2016	Human	-
81	ERR1399398	SDV2		2016	Human	-
82	ERR1399423	SDV1		2016	Human	-
83	ERR1399424	SDV4		Unknown	#N/A	-
84	ERR1399425	SDV2		2016	Human	-
85	ERR1432659	SDV2		2016	Human	-
86	ERR1544012	PV3		2016	Human	-
87	ERR1562562	PV3	IncX4	2016	Human	-
88	ERR1609196	PV3	IncX4	2016	Human	-
89	ERR1609197	SDV2		2016	Human	-
90	ERR1609201	Consensus		2016	Human	-
91	ERR1609215	SDV1		2014	Human	-
92	ERR1609245	SDV1		2014	Human	-
93	ERR1609249	Other		2014	Human	-
94	ERR1609312	SDV1		2014	Human	-
95	ERR1609376	PV1	IncI2	2014	Human	-
96	ERR1609378	PV3		2014	Human	-
97	ERR1609380	Other		2013	Human	-
98	ERR1609434	SDV1		2013	Human	-
99	ERR1609449	PV3	IncX4	2013	Human	-
100	ERR1622034	SDV1		2013	Human	-
101	ERR1622058	SDV1		2013	Human	-
102	ERR1622060	SDV1	IncI2	2013	Human	-
103	ERR1622079	Consensus		2012	Human	-
104	ERR1622107	PV1		2012	Human	-
105	ERR1622305	PV1	IncI2	2012	Human	-
106	ERR1622309	Consensus		2012	Human	-
107	ERR1622310	Consensus		2012	Human	-
108	ERR1622311	PV1	IncI2	2012	Human	-
109	ERR1622312	PV2		2012	Human	-

110	ERR1622314	Consensus		2011	Human	-
111	ERR1622342	Consensus		2012	Human	SRR1788032
112	ERR1622370	Consensus		2012	Human	SRR1788031
113	ERR1622435	Consensus		2012	Human	SRR1788028
114	ERR1622541	Consensus		2012	Human	SRR1788027
115	ERR1622545	Consensus		2012	Human	SRR1788026
116	ERR1622547	Consensus		2012	Human	SRR1788024
117	ERR1622549	Other	IncI2	2016	Human	SRR5350657
118	ERR1622589	Consensus		2012	Pig	SRR5328644
119	ERR1622648	Consensus	IncX4	2014	Chicken	ERR1399398
120	ERR1622651	Consensus		2012	Chicken	ERR1399397
121	ERR1622652	Consensus	IncX4	2012	Chicken	ERR1399396
122	ERR1622653	Consensus	IncX4	2012	Chicken	ERR1399395
123	ERR1622654	Consensus	IncX4	2013	Chicken	ERR1399394
124	ERR1622655	PV1	IncI2	2015	Human	ERR1399393
125	ERR1622670	Consensus		2011	Pig	ERR1800784
126	ERR1622708	Consensus	IncX4	2011	Pig	ERR1800783
127	ERR1622709	Consensus	IncX4	2011	Pig	ERR1800782
128	ERR1622725	Consensus	IncX4	2011	Pig	ERR1800781
129	ERR1622729	Consensus	IncX4	2011	Pig	ERR1800780
130	ERR1622739	Consensus	IncX4	2011	Pig	ERR1800779
131	ERR1622769	Consensus	IncX4	2011	Pig	ERR1800778
132	ERR1622770	Consensus	IncX4	2011	Pig	ERR1800777
133	ERR1622839	Consensus	IncX4	2011	Pig	ERR1800776
134	ERR1622840	Consensus	IncX4	2011	Pig	ERR1800775
135	ERR1622881	Consensus		2011	Pig	ERR1800774
136	ERR1622883	Consensus		2011	Pig	ERR1800773
137	ERR1622928	Consensus		2011	Pig	ERR1800772
138	ERR1622930	Consensus	IncX4	2011	Pig	ERR1800771
139	ERR1622946	Consensus	IncX4			ERR1562562
140	ERR1622987	Consensus		2011	Pig	ERR1800785
141	ERR1623088	Consensus		2013	Cow	DRR065948
142	ERR1623113	Consensus		2012	Cow	DRR065947
143	ERR1623212	Consensus		2008	Cow	DRR065946
144	ERR1623214	Consensus		2014		ERR1759157
145	ERR1623215	Consensus		2014		ERR1759128
146	ERR1623222	Consensus		2014	Chicken	ERR1399425
147	ERR1623223	Consensus		2014	Chicken	ERR1399424
148	ERR1623225	Consensus		2009	Chicken	ERR1399423
149	ERR1623226	Consensus		2014		ERR1759167
150	ERR1623227	Consensus		2014		ERR1759166
151	ERR1623228	Consensus		2016	Human	SRR5201504
152	ERR1623229	SDV1	IncI2	2014	Human	SRR4302302
153	ERR1623230	SDV1		2015	Human	SRR4302224
154	ERR1623237	SDV1	IncI2	2015	Human	SRR4302214
155	ERR1623239	SDV2		2014	Human	SRR4302136
156	ERR1623241	PV3	IncX4	2014	Human	ERR1544012
157	ERR1623277	SDV1		2013	Human	ERR1432659
158	ERR1623278	Consensus		2016	Human	ERR1656450
159	ERR1623279	Consensus		2014		ERR1759207
160	ERR1623444	Consensus		2013	Pig	SRR2054248
161	ERR1656450	Consensus		2013	Pig	SRR2054237
162	ERR1759128	Consensus		2013	Pig	SRR2053340
163	ERR1759157	Consensus		2013	Pig	SRR2075991
164	ERR1759166	Consensus	IncI2	2013	Pig	SRR2015698
165	ERR1759167	Consensus	IncI2	2013	Pig	SRR2010693
166	ERR1759207	Consensus		2015		ERR1218720
167	ERR1800771	Consensus		2015		ERR1218643
168	ERR1800772	Consensus		2015		ERR1218581
169	ERR1800773	Consensus	IncX4		Pig	ERR1366473
170	ERR1800774	SDV1		2015	Pig	ERR1229296
171	ERR1800775	SDV3		2015	Human	SRR1965341
172	ERR1800776	Consensus	IncHI2	2014	Human	SRR1960364
173	ERR1800777	SDV2		2016	Human	SRR3992254
174	ERR1800778	PV3		#N/A	Food	SRR5184275
175	ERR1800779	Consensus			Food	SRR5129179
176	ERR1800780	Consensus				SRR3882972
177	ERR1800781	SDV2		2016	Human	SRR3584989
178	ERR1800782	PV1		2014	Pig	SRR3745275
179	ERR1800783	Consensus	IncI2		Human	ERR715581
180	ERR1800784	Consensus	IncHI1		Human	ERR702345
181	ERR1800785	Consensus				ERR1622648

182	GD43	Consensus				ERR1622589
183	GD88	Consensus				ERR1622549
184	GD190	Consensus				ERR1622547
185	GD200	Consensus				ERR1622545
186	GDA05	SDV3	IncI2			ERR1622541
187	GDA12	Consensus				ERR1622435
188	GDA49	SDV2				ERR1622370
189	GDA77	Consensus				ERR1622342
190	GDA192	SDV3				ERR1622314
191	GDZ16009	SDV3				ERR1622312
192	GDZ16011	SDV3				ERR1622311
193	JS16013	SDV3				ERR1622310
194	KP347127.1	SDV3	IncI2			ERR1622309
195	KU341381.1	SDV3				ERR1622305
196	KU353730.1	SDV3	IncI2			ERR1622107
197	KU647721.2	Consensus				ERR1622079
198	KU743383.1	Consensus				ERR1622060
199	KU743384.1	Consensus				ERR1622058
200	KU761326.1	Consensus				ERR1622034
201	KU761327.1	SDV3				ERR1609449
202	KU870627.1	Consensus				ERR1609434
203	KU922754.1	Consensus				ERR1609380
204	KU934208.1	Consensus				ERR1609378
205	KU934209.1	Consensus				ERR1609376
206	KU994859.1	SDV3				ERR1609312
207	KX013538.1	Consensus				ERR1609249
208	KX013539.1	SDV3				ERR1609245
209	KX013540.1	Consensus				ERR1609215
210	KX032519.1	Consensus				ERR1609201
211	KX032520.1	SDV2				ERR1609197
212	KX034083.1	Other				ERR1609196
213	KX084392.1	SDV1				ERR1360256
214	KX084393.1	Consensus	IncX4	2015		ERR1163331
215	KX084394.1	Consensus		2015		ERR1163291
216	KX129782.1	Consensus		2015	Bird	ERR1149371
217	KX129783.1	Consensus				SRR1814872
218	KX129784.1	Consensus				ERR197184
219	KX236309.1	Other				ERR1623444
220	KX254341.1	Consensus	IncX4			ERR135710
221	KX254342.1	Consensus				ERR1046133
222	KX254343.1	Consensus				ERR1035693
223	KX276657.1	Consensus				ERR1623279
224	KX377410.1	SDV3				ERR1623278
225	KX434879.1	SDV3				ERR1623277
226	KX447768.1	Consensus				ERR1623241
227	KX505142.1	Consensus				ERR1623239
228	KX518745.1	Consensus				ERR1623237
229	KX528699.1	SDV2				ERR1623230
230	KX570748.1	Consensus				ERR1623229
231	KX592672.1	SDV2				ERR1623228
232	KX772391.1	Consensus				ERR1623227
233	KX772777.1	Consensus				ERR1623226
234	KX772778.1	Consensus				ERR1623225
235	KX856065.1	SDV3				ERR1623223
236	KX856066.1	SDV3				ERR1623222
237	KX856067.1	Consensus				ERR1623215
238	KX856068.1	Consensus				ERR1623214
239	KX880944.1	Consensus				ERR1623212
240	KY012274.1	Consensus				ERR1623113
241	KY012275.1	SDV2				ERR1623088
242	KY012276.1	Consensus				ERR1622987
243	KY120363.1	SDV2				ERR1622946
244	KY120364.1	SDV2				ERR1622930
245	KY120365.1	SDV2				ERR1622928
246	KY120366.1	SDV3	IncI2			ERR1622883
247	KY471144.1	SDV3	IncI2			ERR1622881
248	KY471145.1	SDV3				ERR1622840
249	KY471146.1	SDV3				ERR1622839
250	KY624633.1	Consensus				ERR1622770
251	PD1G_WH_A22	Consensus				ERR1622769
252	PD1G_WH_A405	SDV2				ERR1622739
253	PD1G_WH_A412	Consensus				ERR1622729

254	PD1G_WH_A427-160530	Consensus				ERR1622725
255	PD1G_WH_A492	Other				ERR1622709
256	PD1G_WH_A494	Other				ERR1622708
257	PD1G_WH_he1-160530	Consensus				ERR1622670
258	PD1G_WH_hk1-160530	Consensus				ERR1622655
259	PD4G_WH_1107-WH	Consensus				ERR1622654
260	PD4G_WH_1157-WH	Consensus	IncHI1			ERR1622653
261	PD4G_WH_WFA04	Consensus				ERR1622652
262	PD4G_WH_WFA13	Consensus	IncHI1			ERR1622651
263	PD4G_WH_WFA14	Consensus		2016	Human	-
264	PD4G_WH_WFA17	SDV1	IncI2	2015	Human	-
265	PD4G_WH_WFA18	SDV1	IncI2	2015	Human	-
266	PD4G_WH_WFA19	Consensus	IncFII	2011	Pig	-
267	PD4G_WH_WFA20	Consensus		2011	Pig	-
268	PD4G_WH_WFA26	PV4	IncI2	2013	Food	-
269	PD4G_WH_WFA27	Consensus	IncX4	2013	Penguin	-
270	PD4G_WH_WFA29	SDV4	IncX4	2016	Human	-
271	PD4G_WH_WFA32	Consensus	IncX4	2014	Human	-
272	PD4G_WH_WFA40	Consensus	IncX4	2016	Chicken	-
273	PD4G_WH_WFA41	SDV4	IncX4	2016	Chicken	-
274	PD4G_WH_WFA56	Consensus	IncX4	2016	Environmental	-
275	PD4G_WH_WFA60	Consensus		2016	Environmental	-
276	PD4G_WH_WFA62	PV4	IncX4	2016	Environmental	-
277	PD4G_WH_WFA64	Consensus	IncX4	2016	Environmental	-
278	PD4G_WH_WFA65	Consensus	IncX4	2016	Human	-
279	PD4G_WH_WFA66	SDV4	IncX4	2016	Human	-
280	PD4G_WH_WFA67	PV3	IncX4	2016	Chicken	-
281	PD4G_WH_WFA89	PV3	IncX4	2014	Human	-
282	PD4G_WH_WFA97	Consensus	IncI2	2014	Human	-
283	PD4M_WH_wT2	SDV1	IncI2	2014	Human	-
284	SAMEA3930541	Consensus	IncY	2016	Pig	-
285	SAMEA3980467	Other	IncI2	2012	Human	-
286	SAMEA3980468	PV1	IncI2	2013	Human	-
287	SAMEA3980469	SDV2		2016	Human	-
288	SAMEA4031745	Consensus	IncHI2	2015	Pig	-
289	SAMEA4350769	PV1	IncI2	2016	Human	-
290	SAMEA4350770	PV3	IncX4	2015	Human	-
291	SAMEA4350771	SDV2		2016	Human	-
292	SAMEA4350772	Consensus	IncI2	2014	Human	-
293	SAMEA4350773	PV3	IncX4	2016	Pig	-
294	SAMEA4350774	Consensus	IncY	2016	Pig	-
295	SAMEA4350775	SDV2	IncI2	2016	Chicken	-
296	SAMEA4350776	SDV2	IncP1	2015	Environmental	-
297	SAMEA4350777	PV3	IncX4	2014	Pig	-
298	SAMEA4350778	PV1	IncI2	2015	Pig	-
299	SAMEA4350779	Consensus		2015	Pig	-
300	SAMEA4350780	Consensus	IncHI2	2015	Pig	-
301	SAMEA4350781	PV1	IncI2	2015	Pig	-
302	SAMEA4350782	PV1	IncX4	2015	Pig	-
303	SAMEA4350783	Consensus	IncI2	2012	Chicken	-
304	SAMEA4350784	Other	IncI2	2014	Chicken	-
305	SAMEA4350785	PV1	IncI2	2013	Chicken	-
306	SAMEA4350786	Consensus	IncI2	2015	Environmental	-
307	SAMEA4350787	PV3	IncX4	2015	Human	-
308	SAMEA4350788	PV1	IncI2	2015	Human	-
309	SAMEA4350789	PV3	IncX4	2015	Cat	-
310	SAMEA4350790	Consensus	IncHI2	2015	Pig	-
311	SAMN03256164	Other	IncI2	2013	Pig	-
312	SAMN03256224	SDV2		2015	Environmental	-
313	SAMN03256247	SDV2		2015	Chicken	-
314	SAMN04002628	PV1		2014	Chicken	-
315	SAMN04110135	PV1		2015	Chicken	-
316	SAMN04110137	SDV1	IncI2	2015	Chicken	-
317	SAMN04110139	SDV1		2014	Chicken	-
318	SAMN04110140	PV1	IncI2	2014	Chicken	-
319	SAMN04376757	Consensus		2015	Chicken	-
320	SAMN04376760	PV1	IncI2	2015	Chicken	-
321	SAMN04376766	PV1	IncI2	2015	Chicken	-
322	SAMN04376767	Other		2015	Chicken	-
323	SAMN04376786	PV1	IncI2	2015	Chicken	-
324	SAMN04376787	PV1		2015	Chicken	-
325	SAMN04376790	PV2	IncI2	2015	Chicken	-

326	SAMN04376792	SDV1		2015	Chicken	-
327	SAMN04376798	SDV1	IncI2	2015	Chicken	-
328	SAMN04376803	SDV2	IncHI2	2015	Chicken	-
329	SAMN04376805	SDV1		2015	Chicken	-
330	SAMN04376846	PV1		2015	Dog	-
331	SAMN04376847	SDV1	IncI2	2015	Fly	-
332	SAMN04376848	PV1	IncI2	2015	Fly	-
333	SAMN04376857	Consensus		2015	Fly	-
334	SAMN04423147	SDV1		2015	Fly	-
335	SAMN04482604	Consensus	IncX4	2015	Chicken	-
336	SAMN04482605	Consensus	IncX4	2015	Chicken	-
337	SAMN04482606	Consensus	IncX4	2015	Chicken	-
338	SAMN04490314	PV2		2015	Chicken	-
339	SAMN04880556	PV1	IncI2	2015	Chicken	-
340	SAMN04880557	PV2	IncI2	2015	Chicken	-
341	SAMN04884976	PV1	IncI2	2015	Chicken	-
342	SAMN04964663	PV1	IncI2	2015	Chicken	-
343	SAMN05172242	PV1	IncI2	2015	Chicken	-
344	SAMN05177221	PV1	IncI2	2015	Chicken	-
345	SAMN05190012	PV1		2015	Chicken	-
346	SAMN05257099	PV1	IncI2	2015	Chicken	-
347	SAMN05257101	PV1		2015	Environmental	-
348	SAMN05257103	PV2	IncI2	2015	Chicken	-
349	SAMN05294116	PV2	IncI2	2015	Chicken	-
350	SAMN05346848	PV2	IncI2	2015	Chicken	-
351	SAMN05420188	PV1	IncI2	2015	Chicken	-
352	SAMN05510674	PV2	IncI2	2015	Chicken	-
353	SAMN05832830	PV1		2015	Chicken	-
354	SAMN05928858	PV1	IncI2	2014	Chicken	-
355	SAMN05928861	PV1	IncI2	2014	Chicken	-
356	SAMN05928862	PV1	IncI2	2014	Chicken	-
357	SAMN05928864	PV1		2014	Chicken	-
358	SAMN05928865	PV1		2014	Chicken	-
359	SAMN05928876	PV3	IncX4	2016	Human	-
360	SAMN05928890	PV3	IncX4	2016	Human	-
361	SAMN05928895	Consensus		2015	Human	-
362	SAMN05928897	Consensus	IncI2	2013	Sheep	-
363	SAMN05928900	Consensus	IncI2	2013	Sheep	-
364	SAMN05928901	Consensus	IncI2	2013	Sheep	-
365	SAMN05928908	PV1	IncI2	2013	Sheep	-
366	SAMN05928909	Consensus	IncI2	2012	Pig	-
367	SAMN05928914	Consensus	IncI2	2012	Pig	-
368	SAMN05928915	PV3	IncX4	2012	Pig	-
369	SAMN05928916	Consensus	IncI2	2012	Pig	-
370	SAMN05928917	PV3	IncX4	2012	Pig	-
371	SAMN05928918	Other		2012	Pig	-
372	SAMN05928919	Consensus		2012	Pig	-
373	SAMN05928920	PV3	IncX4	2012	Pig	-
374	SAMN05928921	Consensus		2012	Pig	-
375	SAMN05928927	Consensus		2014	Pig	-
376	SAMN05928929	Consensus		2014	Pig	-
377	SAMN05928932	SDV2		2015	Environmental	-
378	SAMN05928943	SDV2		2015	Environmental	-
379	SAMN05928946	Consensus		2015	Environmental	-
380	SAMN05928953	Consensus		2011	Pig	-
381	SAMN05928959	Consensus		2011		-
382	SAMN05928978	Consensus	IncX4	2016	Environmental	-
383	SAMN05928979	Consensus		2013	Environmental	-
384	SAMN05928981	Consensus	IncX4	2012	Environmental	-
385	SAMN05928984	Consensus		2012	Environmental	-
386	SAMN05928988	Consensus		2012	Environmental	-
387	SAMN05928993	Consensus	IncHI2	2015	Human	-
388	SAMN05928994	Consensus	IncI2	2016	Human	-
389	SAMN05928995	Consensus		2010	Chicken	-
390	SAMN05928996	Consensus		2013	Reptile	-
391	SAMN05928997	Consensus		2014	Reptile	-
392	SAMN05929006	Consensus		2012	Environmental	-
393	SAMN05929007	Consensus		2013	Environmental	-
394	SAMN05929008	Consensus	IncX4	2012	Environmental	-
395	SAMN05929009	Consensus	IncX4	2012	Environmental	-
396	SAMN05929010	Consensus	IncX4	2014	Human	-
397	SAMN05929015	Consensus	IncHI2	2016		-

398	SAMN05929018	SDV1	IncI2	2016	Poultry feed	-
399	SAMN05971374	SDV1	IncI2	2016	Environmental	-
400	SAMN05971811	SDV1	IncI2	2016	Chicken	-
401	SAMN06029893	Consensus		2016	Pig	-
402	SAMN06029894	Consensus		2016	Chicken	-
403	SAMN06029895	Consensus		2013	Chicken	-
404	SAMN06029896	SDV1		2013	Chicken	-
405	SAMN06043562	Consensus		2013	Pig	-
406	SAMN06051286	Consensus		2013	Human	-
407	SAMN06159501	Other	IncX4	2015	Turkey	-
408	SAMN06163642	Other	IncX4	2015	Turkey	-
409	SAMN06197014	Consensus		2013	Environmental	-
410	SAMN06215934	Consensus	IncHI2	2012	Human	-
411	SAMN06233851	Consensus		2014	Human	-
412	SAMN06236403	Consensus	IncI2	2014	Human	-
413	SAMN06236581	Consensus	IncI2	2016	Chicken	-
414	SAMN06285083	Consensus	IncX4	2012	Environmental	-
415	SAMN06285143	Consensus		2015	Chicken	-
416	SRR1788024	Consensus	IncI2	2016	Human	-
417	SRR1788026	SDV1	IncI2	2016	Pig	-
418	SRR1788027	PV3	IncX4	2016	Human	-
419	SRR1788028	Consensus	IncX4	2016	Chicken	-
420	SRR1788031	Consensus		2014	Vegetables	-
421	SRR1788032	Consensus	IncI2	2013	Human	-
422	SRR1814872	PV1	IncI2	2016	Pig	-
423	SRR1960364	Consensus	IncX4	2014	Human	-
424	SRR1965341	SDV2		2016	Human	-
425	SRR2010693	Consensus	IncX4	2017	Human	-
426	SRR2015698	Consensus	IncI2	2016	Human	-
427	SRR2053340	Consensus	IncI2	2016	Human	-
428	SRR2054237	Consensus	IncI2	2016	Human	-
429	SRR2054248	Consensus	IncI2	2016	Pig	-
430	SRR2075991	Consensus	IncX4	2014	Human	-
431	SRR3584989	Consensus		2014	Pig	-
432	SRR3745275	SDV2		2013	Human	-
433	SRR3882972	Consensus		2012	Chicken	-
434	SRR3992254	Consensus	IncHI2	2012	Chicken	-
435	SRR4302136	Consensus		2012	Chicken	-
436	SRR4302214	Consensus		2012	Chicken	-
437	SRR4302224	Consensus		2012	Chicken	-
438	SRR4302302	SDV2	IncHI2	2012	Chicken	-
439	SRR5129179	Consensus		2012	Chicken	-
440	SRR5184275	SDV2	IncP1	2012	Chicken	-
441	SRR5201504	Consensus		2012	Chicken	-
442	SRR5328644	Consensus		2012	Chicken	-
443	SRR5350657	Consensus		2012	Chicken	-
444	SY16004	Consensus		2012	Chicken	-
445	WF37	Consensus		2012	Chicken	-
446	WF197	Consensus	IncHI2	2012	Chicken	-
447	WFA05	Consensus		2012	Chicken	-
448	WFA59	SDV2		2012	Chicken	-
449	WFA63	Consensus		2012	Chicken	-
450	WFA160	SDV3	IncI2	2012	Chicken	-
451	WFA174	Consensus		2012	Chicken	-
452	WW05	Consensus		2012	Chicken	-
453	WW09	Consensus		2012	Chicken	-
454	WW12	SDV3	IncI2	2012	Chicken	-
455	XM1416	Consensus	IncX4	2017		-
456	XM1507	PV2	IncI2	2017		-
457	XM1603	PV2	IncI2	2017		-

Shen Dataset						
#	Isolate ID	Promoter	Plasmid	Year	Host	SRA
1	AA008	PV3	IncX4	2016	Pig	SRR15732044
2	AA032	PV3	IncX4	2016	Pig	SRR15732043
3	AA148	Consensus	IncHI2/IncHI2A/pKPC	2016	Pig	SRR15731824
4	AA225	SDV2		2016	Pig	SRR15732037
5	AA226	Consensus		2016	Pig	SRR15731674
6	AA228	Other	IncI2	2016	Pig	SRR15732179
7	AA229	PV3	IncX4	2016	Pig	SRR15732104

8	AA230	Other		2016	Pig	SRR15732065
9	AA231	Consensus	IncY	2016	Pig	SRR15732054
10	AA232	PV3	IncX4	2016	Pig	SRR15732235
11	AA233	Consensus		2016	Pig	SRR15732042
12	AA234	SDV2		2016	Pig	SRR15731995
13	AA235	PV3	IncX4	2016	Pig	SRR15731984
14	AA236	Consensus		2016	Pig	SRR15731973
15	AA237	Other	IncI2	2016	Pig	SRR15731962
16	AA238	PV3	IncX4	2016	Pig	SRR15731951
17	AA239	Consensus		2016	Pig	SRR15731940
18	AA240	PV3	IncX4	2016	Pig	SRR15731857
19	AA241	SDV3	IncHI1A/IncHI1B	2016	Pig	SRR15731846
20	AA242	PV3	IncX4	2016	Pig	SRR15731835
21	AA243	PV3	IncX4	2016	Pig	SRR15731823
22	AA244	PV3	IncX4	2016	Pig	SRR15731812
23	AA246	Consensus		2016	Pig	SRR15731801
24	AA247	Consensus		2016	Pig	SRR11817624
25	AA248	Consensus		2016	Pig	SRR11939516
26	AA249	PV2	IncX4	2016	Pig	SRR15731790
27	AA250	Consensus	IncHI2A	2016	Pig	SRR15731779
28	AA252	Consensus	IncI2	2016	Pig	SRR15731768
29	AA253	Consensus		2016	Pig	SRR15731757
30	AA254	Consensus		2016	Pig	SRR15731746
31	AA255	Other		2016	Pig	SRR15731735
32	AA256	Consensus		2016	Pig	SRR15731724
33	AA257	PV3	IncX4	2016	Pig	SRR15732036
34	AA263	PV3	IncX4	2016	Pig	SRR15732025
35	AA264	Consensus		2016	Pig	SRR15732014
36	AA265	Consensus		2016	Pig	SRR15731931
37	AA266	Consensus		2016	Pig	SRR15731920
38	AA267	Consensus		2016	Pig	SRR15731909
39	AA268	Consensus		2016	Pig	SRR15731898
40	AA269	PV3	IncX4	2016	Pig	SRR15731707
41	AA270	PV2	IncX4	2016	Pig	SRR15731696
42	AA271	Consensus		2016	Pig	SRR15731685
43	AA272	PV3	IncX4	2016	Pig	SRR15731673
44	AA273	PV3	IncX4	2016	Pig	SRR15732326
45	AA274	PV3	IncX4	2016	Pig	SRR15732315
46	AA275	PV1	IncI2	2016	Pig	SRR15732268
47	AA276	PV3	IncX4	2016	Pig	SRR15732257
48	AA278	PV3	IncX4	2016	Pig	SRR15732223
49	AA280	PV3	IncX4	2016	Pig	SRR15732212
50	AA281	PV3	IncX4	2016	Pig	SRR15732201
51	AA282	Consensus		2016	Pig	SRR15732190
52	AA288	Consensus		2016	Pig	SRR15732178
53	AA294	Consensus		2016	Pig	SRR15732167
54	AA295	Other		2016	Pig	SRR15732156
55	AA465	Consensus		2016	Pig	SRR15732301
56	AA477	PV3	IncX4	2016	Pig	SRR15732290
57	AA516	PV3	IncX4	2016	Pig	SRR15732279
58	AA517	PV3		2016	Pig	SRR15732148
59	AA524	Other	IncI2	2016	Pig	SRR15732137
60	AA529	Consensus		2016	Pig	SRR15732126
61	AA531	Consensus		2016	Pig	SRR11939515
62	AB255	Other	IncI2	2016	Pig	SRR15732115
63	AB256	Other	IncI2	2016	Pig	SRR15732103
64	AB257	SDV2		2016	Pig	SRR15732092
65	AB258	Consensus	IncHI2A	2016	Pig	SRR15732081
66	AB259	Consensus	IncHI2/IncHI2A/pKPC	2016	Pig	SRR15731886
67	AB260	Consensus		2016	Pig	SRR15731875
68	AB261	Consensus		2016	Pig	SRR15731864
69	AB262	SDV2		2016	Pig	SRR15732073
70	AB263	Consensus	IncHI2A	2016	Pig	SRR15732068
71	AB264	PV3	IncX4	2016	Pig	SRR15732067
72	AB265	PV2	IncX4	2016	Pig	SRR15732066
73	AB266	PV3	IncX4	2016	Pig	SRR15732064
74	AB267	Consensus		2016	Pig	SRR15732063
75	AB268	Consensus		2016	Pig	SRR15732062
76	AB327	Consensus		2016	Pig	SRR15732061
77	AB335	Other	IncI2	2016	Pig	SRR15732060
78	AC061	Consensus		2016	Healthy human volunteers	SRR11939527
79	AC104	PV3	IncX4	2016	Healthy human volunteers	SRR15732059

80	AC105	PV3	IncX4	2016	Healthy human volunteers	SRR15732058
81	AC106	PV3	IncX4	2016	Healthy human volunteers	SRR15732057
82	AC107	PV3	IncX4	2016	Healthy human volunteers	SRR15732056
83	AC108	SDV2		2016	Healthy human volunteers	SRR15732055
84	AC109	Other	IncI2	2016	Healthy human volunteers	SRR15732053
85	AC111	SDV2		2016	Healthy human volunteers	SRR15732052
86	AC112	Consensus		2016	Healthy human volunteers	SRR15732051
87	AC113	PV2	IncX4	2016	Healthy human volunteers	SRR15732050
88	AC114	Consensus	IncHI2A	2016	Healthy human volunteers	SRR15732049
89	AC115	Consensus		2016	Healthy human volunteers	SRR15732048
90	AC117	Consensus		2016	Healthy human volunteers	SRR15732047
91	AC118	Consensus	IncY	2016	Healthy human volunteers	SRR15732046
92	AC119	PV3	IncX4	2016	Healthy human volunteers	SRR15732045
93	AC120	Consensus	IncHI2A	2016	Healthy human volunteers	SRR15732236
94	AC121	SDV2	IncP1	2016	Healthy human volunteers	SRR15732234
95	AC122	Consensus	IncHI2A	2016	Healthy human volunteers	SRR15732233
96	AC123	Consensus	IncHI2A	2016	Healthy human volunteers	SRR15732232
97	AC124	PV3	IncX4	2016	Healthy human volunteers	SRR15732231
98	AC125	Consensus		2016	Healthy human volunteers	SRR11939523
99	AC126	Consensus		2016	Healthy human volunteers	SRR11939522
100	AC127	PV2	IncX4	2016	Healthy human volunteers	SRR15732230
101	AC128	SDV2	IncI2	2016	Healthy human volunteers	SRR15732229
102	AC129	Consensus		2016	Healthy human volunteers	SRR11939521
103	AC130	SDV2	IncI2	2016	Healthy human volunteers	SRR15732228
104	AC131	PV3	IncX4	2016	Healthy human volunteers	SRR15732227
105	AC132	Consensus		2016	Healthy human volunteers	SRR15732226
106	AC133	SDV2		2016	Healthy human volunteers	SRR15732224
107	AC134	PV3	IncX4	2016	Healthy human volunteers	SRR15732041
108	AC136	Consensus		2016	Healthy human volunteers	SRR11939520
109	AC137	Other	IncHI2A	2016	Healthy human volunteers	SRR15732004
110	AC138	PV3	IncX4	2016	Healthy human volunteers	SRR15732003
111	AC139	Consensus		2016	Healthy human volunteers	SRR15732002
112	AC140	Consensus		2016	Healthy human volunteers	SRR15732001
113	AC141	Consensus		2016	Healthy human volunteers	SRR15732000
114	AC142	SDV2		2016	Healthy human volunteers	SRR15731999
115	AC143	PV3	IncX4	2016	Healthy human volunteers	SRR15731998
116	AC145	Other	IncI2	2016	Healthy human volunteers	SRR15731997
117	AC146	PV3	IncX4	2016	Healthy human volunteers	SRR15731996
118	AC147	Other	IncX4	2016	Healthy human volunteers	SRR15731994
119	AC148	Consensus		2016	Healthy human volunteers	SRR11939519
120	AC150	SDV2	IncP1	2016	Healthy human volunteers	SRR15731993
121	AC154	Consensus		2016	Healthy human volunteers	SRR15731992
122	AC156	PV3	IncX4	2016	Healthy human volunteers	SRR15731991
123	AC157	PV3	IncX4	2016	Healthy human volunteers	SRR15731990
124	AC159	PV3	IncX4	2016	Healthy human volunteers	SRR15731989
125	AC160	Other		2016	Healthy human volunteers	SRR15731988
126	AC161	SDV2	IncP1/ColRNAI1	2016	Healthy human volunteers	SRR15731987
127	AC162	Consensus	IncHI2A	2016	Healthy human volunteers	SRR15731986
128	AC163	PV3	IncX4	2016	Healthy human volunteers	SRR15731985
129	AC232	PV3	IncX4	2016	Healthy human volunteers	SRR15731983
130	AC454	PV3	IncX4	2016	Healthy human volunteers	SRR15731982
131	AC642	PV3	IncX4	2016	Healthy human volunteers	SRR15731981
132	AC703	Other	IncI2	2016	Healthy human volunteers	SRR15731980
133	AC817	Consensus		2016	Healthy human volunteers	SRR15731979
134	AC840	Consensus		2016	Healthy human volunteers	SRR15731978
135	AC844	Consensus		2016	Healthy human volunteers	SRR15731977
136	AC895	PV3	IncX4	2016	Healthy human volunteers	SRR15731976
137	AC922	Consensus		2016	Healthy human volunteers	SRR15731975
138	AD165	Consensus		2016	Patient colonized with Enterobacteriaceae	SRR15731974
139	AD166	SDV2	IncP1	2016	Patient colonized with Enterobacteriaceae	SRR15731972
140	AD167	SDV2	IncP1	2016	Patient colonized with Enterobacteriaceae	SRR15731971
141	AD168	Consensus		2016	Patient colonized with Enterobacteriaceae	SRR15731970
142	AD169	Consensus		2016	Patient colonized with Enterobacteriaceae	SRR15731969
143	AD170	PV3	IncX4	2016	Patient colonized with Enterobacteriaceae	SRR15731968
144	AD171	PV3	IncX4	2016	Patient colonized with Enterobacteriaceae	SRR15731967
145	AD172	Other	IncI2	2016	Patient colonized with Enterobacteriaceae	SRR15731966
146	AD173	Consensus	IncHI2/IncHI2A/pKPC	2016	Patient colonized with Enterobacteriaceae	SRR15731965
147	AD174	Consensus		2016	Patient colonized with Enterobacteriaceae	SRR15731964
148	AD175	SDV2		2016	Patient colonized with Enterobacteriaceae	SRR15731963
149	AD176	SDV2		2016	Patient colonized with Enterobacteriaceae	SRR15731961
150	AD177	Consensus		2016	Patient colonized with Enterobacteriaceae	SRR15731960
151	AD178	PV3	IncX4	2016	Patient colonized with Enterobacteriaceae	SRR15731959

152	AD179	PV3	IncX4	2016	Patient colonized with Enterobacteriaceae	SRR15731958
153	AD180	Consensus		2016	Patient colonized with Enterobacteriaceae	SRR15731957
154	AD181	PV3	IncX4	2016	Patient colonized with Enterobacteriaceae	SRR15731956
155	AD182	Consensus		2016	Patient colonized with Enterobacteriaceae	SRR15731955
156	AD183	PV3		2016	Patient colonized with Enterobacteriaceae	SRR15731954
157	AD184	PV3	IncX4	2016	Patient colonized with Enterobacteriaceae	SRR15731953
158	AD185	Consensus		2016	Patient colonized with Enterobacteriaceae	SRR15731952
159	AD186	Consensus		2016	Patient colonized with Enterobacteriaceae	SRR15731950
160	AD187	Consensus		2016	Patient colonized with Enterobacteriaceae	SRR15731949
161	AD188	Other	IncI2	2016	Patient colonized with Enterobacteriaceae	SRR15731948
162	AD189	SDV2		2016	Patient colonized with Enterobacteriaceae	SRR15731947
163	AD191	Consensus		2016	Patient colonized with Enterobacteriaceae	SRR15731946
164	AD192	Consensus		2016	Patient colonized with Enterobacteriaceae	SRR15731945
165	AD193	PV3		2016	Patient colonized with Enterobacteriaceae	SRR15731944
166	AD194	SDV2	IncP1	2016	Patient colonized with Enterobacteriaceae	SRR15731943
167	AD195	PV3	IncX4	2016	Patient colonized with Enterobacteriaceae	SRR15731942
168	AD196	PV3	IncX4	2016	Patient colonized with Enterobacteriaceae	SRR15731941
169	AD197	Consensus	IncHI2/IncHI2A/pKPC	2016	Patient colonized with Enterobacteriaceae	SRR15731939
170	AD198	SDV2	IncP1	2016	Patient colonized with Enterobacteriaceae	SRR15731938
171	AD199	PV2		2016	Patient colonized with Enterobacteriaceae	SRR15731937
172	AD200	Other	IncI2	2016	Patient colonized with Enterobacteriaceae	SRR15731936
173	AD201	Consensus	IncHI1A/IncHI1B	2016	Patient colonized with Enterobacteriaceae	SRR15731935
174	AD202	Consensus		2016	Patient colonized with Enterobacteriaceae	SRR15731934
175	AD203	Other		2016	Patient colonized with Enterobacteriaceae	SRR15731933
176	AD204	Consensus		2016	Patient colonized with Enterobacteriaceae	SRR15731860
177	AD205	Consensus		2016	Patient colonized with Enterobacteriaceae	SRR15731859
178	AD206	Consensus		2016	Patient colonized with Enterobacteriaceae	SRR15731858
179	AD207	PV3	IncX4	2016	Patient colonized with Enterobacteriaceae	SRR15731856
180	AD208	Consensus		2016	Patient colonized with Enterobacteriaceae	SRR15731855
181	AD209	PV1		2016	Patient colonized with Enterobacteriaceae	SRR15731854
182	AD210	Consensus		2016	Patient colonized with Enterobacteriaceae	SRR11939518
183	AD211	Consensus	IncX4	2016	Patient colonized with Enterobacteriaceae	SRR15731853
184	AD212	PV3	IncX4	2016	Patient colonized with Enterobacteriaceae	SRR15731852
185	AD213	SDV2		2016	Patient colonized with Enterobacteriaceae	SRR15731851
186	AD215	PV3	IncX4	2016	Patient colonized with Enterobacteriaceae	SRR15731850
187	AD216	Consensus		2016	Patient colonized with Enterobacteriaceae	SRR15731849
188	AD2160	Consensus		2016	Patient colonized with Enterobacteriaceae	SRR15731848
189	AD217	Consensus		2016	Patient colonized with Enterobacteriaceae	SRR11939517
190	AD218	PV3	IncX4	2016	Patient colonized with Enterobacteriaceae	SRR15731847
191	AD219	SDV2		2016	Patient colonized with Enterobacteriaceae	SRR15731845
192	AD220	Consensus		2016	Patient colonized with Enterobacteriaceae	SRR11939514
193	AD221	Consensus		2016	Patient colonized with Enterobacteriaceae	SRR15731844
194	AD222	Consensus		2016	Patient colonized with Enterobacteriaceae	SRR15731843
195	AD223	Consensus		2016	Patient colonized with Enterobacteriaceae	SRR15731842
196	AD2473	Other	IncI2	2016	Patient colonized with Enterobacteriaceae	SRR15731841
197	AD2800	PV3	IncX4	2016	Patient colonized with Enterobacteriaceae	SRR15731840
198	AE001	SDV2		2016	Patient infected with Enterobacteriaceae	SRR15731839
199	AE002	Consensus		2016	Patient infected with Enterobacteriaceae	SRR15731838
200	AE003	SDV2		2016	Patient infected with Enterobacteriaceae	SRR15731837
201	AE004	PV3	IncX4	2016	Patient infected with Enterobacteriaceae	SRR15731836
202	AE005	Consensus	IncHI2A	2016	Patient infected with Enterobacteriaceae	SRR15731834
203	AE006	Consensus		2016	Patient infected with Enterobacteriaceae	SRR15731833
204	AE007	PV3	IncX4	2016	Patient infected with Enterobacteriaceae	SRR15731832
205	AE008	Other		2016	Patient infected with Enterobacteriaceae	SRR15731831
206	AE009	Other	IncI2	2016	Patient infected with Enterobacteriaceae	SRR15731830
207	AE011	Other		2016	Patient infected with Enterobacteriaceae	SRR15731829
208	AE012	PV3	IncX4	2016	Patient infected with Enterobacteriaceae	SRR15731828
209	AE013	PV1	IncI2	2016	Patient infected with Enterobacteriaceae	SRR15731827
210	AE047	SDV2	IncHI2A	2016	Patient infected with Enterobacteriaceae	SRR15731826
211	AE052	SDV2		2016	Patient infected with Enterobacteriaceae	SRR15731825
212	AE056	PV1	IncI2	2016	Patient infected with Enterobacteriaceae	SRR15731822
213	AE077	Consensus		2016	Patient infected with Enterobacteriaceae	SRR15731821
214	AE079	Other		2016	Patient infected with Enterobacteriaceae	SRR15731820
215	AE084	Other	IncI2	2016	Patient infected with Enterobacteriaceae	SRR15731819
216	AE109	SDV2		2016	Patient infected with Enterobacteriaceae	SRR15731818
217	AE115	SDV2	IncHI2/IncHI2A/pKPC	2016	Patient infected with Enterobacteriaceae	SRR15731817
218	AE121	SDV2		2016	Patient infected with Enterobacteriaceae	SRR15731816
219	AE148	SDV4	IncI2	2016	Patient infected with Enterobacteriaceae	SRR15731815
220	AE231	Consensus		2016	Patient infected with Enterobacteriaceae	SRR15731814
221	AE262	PV3	IncX4	2016	Patient infected with Enterobacteriaceae	SRR15731813
222	AE344	PV3	IncX4	2016	Patient infected with Enterobacteriaceae	SRR15731811
223	AE404	Consensus		2016	Patient infected with Enterobacteriaceae	SRR15731810

224	AE568	PV3	IncX4	2016	Patient infected with Enterobacteriaceae	SRR15731809
225	AF260	Consensus		2016	Environment	SRR15731808
226	AF269	Other	IncI2	2016	Environment	SRR15731807
227	AF270	PV3	IncX4	2016	Environment	SRR15731806
228	AF271	Other	IncI2	2016	Environment	SRR15731805
229	AF272	Other	IncI2	2016	Environment	SRR15731804
230	AF273	SDV2		2016	Environment	SRR15731803
231	AF274	Other	IncI2	2016	Environment	SRR15731802
232	AF275	Consensus		2016	Environment	SRR15731800
233	AF276	Consensus		2016	Environment	SRR15731799
234	AF277	SDV3	IncHI1A/IncHI1B	2016	Environment	SRR15731798
235	AF278	PV3	IncX4	2016	Environment	SRR15731797
236	AF279	Consensus		2016	Environment	SRR15731796
237	AF280	Consensus		2016	Environment	SRR15731795
238	AF281	Consensus		2016	Environment	SRR15731794
239	AF282	SDV3	IncHI1A/IncHI1B	2016	Environment	SRR15731793
240	AF283	Other	IncI2	2016	Environment	SRR15731792
241	AF284	Consensus		2016	Environment	SRR15731791
242	AF286	Consensus		2016	Environment	SRR15731789
243	AG057	Consensus		2016	Environment	SRR15731788
244	AG060	Consensus		2016	Environment	SRR15731786
245	AG061	Consensus		2016	Environment	SRR15731785
246	AG064	PV3	IncX4	2016	Environment	SRR15731784
247	AG065	PV2	IncX4	2016	Environment	SRR15731783
248	AG067	SDV2		2016	Environment	SRR15731782
249	AG068	PV3	IncX4	2016	Environment	SRR15731781
250	AG069	Other		2016	Environment	SRR15731780
251	AG070	SDV2		2016	Environment	SRR15731778
252	AG071	PV3	IncX4	2016	Environment	SRR15731777
253	AG072	Consensus		2016	Environment	SRR15731776
254	AG074	Consensus		2016	Environment	SRR15731775
255	AG075	Consensus		2016	Environment	SRR15731774
256	AG077	SDV2		2016	Environment	SRR15731773
257	AG078	PV3	IncX4	2016	Environment	SRR15731772
258	AG079	Consensus		2016	Environment	SRR15731771
259	AG080	PV3	IncX4	2016	Environment	SRR15731770
260	AG081	Other		2016	Environment	SRR15731769
261	AG082	Consensus		2016	Environment	SRR15731767
262	AG084	Consensus		2016	Environment	SRR15731766
263	AG085	Consensus		2016	Environment	SRR15731765
264	AG086	Consensus	IncHI2A	2016	Environment	SRR15731764
265	AG087	Consensus		2016	Environment	SRR15731763
266	AG088	Consensus		2016	Environment	SRR15731762
267	AG089	SDV2		2016	Environment	SRR15731761
268	AG102	Other		2016	Environment	SRR15731760
269	AG222	SDV2	IncP1	2016	Environment	SRR15731759
270	AG229	Consensus		2016	Environment	SRR15731758
271	AG261	SDV2	IncHI2/IncHI2A/pKPC	2016	Environment	SRR15731756
272	AG411	SDV2	IncHI2/IncHI2A/pKPC	2016	Environment	SRR15731755
273	AG485	PV3	IncX4	2016	Environment	SRR15731754
274	AH014	Other	IncI2	2016	Food	SRR15731753
275	AH016	PV3	IncX4	2016	Food	SRR15731752
276	AH017	Consensus		2016	Food	SRR15731751
277	AH019	SDV2		2016	Food	SRR15731750
278	AH020	Other		2016	Food	SRR15731749
279	AH021	PV3	IncX4	2016	Food	SRR15731748
280	AH022	Consensus		2016	Food	SRR15731747
281	AH023	Consensus		2016	Food	SRR15731745
282	AH024	PV3	IncX4	2016	Food	SRR15731744
283	AH025	Other	IncI2	2016	Food	SRR15731743
284	AH026	SDV2		2016	Food	SRR15731742
285	AH027	Consensus	IncHI2/IncHI2A/pKPC	2016	Food	SRR15731741
286	AH028	SDV2		2016	Food	SRR15731740
287	AH030	SDV2		2016	Food	SRR15731738
288	AH031	Other	IncI2	2016	Food	SRR15731737
289	AH032	PV3	IncX4	2016	Food	SRR15731736
290	AH033	PV3	IncX4	2016	Food	SRR15731734
291	AH034	PV3	IncX4	2016	Food	SRR15731733
292	AH035	SDV2		2016	Food	SRR15731732
293	AH036	Other	IncI2	2016	Food	SRR15731731
294	AH037	Other	IncI2	2016	Food	SRR15731730
295	AH038	Consensus		2016	Food	SRR15731729

296	AH039	Consensus	IncI2	2016	Food	SRR15731728
297	AH040	Consensus	IncI2	2016	Food	SRR15731727
298	AH041	Consensus	IncI2	2016	Food	SRR15731726
299	AH043	PV3	IncX4	2016	Food	SRR15731725
300	AH047	PV3	IncX4	2016	Food	SRR15731723
301	AH051	PV3	IncX4	2016	Food	SRR15731722
302	AH052	Consensus	IncI2	2016	Food	SRR15731721
303	AH053	Consensus		2016	Food	SRR15731720
304	AH054	Consensus	p01111	2016	Food	SRR15731719
305	AH055	Consensus	p01111	2016	Food	SRR15731718
306	AH056	Other	IncI2	2016	Food	SRR15731717
307	AH091	SDV2		2016	Food	SRR15732040
308	AH093	PV3	IncX4	2016	Food	SRR15732039
309	AH094	Consensus		2016	Food	SRR15732038
310	AH095	Consensus		2016	Food	SRR11939513
311	AH096	Consensus	IncI2	2016	Food	SRR15732035
312	AH097	PV3	IncX4	2016	Food	SRR15732034
313	AH099	PV3	IncX4	2016	Food	SRR15732033
314	AH100	Consensus		2016	Food	SRR11939512
315	AH101	Consensus		2016	Food	SRR11939534
316	AH102	Other		2016	Food	SRR15732032
317	AH103	Consensus		2016	Food	SRR11939533
318	AH285	SDV3	IncHI1A/IncHI1B	2016	Food	SRR15732031
319	AH304	Other	IncI2	2016	Food	SRR15732030
320	AH306	Consensus		2016	Food	SRR15732029
321	AH307	PV3		2016	Food	SRR15732028
322	AH496	PV3	IncX4	2016	Food	SRR15732027
323	AH507	PV3	IncX4	2016	Food	SRR15732026
324	AH509	PV3	IncX4	2016	Food	SRR15732024
325	AH510	PV3	IncX4	2016	Food	SRR15732023
326	AH512	SDV2		2016	Food	SRR15732022
327	AJ262	SDV2	IncP1	2016	Healthy human volunteers	SRR15732021
328	BA015	Consensus		2017	Pig	SRR15732020
329	BA070	PV3	IncX4	2017	Pig	SRR15732019
330	BA172	Consensus		2017	Pig	SRR15732018
331	BA1839	PV3	IncX4	2017	Pig	SRR15732017
332	BA186	PV3	IncX4	2017	Pig	SRR15732016
333	BA188	Consensus	IncHI2A	2017	Pig	SRR15732015
334	BA189	PV3	IncX4	2017	Pig	SRR15732013
335	BA190	Other	IncI2	2017	Pig	SRR15732012
336	BA191	PV3	IncX4	2017	Pig	SRR15732011
337	BA192	Other	IncI2	2017	Pig	SRR15732010
338	BA194	SDV2		2017	Pig	SRR15732009
339	BA196	Other	IncI2	2017	Pig	SRR15732008
340	BA197	Consensus		2017	Pig	SRR15732007
341	BA198	PV3	IncX4	2017	Pig	SRR15732006
342	BA199	Consensus		2017	Pig	SRR15732005
343	BA200	Other	IncI2	2017	Pig	SRR15731932
344	BA201	PV3	IncX4	2017	Pig	SRR15731930
345	BA202	Consensus	IncHI2/IncHI2A/pKPC	2017	Pig	SRR15731929
346	BA203	SDV2		2017	Pig	SRR15731928
347	BA204	PV3	IncX4	2017	Pig	SRR15731927
348	BA206	Other	IncI2	2017	Pig	SRR15731926
349	BA207	SDV2		2017	Pig	SRR15731925
350	BA208	PV3	IncX4	2017	Pig	SRR15731924
351	BA209	PV3	IncX4	2017	Pig	SRR15731923
352	BA211	PV3	IncX4	2017	Pig	SRR15731922
353	BA2116	Other		2017	Pig	SRR15731921
354	BA212	PV2	IncX4	2017	Pig	SRR15731919
355	BA2123	PV3	IncX4	2017	Pig	SRR15731918
356	BA213	PV3	IncX4	2017	Pig	SRR15731917
357	BA214	Consensus		2017	Pig	SRR15731916
358	BA2143	PV3	IncX4	2017	Pig	SRR15731915
359	BA215	Consensus		2017	Pig	SRR15731914
360	BA216	PV3	IncX4	2017	Pig	SRR15731913
361	BA217	PV1	IncI2	2017	Pig	SRR15731912
362	BA218	Consensus		2017	Pig	SRR15731911
363	BA219	Other	IncI2	2017	Pig	SRR15731910
364	BA220	Consensus		2017	Pig	SRR15731908
365	BA221	Other	IncI2	2017	Pig	SRR15731907
366	BA222	Consensus		2017	Pig	SRR15731906
367	BA223	PV1	IncI2	2017	Pig	SRR15731905

368	BA224	Consensus	IncI2	2017	Pig	SRR15731904
369	BA226	Consensus		2017	Pig	SRR15731903
370	BA227	Consensus	IncHI2/IncHI2A/pKPC	2017	Pig	SRR15731902
371	BA228	Consensus	p01111	2017	Pig	SRR15731901
372	BA229	Consensus	IncI2	2017	Pig	SRR15731900
373	BA230	PV1		2017	Pig	SRR15731899
374	BA231	PV3	IncX4	2017	Pig	SRR15731897
375	BA232	Other	IncI2	2017	Pig	SRR15731716
376	BA234	PV3	IncX4	2017	Pig	SRR15731715
377	BA235	Consensus		2017	Pig	SRR15731714
378	BA236	PV3	IncX4	2017	Pig	SRR15731713
379	BA237	Other	IncI2	2017	Pig	SRR15731712
380	BA238	Other	IncI2	2017	Pig	SRR15731711
381	BA240	Consensus		2017	Pig	SRR15731710
382	BA243	PV3	IncX4	2017	Pig	SRR15731709
383	BA245	PV2	IncX4	2017	Pig	SRR15731708
384	BA740	Consensus		2017	Pig	SRR15731706
385	BB287	Consensus	IncI2	2017	Pig	SRR15731703
386	BB294	Other	IncI2	2017	Pig	SRR15731702
387	BB297	PV3	IncX4	2017	Pig	SRR15731701
388	BB497	Other	IncI2	2017	Pig	SRR15731700
389	BC019	PV3	IncX4	2017	Healthy human volunteers	SRR15731699
390	BC020	PV3	IncX4	2017	Healthy human volunteers	SRR15731698
391	BC021	PV3	IncX4	2017	Healthy human volunteers	SRR15731697
392	BC022	Consensus		2017	Healthy human volunteers	SRR15731695
393	BC023	PV3	IncX4	2017	Healthy human volunteers	SRR15731694
394	BC024	PV3	IncX4	2017	Healthy human volunteers	SRR15731693
395	BC025	PV3	IncX4	2017	Healthy human volunteers	SRR15731692
396	BC026	Consensus		2017	Healthy human volunteers	SRR15731691
397	BC027	Other		2017	Healthy human volunteers	SRR15731690
398	BC028	Other	IncI2	2017	Healthy human volunteers	SRR15731689
399	BC029	PV3	IncX4	2017	Healthy human volunteers	SRR15732106
400	BC031	PV3	IncX4	2017	Healthy human volunteers	SRR15731687
401	BC032	SDV2		2017	Healthy human volunteers	SRR15731686
402	BC033	Consensus	IncI2	2017	Healthy human volunteers	SRR15731684
403	BC034	Consensus		2017	Healthy human volunteers	SRR15731683
404	BC035	Consensus		2017	Healthy human volunteers	SRR15731682
405	BC036	SDV2		2017	Healthy human volunteers	SRR15731681
406	BC037	PV3	IncX4	2017	Healthy human volunteers	SRR15731680
407	BC038	Consensus	IncHI2A	2017	Healthy human volunteers	SRR15731679
408	BC039	PV3	IncX4	2017	Healthy human volunteers	SRR15731678
409	BC040	PV3	IncX4	2017	Healthy human volunteers	SRR15731677
410	BC041	Consensus		2017	Healthy human volunteers	SRR11939532
411	BC042	Other	IncI2	2017	Healthy human volunteers	SRR15731676
412	BC043	SDV2		2017	Healthy human volunteers	SRR15731675
413	BC044	PV3	IncX4	2017	Healthy human volunteers	SRR15731672
414	BC045	Other	IncFIB	2017	Healthy human volunteers	SRR15731671
415	BC046	PV3	IncX4	2017	Healthy human volunteers	SRR15731670
416	BC047	Consensus	IncHI2A	2017	Healthy human volunteers	SRR15731669
417	BC049	SDV1	IncI2	2017	Healthy human volunteers	SRR15731668
418	BC050	SDV2	IncHI1A/IncHI1B	2017	Healthy human volunteers	SRR15731667
419	BC051	SDV4	IncI2	2017	Healthy human volunteers	SRR15732330
420	BC052	Consensus		2017	Healthy human volunteers	SRR15732329
421	BC053	Consensus		2017	Healthy human volunteers	SRR15732328
422	BC055	PV2	IncX4	2017	Healthy human volunteers	SRR15732325
423	BC056	SDV1	IncI2	2017	Healthy human volunteers	SRR15732324
424	BC057	Consensus		2017	Healthy human volunteers	SRR15732323
425	BC058	Other	IncI2	2017	Healthy human volunteers	SRR15732322
426	BC059	Other	IncI2	2017	Healthy human volunteers	SRR15732321
427	BC060	PV1		2017	Healthy human volunteers	SRR15732320
428	BC061	SDV2		2017	Healthy human volunteers	SRR15732319
429	BC062	PV3	IncX4	2017	Healthy human volunteers	SRR15732318
430	BC063	Other		2017	Healthy human volunteers	SRR15732317
431	BC064	PV3	IncX4	2017	Healthy human volunteers	SRR15732316
432	BC065	PV1	IncI2	2017	Healthy human volunteers	SRR15731688
433	BC066	SDV3		2017	Healthy human volunteers	SRR15732313
434	BC067	PV3	IncX4	2017	Healthy human volunteers	SRR15732312
435	BC068	PV3	IncX4	2017	Healthy human volunteers	SRR15732311
436	BC069	SDV3		2017	Healthy human volunteers	SRR15732310
437	BC070	SDV3		2017	Healthy human volunteers	SRR15732309
438	BC071	SDV3		2017	Healthy human volunteers	SRR15732272
439	BC072	SDV3		2017	Healthy human volunteers	SRR15732271

440	BC073	PV3	IncX4	2017	Healthy human volunteers	SRR15732270
441	BC074	SDV3		2017	Healthy human volunteers	SRR15732269
442	BC075	SDV2		2017	Healthy human volunteers	SRR15732267
443	BC076	SDV3		2017	Healthy human volunteers	SRR15732266
444	BC077	SDV3	IncI2	2017	Healthy human volunteers	SRR15732265
445	BC078	SDV3		2017	Healthy human volunteers	SRR15732264
446	BC079	Other	IncI2	2017	Healthy human volunteers	SRR15732263
447	BC080	Other	IncI2	2017	Healthy human volunteers	SRR15732262
448	BC081	Other	IncI2	2017	Healthy human volunteers	SRR15732261
449	BC082	SDV2		2017	Healthy human volunteers	SRR11939531
450	BC084	PV3	IncX4	2017	Healthy human volunteers	SRR15732259
451	BC085	Consensus		2017	Healthy human volunteers	SRR11939530
452	BD086	Other		2017	Patient colonized with Enterobacteriaceae	SRR15732258
453	BD087	Consensus		2017	Patient colonized with Enterobacteriaceae	SRR15732256
454	BD088	PV3	IncX4	2017	Patient colonized with Enterobacteriaceae	SRR15732255
455	BD089	PV3	IncX4	2017	Patient colonized with Enterobacteriaceae	SRR15732254
456	BD090	PV3	IncX4	2017	Patient colonized with Enterobacteriaceae	SRR15732253
457	BD091	SDV2	IncHI2/IncHI2A/pKPC	2017	Patient colonized with Enterobacteriaceae	SRR15732252
458	BD092	SDV2	IncHI2/IncHI2A/pKPC	2017	Patient colonized with Enterobacteriaceae	SRR15732251
459	BD093	PV3	IncX4	2017	Patient colonized with Enterobacteriaceae	SRR15732250
460	BD094	SDV3	IncHI1A/IncHI1B	2017	Patient colonized with Enterobacteriaceae	SRR15732249
461	BD099	PV3	IncX4	2017	Patient colonized with Enterobacteriaceae	SRR15732248
462	BD100	Other	IncI2	2017	Patient colonized with Enterobacteriaceae	SRR15732247
463	BD101	Consensus	IncHI2/IncHI2A/pKPC	2017	Patient colonized with Enterobacteriaceae	SRR15732245
464	BD102	Other		2017	Patient colonized with Enterobacteriaceae	SRR15732244
465	BD104	Consensus	IncHI2A	2017	Patient colonized with Enterobacteriaceae	SRR15732242
466	BD105	Consensus	IncHI2A	2017	Patient colonized with Enterobacteriaceae	SRR15732241
467	BD106	Consensus	IncHI2A	2017	Patient colonized with Enterobacteriaceae	SRR15732240
468	BD107	Consensus	IncHI2A	2017	Patient colonized with Enterobacteriaceae	SRR15732239
469	BD108	PV3	IncX4	2017	Patient colonized with Enterobacteriaceae	SRR15732238
470	BD109	Consensus	IncHI2A	2017	Patient colonized with Enterobacteriaceae	SRR15732237
471	BD111	Consensus	IncHI2A	2017	Patient colonized with Enterobacteriaceae	SRR15732222
472	BD113	SDV2		2017	Patient colonized with Enterobacteriaceae	SRR15732314
473	BD114	PV2	IncX4	2017	Patient colonized with Enterobacteriaceae	SRR15732220
474	BD115	PV3	IncX4	2017	Patient colonized with Enterobacteriaceae	SRR15732219
475	BD116	Consensus	IncHI2A	2017	Patient colonized with Enterobacteriaceae	SRR15732218
476	BD117	PV3	IncX4	2017	Patient colonized with Enterobacteriaceae	SRR15732217
477	BD118	Other	IncX4	2017	Patient colonized with Enterobacteriaceae	SRR15732216
478	BD119	Consensus	IncHI2A	2017	Patient colonized with Enterobacteriaceae	SRR15732215
479	BD120	Other		2017	Patient colonized with Enterobacteriaceae	SRR15732214
480	BD121	PV3	IncX4	2017	Patient colonized with Enterobacteriaceae	SRR15732213
481	BD122	Other	IncI2	2017	Patient colonized with Enterobacteriaceae	SRR15732211
482	BD123	SDV2		2017	Patient colonized with Enterobacteriaceae	SRR15732210
483	BD124	PV2	IncX4	2017	Patient colonized with Enterobacteriaceae	SRR15732209
484	BD127	SDV2		2017	Patient colonized with Enterobacteriaceae	SRR15732207
485	BD128	PV3		2017	Patient colonized with Enterobacteriaceae	SRR15732206
486	BD129	PV3		2017	Patient colonized with Enterobacteriaceae	SRR15732205
487	BD130	Consensus		2017	Patient colonized with Enterobacteriaceae	SRR15732204
488	BD3620	PV3	IncX4	2017	Patient colonized with Enterobacteriaceae	SRR15732203
489	BD4077	SDV2	IncHI2/IncHI2A/pKPC	2017	Patient colonized with Enterobacteriaceae	SRR15732202
490	BE001	PV3	IncX4	2017	Patient infected with Enterobacteriaceae	SRR15732200
491	BE026	Consensus		2017	Patient infected with Enterobacteriaceae	SRR15732199
492	BE055	Consensus		2017	Patient infected with Enterobacteriaceae	SRR15732198
493	BE079	Consensus		2017	Patient infected with Enterobacteriaceae	SRR15732197
494	BE082	Consensus	IncHI2A	2017	Patient infected with Enterobacteriaceae	SRR15732196
495	BE085	PV3	IncX4	2017	Patient infected with Enterobacteriaceae	SRR15732195
496	BE162	Consensus		2017	Patient infected with Enterobacteriaceae	SRR15732194
497	BE166	Consensus		2017	Patient infected with Enterobacteriaceae	SRR15732193
498	BE169	Consensus		2017	Patient infected with Enterobacteriaceae	SRR15732192
499	BE192	PV2	IncX4	2017	Patient infected with Enterobacteriaceae	SRR15732191
500	BE303	Consensus	IncHI2A	2017	Patient infected with Enterobacteriaceae	SRR15732189
501	BE333	Other		2017	Patient infected with Enterobacteriaceae	SRR15732188
502	BE352	PV3	IncX4	2017	Patient infected with Enterobacteriaceae	SRR15732187
503	BE384	PV3	IncX4	2017	Patient infected with Enterobacteriaceae	SRR15732186
504	BE410	SDV2	IncHI2A	2017	Patient infected with Enterobacteriaceae	SRR15732185
505	BE411	SDV2	IncHI2A	2017	Patient infected with Enterobacteriaceae	SRR15732184
506	BE426	SDV2	IncHI2A	2017	Patient infected with Enterobacteriaceae	SRR15732183
507	BF018	PV1		2017	Environment	SRR15732182
508	BF299	Consensus		2017	Environment	SRR15732181
509	BF300	Other	IncI2	2017	Environment	SRR15732180
510	BF301	Consensus		2017	Environment	SRR15732177
511	BF302	PV3	IncX4	2017	Environment	SRR15732176

512	BF303	Consensus		2017	Environment	SRR15732175
513	BF304	PV3		2017	Environment	SRR15732174
514	BF305	PV3	IncX4	2017	Environment	SRR15732173
515	BG001	SDV2		2017	Environment	SRR15732172
516	BG002	Consensus		2017	Environment	SRR15732171
517	BG003	PV3	IncX4	2017	Environment	SRR15732170
518	BG004	Consensus		2017	Environment	SRR15732105
519	BG005	SDV2		2017	Environment	SRR15732168
520	BG006	SDV2		2017	Environment	SRR15732166
521	BG007	SDV2	IncHI2A	2017	Environment	SRR15732165
522	BG008	Consensus	IncHI2/pKPC	2017	Environment	SRR15732164
523	BG009	Consensus	p01111	2017	Environment	SRR15732163
524	BG010	SDV2		2017	Environment	SRR11939529
525	BG013	Consensus	IncY	2017	Environment	SRR15732162
526	BG014	PV3	IncX4	2017	Environment	SRR15732161
527	BG015	PV3	IncX4	2017	Environment	SRR15732160
528	BG016	Other	IncI2	2017	Environment	SRR15732159
529	BH101	Other	IncI2	2017	Food	SRR15732158
530	BH1226	PV3	IncX4	2017	Food	SRR15732157
531	BH131	Other	IncI2	2017	Food	SRR15732155
532	BH133	PV3	IncX4	2017	Food	SRR15732154
533	BH135	PV3	IncX4	2017	Food	SRR15732153
534	BH136	Consensus		2017	Food	SRR11939528
535	BH138	PV3	IncX4	2017	Food	SRR15732308
536	BH139	PV3	IncX4	2017	Food	SRR15732307
537	BH140	PV3	IncX4	2017	Food	SRR15732306
538	BH141	Other	IncI2	2017	Food	SRR15732305
539	BH143	Other		2017	Food	SRR15732303
540	BH144	Other		2017	Food	SRR15732302
541	BH146	PV2	IncX4	2017	Food	SRR15732300
542	BH149	SDV2		2017	Food	SRR15732298
543	BH151	PV3	IncX4	2017	Food	SRR15732296
544	BH152	Consensus	IncHI2A	2017	Food	SRR15732295
545	BH153	PV3	IncX4	2017	Food	SRR15732294
546	BH154	SDV2		2017	Food	SRR15732293
547	BH155	SDV2		2017	Food	SRR15732292
548	BH157	SDV2		2017	Food	SRR15732291
549	BH158	PV3	IncX4	2017	Food	SRR15732289
550	BH159	PV3	IncX4	2017	Food	SRR15732288
551	BH160	SDV2		2017	Food	SRR15732287
552	BH161	SDV2		2017	Food	SRR15732286
553	BH162	SDV2		2017	Food	SRR15732285
554	BH164	SDV2		2017	Food	SRR15732284
555	BH165	SDV2		2017	Food	SRR15732283
556	BH166	SDV2		2017	Food	SRR15732282
557	BH169	PV3	IncX4	2017	Food	SRR15732281
558	BH170	Consensus		2017	Food	SRR15732280
559	BH171	Consensus		2017	Food	SRR15732278
560	BH173	Consensus	p01111	2017	Food	SRR15732277
561	BH174	Other		2017	Food	SRR15732276
562	BH175	PV3	IncX4	2017	Food	SRR15732275
563	BH176	Consensus		2017	Food	SRR11939526
564	BH177	Consensus		2017	Food	SRR15732274
565	BH178	PV3	IncX4	2017	Food	SRR15732273
566	BH179	SDV2	IncI2	2017	Food	SRR15732152
567	BH180	PV3		2017	Food	SRR15732151
568	BH181	Other	IncX4	2017	Food	SRR15732150
569	BH182	Other	IncX4	2017	Food	SRR15732149
570	BH183	PV3	IncX4	2017	Food	SRR15732147
571	BH184	PV3	IncX4	2017	Food	SRR15732146
572	BH185	PV3	IncX4	2017	Food	SRR15732145
573	BH1962	PV3	IncX4	2017	Food	SRR15732144
574	BH1972	Consensus		2017	Food	SRR15732143
575	BH825	PV3	IncX4	2017	Food	SRR15732142
576	BH829	PV2	IncX4	2017	Food	SRR15732141
577	BJ288	Other		2017	Healthy human volunteers	SRR15732140
578	BJ289	PV3	IncX4	2017	Healthy human volunteers	SRR15732139
579	BJ290	Consensus	IncX4	2017	Healthy human volunteers	SRR15732138
580	BJ291	Other	IncI2	2017	Healthy human volunteers	SRR15732136
581	BJ292	Other	IncI2	2017	Healthy human volunteers	SRR15732135
582	BJ293	Other	IncI2	2017	Healthy human volunteers	SRR15732134
583	BJ295	Other	IncHI2/IncHI2A/pKPC	2017	Healthy human volunteers	SRR15732133

584	BJ296	Other	IncHI2/IncHI2A/pKPC	2017	Healthy human volunteers	SRR15732132
585	BJ298	PV1	IncI2	2017	Healthy human volunteers	SRR15732131
586	BJ386	Other	IncI2	2017	Healthy human volunteers	SRR15732130
587	CA1003	PV3	IncX4	2018	Pig	SRR15732129
588	CA270	PV3	IncX4	2018	Pig	SRR15732128
589	CA297	Other		2018	Pig	SRR15732127
590	CA305	PV3	IncX4	2018	Pig	SRR15732125
591	CA314	Other	IncI2	2018	Pig	SRR15732124
592	CA317	PV3	IncX4	2018	Pig	SRR15732123
593	CA320	Consensus		2018	Pig	SRR11939525
594	CA331	SDV3		2018	Pig	SRR15732122
595	CA332	PV3	IncX4	2018	Pig	SRR15732121
596	CA337	Other	IncI2	2018	Pig	SRR15732120
597	CA357	PV3	IncX4	2018	Pig	SRR15732119
598	CA364	Consensus		2018	Pig	SRR15732118
599	CA370	PV3	IncX4	2018	Pig	SRR15732117
600	CA383	PV3	IncX4	2018	Pig	SRR15732116
601	CA387	PV2	IncX4	2018	Pig	SRR15732114
602	CA392	Consensus		2018	Pig	SRR15732113
603	CA394	PV2	IncX4	2018	Pig	SRR15732112
604	CA398	SDV2	IncHI1A/IncHI1B/IncFIA	2018	Pig	SRR15732111
605	CA400	PV3	IncX4	2018	Pig	SRR15732110
606	CA411	PV2	IncX4	2018	Pig	SRR15732109
607	CA418	Consensus		2018	Pig	SRR15732108
608	CA423	Consensus		2018	Pig	SRR15732107
609	CA425	Other	IncI2	2018	Pig	SRR15732100
610	CA429	PV3		2018	Pig	SRR15731892
611	CA437	PV3	IncX4	2018	Pig	SRR15732102
612	CA438	Consensus		2018	Pig	SRR15732101
613	CA443	Other	IncI2	2018	Pig	SRR15731891
614	CA464	PV1	IncI2	2018	Pig	SRR15732099
615	CA488	Consensus		2018	Pig	SRR15732098
616	CA504	PV3	IncX4	2018	Pig	SRR15732097
617	CA512	PV3	IncX4	2018	Pig	SRR15732096
618	CA854	PV3	IncX4	2018	Pig	SRR15732095
619	CA894	PV3	IncX4	2018	Pig	SRR15732094
620	CA927	PV3	IncX4	2018	Pig	SRR15732093
621	CA930	Consensus		2018	Pig	SRR15732091
622	CA931	PV3	IncX4	2018	Pig	SRR15732090
623	CA941	Other	IncI2	2018	Pig	SRR15732089
624	CA943	PV3	IncX4	2018	Pig	SRR15732088
625	CA946	PV3	IncX4	2018	Pig	SRR15732087
626	CA958	PV3	IncX4	2018	Pig	SRR15732086
627	CA973	PV3	IncX4	2018	Pig	SRR15732085
628	CA979	Consensus		2018	Pig	SRR15732084
629	CA993	PV3	IncX4	2018	Pig	SRR15732083
630	CA998	PV1	IncI2	2018	Pig	SRR15732082
631	CB1564	Consensus	p01111	2018	Pig	SRR15731896
632	CB1574	Consensus		2018	Pig	SRR15731895
633	CB1583	Consensus	p01111	2018	Pig	SRR15731894
634	CB1584	Consensus	p01111	2018	Pig	SRR15731893
635	CB1599	Consensus		2018	Pig	SRR15732221
636	CB1903	Consensus		2018	Pig	SRR11939524
637	CB1943	Consensus		2018	Pig	SRR15732169
638	CB1947	Other	IncI2	2018	Pig	SRR15731890
639	CB1955	PV3	IncX4	2018	Pig	SRR15731889
640	CB2078	PV3	IncX4	2018	Pig	SRR15731888
641	CB595	Other		2018	Pig	SRR15731887
642	CB619	PV3	IncX4	2018	Pig	SRR15731885
643	CB631	Other	IncX4	2018	Pig	SRR15731884
644	CB644	Other	IncX4	2018	Pig	SRR15731883
645	CC1249	Consensus		2018	Healthy human volunteers	SRR15731882
646	CC369	SDV2		2018	Healthy human volunteers	SRR15731880
647	CC439	PV3	IncX4	2018	Healthy human volunteers	SRR15731879
648	CC450	PV3	IncX4	2018	Healthy human volunteers	SRR15731878
649	CC454	PV3	IncX4	2018	Healthy human volunteers	SRR15731876
650	CC473	PV3	IncX4	2018	Healthy human volunteers	SRR15731874
651	CD071	Other	IncI2	2018	Patient colonized with Enterobacteriaceae	SRR15731873
652	CD163	Other	IncI2	2018	Patient colonized with Enterobacteriaceae	SRR15731872
653	CD175	SDV1	IncI2	2018	Patient colonized with Enterobacteriaceae	SRR15731871
654	CD240	SDV2		2018	Patient colonized with Enterobacteriaceae	SRR15731870
655	CD266	Consensus	IncHI2A	2018	Patient colonized with Enterobacteriaceae	SRR15731869

656	CD4812	SDV2	IncHI2/IncHI2A/pKPC	2018	Patient colonized with Enterobacteriaceae	SRR15731868
657	CD4925	PV1	IncI2	2018	Patient colonized with Enterobacteriaceae	SRR15731867
658	CD4968	SDV2	IncHI2/IncHI2A/pKPC	2018	Patient colonized with Enterobacteriaceae	SRR15731866
659	CD5013	SDV2		2018	Patient colonized with Enterobacteriaceae	SRR15731865
660	CE003	SDV2	IncHI2/IncHI2A/pKPC	2018	Patient infected with Enterobacteriaceae	SRR15731863
661	CE004	SDV2	IncHI2/IncHI2A/pKPC	2018	Patient infected with Enterobacteriaceae	SRR15731862
662	CE036	Consensus		2018	Patient infected with Enterobacteriaceae	SRR15731861
663	CE049	Consensus	IncX4	2018	Patient infected with Enterobacteriaceae	SRR15732080
664	CE057	SDV2	IncHI2/IncHI2A/pKPC	2018	Patient infected with Enterobacteriaceae	SRR15732079
665	CE096	Other	IncI2	2018	Patient infected with Enterobacteriaceae	SRR15732078
666	CE101	Other		2018	Patient infected with Enterobacteriaceae	SRR15732077
667	CE107	SDV4	IncI2	2018	Patient infected with Enterobacteriaceae	SRR15732076
668	CE123	SDV2		2018	Patient infected with Enterobacteriaceae	SRR15732075
669	CE199	Other	IncI2	2018	Patient infected with Enterobacteriaceae	SRR15732074
670	CE227	SDV2		2018	Patient infected with Enterobacteriaceae	SRR15732072
671	CG185	SDV3		2018	Environment	SRR15732071
672	CH719	SDV2	IncHI1A/IncHI1B	2018	Food	SRR15732070
673	CH721	SDV2		2018	Food	SRR15732069

References

Aarts, H. and Margolles, A. (2015) 'Antibiotic resistance genes in food and gut (non-pathogenic) bacteria. Bad genes in good bugs', *Frontiers in Microbiology*, 5. doi: 10.3389/fmicb.2014.00754.

Adedeji, W. A. (2016) 'THE TREASURE CALLED ANTIBIOTICS.', *Annals of Ibadan postgraduate medicine*.

Alderliesten, J. B. *et al.* (2020) 'Effect of donor-recipient relatedness on the plasmid conjugation frequency: a meta-analysis', *BMC Microbiology*, 20(1), p. 135. doi: 10.1186/s12866-020-01825-4.

Altschul, S. F. *et al.* (1990) 'Basic local alignment search tool', *Journal of Molecular Biology*. doi: 10.1016/S0022-2836(05)80360-2.

Aminov, R. I. (2010) 'A brief history of the antibiotic era: Lessons learned and challenges for the future', *Frontiers in Microbiology*. doi: 10.3389/fmicb.2010.00134.

Andersson, D. I. and Hughes, D. (2010a) 'Antibiotic resistance and its cost: Is it possible to reverse resistance?', *Nature Reviews Microbiology*. doi: 10.1038/nrmicro2319.

Andersson, D. I. and Hughes, D. (2010b) 'Antibiotic resistance and its cost: Is it possible to reverse resistance?', *Nature Reviews Microbiology*. doi: 10.1038/nrmicro2319.

Andersson, D. I. and Levin, B. R. (1999) 'The biological cost of antibiotic resistance', *Current Opinion in Microbiology*. doi: 10.1016/S1369-5274(99)00005-3.

B McPhee, J. and Lewenza, S. (2016) 'From Pigs to Patients: Transmissible, Single Gene-mediated Resistance to Colistin', *Journal of Medical Microbiology & Diagnosis*. doi: 10.4172/2161-0703.1000221.

Bailey, S. F., Guo, Q. and Bataillon, T. (2018) 'Identifying Drivers of Parallel Evolution: A Regression Model Approach', *Genome Biology and Evolution*. Edited by R. Hershberg, 10(10), pp. 2801–2812. doi: 10.1093/gbe/evy210.

Baltrus, D. A. (2013) 'Exploring the costs of horizontal gene transfer', *Trends in Ecology and Evolution*. doi: 10.1016/j.tree.2013.04.002.

Barlow, M. (2009) 'What Antimicrobial Resistance Has Taught Us About Horizontal Gene Transfer', in, pp. 397–411. doi: 10.1007/978-1-60327-853-9_23.

Basra, P. *et al.* (2018) 'Fitness Tradeoffs of Antibiotic Resistance in Extraintestinal Pathogenic Escherichia coli', *Genome Biology and Evolution*. doi: 10.1093/gbe/evy030.

Bauer, B. F. *et al.* (1988) 'Sequence determinants for promoter strength in the leuV operon of Escherichia coli', *Gene*, 63(1), pp. 123–134. doi: 10.1016/0378-1119(88)90551-3.

Baym, M. *et al.* (2016) 'Spatiotemporal microbial evolution on antibiotic landscapes', *Science*. doi: 10.1126/science.aag0822.

Bell, G. and MacLean, C. (2018) 'The Search for "Evolution-Proof" Antibiotics', *Trends in Microbiology*. doi: 10.1016/j.tim.2017.11.005.

Benler, S. *et al.* (2021) 'Cargo Genes of Tn 7 -Like Transposons Comprise an Enormous Diversity of Defense Systems, Mobile Genetic Elements, and Antibiotic Resistance Genes', *mBio*. Edited by S. J. Giovannoni, 12(6). doi: 10.1128/mBio.02938-21.

Bentley, W. E. *et al.* (1990) 'Plasmid-encoded protein: The principal factor in the "metabolic burden" associated with recombinant bacteria', *Biotechnology and Bioengineering*. doi: 10.1002/bit.260350704.

Bergstrom, C. T., Lipsitch, M. and Levin, B. R. (2000) 'Natural selection, infectious transfer and the existence conditions for bacterial plasmids', *Genetics*.

Besier, S. *et al.* (2005) 'Compensatory adaptation to the loss of biological fitness associated with acquisition of fusidic acid resistance in Staphylococcus aureus', *Antimicrobial Agents and Chemotherapy*. doi:

10.1128/AAC.49.4.1426-1431.2005.

Bhattacharyya, S. *et al.* (2018) 'Accessibility of the Shine-Dalgarno Sequence Dictates N-Terminal Codon Bias in E. coli', *Molecular Cell*, 70(5), pp. 894-905.e5. doi: 10.1016/j.molcel.2018.05.008.

Bialvaei, A. Z. and Samadi Kafil, H. (2015) 'Colistin, mechanisms and prevalence of resistance', *Current Medical Research and Opinion*. doi: 10.1185/03007995.2015.1018989.

Biswas, S. *et al.* (2012) 'Colistin: An update on the antibiotic of the 21st century', *Expert Review of Anti-Infective Therapy*. doi: 10.1586/eri.12.78.

Blair, J. M. A. *et al.* (2015) 'Molecular mechanisms of antibiotic resistance', *Nature Reviews Microbiology*. doi: 10.1038/nrmicro3380.

Bobay, L.-M. and Ochman, H. (2017) 'The Evolution of Bacterial Genome Architecture', *Frontiers in Genetics*, 8. doi: 10.3389/fgene.2017.00072.

Bosshard, L. *et al.* (2019) 'Mutational and Selective Processes Involved in Evolution during Bacterial Range Expansions', *Molecular Biology and Evolution*. doi: 10.1093/molbev/msz148.

Bottery, M. J., Wood, A. J. and Brockhurst, M. A. (2017) 'Adaptive modulation of antibiotic resistance through intragenomic coevolution', *Nature Ecology and Evolution*. doi: 10.1038/s41559-017-0242-3.

Bouma, J. E. and Lenski, R. E. (1988) 'Evolution of a bacteria/plasmid association', *Nature*, 335(6188), pp. 351–352. doi: 10.1038/335351a0.

Brockhurst, M. A. *et al.* (2019) 'The Ecology and Evolution of Pangenomes', *Current Biology*. doi: 10.1016/j.cub.2019.08.012.

Bulyk, M. L. (2005) 'Discovering DNA regulatory elements with bacteria', *Nature Biotechnology*, 23(8), pp. 942–944. doi: 10.1038/nbt0805-942.

Cannatelli, A. *et al.* (2013) 'In vivo emergence of colistin resistance in Klebsiella pneumoniae producing KPC-type carbapenemases mediated by insertional inactivation of the PhoQ/PhoP mgrB regulator', *Antimicrobial Agents and Chemotherapy*. doi: 10.1128/AAC.01480-13.

Carretto, E. *et al.* (2018) 'Detection of mcr-4 positive Salmonella enterica serovar Typhimurium in clinical isolates of human origin, Italy, october to November 2016', *Eurosurveillance*. doi: 10.2807/1560-7917.ES.2018.23.2.17-00821.

Cassiano, M. H. A. and Silva-Rocha, R. (2020) 'Benchmarking Bacterial Promoter Prediction Tools: Potentialities and Limitations', *mSystems*. Edited by A. Fodor, 5(4). doi: 10.1128/mSystems.00439-20.

Cassini, A. *et al.* (2019) 'Attributable deaths and disability-adjusted life-years caused by infections with antibiotic-resistant bacteria in the EU and the European Economic Area in 2015: a population-level modelling analysis', *The Lancet Infectious Diseases*. doi: 10.1016/S1473-3099(18)30605-4.

Chalabaev, S. *et al.* (2014) 'Biofilms Formed by Gram-Negative Bacteria Undergo Increased Lipid A Palmitoylation, Enhancing In Vivo Survival', *mBio*. Edited by S. Trent and Y. V. Brun, 5(4). doi: 10.1128/mBio.01116-14.

Comas, I. *et al.* (2012) 'Whole-genome sequencing of rifampicin-resistant Mycobacterium tuberculosis strains identifies compensatory mutations in RNA polymerase genes', *Nature Genetics*. doi: 10.1038/ng.1038.

Costelloe, C. *et al.* (2010) 'Effect of antibiotic prescribing in primary care on antimicrobial resistance in individual patients: Systematic review and meta-analysis', *BMJ (Online)*. doi: 10.1136/bmj.c2096.

Dadgostar, P. (2019) 'Antimicrobial resistance: implications and costs', *Infection and Drug Resistance*. doi: 10.2147/IDR.S234610.

Dahlberg, C. and Chao, L. (2003) 'Amelioration of the Cost of Conjugative Plasmid Carriage in Eschericha coli K12', *Genetics*.

Darveau, R. P. (1998) 'Lipid A diversity and the innate host response to bacterial infection', *Current Opinion in Microbiology*, 1(1), pp. 36–42. doi: 10.1016/S1369-5274(98)80140-9.

Davies, J. and Davies, D. (2010) 'Origins and Evolution of Antibiotic Resistance', *Microbiology and Molecular*

Biology Reviews. doi: 10.1128/MMBR.00016-10.

Davies, M. and Walsh, T. R. (2018) 'A colistin crisis in India', *The Lancet. Infectious diseases*. doi: 10.1016/S1473-3099(18)30072-0.

Davis, B. H., Poon, A. F. Y. and Whitlock, M. C. (2009) 'Compensatory mutations are repeatable and clustered within proteins', *Proceedings of the Royal Society B: Biological Sciences*, 276(1663), pp. 1823–1827. doi: 10.1098/rspb.2008.1846.

Depardieu, F. *et al.* (2007) 'Modes and Modulations of Antibiotic Resistance Gene Expression', *Clinical Microbiology Reviews*, 20(1), pp. 79–114. doi: 10.1128/CMR.00015-06.

Dimitriu, T. *et al.* (2019) 'Negative frequency dependent selection on plasmid carriage and low fitness costs maintain extended spectrum β-lactamases in Escherichia coli', *Scientific Reports*. doi: 10.1038/s41598-019-53575-7.

e Silva, S. de A. and Echeverrigaray, S. (2012) 'Bacterial Promoter Features Description and Their Application on E. coli in silico Prediction and Recognition Approaches', in *Bioinformatics*. InTech. doi: 10.5772/48149.

'ECDC/EFSA/EMA first joint report on the integrated analysis of the consumption of antimicrobial agents and occurrence of antimicrobial resistance in bacteria from humans and food-producing animals' (2015) *EFSA Journal*. doi: 10.2903/j.efsa.2015.4006.

ESFA (2018) 'The European Union summary report on antimicrobial resistance in zoonotic and indicator bacteria from humans, animals and food in 2016', *EFSA Journal*. doi: 10.2903/j.efsa.2018.5182.

Eyre-Walker, A. and Keightley, P. D. (2007) 'The distribution of fitness effects of new mutations', *Nature Reviews Genetics*, 8(8), pp. 610–618. doi: 10.1038/nrg2146.

Falagas, M. E., Kasiakou, S. K. and Saravolatz, L. D. (2005) 'Colistin: The Revival of Polymyxins for the Management of Multidrug-Resistant Gram-Negative Bacterial Infections', *Clinical Infectious Diseases*. doi: 10.1086/429323.

Feklistov, A. and Darst, S. A. (2011) 'Structural Basis for Promoter −10 Element Recognition by the Bacterial RNA Polymerase σ Subunit', *Cell*, 147(6), pp. 1257–1269. doi: 10.1016/j.cell.2011.10.041.

Fernandez-Astorga, A. *et al.* (1992) 'Biotic and abiotic factors affecting plasmid transfer in Escherichia coli strains', *Applied and Environmental Microbiology*. doi: 10.1128/aem.58.1.392-398.1992.

Freudl, R. (2018) 'Signal peptides for recombinant protein secretion in bacterial expression systems', *Microbial Cell Factories*, 17(1), p. 52. doi: 10.1186/s12934-018-0901-3.

Gharaibeh, M. H. and Shatnawi, S. Q. (2019) 'An overview of colistin resistance, mobilized colistin resistance genes dissemination, global responses, and the alternatives to colistin: A review', *Veterinary World*. doi: 10.14202/vetworld.2019.1735-1746.

Giacomucci, S. *et al.* (2019) 'Flagella-dependent inhibition of biofilm formation by sub-inhibitory concentration of polymyxin B in Vibrio cholerae', *PLOS ONE*. Edited by I. Karunasagar, 14(8), p. e0221431. doi: 10.1371/journal.pone.0221431.

Gifford, D. R. and MacLean, R. C. (2013) 'EVOLUTIONARY REVERSALS OF ANTIBIOTIC RESISTANCE IN EXPERIMENTAL POPULATIONS OF PSEUDOMONAS AERUGINOSA', *Evolution*, p. n/a-n/a. doi: 10.1111/evo.12158.

Gullberg, E. *et al.* (2011) 'Selection of resistant bacteria at very low antibiotic concentrations', *PLoS Pathogens*. doi: 10.1371/journal.ppat.1002158.

Gunn, J. S. (2008) 'The Salmonella PmrAB regulon: lipopolysaccharide modifications, antimicrobial peptide resistance and more', *Trends in Microbiology*. doi: 10.1016/j.tim.2008.03.007.

Hall, J. P. J. *et al.* (2017) 'The evolution of plasmid stability: Are infectious transmission and compensatory evolution competing evolutionary trajectories?', *Plasmid*, 91, pp. 90–95. doi: 10.1016/j.plasmid.2017.04.003.

Harrison, E. *et al.* (2012) 'The cost of copy number in a selfish genetic element: The 2-µm plasmid of Saccharomyces cerevisiae', *Journal of Evolutionary Biology*. doi: 10.1111/j.1420-9101.2012.02610.x.

Harrison, E. *et al.* (2015) 'Parallel Compensatory Evolution Stabilizes Plasmids across the Parasitism-Mutualism

Continuum', *Current Biology*, 25(15), pp. 2034–2039. doi: 10.1016/j.cub.2015.06.024.

Harrison, E. and Brockhurst, M. A. (2012) 'Plasmid-mediated horizontal gene transfer is a coevolutionary process', *Trends in Microbiology*. doi: 10.1016/j.tim.2012.04.003.

He, Y.-Z. *et al.* (2019) 'The ISApl12 Dimer Circular Intermediate Participates in mcr-1 Transposition', *Frontiers in Microbiology*, 10. doi: 10.3389/fmicb.2019.00015.

Headd, B. and Bradford, S. A. (2018) 'Physicochemical Factors That Favor Conjugation of an Antibiotic Resistant Plasmid in Non-growing Bacterial Cultures in the Absence and Presence of Antibiotics', *Frontiers in Microbiology*, 9. doi: 10.3389/fmicb.2018.02122.

Hegde, R. S. and Bernstein, H. D. (2006) 'The surprising complexity of signal sequences', *Trends in Biochemical Sciences*. doi: 10.1016/j.tibs.2006.08.004.

Hüttener, M. *et al.* (2022) 'Roles of Proteins Containing Immunoglobulin-Like Domains in the Conjugation of Bacterial Plasmids', *mSphere*. Edited by C. D. Ellermeier, 7(1). doi: 10.1128/msphere.00978-21.

IDT (no date) *OligoAnalyzer™ Tool*. Available at: https://eu.idtdna.com/calc/analyzer.

Kaberdin, V. R. and Bläsi, U. (2006) 'Translation initiation and the fate of bacterial mRNAs', *FEMS Microbiology Reviews*, 30(6), pp. 967–979. doi: 10.1111/j.1574-6976.2006.00043.x.

Kallel, H. *et al.* (2008) 'Correlation between antibiotic use and changes in susceptibility patterns of Pseudomonas aeruginosa in a medical-surgical intensive care unit', *Indian Journal of Critical Care Medicine*. doi: 10.4103/0972-5229.40945.

Kieffer, N., Nordmann, P. and Poirel, L. (2017) 'Moraxella Species as Potential Sources of MCR-Like Polymyxin Resistance Determinants', *Antimicrobial Agents and Chemotherapy*, 61(6). doi: 10.1128/AAC.00129-17.

Klein, E. Y. *et al.* (2018) 'Global increase and geographic convergence in antibiotic consumption between 2000 and 2015', *Proceedings of the National Academy of Sciences of the United States of America*. doi: 10.1073/pnas.1717295115.

Kües, U. and Stahl, U. (1989) 'Replication of plasmids in gram-negative bacteria', *Microbiological Reviews*, 53(4), pp. 491–516. doi: 10.1128/mr.53.4.491-516.1989.

Kumar, A. and Bansal, M. (2018) 'Modulation of Gene Expression by Gene Architecture and Promoter Structure', in *Bioinformatics in the Era of Post Genomics and Big Data*. InTech. doi: 10.5772/intechopen.76051.

Levin, B. R., Perrot, V. and Walker, N. (2000) 'Compensatory Mutations, Antibiotic Resistance and the Population Genetics of Adaptive Evolution in Bacteria', *Genetics*, 154(3), pp. 985–997. doi: 10.1093/genetics/154.3.985.

Levy, S. B. and Bonnie, M. (2004) 'Antibacterial resistance worldwide: Causes, challenges and responses', *Nature Medicine*. doi: 10.1038/nm1145.

Licht, T. R. *et al.* (1999) 'Plasmid transfer in the animal intestine and other dynamic bacterial populations: the role of community structure and environment', *Microbiology*, 145(9), pp. 2615–2622. doi: 10.1099/00221287-145-9-2615.

Liu, G. *et al.* (2019) 'Antibiotic-Induced, Increased Conjugative Transfer Is Common to Diverse Naturally Occurring ESBL Plasmids in Escherichia coli', *Frontiers in Microbiology*, 10. doi: 10.3389/fmicb.2019.02119.

Liu, X. *et al.* (2017) 'Protein secretion in Corynebacterium glutamicum', *Critical Reviews in Biotechnology*, 37(4), pp. 541–551. doi: 10.1080/07388551.2016.1206059.

Liu, Y. Y. *et al.* (2016) 'Emergence of plasmid-mediated colistin resistance mechanism MCR-1 in animals and human beings in China: A microbiological and molecular biological study', *The Lancet Infectious Diseases*. doi: 10.1016/S1473-3099(15)00424-7.

Liu, Z. *et al.* (2021) 'Genetic Features of Plasmid- and Chromosome-Mediated mcr-1 in Escherichia coli Isolates From Animal Organs With Lesions', *Frontiers in Microbiology*, 12. doi: 10.3389/fmicb.2021.707332.

Long, H. *et al.* (2016) 'Antibiotic treatment enhances the genome-wide mutation rate of target cells', *Proceedings of the National Academy of Sciences of the United States of America*. doi: 10.1073/pnas.1601208113.

Lopatkin, A. J. *et al.* (2016) 'Antibiotics as a selective driver for conjugation dynamics', *Nature Microbiology*, 1(6), p. 16044. doi: 10.1038/nmicrobiol.2016.44.

Lopatkin, A. J. *et al.* (2017) 'Persistence and reversal of plasmid-mediated antibiotic resistance', *Nature Communications*, 8(1), p. 1689. doi: 10.1038/s41467-017-01532-1.

Ma, G. *et al.* (2016) 'High resolution crystal structure of the catalytic domain of MCR-1', *Scientific Reports*, 6(1), p. 39540. doi: 10.1038/srep39540.

Maciuca, I. E. *et al.* (2019) 'Genetic Features of mcr-1 Mediated Colistin Resistance in CMY-2-Producing Escherichia coli From Romanian Poultry', *Frontiers in Microbiology*. doi: 10.3389/fmicb.2019.02267.

MacLean, R. C. *et al.* (2010) 'The population genetics of antibiotic resistance: Integrating molecular mechanisms and treatment contexts', *Nature Reviews Genetics*. doi: 10.1038/nrg2778.

MacLean, R. C. and Vogwill, T. (2015) 'Limits to compensatory adaptation and the persistence of antibiotic resistance in pathogenic bacteria', *Evolution, Medicine and Public Health*. doi: 10.1093/emph/eou032.

Maduro (no date) *Random DNA Sequence Generator*. Available at: http://www.faculty.ucr.edu/~mmaduro/random.htm.

Maiden, M. C. J. (1998) 'Horizontal Genetic Exchange, Evolution, and Spread of Antibiotic Resistance in Bacteria', *Clinical Infectious Diseases*, 27(s1), pp. S12–S20. doi: 10.1086/514917.

Martinez, N. *et al.* (2007) 'Detailed structure of integrons and transposons carried by large conjugative plasmids responsible for multidrug resistance in diverse genomic types of Salmonella enterica serovar Brandenburg', *Journal of Antimicrobial Chemotherapy*, 60(6), pp. 1227–1234. doi: 10.1093/jac/dkm336.

Matsumura, Y., Peirano, G. and Pitout, J. D. D. (2018) 'Complete Genome Sequence of Escherichia coli J53, an Azide-Resistant Laboratory Strain Used for Conjugation Experiments', *Genome Announcements*, 6(21). doi: 10.1128/genomeA.00433-18.

McClaine, J. W. and Ford, R. M. (2002) 'Reversal of Flagellar Rotation Is Important in Initial Attachment of Escherichia coli to Glass in a Dynamic System with High- and Low-Ionic-Strength Buffers', *Applied and Environmental Microbiology*, 68(3), pp. 1280–1289. doi: 10.1128/AEM.68.3.1280-1289.2002.

Meek, R. W., Vyas, H. and Piddock, L. J. V. (2015) 'Nonmedical Uses of Antibiotics: Time to Restrict Their Use?', *PLoS Biology*. doi: 10.1371/journal.pbio.1002266.

Melnyk, A. H., Wong, A. and Kassen, R. (2015) 'The fitness costs of antibiotic resistance mutations', *Evolutionary Applications*. doi: 10.1111/eva.12196.

Mendes Oliveira, V. R., Paiva, M. C. and Lima, W. G. (2019) 'Plasmid-mediated colistin resistance in Latin America and Caribbean: A systematic review', *Travel Medicine and Infectious Disease*, 31, p. 101459. doi: 10.1016/j.tmaid.2019.07.015.

Millan, A. S. *et al.* (2014) 'Positive selection and compensatory adaptation interact to stabilize non-transmissible plasmids', *Nature Communications*. doi: 10.1038/ncomms6208.

Murakami, K. S. and Darst, S. A. (2003) 'Bacterial RNA polymerases: the wholo story', *Current Opinion in Structural Biology*, 13(1), pp. 31–39. doi: 10.1016/S0959-440X(02)00005-2.

Nakao, R. *et al.* (2012) 'Enhanced Biofilm Formation by Escherichia coli LPS Mutants Defective in Hep Biosynthesis', *PLoS ONE*. Edited by U. Dobrindt, 7(12), p. e51241. doi: 10.1371/journal.pone.0051241.

Nang, S. C. *et al.* (2018) 'Fitness cost of mcr-1-mediated polymyxin resistance in Klebsiella pneumoniae', *Journal of Antimicrobial Chemotherapy*. doi: 10.1093/jac/dky061.

NDARO (no date) *MCR-1 family phosphoethanolamine--lipid A transferase gene family (National Database of Antibiotic Resistant Organisms)*. Available at: https://www.ncbi.nlm.nih.gov/pathogens/refgene/#gene_family:(mcr-1).

Norman, A., Hansen, L. H. and Sørensen, S. J. (2009) 'Conjugative plasmids: vessels of the communal gene pool', *Philosophical Transactions of the Royal Society B: Biological Sciences*, 364(1527), pp. 2275–2289. doi: 10.1098/rstb.2009.0037.

ONS (no date) *Causes of death over 100 years*.

Ortega-Paredes, D. *et al.* (2020) 'Broiler Farms and Carcasses Are an Important Reservoir of Multi-Drug Resistant Escherichia coli in Ecuador', *Frontiers in Veterinary Science*. doi: 10.3389/fvets.2020.547843.

Palmer, A. C. and Kishony, R. (2014) 'Opposing effects of target overexpression reveal drug mechanisms', *Nature Communications*, 5(1), p. 4296. doi: 10.1038/ncomms5296.

Pan, H. *et al.* (2014) 'A comparison of conventional methods for the quantification of bacterial cells after exposure to metal oxide nanoparticles', *BMC Microbiology*, 14(1), p. 222. doi: 10.1186/s12866-014-0222-6.

Patel, V. and Matange, N. (2021) 'Adaptation and compensation in a bacterial gene regulatory network evolving under antibiotic selection', *eLife*, 10. doi: 10.7554/eLife.70931.

Poirel, L. *et al.* (2016) 'Genetic Features of MCR-1-Producing Colistin-Resistant Escherichia coli Isolates in South Africa', *Antimicrobial Agents and Chemotherapy*, 60(7), pp. 4394–4397. doi: 10.1128/AAC.00444-16.

Poon, A., Davis, B. H. and Chao, L. (2005) 'The Coupon Collector and the Suppressor Mutation', *Genetics*. doi: 10.1534/genetics.104.037259.

Prestinaci, F., Pezzotti, P. and Pantosti, A. (2015) 'Antimicrobial resistance: A global multifaceted phenomenon', *Pathogens and Global Health*. doi: 10.1179/2047773215Y.0000000030.

Price, M. N. and Arkin, A. P. (2015) 'Weakly deleterious mutations and low rates of recombination limit the impact of natural selection on bacterial genomes', *mBio*. doi: 10.1128/mBio.01302-15.

Qi, Q. *et al.* (2016) 'The genomic basis of adaptation to the fitness cost of rifampicin resistance in pseudomonas aeruginosa', *Proceedings of the Royal Society B: Biological Sciences*. doi: 10.1098/rspb.2015.2452.

Renner, L. D. and Weibel, D. B. (2011) 'Physicochemical regulation of biofilm formation', *MRS Bulletin*, 36(5), pp. 347–355. doi: 10.1557/mrs.2011.65.

Rossetti, F. F. *et al.* (2004) 'Interaction of Poly(L-Lysine)-g-Poly(Ethylene Glycol) with Supported Phospholipid Bilayers', *Biophysical Journal*, 87(3), pp. 1711–1721. doi: 10.1529/biophysj.104.041780.

Le Roux, F. *et al.* (2007) 'Construction of a Vibrio splendidus Mutant Lacking the Metalloprotease Gene vsm by Use of a Novel Counterselectable Suicide Vector', *Applied and Environmental Microbiology*, 73(3), pp. 777–784. doi: 10.1128/AEM.02147-06.

Rozwandowicz, M. *et al.* (2018) 'Plasmids carrying antimicrobial resistance genes in Enterobacteriaceae', *Journal of Antimicrobial Chemotherapy*, 73(5), pp. 1121–1137. doi: 10.1093/jac/dkx488.

Saiful, I. K. ., Shiraj-Um-Mahmuda, S. and Hazzaz-Bin-Kabir, M. (2016) 'Antibiotic usage patterns in selected broiler farms of Bangladesh and their public health implications', *Journal of Public Health in Developing Countries J Public Health Dev Ctries*.

Saito, K., Green, R. and Buskirk, A. R. (2020) 'Translational initiation in E. coli occurs at the correct sites genome-wide in the absence of mRNA-rRNA base-pairing', *eLife*, 9. doi: 10.7554/eLife.55002.

San Millan, A. and MacLean, R. C. (2017) 'Fitness Costs of Plasmids: a Limit to Plasmid Transmission', *Microbiology Spectrum*. doi: 10.1128/microbiolspec.mtbp-0016-2017.

Segev-Zarko, L. *et al.* (2018) 'Deficient Lipid A Remodeling by the arnB Gene Promotes Biofilm Formation in Antimicrobial Peptide Susceptible Pseudomonas aeruginosa', *Biochemistry*, 57(13), pp. 2024–2034. doi: 10.1021/acs.biochem.8b00149.

Shen, C. *et al.* (2020) 'Dynamics of mcr-1 prevalence and mcr-1-positive Escherichia coli after the cessation of colistin use as a feed additive for animals in China: a prospective cross-sectional and whole genome sequencing-based molecular epidemiological study', *The Lancet Microbe*. doi: 10.1016/s2666-5247(20)30005-7.

Shen, Y. *et al.* (2019) 'Integrated aquaculture contributes to the transfer of mcr-1 between animals and humans via the aquaculture supply chain', *Environment International*, 130, p. 104708. doi: 10.1016/j.envint.2019.03.056.

Sheppard, S. K., Guttman, D. S. and Fitzgerald, J. R. (2018) 'Population genomics of bacterial host adaptation', *Nature Reviews Genetics*, 19(9), pp. 549–565. doi: 10.1038/s41576-018-0032-z.

Shine, J. and Dalgarno, L. (1975) 'Determinant of cistron specificity in bacterial ribosomes', *Nature*, 254(5495), pp. 34–38. doi: 10.1038/254034a0.

Shterzer, N. and Mizrahi, I. (2015) 'The animal gut as a melting pot for horizontal gene transfer', *Canadian Journal of Microbiology*, 61(9), pp. 603–605. doi: 10.1139/cjm-2015-0049.

Shultzaberger, R. K. *et al.* (2007) 'Anatomy of Escherichia coli σ 70 promoters', *Nucleic Acids Research*, 35(3), pp. 771–788. doi: 10.1093/nar/gkl956.

Silhavy, T. J., Kahne, D. and Walker, S. (2010) 'The bacterial cell envelope.', *Cold Spring Harbor perspectives in biology*. doi: 10.1101/cshperspect.a000414.

Silva-Rocha, R. *et al.* (2013) 'The Standard European Vector Architecture (SEVA): a coherent platform for the analysis and deployment of complex prokaryotic phenotypes', *Nucleic Acids Research*, 41(D1), pp. D666–D675. doi: 10.1093/nar/gks1119.

Simonsen, L. *et al.* (1990) 'Estimating the rate of plasmid transfer: An end-point method', *Journal of General Microbiology*. doi: 10.1099/00221287-136-11-2319.

Sommer, M. O. A., Dantas, G. and Church, G. M. (2009) 'Functional characterization of the antibiotic resistance reservoir in the human microflora', *Science*. doi: 10.1126/science.1176950.

Sota, M. *et al.* (2010) 'Shifts in the host range of a promiscuous plasmid through parallel evolution of its replication initiation protein', *ISME Journal*. doi: 10.1038/ismej.2010.72.

Stern, D. L. (2013) 'The genetic causes of convergent evolution', *Nature Reviews Genetics*, 14(11), pp. 751–764. doi: 10.1038/nrg3483.

Stevenson, K. *et al.* (2016) 'General calibration of microbial growth in microplate readers', *Scientific Reports*, 6(1), p. 38828. doi: 10.1038/srep38828.

Stewart, F. M. and Levin, B. R. (1977) 'THE POPULATION BIOLOGY OF BACTERIAL PLASMIDS: A PRIORI CONDITIONS FOR THE EXISTENCE OF CONJUGATIONALLY TRANSMITTED FACTORS', *Genetics*, 87(2), pp. 209–228. doi: 10.1093/genetics/87.2.209.

Stoebel, D. M. *et al.* (2009) 'Compensatory Evolution of Gene Regulation in Response to Stress by Escherichia coli Lacking RpoS', *PLoS Genetics*. Edited by D. S. Guttman, 5(10), p. e1000671. doi: 10.1371/journal.pgen.1000671.

Stojanoski, V. *et al.* (2016) 'Structure of the catalytic domain of the colistin resistance enzyme MCR-1', *BMC Biology*. doi: 10.1186/s12915-016-0303-0.

Sun, J. *et al.* (2018) 'Towards Understanding MCR-like Colistin Resistance', *Trends in Microbiology*. doi: 10.1016/j.tim.2018.02.006.

the Maduro lab (no date) *Random DNA Sequence Generator*. Available at: http://www.faculty.ucr.edu/~mmaduro/random.htm.

Tietgen, M. *et al.* (2018) 'Impact of the colistin resistance gene mcr-1 on bacterial fitness', *International Journal of Antimicrobial Agents*. doi: 10.1016/j.ijantimicag.2017.11.011.

Trunk, T., S. Khalil, H. and C. Leo, J. (2018) 'Bacterial autoaggregation', *AIMS Microbiology*, 4(1), pp. 140–164. doi: 10.3934/microbiol.2018.1.140.

Uphoff, S. (2018) 'Real-time dynamics of mutagenesis reveal the chronology of DNA repair and damage tolerance responses in single cells', *Proceedings of the National Academy of Sciences of the United States of America*. doi: 10.1073/pnas.1801101115.

Ventola, C. L. (2015) 'The antibiotic resistance crisis: part 1: causes and threats.', *P & T : A peer-reviewed journal for formulary management (2015)*. doi: Article.

Vigeant, M. A.-S. *et al.* (2002) 'Reversible and Irreversible Adhesion of Motile Escherichia coli Cells Analyzed by Total Internal Reflection Aqueous Fluorescence Microscopy', *Applied and Environmental Microbiology*, 68(6), pp. 2794–2801. doi: 10.1128/AEM.68.6.2794-2801.2002.

Vogwill, T., Kojadinovic, M. and Maclean, R. C. (2016) 'Epistasis between antibiotic resistance mutations and genetic background shape the fitness effect of resistance across species of pseudomonas', *Proceedings of the*

Royal Society B: Biological Sciences. doi: 10.1098/rspb.2016.0151.

Vogwill, T. and Maclean, R. C. (2015a) 'The genetic basis of the fitness costs of antimicrobial resistance: A meta-analysis approach', *Evolutionary Applications*. doi: 10.1111/eva.12202.

Vogwill, T. and Maclean, R. C. (2015b) 'The genetic basis of the fitness costs of antimicrobial resistance: A meta-analysis approach', *Evolutionary Applications*. doi: 10.1111/eva.12202.

Wagner, L. A. *et al.* (1994) 'An efficient Shine-Dalgarno sequence but not translation is necessary for lacZ mRNA stability in Escherichia coli', *Journal of Bacteriology*, 176(6), pp. 1683–1688. doi: 10.1128/jb.176.6.1683-1688.1994.

Wakabayashi, H., Warnasooriya, C. and Ermolenko, D. N. (2020) 'Extending the Spacing between the Shine–Dalgarno Sequence and P-Site Codon Reduces the Rate of mRNA Translocation', *Journal of Molecular Biology*, 432(16), pp. 4612–4622. doi: 10.1016/j.jmb.2020.06.008.

Wale, N. *et al.* (2017) 'Resource limitation prevents the emergence of drug resistance by intensifying within-host competition', *Proceedings of the National Academy of Sciences of the United States of America*. doi: 10.1073/pnas.1715874115.

Wang, R. *et al.* (2018a) 'The global distribution and spread of the mobilized colistin resistance gene mcr-1', *Nature Communications*. doi: 10.1038/s41467-018-03205-z.

Wang, R. *et al.* (2018b) 'The global distribution and spread of the mobilized colistin resistance gene mcr-1', *Nature Communications*. doi: 10.1038/s41467-018-03205-z.

Wang, Y., Zhang, R., *et al.* (2017) 'Comprehensive resistome analysis reveals the prevalence of NDM and MCR-1 in Chinese poultry production', *Nature Microbiology*. doi: 10.1038/nmicrobiol.2016.260.

Wang, Y., Tian, G.-B., *et al.* (2017) 'Prevalence, risk factors, outcomes, and molecular epidemiology of mcr-1-positive Enterobacteriaceae in patients and healthy adults from China: an epidemiological and clinical study', *The Lancet Infectious Diseases*. doi: 10.1016/S1473-3099(16)30527-8.

Wang, Yang *et al.* (2020) 'Changes in colistin resistance and mcr-1 abundance in Escherichia coli of animal and human origins following the ban of colistin-positive additives in China: an epidemiological comparative study', *The Lancet Infectious Diseases*. doi: 10.1016/s1473-3099(20)30149-3.

Wertheim, H. *et al.* (2013) 'Global survey of polymyxin use: A call for international guidelines', *Journal of Global Antimicrobial Resistance*. doi: 10.1016/j.jgar.2013.03.012.

World Health Organization (2018) *WHO report on surveillance of antibiotic consumption: 2016-2018 early implementation*. Geneva. Available at: https://www.who.int/medicines/areas/rational_use/who-amr-amc-report-20181109.pdf.

Yang, P. *et al.* (2018) 'Association between antibiotic consumption and the rate of carbapenem-resistant Gram-negative bacteria from China based on 153 tertiary hospitals data in 2014', *Antimicrobial Resistance and Infection Control*. doi: 10.1186/s13756-018-0430-1.

Yang, Q. *et al.* (2017a) 'Balancing mcr-1 expression and bacterial survival is a delicate equilibrium between essential cellular defence mechanisms', *Nature Communications*. doi: 10.1038/s41467-017-02149-0.

Yang, Q. *et al.* (2017b) 'Balancing mcr-1 expression and bacterial survival is a delicate equilibrium between essential cellular defence mechanisms', *Nature Communications*, 8(1), p. 2054. doi: 10.1038/s41467-017-02149-0.

Yang, Q. E. *et al.* (2020) 'Compensatory mutations modulate the competitiveness and dynamics of plasmid-mediated colistin resistance in Escherichia coli clones', *The ISME Journal*, 14(3), pp. 861–865. doi: 10.1038/s41396-019-0578-6.

Yi, H. *et al.* (2012) 'Genome sequence of Escherichia coli J53, a reference strain for genetic studies', *Journal of Bacteriology*. doi: 10.1128/JB.00641-12.

Zaman, S. Bin *et al.* (2017) 'A Review on Antibiotic Resistance: Alarm Bells are Ringing', *Cureus*. doi: 10.7759/cureus.1403.